Université du Québec

INRS (Centre Énergie Matériaux Télécommunications)

Electron kinetic simulations using Maxwellians and generalized Laguerre polynomials

Par

Amir Abbas Haji Abolhassani

Mémoire présenté

pour l'obtention

du grade de Maître ès sciences (M.Sc.)

en Sciences de l'énergie et des matériaux

Jury d'évaluation

Président du jury   François Vidal
et examinateur interne   INRS (EMT)

Examinateur externe   Lora Ramunno
                                    Département de Physique
                                    Université d'Ottawa

Directeur de recherche   Jean-Pierre Matte
                                    INRS (EMT)

Abstract

Electron heat flow in steep temperature gradients is known to produce distinctly non-Maxwellian electron velocity distributions: In the cold regions, there is a considerable surplus of hot electrons which have streamed from the hot regions before being thermalized. In electron kinetic codes, the velocity distribution function is represented on a grid in velocity space. Expanding the angular dependence in Legendre polynomials greatly reduces the computational requirements, but the energy grid is still a burden. Here, we propose to represent the energy dependence as a sum of one, two or three Maxwellians, each multiplied by a finite sum of generalized Laguerre polynomials, to represent, for example, the streaming of energetic electrons into cold plasma.

In the Vlasov-Fokker-Planck electron kinetic equation, if we assume that the spatial variation is in 1 dimension, along x, and that the velocity variation has azimutal symmetry about the x axis, and we expand the angular μ dependence in Legendre polynomials, we can derive the kinetic equation (eq. 2 of F. Alouani_Bibi *et al.*, Comp. Phys. Comm. **164**, 60 (2004)), assuming there is no magnetic field, except possibly along x.

In the present "FPI" electron kinetic code, these Legendre coefficients $f_l(x, v, t)$ are advanced in time, using finite difference grids in x and v. The aim of our project is to replace the grid in v by one, two or three Maxwellians, each multiplied by a sum of generalized Laguerre polynomials on each point of the spatial grid, and then to compute the time evolution of the electron distribution function for different temperature ratios using generalized Laguerre polynomials:

$$f_l(x, v, t) = \sum_{\eta=c,m,h} \left(\frac{m_e}{2\pi k_B T_\eta(x,t)} \right)^{\frac{3}{2}} \exp\left\{ -\frac{m_e v^2}{2 k_B T_\eta(x,t)} \right\} \sum_{j=0}^{N_L} a_{\eta l j}(x,t) L_j^{(l+1/2)}\left(\frac{m_e v^2}{2 k_B T_\eta(x,t)} \right)$$

where m_e is the electron mass, v is velocity, η denotes the population, c for cold, m for medium and h for hot. $T_\eta(x,t)$'s are the temperatures of each population, $a_{\eta l j}(x,t)$'s are the coefficients of the generalized Laguerre polynomials (The $T_\eta(x,t)$ and the $a_{\eta l j}(x,t)$'s are the fitting parameters).

As electron-electron (*e-e*) collisions are the most complex part of this problem, we focus on this aspect in the present research. We study the relaxation of a hot Maxwellian initially embedded in a colder and denser one towards a single Maxwellian. First, we fitted the distribution functions from the "FPI" finite difference electron code for this problem to a single/two/three Maxwellian(s) each multiplied by a finite sum of generalized Laguerre polynomials, at several

times, to show that this expansion is viable. Then, we provided a moment evolving and fitting method for advancing the parameters (the temperatures $T_\eta(x,t)$'s and the coefficients of the generalized Laguerre polynomials $a_{\eta l j}(x,t)$'s) in time, and a comparison to "FPI" code results at several times was made. Good agreement was obtained, if proper choices of the number of Maxwellians and of Laguerre terms were made   It was found that a single temperature expansion is viable only for low initial temperature ratios (2:1 or less), but that for initial temperature ratios above 10:1, a three temperature expansion is best, and was seen to give good results (i.e. good agreement with "FPI") for temperature ratios as high as 1000:1.

Étudiant
　　　Amir Abbas Haji Abolhassani

Directeur de recherche
　　　Jean-Pierre Matte

"Free your perception to feel the flow of knowledge."

To:

my mother for her prayers;

my brother Amin for his support;

And Mahsan for her love;

Acknowledgements

Résumé en français

Introduction

Les plasmas composent 99% de la matière dans l'univers. Sur terre, ils ont de nombreuses applications dans plusieurs domaines de la science et de la technologie. Il est donc important de pouvoir les modéliser correctement, et les modèles numériques sont un complément nécessaire pour les expériences, souvent difficiles et coûteuses, et pour les modèles analytiques, qui, bien souvent, ne sont applicables qu'aux situations très simples ou très idéalisées.

Il y a deux grandes familles de modèles:

1) Les modèles macroscopiques, aussi appelés modèles fluides ou hydrodynamiques, dans lesquels les profils de densité, de vitesse moyenne et de température sont calculés et avancés en temps en utilisant les équations de conservation des particules, de la quantité de mouvement et de l'énergie.

2) Les modèles microscopiques, ou modèles cinétiques, où c'est la densité de particules dans l'espace de phase qui est avancée en temps. Il y a deux grandes familles de codes cinétiques:

    a) Les codes à particules (PIC), Monte Carle (MC) ou de dynamique moléculaire (MD), dans lesquels les équations du mouvement sont résolues pour un grand nombre de particules qui représentent le comportement des particules du plasma.

    b) Les codes cinétiques dans lesquels la densité de particules dans l'espace de phase est avancée en temps directement sur une grille aux différences finies. Dans l'équation cinétique générale de Boltzmann, le terme de collision entre les particules est obtenu en supposant simplement des collisions binaires et une absence de corrélations entre particules avant la collision [5]. Cependant, pour des collisions élastiques entre particules chargées dans un plasma, une forme particulière du terme de collision, conduisant à l'équation de Fokker-Planck, en donne une bonne approximation [6, 7].

Les codes fluides sont les plus utilisés, parce qu'ils sont beaucoup moins exigeants en ressources informatiques, mais il y a plusieurs cas où ils sont incorrects ou insuffisants, puisque la densité, la vitesse moyenne et la température ne suffisent pas pour bien caractériser un plasma. Les taux d'ionisation et d'excitation, par exemple, exigent une intégration sur la partie de la fonction de distribution qui est au dessus du seuil et en tenant compte de la dépendance de la section efficace sur la vitesse. Dans les codes fluides, on suppose que la fonction de distribution

est maxwellienne, puisque c'est la solution d'équilibre des équations de Boltzmann et de Fokker-Planck, mais cette hypothèse n'est pas valide dans des gradients raides ou en présence de champs forts. De même, les conductivités électrique et thermique classiques obtenues par Spitzer et Härm [8] ne sont valides que pour des champs faibles et des gradients doux. Quand il y a des gradients de température très raides, par contre, il y a des électrons rapides qui vont de la zone chaude à la zone froide avant d'être thermalisés, ce qui fait qu'y coexistent une maxwellienne froide et une minorité à une température voisine de celle de la zone chaude [15, 16]. Ceci implique aussi qu'il y a du pré-chauffage, de sorte que le profil de température n'est plus concave jusqu'à la région froide, avec une discontinuité abrupte de la pente à cet endroit (comme le prédit la théorie classique de la diffusion de la chaleur), mais plutôt une région où le profil est convexe, à cause de ces électrons plus rapides qui y déposent leur énergie graduellement [17, 18]. Ce préchauffage peut être décrit par des formules de flux de chaleur non local, où on fait une convolution en espace sur le flux classique (de Spitzer-Härm) et il y eu de très nombreux travaux sur ce sujet [17-32]. Des simulations fluides utilisant certaines de ces formules pour le flux de chaleur ont été comparées à des simulations cinétiques [33, 34] et à des expériences [35-37], et il s'avère qu'aucune de ces formules ne permet de bien rendre compte de toutes les situations. De plus, ces formules ne rendent aucunement compte de l'aspect non-maxwellien des fonctions de distribution, et des corrections nécessaires aux taux d'ionisation et d'excitation, par exemple. Il est donc évident qu'il serait très désirable de développer des codes cinétiques plus rapides et plus légers.

Dans les codes cinétiques en espace de phase (2b dans l'énumération ci-dessus), la dépendance angulaire de la distribution des vitesses est très souvent dévelopée en harmoniques sphériques, ce qui réduit beaucoup la lourdeur des calculs, mais il reste quand même la grille pour l'énergie ou le module de la vitesse. C'est là ce que nous voulons alléger, en remplaçant la grille en énergie par une série d'une, deux ou trois maxwelliennes, dont chacune serait multipliée par une série de polynômes de Laguerre (ou de Sonine) généralisés.

De tels développements ont été utilisés dans le passé, mais avec une seule température. D'abord, pour les gaz, la méthode de Chapman-Enskog [38] consistait à utiliser ces polynômes pour calculer l'effet de forces externes ou de gradients sur $f_1(v)$, l'anisotropie de 1er ordre dans le développement de Legendre, en supposant que $f_0(v)$ est une maxwellienne. C'est cette méthode qui a été appliquée aux plasmas par Spitzer et Härm pour calculer les conductivités électrique et thermiques [8]. Ce développement a aussi été utilisé pour simuler la relaxation de $f_0(v)$ d'un gaz [39] ou d'un plasma [40, 41] uniforme vers l'équilibre. Held et coll. ont développé un code cinétique avec gradients spatiaux, dans le contexte du plasma central d'un Tokamak, où les différences de température sont modestes, mais les libres parcours moyens très longs, car ces

plasmas sont très chauds (contrairement aux plasmas des déflecteurs) [42-48], et ils ont pu ainsi développer des formules non-locales et les inclure dans le code hydrodynamique "NIMROD" [49-52]. Toutefois, si on veut simuler l'interaction entre des électrons froids et des électrons chauds, un développement à une seule température n'est pas pratique parce que le nombre de termes requis devient prohibitif, et nous verrons qu'il vaut mieux utiliser deux ou même trois températures, si le rapport des deux températures initiales est supérieur à 2.

Dans le but d'étudier l'utilisation de fonctions de distribution comportant plusieurs températures, nous avons considéré le problème particulier de la relaxation collisionnelle de plasmas uniformes, consistant initialement en deux populations maxwelliennes, vers une seule maxwellienne. C'est là la partie la plus complexe pour développer un code cinétique, puisque l'opérateur de collision électron-électron est nonlinéaire, et nous nous sommes limités à cet aspect. Donc, il n'y a pas de champ électrique extérieur ni de gradient, et la fonction de distribution en vitesse est isotrope. Un code numérique a été mis au point pour calculer l'évolution temporelle de la fonction de distribution développée ainsi, et les résultats ont été comparés à ceux obtenus au moyen d'un code cinétique électronique aux différences finies "FPI" ("Fokker Planck International") développé par Matte et coll. [13, 16, 28, 37, 58] et un bon accord est obtenu.

Ce mémoire est divisé en cinq chapitres.

Au chapitre 1, l'équation de Vlasov-Fokker-Planck est décrite plus en détail. Nous décrivons les simplifications effectuées pour un modèle à une dimension (ce qui sera une brève description du code "FPI"), puis à zéro dimension en espace, soit le cadre du présent travail. Au chapitre 2, nous montrons qu'on peut représenter correctement les fonctions non-maxwelliennes calculées par "FPI", au moyen de fits ou d'ajustements des paramètres en utilisant une méthode de moments, c'est-à-dire en calculant numériquement des intégrales de la fonction de distribution multipliées par différentes puissances de la vitesse, et en faisant en sorte que ces fonctions de distribution analytiques aient les mêmes valeurs pour ces moments que les fonctions de distribution numériques. Au chapitre 3, nous expliquons notre algorithme pour calculer l'évolution temporelle de la composante isotrope des fonctions de distribution représentées par ce développement de Laguerre, et donc le taux de changement des moments, comme moyen d'avancer les températures et les coefficients des polynômes de Laguerre en temps, en utilisant en partie des éléments de l'algorithme utilisé pour le chapitre 2. Les dérivations des formules sont expliquées en détail aux appendices A, B, et C. Au chapitre 4, nous présentons les résultats des calculs d'évolution temporelle pour différents cas, c'est-à-dire pour différents rapports initiaux de température et de densité, effectués avec la méthode décrite au chapitre 3, et comparons aux résultats obtenus avec le code cinétique électronique aux différences finies "FPI", pour les mêmes conditions initiales.

Enfin, le chapitre 5 conclut par un sommaire du travail et une brève explication de ce qu'il resterait à faire pour développer un code capable de simuler l'évolution temporelle de la fonction de distribution en présence de champs électriques et de gradients.

1. Chapitre 1 – Équation deVlasov-Fokker-Planck

1.1. Équation deVlasov-Fokker-Planck

L'équation de Vlasov-Fokker-Planck décrit les effets d'un champ électro-magnétique et de gradients spatiaux dans un plasma, en utilisant les équations du mouvement et l'équation de continuité dans l'espace de phase. Si les champs électrique et magnétique ainsi que les gradients spatiaux sont dans une seule direction (disons l'axe $\hat{x}$), et si on suppose une symétrie azimutale autour de cet axe, on peut réduire le nombre de dimensions dans l'espace de phase de 6 à seulement 3, soit (x,v,μ) où $\mu = \frac{v_x}{v}$. Ensuite, en développant la dépendance en μ en polynômes de Legendre, on peut réécrire l'équation de Vlasov-Fokker-Planck comme une série d'équations couplées en 2 dimensions (x,v) [16,37] :

$$\frac{\partial}{\partial t} f_l(x,v,t) + v\left[\frac{l}{2l-1}\frac{\partial f_{l-1}}{\partial x} + \frac{l+1}{2l+3}\frac{\partial f_{l+1}}{\partial x}\right] - \frac{eE}{m_e}\left[\frac{l}{2l-1}v^{l-1}\frac{\partial}{\partial v}\left(\frac{f_{l-1}}{v^{l-1}}\right) + \frac{l+1}{2l+3}\frac{1}{v^{l+2}}\frac{\partial}{\partial v}\left(v^{l+2}f_{l+1}\right)\right] =$$
$$\left(\frac{\partial f_l}{\partial t}\right)_{e-i} + \left(\frac{\partial f_l}{\partial t}\right)_{e-e} \tag{1}$$

À droite, il y a les termes de collision électrons-ions $e-i$ et électrons-électrons $e-e$, qui s'expriment comme suit dans l'aproximation de Fokker-Planck:

$$\left(\frac{\partial f_l}{\partial t}\right)_{e-i} = -\frac{l(l+1)}{2}\frac{4\pi Z^2 n_i e^4 Ln\Lambda}{m_e^2 v^3}f_l \tag{2}$$

$$\left(\frac{\partial f_l}{\partial t}\right)_{e-e} = \frac{1}{v^2}\frac{\partial}{\partial v}\left[v^2\left(D_{\parallel-0}(v)\frac{\partial f_l}{\partial v} + C_0(v)f_l\right)\right] - \frac{l(l+2)}{2v^2}D_{\perp-0}(v)f_l \tag{3}$$

Le terme de collision $e-e$ est nonlinéaire et c'est la partie la plus compliquée de l'équation de Vlasov-Fokker-Planck. Ici, $C_0(v)$, $D_{\parallel-0}(v)$ et $D_{\perp-0}(v)$ sont les coefficients de friction, de diffusion paralllèle et de diffusion perpendiculaire. Dans l'approximation des potentiels de Rosenbluth isotropes, que nous adoptons, on tient compte seulement de la composante $f_0(v)$ (moyennée sur les angles) de la fonction de distribution dans le calcul des opérateurs de collision (car tenir compte des termes supplémentaires alourdirait beaucoup les calculs [63]). Les coefficients s'expriment alors:

$$C_0(v) = \frac{4\pi\alpha}{v^2}\int_0^v u^2 f_0(u)\,du \tag{4}$$

$$D_{\parallel-0}(v) = \frac{8\pi\alpha}{3}\left(\int_v^\infty u\,f_0(u)\,du + \left(\frac{1}{v^3}\right)\int_0^v u^4 f_0(u)\,du\right) \tag{5}$$

$$D_{\perp-0}(v) = \frac{4\pi\alpha}{3}\left(2\int_v^\infty u\, f_0\,(u)\,\mathrm{d}u + \left(\frac{3}{v}\right)\int_0^v u^2 f_0\,(u)\,\mathrm{d}u\right) \tag{6}$$

$$\alpha = \frac{4\pi\mathrm{e}^4 \mathrm{Ln}\,(\Lambda)}{m_e^4}\;(\mathrm{cgs}) \tag{7}$$

e est la charge d'un électron, m_e sa masse et $Ln(\Lambda)$ est le logarithme de Coulomb. Ici, nous avons utilise le système d'unités (cgs).

1.2. La fonction de distribution électronique de Laguerre généralisée

Dans les codes cinétiques, la fonction de distribution des vitesses est représentée sur une grille dans l'espace des vitesses. Les développements de la dépendance angulaire en harmoniques sphériques a réduit de beaucoup les exigences en temps de calcul et en mémoire, mais la résolution sur la grille en vitesse est quand même encore lourde pour des codes cinétiques comme « FPI » qui résolvent les équations (1) à (7) sur des grilles aux différences finies en x et en v. Ici, nous proposons de représenter la dépendence en énergie de chacune des composantes de Legendre $f_l(x,v,t)$ par une somme de deux maxwelliennes (ou trois, lorsque le rapport des températures est élevé), dont chacune est multipliée par une somme finie de polynômes de Laguerre généralisés, pour représenter l'interaction entre des électrons chauds et des électrons froids, comme, par exemple, lorsque des électrons rapides de la région chaude du plasma pénètrent dans la région froide.

$$f_l(x,v,t) = \sum_\eta \left(\frac{m_e}{2\pi k_B T_\eta(x,t)}\right)^{\frac{3}{2}} exp\left\{-\frac{m_e v^2}{2k_B T_\eta(x,t)}\right\} \sum_{j=0}^{N_{\eta l}} a_{\eta l j}(x,t)\, L_j^{(\alpha_l)}\left(\frac{m_e v^2}{2k_B T_\eta(x,t)}\right) \tag{8}$$

où $\alpha_l = l + \frac{1}{2}$.

L'indice η = c (froid), m (moyen), h (chaud) indique les différentes températures utilisées pour représenter la fonction de distribution. Par ailleurs: $L_i^{(\alpha)}(x)$ est le polynôme de Laguerre généralisé, défini par [53], équation 22.3.9:

$$L_n^{(\alpha)}(x) = \sum_{i=0}^n \frac{(-1)^i}{i!}\binom{n+\alpha}{n-i}x^i \tag{9}$$

$\binom{\alpha}{n}$ est le coefficient binomial généralisé (voir [65], section: "Generalization and connection to the binomial series") .

Dans ce travail, nous ne considérerons que la composante isotrope (l=0), et seulement les collisions électron-électron. Pour cette composante, on a $\alpha_0 = 1/2$. La fonction de distribution (8) s'exprime donc comme:

$$f_0(x,v,t) = \sum_{\eta=c,h} \left(\frac{m_e}{2\pi k_B T_\eta(x,t)}\right)^{\frac{3}{2}} \exp\left\{-\frac{m_e v^2}{2k_B T_\eta(x,t)}\right\} \sum_{j=0}^{N_L} a_{\eta 0 j}(x,t) L_j^{\left(\frac{1}{2}\right)}\left(\frac{m_e v^2}{2k_B T_\eta(x,t)}\right) \tag{10}$$

De plus, nous laisserons tomber la dependance en x, puisque nous traitons des plasmas uniformes.

2. Chapitre 2 Fits en polynômes de Laguerre généralisés aux fonctions de distribution "FPI"

Pour étudier l'évolution temporelle de la fonction de distribution causée par les collisions $e - e$, il faut une fonction de distribution initiale, et dans ce travail, ce sera toujours la somme de deux maxwelliennes. À chaque pas de temps, cette fonction de distribution évolue à cause de l'effet des collisions $e - e$. Nous utilisons les fonctions de distribution calculées par le code "FPI" au même temps physique comme base de comparaison. Dans ce chapitre, nous définissons d'abord différentes formes de fonction de distribution de Laguerre (définie par l'équation (10)), et ensuite, nous écrivons les équations de moments et la méthode de régression pour obtenir les températures et les coefficients à partir des moments obtenus par intégration numérique sur les fonctions de distribution calculées numériquement avec le code "FPI", et nous comparons les fonctions de distribution ainsi obtenues à celles de "FPI". Ceci nous permettra de vérifier la validité du développement, et nous guidera pour le calcul direct de l'évolution temporelle sans utiliser de différences finies au chapitre 4.

2.1. Diverses formes de la fonction de distribution de Laguerre

Dans ce contexte, nous définissons maintenant 5 variantes de la fonction de distribution de Laguerre, selon les termes retenus dans la double somme:

Fonction de distribution à une seule maxwellienne:

$$f_{\{0\}}(v,t) = a_0(t)\left(\frac{m_e}{2\pi k_B T(t)}\right)^{\frac{3}{2}}\exp\left\{-\frac{m_e v^2}{2k_B T(t)}\right\} \tag{11}$$

Fonction de distribution à une température:

$$f_{\{N_c\}}(v,t) = \left(\frac{m_e}{2\pi k_B T(t)}\right)^{\frac{3}{2}}\exp\left\{-\frac{m_e v^2}{2k_B T(t)}\right\}\sum_{j=0}^{N_c} a_j(t)L_j^{\left(\frac{1}{2}\right)}\left(\frac{m_e v^2}{2k_B T(t)}\right) \tag{12}$$

Fonction de distribution à deux maxwelliennes:

$$f_{\{0,0\}}(v,t) = \sum_{\eta=c,h} a_{\eta 0}(t)\left(\frac{m_e}{2\pi k_B T_\eta(t)}\right)^{\frac{3}{2}}\exp\left\{-\frac{m_e v^2}{2k_B T_\eta(t)}\right\} \tag{13}$$

Pour toutes les simulations présentées dans ce travail, la fonction de distribution initiale (t=0) a cette forme.

Fonction de distribution à deux températures:

$$f_{\{N_c,N_h\}}(v,t) = \sum_{\eta=c,h}\left(\frac{m_e}{2\pi k_B T_\eta(t)}\right)^{\frac{3}{2}}\exp\left\{-\frac{m_e v^2}{2k_B T_\eta(t)}\right\}\sum_{j=0}^{N_\eta} a_{\eta j}(t)L_j^{\left(\frac{1}{2}\right)}\left(\frac{m_e v^2}{2k_B T_\eta(t)}\right) \tag{14}$$

Fonction de distribution à trois températures:

$$f_{\{N_c,N_m,N_h\}}(v,t) = \sum_{\eta=c,m,h} \left(\frac{m_e}{2\pi k_B T_\eta(t)}\right)^{\frac{3}{2}} \exp\left\{-\frac{m_e v^2}{2 k_B T_\eta(t)}\right\} \sum_{j=0}^{N_\eta} a_{\eta j}(t) L_j^{\left(\frac{1}{2}\right)}\left(\frac{m_e v^2}{2 k_B T_\eta(t)}\right) \quad (15)$$

2.2. Moments de la fonction de distribution de Laguerre et normalisation.

Les moments sont des instruments puissants pour extraire de l'information globale sur les fonctions de distribution et sont définis comme des intégrales sur la variable d'énergie. Le k$^{\text{ème}}$ moment correspond à la densité multipliée par la valeur moyenne de la vitesse à la puissance $(k-2)$:

$$M_k(t) = N_e < v^{k-2} > (t) = 4\pi \int_0^\infty f_0(v,t) v^k \, dv \qquad (16)$$

Ici, k est le numéro du moment et $<>$ indique une moyenne sur la fonction de distribution.

Par commodité, nous avons normalisé les températures $T_\eta(t)$ en keV et v^2 en 2 keV/m_e, l'unité de densité où $a_{\eta 0}(t) = 1$ correspond à 10^{21} cm^{-3} et le facteur 4π est absorbé dans $f(v)$, de sorte que la fonction de distribution de Laguerre s'écrit maintenant :

$$F_{\{N_c,N_m,N_h\}}(v,t) = \frac{4}{\sqrt{\pi}} \sum_\eta T_\eta(t)^{-\frac{3}{2}} \exp\left(-\frac{v^2}{T_\eta(t)}\right) \sum_{i=0}^{N_\eta} a_{\eta i}(t) L_i^{\left(\frac{1}{2}\right)}\left(\frac{v^2}{T_\eta(t)}\right) \qquad (17)$$

Nous pouvons maintenant calculer les moments de la fonction de distribution de Laguerre (avec la 2$^{\text{ème}}$ équation de la section "Orthogonality" de la réf. [66]).

$$M_{\{N_c,N_m,N_h\},k} = \frac{2}{\sqrt{\pi}} \sum_\eta T_\eta(t)^{\left(\frac{k}{2}-1\right)} \sum_{i=0}^{N_\eta} \binom{-\frac{k}{2}+i}{i} a_{\eta i}(t) \, \Gamma\left(\frac{k+1}{2}\right) \qquad (18)$$

2.3. Fit d'une distribution de Laguerre par égalisation des moments:

Pour construire les distributions de Laguerre définies plus haut, il faut trouver $\sum_\eta (N_\eta + 2)$ inconnues, soit: $T_\eta(t), a_{\eta 0}(t), \ldots, a_{\eta N_\eta}(t)$. Par exemple, pour trois températures, il y en a a $(N_c + N_m + N_h + 6)$. Nous égalisons $N_M = \sum_\eta (N_\eta + 2)$ moments de la fonction de distribution de Laguerre $M_{\{N_c,N_m,N_h\},k}$ à autant de moments M_k obtenus par intégration numérique des fonctions de distribution "FPI". Nous n'utilisons que des moments pairs ici $(k = 0,2,4,\ldots,2(N_M - 1))$, ce qui facilite la solution des équations de fit pour les températures (appendice A), celles-ci n'intervenant qu'avec des puissances entières.

$$M_{\{N_c,N_m,N_h\},k} = \left(\frac{2}{\sqrt{\pi}}\right) \Gamma\left(\frac{k+1}{2}\right) \sum_\eta T_\eta(t)^{\left(\frac{k}{2}-1\right)} \sum_{i=0}^{N_\eta} C_{ki} \, a_{\eta i}(t) = M_k,$$

$$k = 0,2,\ldots,2(N_M - 1)$$

où:

$$C_{ki} = \binom{-\frac{k}{2}+i}{i}. \qquad (19)$$

Ce système d'équations est linéaire dans les $a_{\eta i}(t)$ mais nonlinéaire dans les $T_\eta(t)$. Il faut d'abord chercher les valeurs des $T_\eta(t)$'s puis résoudre le système d'équations linéaires pour les coefficients $a_{\eta i}(t)$. On peut itérer sur les $T_\eta(t)$ jusqu'à ce qu'un accord satisfaisant soit obtenu.

Supposons une fonction de distribution de Laguerre avec (s) températures différentes, c.-à-d. $\eta = 1,2, \ldots, s$ et qu'il y a $N_\eta + 1$ polynômes Laguerre pour chaque température. En éliminant les $a_{\eta i}(t)$ dans (19) on obtient (s) équations pour les températures (Appendice A):

$$\sum_{i_1=0}^{N_1+1} \sum_{i_2=0}^{N_2+1} \cdots \sum_{i_s=0}^{N_s+1} \binom{N_1+1}{i_1} (-T_1)^{N_1+1-i_1} \times \binom{N_2+1}{i_2} (-T_2)^{N_2+1-i_2} \times \ldots \times$$

$$\binom{N_s+1}{i_s} (-T_s)^{N_s+1-i_s} \times \bar{M}_{\{N_1+1,N_2+1,\ldots,N_s+1\},2(l+i_1+i_2+\cdots+i_s)} = 0, \ l = 0,1,2, \ldots, s-1 \quad (20)$$

Ici, nous utilisons les moments normalisés $\bar{M}_k = \frac{M_k}{\Gamma\left(\frac{k+1}{2}\right)} \left(\frac{\sqrt{\pi}}{2}\right)$, car ainsi les ordres de grandeur sont semblables, ce qui évite des erreurs d'arrondi.

On trouve les $T_1, T_2, \ldots, T_s$ numériquement par itération de Newton-Raphson. Bien sûr, il faut toujours un estimé initial suffisamment rapproché pour chacune des températures pour que la méthode converge. Pour les calculs d'évolution temporelle, les températures obtenues au pas de temps précédent servent d'estimé. Ensuite, on peut résoudre le système d'équations linéaires (19) pour obtenir les $\boldsymbol{a_{\eta i}(t)}$.

2.4. Résultats du fit d'une fonction de distribution de Laguerre à trois températures aux résultats obtenus de "FPI" pour un rapport des températures 1000:1

La Figure (1) montre le résultat du fit à une fonction de distribution "FPI" après un demi temps de collision (pour des électrons d'un keV) pour un plasma dans lequel les rapports initiaux de température et de densité étaient $\left(\frac{T_c(0)}{T_h(0)} = 0.001, \frac{n_c(0)}{n_h(0)} = \frac{a_{c0}(0)}{a_{h0}(0)} = 9\right)$ avec la forme à trois températures de la fonction de distribution Laguerre, en variant le nombre de polynômes de Laguerre pour la température intermédiaire.
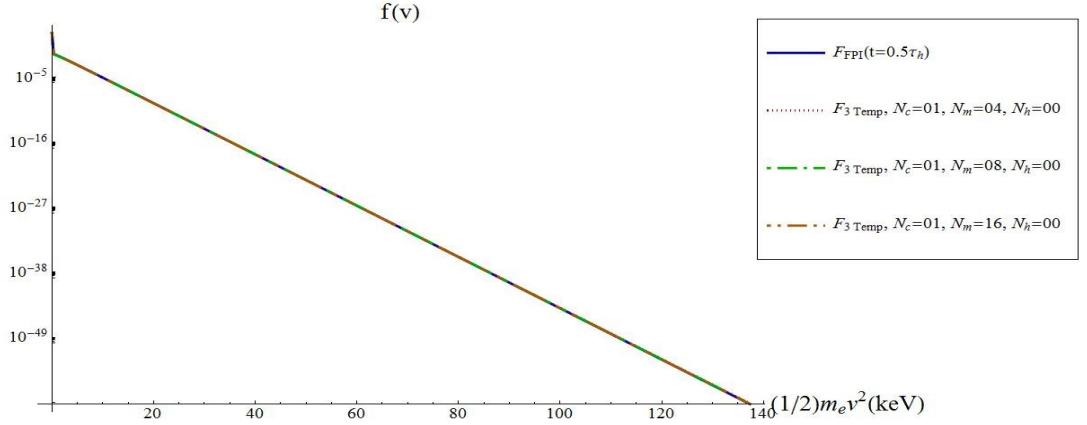
Figure (1): Résultat des fits pour la forme à trois températures de la fonction de distribution de Laguerre $\left(\frac{T_c(0)}{T_h(0)} = 0.001, \frac{a_{c0}(0)}{a_{h0}(0)} = 9, t = 0.5\tau_{T_h}\right)$.
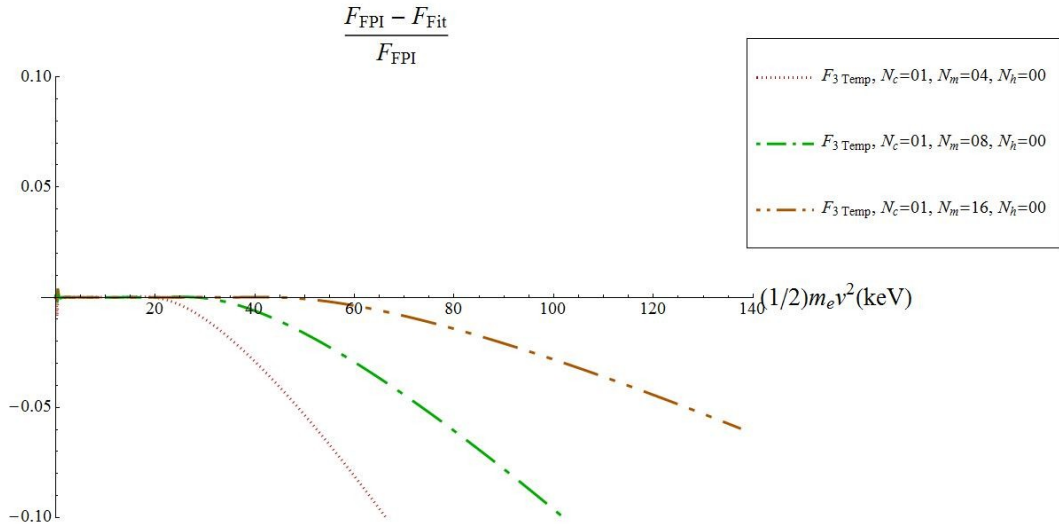

Figure (2): Erreur relative des résultats des fits tracés à la Figure (1).

Pour conclure ce chapitre, plusieurs fits aux résultats obtenus par le code "FPI" ont été effectués, avec différents rapports initiaux des températures, et nous en avons déduit un critère pour le choix de la forme la plus appropriée pour la fonction de distribution de l'évolution temporelle Laguerre:

$$\begin{cases} 0.5 \leq \frac{T_c(0)}{T_h(0)} < 1 \implies forme \ \text{à} \ une \ température \\ 0.1 < \frac{T_c(0)}{T_h(0)} < 0.5 \implies forme \ \text{à} \ deux \ températures \\ \frac{T_c(0)}{T_h(0)} \leq 0.1 \implies forme \ \text{à} \ trois \ températures \end{cases} \tag{21}$$

3. Chapitre 3 - Évolution temporelle de la fonction de distribution de Laguerre

La simulation de l'évolution temporelle de la fonction de distribution de Laguerre comporte cinq parties essentielles.

1- Initialiser la fonction de distribution, c.-à-d. définir deux maxwelliennes avec les températures et les densités prescrites (pour les distributions froides et chaudes) selon l'équation (13).

2- Calculer les moments pour une fonction de distribution de Laguerre décrite à la section 1.2 (pour une forme à une, deux ou trois températures de la fonction de distribution de Laguerre, si on connait les températures et les coefficients des polynômes de Laguerre, les moments se calculent facilement).

3- Choisir la forme appropriée de la fonction de distribution de Laguerre compte tenu du rapport initial des températures $\left(\frac{T_c(0)}{T_{h(0)}}\right)$ selon (21), c.-à-d. une, deux out trois températures.

4- Calculer les taux de variation des moments sous l'effet des collisions $e - e$ à chaque pas de temps à partir de la fonction de distribution de Laguerre. Les moments sont réactualisés en conséquence.

5- Par régression, trouver les nouvelles températures et les nouveaux coefficients $(a_{\eta i}(t)$, $T_\eta(t))$ de la fonction de distribution de Laguerre pour que les moments correspondent aux moments réactualisés, selon la technique décrite à la section 2.3.

3.1. Taux de variation des moments par collisions $e - e$ pour une fonction de distribution de Laguerre donnée

Il est commode d'écrite la forme générale de la fonction de distribution de Laguerre comme une somme de fonctions de base, dont chacune est multipliée par son coefficient :

$$\begin{cases} f_0(v,t) = F_{\{N_c,N_m,N_h\}}(v,t) = \sum_\eta \sum_{i=0}^{N_\eta} a_{\eta i}(t) F_{\eta i}(v,t) \\ \quad F_{\eta i}(v,t) = \frac{4}{\sqrt{\pi}} T_\eta(t)^{-\frac{3}{2}} \exp\left(-\frac{v^2}{T_\eta(t)}\right) L_i^{\left(\frac{1}{2}\right)}\left(\frac{v^2}{T_\eta(t)}\right) \end{cases} \quad (22)$$

Les équations (3) à (7) représentaient l'opérateur de collisions $e - e$. Ici, nous réécrivons l'opérateur de collision comme une somme sur toutes les combinaisons de ces fonctions de base, puisque l'opérateur est bilinéaire (dans l'approximation des potentiels de Rosenbluth isotropes [6]) pour la partie isotrope de la fonction de distribution ($l = 0$), et i. Il vient:

$$\left(\frac{\partial F(v,t)}{\partial t}\right)_{e-e} = \sum_\eta \sum_{p=0}^{N_\eta} \sum_\zeta \sum_{q=0}^{N_\zeta} a_{\zeta q}(t) a_{\eta p}(t) Coll\{F_{\zeta q}(v,t), F_{\eta p}(v,t)\} \quad (23)$$

$$\begin{cases} Coll\{F_{\zeta q}(v,t), F_{\eta p}(v,t)\} \stackrel{\text{def}}{=} \dfrac{1}{v^2}\dfrac{\partial}{\partial v}\left[v^2\left(D_{\eta p}(v,t)\dfrac{\partial F_{\zeta q}(v,t)}{\partial v} + C_{\eta p}(v,t)F_{\zeta q}(v,t)\right)\right] \\[2mm] C_{\eta p}(v,t) \stackrel{\text{def}}{=} \dfrac{4\pi\alpha}{v^2}\displaystyle\int_0^v u^2 F_{\eta p}(u,t)\,\mathrm{d}u \\[2mm] D_{\eta p}(v,t) \stackrel{\text{def}}{=} \dfrac{4\pi\alpha}{3}\left(\displaystyle\int_v^\infty u\,F_{\eta p}(u,t)\,\mathrm{d}u + \left(\dfrac{1}{v^3}\right)\int_0^v u^4 F_{\eta p}(u,t)\,\mathrm{d}u\right) \end{cases} \tag{24}$$

Note:

Maintenant, les taux de variation des moments sous l'effet des collisions $e-e$ pour une fonction de distribution de Laguerre $F(v,t)$ sont donc donnés par :

$$\left(\frac{\partial M_k}{\partial t}\right)_{e-e} = \int_0^\infty v^k\left(\frac{\partial F(v,t)}{\partial t}\right)_{e-e} dv = \sum_\zeta \sum_{q=0}^{N_\zeta} a_{\zeta q}(t)\int_0^\infty v^k\left(\frac{\partial F_{\zeta q}(v,t)}{\partial t}\right)_{e-e} dv =$$

$$\sum_\eta \sum_{p=0}^{N_\eta}\sum_\zeta \sum_{q=0}^{N_\zeta} a_{\zeta q}(t)a_{\eta p}(t)\int_0^\infty v^k Coll\{F_{\zeta q}(v,t), F_{\eta p}(v,t)\}dv =$$

$$\sum_\eta \sum_{p=0}^{N_\eta}\sum_\zeta \sum_{q=0}^{N_\zeta} a_{\zeta q}(t)a_{\eta p}(t)\xi_{k\zeta q\eta p}(T_\zeta, T_\eta) \tag{25}$$

où les $\xi_{k\zeta q\eta p}(T_\zeta, T_\eta)$ sont définis comme :

$$\xi_{k\zeta q\eta p}(T_\zeta, T_\eta) = \int_0^\infty v^k Coll\{F_{\zeta q}(v,t), F_{\eta p}(v,t)\}dv =$$

$$= -\left(\frac{\sqrt\pi}{4}\right)Co_{\zeta q\eta 0}\gamma_{\zeta\eta}T_\eta(t)^{\frac{k+1}{2}}S1_{\zeta\eta q\left(\frac32\right)\left(\frac k2-1\right)} + \left(\frac{\sqrt\pi}{4}\right)Co_{\zeta q\eta 0}\gamma_{\zeta\eta}^2 T_\eta(t)^{\frac{k+1}{2}}S1_{\zeta\eta q\left(\frac52\right)\left(\frac k2-1\right)}$$

$$+\left(\frac12\right)Co_{\zeta q\eta 0}T_\eta(t)^{\frac{k+1}{2}}S2_{\zeta\eta q0\left(\frac12\right)\left(\frac12\right)\left(\frac{k-1}{2}\right)}$$

$$-\left(\frac12\right)Co_{\zeta q\eta 0}\gamma_{\zeta\eta}{}^2 T_\eta(t)^{\frac{k+1}{2}}S2_{\zeta\eta q0\left(\frac52\right)\left(\frac12\right)\left(\frac{k-1}{2}\right)}, \qquad \text{pour } p=0;$$

$$= -\left(\frac14\right)Co_{\zeta q\eta 1}\gamma_{\zeta\eta}T_\eta(t)^{\frac{k+1}{2}}S2_{\zeta\eta q0\left(\frac32\right)\left(\frac12\right)\left(\frac{k-1}{2}\right)} + \left(\frac34\right)Co_{\zeta q\eta 1}T_\eta(t)^{\frac{k+1}{2}}S2_{\zeta\eta q0\left(\frac12\right)\left(\frac12\right)\left(\frac{k-1}{2}\right)}$$

$$-\left(\frac12\right)Co_{\zeta q\eta 1}T_\eta(t)^{\frac{k+1}{2}}S2_{\zeta\eta q0\left(\frac12\right)\left(\frac12\right)\left(\frac{k+1}{2}\right)} - \left(\frac{\sqrt\pi}{4}\right)Co_{\zeta q\eta 1}\gamma_{\zeta\eta}{}^2 T_\eta(t)^{\frac{k+1}{2}}S1_{\zeta\eta q\left(\frac52\right)\left(\frac k2-1\right)}$$

$$+\left(\frac12\right)Co_{\zeta q\eta 1}\gamma_{\zeta\eta}{}^2 T_\eta(t)^{\frac{k+1}{2}}S2_{\zeta\eta q0\left(\frac52\right)\left(\frac12\right)\left(\frac{k+1}{2}\right)}$$

$$+\left(\frac12\right)Co_{\zeta q\eta 1}\gamma_{\zeta\eta}{}^2 T_\eta(t)^{\frac{k+1}{2}}S2_{\zeta\eta q0\left(\frac52\right)\left(\frac12\right)\left(\frac{k-1}{2}\right)}, \qquad \text{pour } p=1;$$

$$= \left(\frac12\right)Co_{\zeta q\eta p}T_\eta(t)^{\frac{k+1}{2}}S2_{\zeta\eta qp\left(\frac12\right)\left(\frac12\right)\left(\frac{k-1}{2}\right)} + \left(\frac12\right)\left(\frac{1}{p-1}\right)Co_{\zeta q\eta p}\gamma_{\zeta\eta}^2 T_\eta(t)^{\frac{k+1}{2}}S2_{\zeta\eta q(p-1)\left(\frac52\right)\left(\frac12\right)\left(\frac{k+1}{2}\right)} -$$

$$\left(\frac12\right)\left(\frac{1}{p(p-1)}\right)Co_{\zeta q\eta p}\gamma_{\zeta\eta}^2 T_\eta(t)^{\frac{k+1}{2}}S2_{\zeta\eta q(p-1)\left(\frac52\right)\left(\frac32\right)\left(\frac{k+1}{2}\right)} -$$

$$\left(\frac14\right)\left(\frac{1}{p}\right)Co_{\zeta q\eta p}\gamma_{\zeta\eta}T_\eta(t)^{\frac{k+1}{2}}S2_{\zeta\eta q(p-1)\left(\frac32\right)\left(\frac12\right)\left(\frac{k-1}{2}\right)}, \qquad \text{pour } p\geq 2 \tag{26}$$

Rappelons que dans notre travail, nous utilisons toujours des moments pairs c.-à-d. k est un entier pair supérieur ou égal à 0 $\left(\frac{k}{2}\epsilon\mathbb{Z}^+\right)$. $S1_{\zeta\eta n\alpha_1 i}$ et $S2_{\zeta\eta nm\alpha_1\alpha_2 h}$ sont donnés par les formules:

$$S1_{\zeta\eta n\alpha_1 i} = \sum_{w=0}^{n} \frac{(-1^w)}{w!} \binom{n+\alpha_1}{n-w} \gamma_{\zeta\eta}^w \overline{S1}_{\zeta\eta n\alpha_1(i+w)}, \qquad i \in \mathbb{Z} \geq -1, \qquad w \in \mathbb{Z}^+$$

$$\overline{S1}_{\zeta\eta n\alpha_1 j} = \int_0^\infty x_\eta{}^j Erf\left[\sqrt{x_\eta}\right] e^{-(\gamma_{\zeta\eta}x_\eta)} dx_\eta, \; j \in \mathbb{Z} \geq -1 \tag{27}$$

Pour $(j = -1)$ le développement en série de Taylor expansion mène au résultat suivant:

$$\overline{S1}_{\zeta\eta n\alpha_1(-1)} = \text{Ln}\left[\sqrt{\frac{1}{\gamma_{\zeta\eta}}} + \sqrt{\frac{1}{\gamma_{\zeta\eta}}+1}\right] = 2\,\text{ArcSinh}\left[\sqrt{\frac{1}{\gamma_{\zeta\eta}}}\right], \; j = -1 \tag{28}$$

Pour $(j \geq 0)$, en intégrant par parties, on a,

$$\overline{S1}_{\zeta\eta n\alpha_1 j} = \left(\frac{1}{\sqrt{\pi}}\right)\left(\frac{1}{\gamma_{\zeta\eta}}\right)\left(\frac{1}{\gamma_{\zeta\eta}+1}\right)^{j+\frac{1}{2}} \Gamma\left[j+\frac{1}{2}\right] + \left(\frac{j}{\gamma_{\zeta\eta}}\right)\overline{S1}_{\zeta\eta n\alpha_1(j-1)}, \; j \geq 0 \tag{29}$$

(29) est une relation de récurrence pour calculer $\left(\overline{S1}_{\zeta\eta n\alpha_1 j}\right)$.

La définition de $S2_{\zeta\eta nm\alpha_1\alpha_2 h}$ est :

$$S2_{\zeta\eta nm\alpha_1\alpha_2 h} = \int_0^\infty x_\eta{}^h e^{-\left((\gamma_{\zeta\eta}+1)x_\eta\right)} L_n^{(\alpha_1)}(\gamma_{\zeta\eta}x_\eta) L_m^{(\alpha_2)}(x_\eta) dx_\eta, \; \left(h+\frac{1}{2}\right) \in \mathbb{Z}^+ \tag{30}$$

Maintenant, pour (25) en développant les polynômes de Laguerre :

$$S2_{\zeta\eta nm\alpha_1\alpha_2 h} = \sum_{i=0}^{n}\sum_{j=0}^{m} \frac{(-1)^{i+j}}{i!j!}\binom{n+\alpha_1}{n-i}\binom{m+\alpha_2}{m-j}\gamma_{\zeta\eta}^i\left(\frac{1}{1+\gamma_{\zeta\eta}}\right)^{h+i+j+1}\Gamma[h+i+j+1],$$

$$\left(h+\frac{1}{2}\right) \in \mathbb{Z}^+ \tag{31}$$

où:

$$\begin{cases} Co_{\zeta q\eta p} = 64\,\alpha\,T_\zeta(t)^{-\frac{3}{2}}T_\eta(t)^{-\frac{3}{2}} \\ x_\eta = \frac{v^2}{T_\eta(t)} \\ x_\zeta = \frac{v^2}{T_\zeta(t)} = \gamma_{\zeta\eta}x_\eta \\ \gamma_{\zeta\eta} = \left(\frac{T_\eta(t)}{T_\zeta(t)}\right) \\ \mathcal{F}_{\eta p}(x_\eta) = F_{\eta p}(v,t) \\ \mathcal{F}_{\zeta q}(x_\zeta) = F_{\zeta q}(v,t) = \mathcal{F}_{\eta p}(\gamma_{\zeta\eta}x_\eta) \end{cases} \tag{32}$$

3.2. Évolution temporelle des moments

En calculant l'évolution temporelle des moments (résultant de l'évolution temporelle de la fonction de distribution), nous utilisons une approximation de 1er ordre pour la dépendance temporelle des moments, et nous négligeons les termes de 2ème, 3ème,…, *etc.* ordre: Autrement dit:

$$M_k^{t_{n+1}} = M_k^{t_n} + \left(\frac{\partial M_k}{\partial t}\right)_{e-e}^{t_n} \Delta t + \underbrace{\frac{1}{2}\left(\frac{\partial^2 M_k}{\partial t^2}\right)_{e-e}^{t_n} \Delta t^2 + \cdots}_{\simeq 0} \tag{33}$$

ce qui est valide pourvu que le pas de temps soit suffisamment petit.

4. Chapitre 4 - Résultats numériques pour l'évolution temporelle de la fonction de distribution

Nous pouvons maintenant simuler l'évolution temporelle de la fonction de distribution sur la base de la procédure expliquée au chapitre précédent, qui est rappelée et résumée dans la figure (3).

1 Initialiser la fonction de distribution c.-à-d. deux maxwelliennes

2 Calculer les moments (section 2.2)
$$M_k(t_n = 0), \qquad n = 0$$

3 Choisir la forme appropriée de la fonction de distribution de Laguerre (une, deux ou trois températures) selon l'équation (20)

4 Calculer les taux de changement des moments (section 3.3)
$$\frac{\partial M_k(t_n)}{\partial t}$$

5 Avancer le temps
$$t_{n+1} = t_n + \Delta t$$

6 Réactualiser les moments pour le nouveau pas de temps (section 3.4)
$$M_k(t_{n+1}) = M_k(t_n) + \frac{\partial M_k(t_n)}{\partial t}\Delta t$$

7 Réactualiser les coefficients et la(es) température(s) de la fonction de distribution de Laguerre par un fit aux nouveaux moments (section 2.3)
$$\left(a_{\eta i}(t_{n+1}), T_\eta(t_{n+1})\right)$$

8 Préparation du prochain pas de temps : $n = n + 1$

Figure (3): Procédure pour simuler l'évolution temporelle de la fonction de distribution de Laguerre.

4.1. Évolution temporelle d'une forme à trois températures de la fonction de distribution de Laguerre $(N_c = 02, N_m = 08, N_h = 00)$; pour un rapport initial des températures 1:1000 $\left(\frac{T_c(t=0)}{T_h(t=0)} = \frac{1}{1000}\right)$ et un rapport initial des densités 9:1 $\left(\frac{a_{c0}(t=0)}{a_{h0}(t=0)} = 9\right)$ (cas no. 46 dans le tableau 4.1, pp. 53-54)

Nous avons simulé un grand nombre de cas résumés au tableau 4.1 (pp. 53-54), et montré les résultats pour plusieurs d'entre eux. En voici un exemple. La Figure (4) montre l'évolution temporelle d'une forme à trois températures de la fonction de distribution de Laguerre ($N_c = 02$, $N_m = 08$, $N_h = 00$) pour une distribution initiale à deux maxwelliennes $\left(\frac{T_c(t=0)}{T_h(t=0)} = \frac{1}{1000}\right.$, $\left.\frac{a_{c0}(t=0)}{a_{h0}(t=0)} = 9\right)$. La figure 4 montre les fonctions de distribution. On remarque que la pente de la fonction de distribution est encore plus faible aux énergies intermédiaires qu'aux hautes énergies. La Figure (5) montre les erreurs relatives de la fonction de distribution comparée à "FPI" à différents temps $\left(\frac{t}{\tau} = 1, 2, 5, 10, 20, 50, 100\right)$. Dans ce cas, nous avons $(N_c + N_m + N_h + 6 = 16)$ inconnues dans la fonction de distribution de Laguerre. Il nous faut donc calculer l'évolution temporelle de 16 moments $(MLag_0(t), MLag_2(t), ..., MLag_{30}(t))$ pour trouver les bons coefficients et les températures à chaque pas de temps en appliquant la méthode décrite à la section 2.3 et au chapitre 3.

La Figure (6) montre l'évolution temporelle des trois températures. Éventuellement, après plusieurs temps de collision, $T_c(t)$ tend vers la température d'équilibre $(T_e = 0.1009 \text{ keV})$. Même si $T_h(t)$ aumente un peu et atteint $(T_h(100\tau_h) \simeq 1.2 \text{ keV})$, après 100 temps de collision, presque toute l'énergie est dans les électrons froids, (surtout le terme $a_{c0}(t)$) parce que a_{h0} et a_{hm0} sont très petits.

Pendant l'évolution temporelle de la fonction de distribution de Laguerre, les populations chaude et intermédiaire diminuent (c.-à-d $a_{m0}(t)$ et , $a_{h0}(t)$).

Les figures (7) et (8) montrent l'évolution temporelle des coefficients de la fonction de distribution de Laguerre. Tous les coefficients diminuent graduellement durant l'évolution temporelle de la fonction de distribution de Laguerre sauf $a_{c0}(t)$. La décroissance de $a_{h0}(t)$ est particulièrement remarquable.

La Figure (9) montre la déviation des moments de ceux d'une seule maxwellienne. Dans ce cas, comme le rapport initial des températures est petit $\left(\frac{T_c(0)}{T_h(0)} = \frac{1}{1000}\right)$, il faut beaucoup de temps pour que les moments se rapprochent de leur valeur ultime (c.-à-d les moments d'une seule maxwellienne à la température d'équilibre) et après 100 temps de collision la plupart des moment n'ont pas encore fini de relaxer. Pour les moments 2 et 4, ces différences sont toujours minuscules

car ces quantités (densité et énergie) sont conservées (Ces moments correspondent respectivement au nombre total d'électrons et à l'énergie).
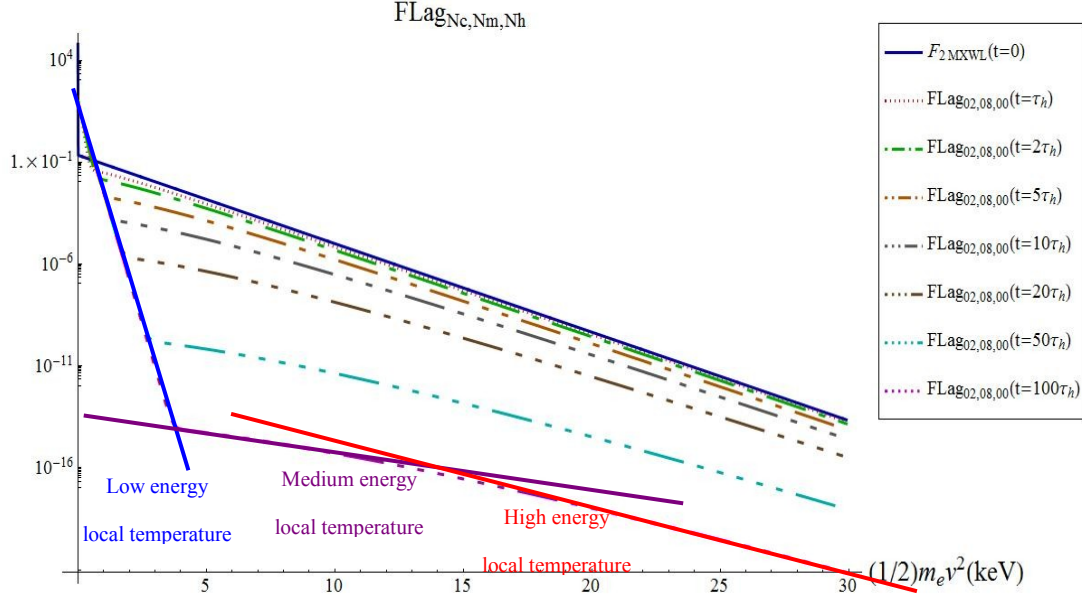
Figure (4): Évolution temporelle de la fonction de distribution de Laguerre à trois températures ($N_c = 02, N_m = 08, N_h = 00, \frac{T_c(t=0)}{T_h(t=0)} = \frac{1}{1000}, \frac{a_{c0}(t=0)}{a_{h0}(t=0)} = 9$).
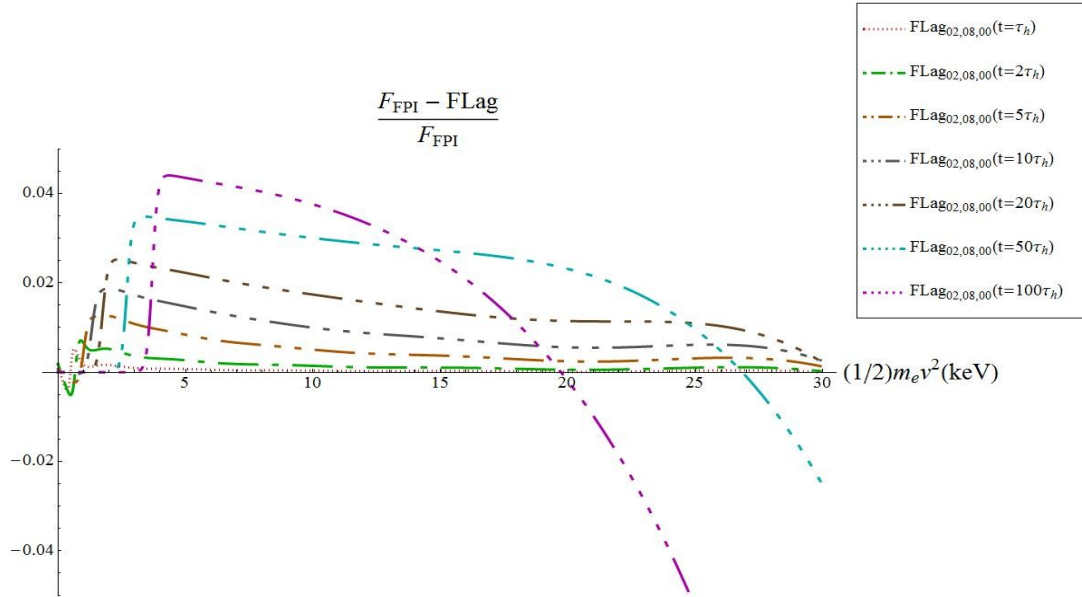
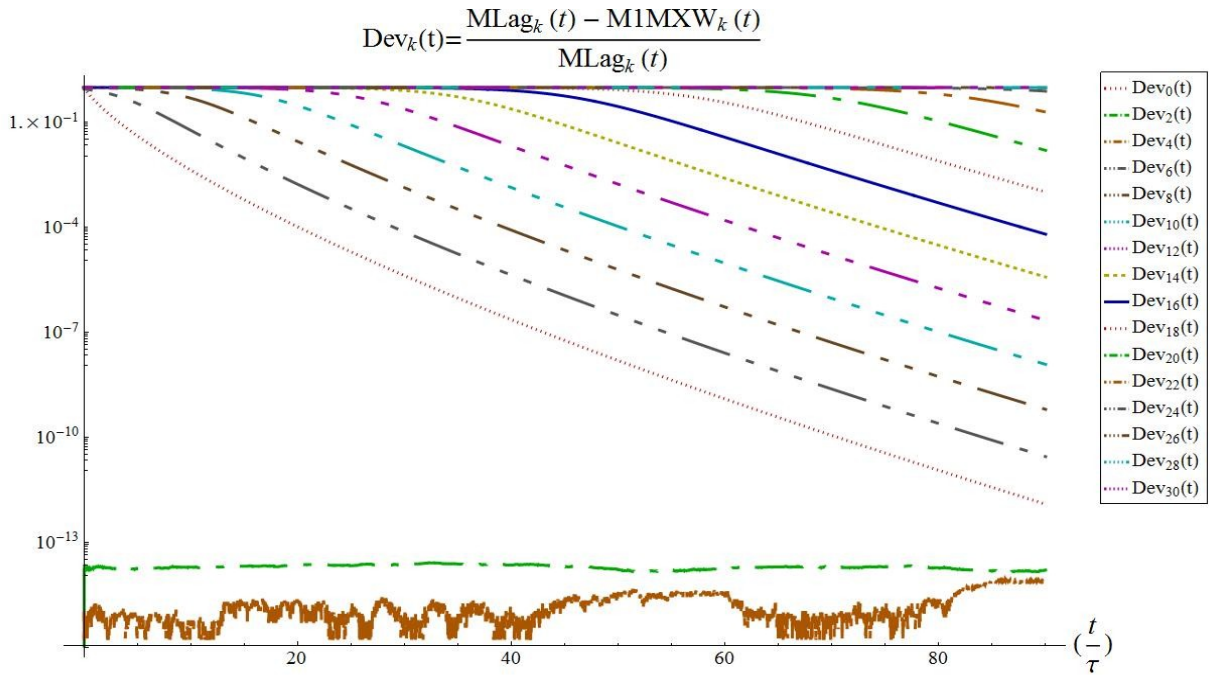Figure (5): Erreur relative sur la fonction de distribution de Laguerre à trois températures ($N_c = 02, N_m = 08, N_h = 00, \frac{T_c(t=0)}{T_h(t=0)} = \frac{1}{1000}, \frac{a_{c0}(t=0)}{a_{h0}(t=0)} = 9$) à différents temps.
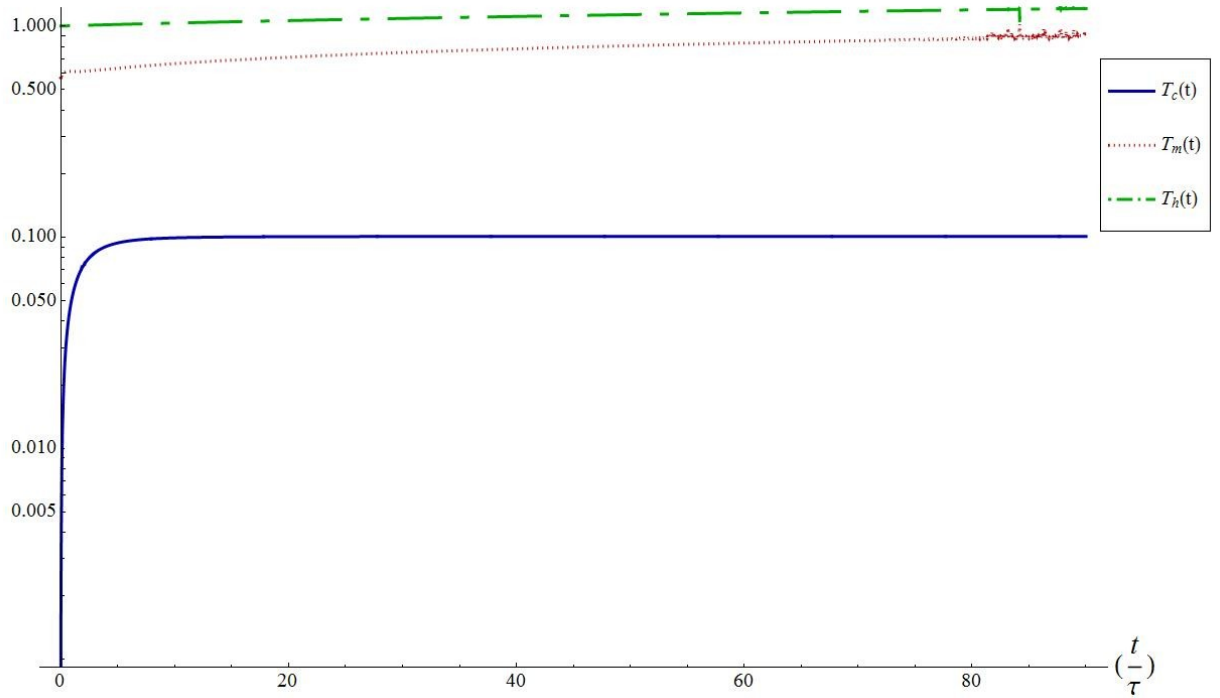
Figure (6): Évolution temporelle des températures de la fonction de distribution de Laguerre $(N_c = 02, N_m = 08, N_h = 00, \frac{T_c(t=0)}{T_h(t=0)} = \frac{1}{1000}, \frac{a_{c0}(t=0)}{a_{h0}(t=0)} = 9)$.
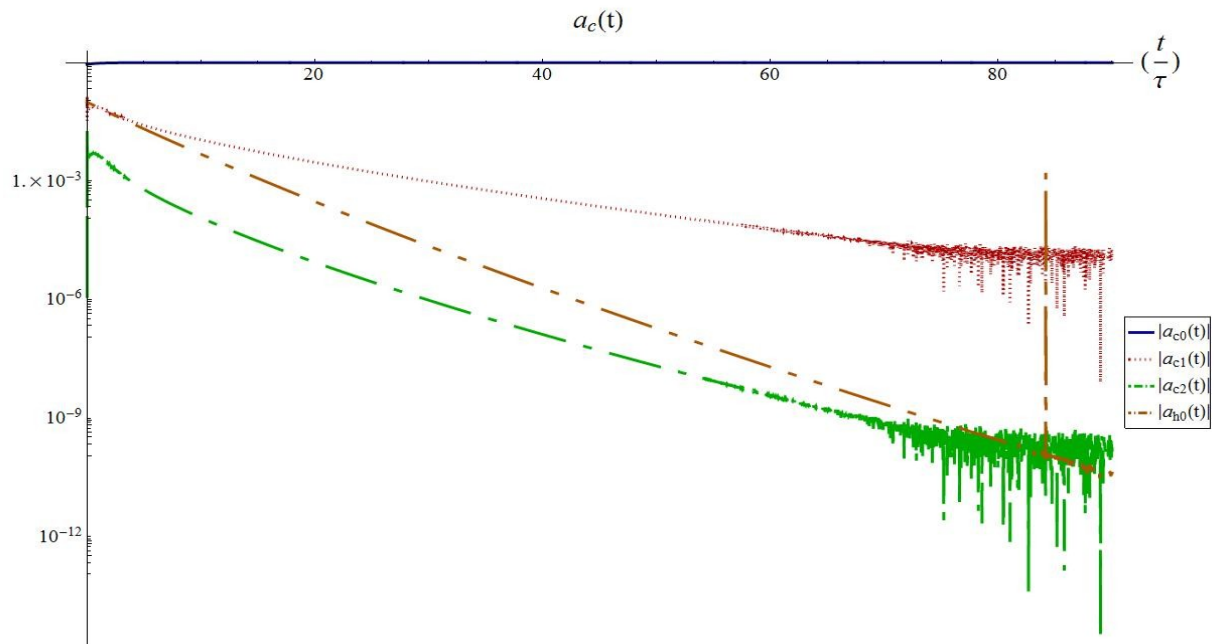
Figure (7): Évolution temporelle des coefficients (chaud et froids) de la fonction de distribution de Laguerre $(N_c = 02, N_m = 08, N_h = 00, \frac{T_c(t=0)}{T_h(t=0)} = \frac{1}{1000}, \frac{a_{c0}(t=0)}{a_{h0}(t=0)} = 9)$.
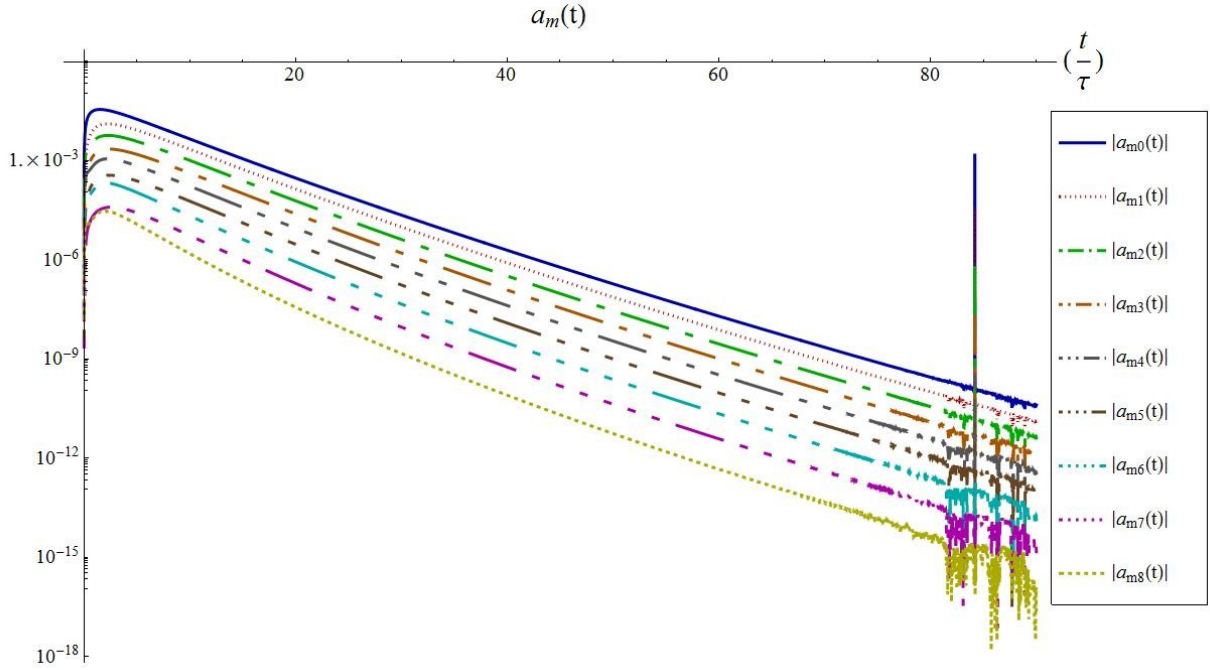
Figure (8): Évolution temporelle des coefficients (intermédiaires) de la fonction de distribution de Laguerre $(N_c = 02, N_m = 08, N_h = 00, \frac{T_c(t=0)}{T_h(t=0)} = \frac{1}{1000}, \frac{a_{c0}(t=0)}{a_{h0}(t=0)} = 9)$.

Figure (9): Évolution temporelle de la déviation des moments de la fonction de distribution de Laguerre des moments d'une seule maxwellienne $(N_c = 02, N_m = 08, N_h = 00, \frac{T_c(t=0)}{T_h(t=0)} = \frac{1}{1000}, \frac{a_{c0}(t=0)}{a_{h0}(t=0)} = 9)$.

Conclusion

L'équation Vlasov-Fokker-Planck décrit les effets d'un champ électro-magnétique et de gradients spatiaux dans le plasma, en utilisant les équations du mouvement et l'équation de continuité ou de conservation dans l'espace de phase. En l'absence de champ magnétique (sauf peut-être le long de l'axe $\hat{x}$) et en supposant une symétrie azimutale le long de l'axe $\hat{x}$ (la direction du champ électrique ou des gradients spatiaux) on peut réduire les 6 dimensions de l'espace de phase pour la fonction de distribution à seulement 3 (x, v, μ). Puis, en développant la dépendance angulaire μ en termes de polynômes de Legendre, on peut réécrire l'équation Vlasov-Fokker-Planck sous la forme (1). Un maillage en x est la meilleure façon de simuler l'évolution temporelle de la fonction de distribution à différentes positions. Mais, il faut d'abord résoudre les termes de collision sur le côté droit de cette équation. Une solution est d'utiliser une autre grille aux différences finies en v, comme dans le code "FPI" [16] et les résultats obtenus avec ce code sont proches des résultats expérimentaux. Même s'il n'y a pas de gradients, la présence de forces implique qu'il faut une grille en vitesses pour les termes de Vlasov correspondants. Le seul problème avec ce code est que les calculs prennent beaucoup de temps, surtout pour les rapports de température élevés, car il faut alors une résolution fine aux basses énergies. Dans ce travail, une nouvelle forme de la fonction de distribution, c.-à-d. la fonction de distribution de Laguerre, est introduite. Nous suggérons de remplacer la grille aux différences finies en v par la fonction de distribution de Laguerre (10). Jusqu'ici, nous avons calculé l'évolution temporelle de la composante isotrope de la fonction de distribution électronique pour les collisions e-e. C'est la partie la plus compliquée de l'équation de Vlasov-Fokker-Planck (toutes les autres parties sont linéaires). Nous avons d'abord montré au chapitre 2 qu'il est possible d'exprimer les fonctions de distribution (c.-à-d. les résultats de l'évolution temporelle de la fonction de distribution calculée par "FPI" pour les collisions e-e) initialisée avec différents rapports de température, avec la fonction de distribution de Laguerre en égalisant les moments des deux fonctions de distribution (section 2.3). Bien sûr, cette méthode est non-triviale et, au-delà d'une certaine énergie, la fonction de distribution de Laguerre ne peut plus exprimer la fonction de distribution. Mais, on peut obtenir un bon fit aux énergies supérieures en ajoutant plus de polynômes de Laguerre et en utilisant plus de températures dans la forme de la fonction de distribution de Laguerre (10). Puis, au chapitre 3 nous avons donné les equations du taux de variation des moments à cause des collisions *e-e* et nous avons aussi décrit un algorithme pour calculer l'évolution temporelle de la fonction de distribution de Laguerre. Nous avons montré, au chapitre 4, que l'évolution temporelle ainsi calculée était en bon accord avec les calculs du code "FPI".

Perspectives

Les prochaines étapes, pour émuler "FPI" seront:

Calculer les composantes non-isotropes de la fonction de distribution (termes $l > 0$ dans le développement en polynômes de Legendre de la dépendance en μ). Un plasma initialement anisotrope relaxera vers l'isotropie par collisions *e-e* et *e-i* (électron-ion).

Calculer la partie Vlasov de l'equation cinétique (c.-à-d. $\left(E \frac{\partial f}{\partial v_x} \right)$ et $\left(v_x \frac{\partial f}{\partial x} \right)$)

Généraliser les calculs à des plasmas de densité et de température inhomogènes.

Table of contents

xxx

List of figures

List of Tables

Introduction

A plasma is a medium in which an important fraction of the atoms is ionized into charged particles known as electrons and ions. This ionization may be due to an imposed electric field or to the very high temperature of the medium. The degree of ionization increases with the temperature, and in very hot plasmas, one has only electrons and nuclei. These charged particles move under the influence of internal and externally imposed electromagnetic fields. The charges inside the plasma move in order to screen out any internal electric fields. Amazingly, 99% of our universe consists of plasma, whereas here on earth, the plasma state is rare compared to the other three well known states of matter (solid, liquid and gaseous).

Very hot and dense plasmas exist in the core of stars (including our own sun), and this makes possible the nuclear fusion reactions which make stars like our sun shine, and hence make life possible on earth. The interstellar medium is a cold and very tenuous plasma, and around our planet, the ionosphere is a cool and tenuous plasma. Other relatively cold plasmas in flames and lightning are some of the most famous plasmas found in nature whereas very hot plasmas produced in experiments on magnetic fusion (Tokamaks [1]) and inertial confinement fusion [2, 3] are examples of hot man-made plasmas, with the aim of creating an abundant and clean energy source.

Nowadays, plasmas have a key role in many laboratory studies and major applications in industry, medicine and for improving the environment. Some of these applications include [4]:

- Materials treatment (etching, deposition, cleaning, surface modification, element analysis);
- Light sources (at visible wavelengths in plasma screens; but hot plasmas can be the source of vuv, xuv (vacuum and extreme ultraviolet) and x-ray radiation;
- Toxic waste treatment;
- Sterilization;
- Spray deposition;
- Chemistry;
- Cutting;
- Laser drilling;

Categorizing the plasma is normally based on three fundamental parameters:

- The temperature T of each species (usually measured in eV (electron-Volt), where $1 eV = 11,605$ K),

- The particle density n (measured in particles per cubic meter or centimetre),
- The steady state magnetic field (measured in Tesla or Gauss).

Other parameters, e.g. Debye length, Larmor radius, plasma frequency, cyclotron frequency and thermal velocity can be derived and calculated from these three main parameters. For partially ionized plasmas, ionization and excitation rates are also important. The spatial and temporal variations of these parameters also affect the plasma properties considerably, especially if gradients are steep or changes are rapid. It is useful to recall that charged particles are not the only components of the plasma. A low temperature plasma usually also contains neutral molecules, atoms and radicals. The density of the neutrals is mostly based on the ratio of the ionization and recombination rates in the plasma. The ionization rate increases and the recombination rate decreases with increasing temperature, and therefore the ratio of the density of the charged particles to the neutrals is higher in a hot plasma than in a cold plasma. One of the significant advantages of using plasmas is the existence of the charged particles. The interactions of these particles with each other and with neutrals inside the plasma produce short-lived radical species carrying significant chemical energy. These species can initiate many types of reactions which could not be provided by any of the other existing thermalization methods, such as simply heating to high temperatures. In this work, we will consider only hot, fully stripped plasmas, but the formalism which we develop could also be applied to charged particles in cooler, partially ionized plasmas.

Due to the many present and future applications of plasmas, and to their importance in nature, it is important to be able to numerically simulate their behaviour and their response to externally imposed fields. This is useful because it complements and guides experiments while analytic theory can usually be applied only in relatively simple or highly idealized cases.

There are two main families of plasma models:

1) Macroscopic models, also called fluid or hydrodynamic models, in which (usually) the profiles of density, average velocity and temperature are computed and advanced in time, using the equations of particle, momentum and energy conservation.

2) Microscopic models, also called kinetic models, in which it is the density of particles in phase space which is advanced in time. There are two main types of kinetic codes:

   a) Particle in Cell (PIC), Monte Carlo (MC) or Molecular Dynamics (MD) codes, in which the equations of motion are solved for a large number of particles, which represent the behaviour of real plasma particles.

b) Kinetic codes in which the phase space density is advanced in time directly on a finite difference grid.   In many such codes, the velocity dependence is simplified by an expansion of the angular dependence in spherical harmonics.

The present work aims to improve the performance of such kinetic codes by an appropriate expansion of the energy dependence, to replace the grid in energy or (v). In the general Boltzmann kinetic equation, the colision term (between the particles) is obtained by simply assuming binary collisions and a lack of correlations between particles before the collision [5]. However, for elastic collisions between charged particles in plasmas, it is approximated by the Fokker-Planck equation [6, 7].

In kinetic simulations, the fluid quantities can be obtained by integrating the distribution function over velocity space, multiplied by (1), (mv_i), $\left(\frac{mv^2}{2}\right)$ for the particle, momentum (component i) and energy densities respectively. These are the zeroth, first and second order moments of the distribution function. The conservation equations are obtained by taking the corresponding moments of the kinetic equation.

While fluid simulations are the most widely used, because of their simplicity and much lower computer time and memory use, there are many cases in which they are not correct, or do not provide enough information, as the density, momentum density and temperature do not fully describe a plasma: The rates of ionization and excitation, for example, demand an integration on the part of the velocity distribution function above the threshold energy, and taking into account the energy dependence of the cross section. It is usual to assume, in such codes, that the distribution function is Maxwellian, as this is the equilibrium solution of the Boltzmann or Fokker-Planck equations. Furthermore, even in fluid simulations, one needs the heat flux, to update the energy equation, which is a higher order moment of the distribution function. The calculation of the current in a plasma, due to an electric field, is another example of a quantity which is not immediately obtained by fluid calculations.

For the electrical and thermal conductivity, Spitzer and Härm [8] have obtained solutions by assuming that the field and the temperature gradient are relatively weak, and a perturbation solution (with a Maxwellian as the zeroth order description) of the Fokker-Planck kinetic equation was found. Similarly, the absorption of a plasma heated by a low intensity laser beam was obtained by Dawson and Oberman, and Johnston and Dawson [9-11]. However, when fields are strong or gradients are steep, such perturbation calculations are no longer valid, and the energy distribution function may no longer be assumed to be a simple Maxwellian. In laser heated plasmas, at higher but moderate intensities (where the oscillation energy of the electrons in the laser field is lower than the local temperature, but high enough so that the heating is faster than

the relaxation towards a maxwellian by e-e collisions), the velocity distribution takes a super-Gaussian form, which is distinctly non-Maxwellian [12, 13]; however, we will not address this aspect further in this work. On the other hand, when the intensity is very high, and especially for short pulses, a minority of electrons are heated to very high temperatures, but with an approximately Maxwellian distribution [14]. Of course, these energetic electrons interact with the local thermal electrons, and they also stream into the unheated plasma.

In steep temperature gradients, faster electrons stream into the cold plasma, so that in the cold regions, there is a cold Maxwellian and a minority population of hotter ones, at a temperature close to that of the hot region [15, 16]. This also implies that there is preheat, *i.e.* the energy density profile is not concave all the way down to the cold region with an abrupt discontinuity of the slope there, as predicted by classical heat diffusion theory, but there is a region where it is convex, and decreases smoothly to the cold temperature, due to the effect of these faster electrons which gradually lose their energy in this region [17, 18].

Even in some other cases where there is no laser plasma interaction, some researchers have shown that steep temperature gradients and non-Maxwellian distributions exist, *e.g.* in plasmas created in the divertor chamber of a tokamak [1]. These experiments also show the necessity of studying non-Maxwellian plasmas.

The problem of describing electron heat flow in steep temperature gradients with fluid codes was shown to be solvable with nonlocal heat flow formulas which consist of spatial convolutions over the classical (Spiter-Härm) heat flux. There has been very considerable theoretical and numerical work on this topic [17, 19-30], and it was reviewed in Refs. [18, 31, 32]. Comparisons of fluid simulations using such formulas for the electron heat flux with Fokker-Planck kinetic simulations were done [33, 34], as well as comparisons with experiments [35, 36], but it seems that no single formula is satisfactory for all cases. Furthermore, these do not address the issue of the non-Maxwellian shape of the energy distribution function, which can affect the rates of ionization and excitation, and hence the x-ray line spectrum [37]. Therefore, it is clearly desirable to devise an alternative formulation of the kinetic model which could run with a reduced computer time, compared to full finite difference Fokker-Planck codes, and the present work aims to contribute to this goal.

The use of generalized Laguerre (or Sonine) polynomials in kinetic theory is not new. For gases, they were used to compute fluxes *etc.* from perturbation analyses, for small gradients or under moderate external forces, assuming that the isotropic component velocity distribution function (or its angle averaged value at each given energy) is a Maxwellian, in the well known Chapman-Enskog method [38]. This method was adapted for plasmas by Spitzer and Härm [8].

More recently, they were used by Abe for the isotropic component of the distribution function for a uniform gas, by assuming that it was a Maxwellian energy distribution function multiplied by a finite series of generalized Laguerre polynomials [39]. The relaxation of an initially non-Maxwellian plasma was simulated with the Fokker-Planck equation (which we will describe in Chapter 1) by Abe and Ushimi **[40]** and by Khabibrakhmanov and Summers [41] by using such an expansion. More recently, it has been used by Held *et al*. to simulate nonlocal heat flow in a hot Tokamak core plasma, where temperature differences are modest, but the mean free path is extremely long (contrary to the divertor plasma) **[42-48]**. This nonlocal prescription was implemented in the Tokamak fluid simulation code "NIMROD" **[49-52]**. This technique, however, is applicable only to the distribution functions that deviate slightly from a single Maxwellian or two-Maxwellian distribution with a close to 1 temperature ratios. This is easily seen if, for example, we try to expand a Maxwellian in terms of such an expansion around a Maxwellian at another temperature [53] (equation 22.9.15): The series diverges or needs an impractically large number of terms, unless the two temperatures are close, as will be shown in section 2.4. This is why we have extended the technique to using two or three Maxwellians of different temperatures, each multiplied by such a series of generalized polynomials. These polynomials have two useful properties for our purpose. First, orthogonality relations which simplifiy calculating the moment equations (2-9); *i.e.* thanks to orthogonality, M_2 (density) depends only on the first Laguerre term, M_4 (energy density) depends only on the first two Laguerre terms and so on. Second, the adjustable parameter α is useful for expressing the expansion of the angular dependency of the distribution function in Legendre polynomials (1-15) and (1-7). We will see that this allows the description of the collisional interaction of hot and cold populations with very high temperature ratios.

In this work, we study the effect of the non-Maxwellian distribution function by calculating the time evolution of the distribution function.

We assume there are no spatial gradients, nor any applied electric field, and that the velocity distribution function is isotropic. Thus, only the electron-electron collisions, affecting the isotropic part of the velocity distribution will be treated here, as this is the most complicated part of the Vlasov-Fokker-Planck equation (explained in chapter 1), due to its nonlinear character. The problem which we solve in this work is the relaxation of a plasma which consists, initially, of a mixture of a cold and a hot plasma. Then we introduce generalized Laguerre polynomials and finally, we define the new form for the electron distribution function using these polynomials.

We have developed a code to calculate the time evolution of the isotropic component of the electron distribution function due to electron-electron collisions. We propose a finite sum of generalized Laguerre polynomials multiplied by one, two or three Maxwellians (in higher temperature ratios, three different temperatures are used) to represent the electron velocity distribution function. The results of the time evolution of the distribution function are compared with the results obtained from the finite difference code "FPI" (Fokker Planck international) code developed by Matte *et al.* **[**13, 16, 28, 34, 37, 54-58**]** and very briefly described in chapter 1. Good agreement is obtained.

This thesis is divided in 5 chapters:

Chapter 1: Vlasov-Fokker-Planck equation.

In this chapter, the Vlasov-Fokker-Planck equation (this equation is derived from the Boltzmann equation) is described explicitly. It is the main equation of the present work. It governs the time evolution of the distribution function. This equation consists of two parts; first, the Vlasov part of the equation which describes the effects of spatial gradients and of the electric field on the distribution function. By assuming azimuthal symmetry along one axis in space and the absence of the magnetic field (except, possibly, along the spatial gradients and the electric field), the first part of the equation can be simplified and the pitch angle dependence of the velocity distribution function can be expanded in Legendre polynomials which hugely reduces the size of the computations. The second part describes the effect of electron-electron *e-e* collisions, and the present work will concentrate on this.

Chapter 2: Generalized Laguerre polynomials expansion fits to "FPI" distribution functions:

Using the moments calculated numerically (*i.e.* integrals of the distribution function multiplied by different powers of the velocity) from the results obtained from the "FPI" code, a technique is provided to compute the temperatures and the coefficients of the generalized Laguerre polynomials to approximate the distribution function, and a technical part of the algorithm is explained in appendix A. Then we compare some of the results (velocity distribution functions) as proof of the validity of this expansion, and to see how many temperatures and generalized Laguerre polynomial terms for each are required, and how this depends on the ratio of the hot to the cold initial temperatures.

Chapter 3: Time evolution of the distribution function.

We introduce an algorithm for calculating the time evolution of the distribution function. It consists in calculating the *e-e* collision operator, for a distribution function written in this

Laguerre form, and hence the rates of change of the moments for the isotropic component of the electron velocity distribution function, as a means for advancing the temperatures and the coefficients of the generalized Laguerre polynomials in time. The derivations of the formulas used are explained in more detail in appendices B and C.

Chapter 4: Numerical results for the time evolution of the distribution function

For several cases *i.e.* different initial temperature and density ratios, we compute the time evolution of the Laguerre distribution function obtained with the moments method described in chapter 3, and for each case, we compare to the results obtained from the "FPI" finite difference electron kinetic code, for the same initial conditions.

Conclusion and future work

We summarize and conclude the work, and explain briefly what would remain to be done to develop a code capable of advancing the distribution function in time in the presence of electric fields and spatial gradients.

Chapter 1

Vlasov-Fokker-Planck equation

1.1. **Vlasov-Fokker-Planck equation:**

In 1917, Planck published a paper [59] where he explained and gave a proof of an equation which plays an important role in the statistical description of many body problems. Using the results of the work of Einstein [60] and Fokker [61] as references he represented the Einstein-Fokker equation which is now known as the Fokker-Planck equation to describe collisions in the approximation that each collision weakly deflects the particles.

This equation has many applications in many different fields. One of these applications is the physics of fully ionised plasmas, which is the interest of the present work.

1.1.1. **The Fokker-Planck collision term in plasmas**

In plasma physics the most important application of the Fokker-Planck equation is describing the effect of Coulomb interactions between the particles (*i.e.* collisions) on the evolution of the plasma. The application of this equation is for cases where we have ideal plasma, with many particles in the so-called Debye sphere.

An equivalent criterion to determine whether plasma is ideal is that the Coulomb logarithm $\ln\Lambda \gg 1$. For example, in the present work, we suggest choosing $\ln\Lambda > 10$, and apply the definition of the Coloumb Logarithm for e-e collisions in Ref. [69]:

$$\ln\Lambda = 23 - \ln\left(n_e^{\frac{1}{2}} T_e^{-\frac{3}{2}} \right), \qquad T_e < 10\ eV$$

$$= 24 - \ln\left(n_e^{\frac{1}{2}} T_e^{-1} \right), \qquad T_e \geq 10\ eV$$

As a result, to have an ideal plasma, the density must not be higher than the following temperature dependent limit:

$$\frac{n}{T^3} \leq \exp(26) \simeq 1.96 \times 10^{11} \text{cm}^{-3} \text{eV}^{-3}, \qquad T_e < 10\ eV$$

$$\frac{n}{T^2} \leq \exp(28) \simeq 1.45 \times 10^{12} \text{cm}^{-3} \text{eV}^{-2}, \qquad T_e \geq 10\ eV$$

In such situations, small angle collisions can be assumed to dominate (which has been shown to be a good approximation [7]) and we can use the Fokker-Planck equation to simulate collisions. The derivation of the Fokker-Planck equation for Coulomb collisions was first presented by Landau [62].

A system with two particles species is assumed and f_1 and f_2 are defined to be the distribution functions or densities of species 1 and 2 in 6 dimension phase space (*i.e.* $(\boldsymbol{x}, \boldsymbol{v})$) at any given time.

$$\frac{\partial f_1(\boldsymbol{v_1}, t)}{\partial t} = \frac{2\pi\, e_1^2\, e_2^2 \ln \Lambda}{m_1} \frac{\partial}{\partial \boldsymbol{v_1}} \int d^3\boldsymbol{v_2} \left(\frac{g^2\, \bar{\mathbf{I}} - \boldsymbol{g}\boldsymbol{g}}{g^3}\right) \cdot \left[\frac{f_2(\boldsymbol{v_2}, t) \partial f_1(\boldsymbol{v_1}, t)}{m_1\, \partial \boldsymbol{v_1}} - \frac{f_1(\boldsymbol{v_1}, t) \partial f_2(\boldsymbol{v_2}, t)}{m_2\, \partial \boldsymbol{v_2}}\right] \qquad (1\text{-}1)$$

Where, g is the relative velocity $g = v_1 - v_2$, $\mathbf{I}$ is the unit tensor, and e_1 and e_2 are the electrical charges of particles of type 1 and 2 respectively.

This is the Fokker-Planck collision operator in Landau form. (1-1) is the collision term for particles of species 1 (distribution function $f_1(\boldsymbol{v_1}, t)$) colliding with all the particles of species 2 (distribution function $f_2(\boldsymbol{v_2}, t)$). Thus, for electron-ion (*e-i*) collisions, $f_1(\boldsymbol{v_1}, t)$ is the electron velocity distribution function and $f_2(\boldsymbol{v_2}, t)$ is the ion velocity distribution function, while for electron-electron *e-e* collisions, they both represent the electron velocity distribution function. The collision operator is a local operator so all distribution functions mentioned in Eq. 10 are at the same position in space $\boldsymbol{x}$. This is why we have dropped the dependence on $\boldsymbol{x}$ in (1-1), but it is implicitly understood.

1.1.2. The Vlasov-Fokker-Planck equation and the Legendre polynomial expansion

In order to describe the effect of an electro-magnetic field and spatial gradients inside the plasma, using the equations of motion and considering the continuity equation in phase space, one can write the Vlasov-Fokker-Planck equation as follows:

$$\frac{\partial f(x,v,t)}{\partial t} + \boldsymbol{v} \cdot \frac{\partial f(x,v,t)}{\partial x} + \frac{e}{m}\left[\boldsymbol{E} + \frac{\boldsymbol{v} \times \boldsymbol{B}}{c}\right] \cdot \frac{\partial f(x,v,t)}{\partial v} = \left(\frac{\partial f(x,v,t)}{\partial t}\right)_{e-e} + \left(\frac{\partial f(x,v,t)}{\partial t}\right)_{e-i} \qquad (1\text{-}2)$$

On the right hand side of the equation we have the collision operator (electron-electron and electron-ion collisions) described by equation (1-1) and it can be calculated for any position in space, and, on the left hand side, the effects of the electro-magnetic fields (externally imposed and self-consistent) and spatial gradients on the evolution of the velocity distribution of the particles is described by the Vlasov equation, which is the continuity equation in phase space.

If we assume that the spatial variation is in 1 dimension, along $\hat{\boldsymbol{x}}$, and that the velocity distribution has azimutal symmetry about the $\hat{\boldsymbol{x}}$ axis, we can express the distribution function in 3 dimensions (i.e. 1 dimension in x and 2 dimensions in v), *i.e.* $f(\boldsymbol{x}, \boldsymbol{v}, t)$ can be expressed as $f(x, v, \mu, t)$:

$$f(\boldsymbol{x}, \boldsymbol{v}, t) \rightarrow f(x, v, \mu, t) \tag{1-3}$$

where,

$$v = \sqrt{v_x^2 + v_y^2 + v_z^2}\ ; \quad \mu = v_x/v \tag{1-4}$$

We may then expand the angular μ dependence in Legendre polynomials,

$$f(x, v, \mu, t) = \sum_{l=0}^{N_P} f_l(x, v, t) P_l(\mu) \tag{1-5}$$

where,

$$f_l(x, v, t) = \frac{2}{2l+1} \int_{-1}^{1} f(x, v, \mu, t) P_l(\mu) d\mu \tag{1-6}$$

The first Legendre polynomials are:

$P_0(\mu) = 1$; $P_1(\mu) = \mu$; $P_2(\mu) = 1/2(3\mu^2 - 1)$; *etc.*

$f_0(v)$ is the isotropic component of the velocity distribution or its angle averaged value.

Considering (1-3) through (1-6) we can write (1-2) as (1-7) (assuming there is no magnetic field, except possibly along $\hat{x}$):

$$\frac{\partial}{\partial t} f_l(x, v, t) + v \left[\frac{l}{2l-1} \frac{\partial f_{l-1}}{\partial x} + \frac{l+1}{2l+3} \frac{\partial f_{l+1}}{\partial x} \right] -$$

$$\frac{eE}{m_e} \left[\frac{l}{2l-1} v^{l-1} \frac{\partial}{\partial v} \left(\frac{f_{l-1}}{v^{l-1}} \right) + \frac{l+1}{2l+3} \frac{1}{v^{l+2}} \frac{\partial}{\partial v} \left(v^{l+2} f_{l+1} \right) \right] = \left(\frac{\partial f_l}{\partial t} \right)_{e-i} + \left(\frac{\partial f_l}{\partial t} \right)_{e-e} \tag{1-7}$$

On the right hand side of the (1-7) we have the $e-i$ and $e-e$ collision terms (electron-ion and electron-electron collision term respectively). One could derive (1-8) and (1-9) from the Fokker-Planck collision term (1-1):

$$\left(\frac{\partial f_l}{\partial t} \right)_{e-i} = -\frac{l(l+1)}{2} \frac{4\pi Z^2 n_i e^4 Ln\Lambda}{m_e^2 v^3} f_l \tag{1-8}$$

$$\left(\frac{\partial f_l}{\partial t} \right)_{e-e} = \frac{1}{v^2} \frac{\partial}{\partial v} \left[v^2 \left(D_{\parallel-0}(v) \frac{\partial f_l}{\partial v} + C_0(v) f_l \right) \right] - \frac{l(l+2)}{2v^2} D_{\perp-0}(v) f_l \tag{1-9}$$

In the $e-i$ collision term we assume the ions to be immobile while they collide with electrons, due to the very large mass of the ions compared to the electrons. Thus, Eq.(1-8) depends linearly on the electron distribution function. On the other hand, the $e-e$ collision term is highly nonlinear and is the most complicated term in the Vlasov-Fokker-Planck electron kinetic equation and is provided in (1-9). Here $D_{\perp-0}(v)$ is the perpendicular diffusion coefficient due to e-e collisions while $D_{\parallel-0}(v)$ and $C_0(v)$ are the diffusion and friction coefficients of the collision operator, respectively, and can be calculated by integrating on the isotropic part of the distribution function:

$$C_0(v) = \frac{4\pi\alpha}{v^2} \int_0^v u^2 f_0(u) \, du \tag{1-10}$$

$$D_{\parallel-0}(v) = \frac{8\pi\alpha}{3} \left(\int_v^\infty u f_0(u) \, du + \left(\frac{1}{v^3} \right) \int_0^v u^4 f_0(u) \, du \right) \tag{1-11}$$

$$D_{\perp-0}(v) = \frac{4\pi\alpha}{3} \left(2 \int_v^\infty u f_0(u) \, du + \left(\frac{3}{v} \right) \int_0^v u^2 f_0(u) \, du \right) \tag{1-12}$$

$$\alpha = \frac{4\pi e^4 Ln(\Lambda)}{m_e^4} \text{ (cgs)} \tag{1-13}$$

In these expressions, e is electron charge, m_e is electron mass and $Ln(\Lambda)$ is the Coulomb logarithm. Here, we have used the (cgs) system of units.

It is important to note that equations (1-10) through (1-13) are an approximation, often called the "spherical Rosenbluth potentials approximation", and it amounts to taking into account only the angle averaged term in the representation of the target electrons (the $f_2(v_2)$ in (1-1)); in other words, the "target" electrons are assumed to have an isotropic distribution function. This approximation is often used because the inclusion of the anisotropic terms makes the calculation much more complicated [63]. Of course, it is exact in the cases where the distribution function is isotropic.

1.1.3. The generalized Laguerre electron distribution function

In electron kinetic codes, the velocity distribution function is represented on a grid in velocity space. Expanding the angular dependence in Legendre polynomials has greatly reduced the computation time and memory requirements, but the energy grid is still a burden, in codes such as the electron kinetic code "FPI" which solves Equations (1-7) through (1-13) on finite difference grids in both x and v. Here, we propose to represent the energy dependence as a sum of two-Maxwellian (in high temperature ratios, 3 Maxwellians), each multiplied by a finite sum of generalized Laguerre polynomials, to represent the interaction of hot and cold electrons. This occurs when, for example, energetic electrons stream from a hot plasma into a cold plasma. The electron distribution function would thus read, with the temperatures and coefficients dependent on time and space:

$$f_l(x,v,t) = \sum_\eta \left(\frac{m_e}{2\pi k_B T_\eta(x,t)}\right)^{\frac{3}{2}} \exp\left\{-\frac{m_e v^2}{2k_B T_\eta(x,t)}\right\} \sum_{j=0}^{N_{\eta l}} a_{\eta l j}(x,t) \, L_j^{(\alpha_l)}\left(\frac{m_e v^2}{2k_B T_\eta(x,t)}\right) \quad (1\text{-}14)$$

All units are in cgs. The $a_{\eta l j}(x,t)$'s are in density units cm^{-3}.

where,

$$\alpha_l = l + \frac{1}{2}$$

(Note: These α_l's must not be confused with the value of α defined by equation (1-13).)

$l = 0$ represents the isotropic component of the distribution function. We have $\alpha_0 = \frac{1}{2}$.

This choice of the values of the α_l's is the usual one, and it makes these polynomials more convenient because for the lowest moment of greatest interest for each l (density for l=0, flux for l=1, traceless pressure tensor for l=2), only the coefficient of the 0th order generalized Laguerre polynomials j=0 contributes; and for the next moments (energy density for l=0 and energy flux for l=1), only the first two terms contribute, and so on.

The index η = c (cold), m (medium), h (hot) denotes different temperatures used to represent the distribution function. When the initial temperature ratio is close to 1, a single Maxwellian

multiplied by a sum of generalized polynomials with a reasonable number of Laguerre terms (less than 20 terms) can be sufficient to fit the actual distribution function with an acceptable accuracy.

The generalized Laguerre polynomials are defined as (see ref. [53] equation 22.3.9):

$$L_n^{(\alpha)}(x) = \sum_{i=0}^{n} \frac{(-1)^i}{i!} \binom{n+\alpha}{n-i} x^i \tag{1-15}$$

where $\binom{\alpha}{n} = \frac{\alpha(\alpha-1)...(\alpha-n+1)}{n!}, \quad \alpha \in \mathbb{R}, n \in \mathbb{Z}^+$ (1-16)

is the generalized Binomial (see ref. [64] section "y = m" in page 6 and [65] section: "Generalization and connection to the binomial series").

In the particular case of a positive α:

$$\binom{\alpha}{n} = \frac{\Gamma(\alpha+1)}{\Gamma(n+1)\Gamma(\alpha-n+1)}, \quad \alpha \in \mathbb{R}^+, n \in \mathbb{Z}^+ \tag{1-17}$$

And for a negative α:

$$\binom{\alpha}{n} = (-1)^n \frac{\Gamma(-\alpha+n)}{\Gamma(n+1)\Gamma(-\alpha)}, \quad \alpha \in \mathbb{R}^-, n \in \mathbb{Z}^+ \tag{1-18}$$

where, $\Gamma(\alpha)$ is the Gamma function.

In the present "FPI" electron kinetic code, the $f_l(x,v,t)$'s are advanced in time, using finite difference grids in x and v. The ultimate aim of our project is to replace the grid in v by two or three Maxwellians, each multiplied by a sum of generalized Laguerre polynomials, on each point of the spatial grid, as expressed in equation (1-14), for the components of the distribution function. In the present work, we simulate the collisional relaxation of hot and cold electrons in a uniform and isotropic plasma, and therefore only the isotropic component *l*=0 will be considered (equation (1-9) with *l*=0, with the friction and parallel diffusion coefficients given by equations (1-10) and (1-11)). This may be considered as a first step in the elaboration of a full kinetic code.

Chapter 2

Generalized Laguerre polynomials expansion fits to "FPI" distribution functions

In order to study the time evolution of the distribution function due to $e - e$ collisions, we need to start with an initial distribution function, and in this work we always use the sum of two Maxwellians as the initial distribution function where T_c and T_h denote the temperatures of the cold and hot Maxwellians respectively. At each time step, this distribution function evolves under the effect of the $e - e$ collisions. We use the "FPI" distribution function at any given time step as our reference.

In this chapter, we first define different forms of the Laguerre distribution function, then we describe the moment equations and also, we explain the fitting method that we use to calculate the Laguerre distribution function for any given set of moments at any timestep *i.e.* obtained from "FPI" distribution function or the result of the time evolution of the distribution function calculated by using the previous time step. Finally, we compare some results obtained from the "FPI" distribution function at different timesteps and for different initial temperature ratios to our calculated (fitted) Laguerre distribution function. This will give us a verification of the viability and validity of the expansion and give us some guidance as to the number of required terms, when we will directly compute the time evolution with this expansion, without using finite differences in v in Chapter 4.

In chapter 1, we introduced (1-14)) as the Laguerre expansion of the distribution function. As the distribution function is assumed to be isotropic, we have only the $l = 0$ terms in the Legendre expansion, and thus, we obtain:

$$f(v,t) = \sum_\eta \left(\frac{m_e}{2\pi k_B T_\eta(t)}\right)^{\frac{3}{2}} \exp\left\{-\frac{m_e v^2}{2k_B T_\eta(t)}\right\} \sum_{j=0}^{N_\eta} a_{\eta j}(t) L_j^{\left(\frac{1}{2}\right)}\left(\frac{m_e v^2}{2k_B T_\eta(t)}\right) \qquad (2\text{-}1)$$

Notes:

In the rest of this thesis, we will drop the dependence on x, as the spatial dependence will not be included in our work, since we consider a uniform plasma. We will also drop the "l" index, as only the isotropic component $l = 0$ will be treated here.

To shorten the text, we will use: "Laguerre distribution function" instead of "the isotropic electron distribution function represented as 1, 2 or 3 Maxwellians, each multiplied by a finite series of generalized Laguerre polynomials", and "FPI distribution function" instead of "isotropic electron distribution function result of the time evolution of the distribution function due to electron-electron collisions computed by the "FPI" finite difference electron kinetic code".

2.1. **Different forms of the Laguerre distribution function**

In this context we now define 5 different forms of the Laguerre distribution function:

2.1.1. Single Maxwellian distribution function (thermal equilibrium)

In (2-1) by deleting the summations over (η) and (j) $N_\eta = 0$ we have a single Maxwellian:

$$f_{\{0\}}(v,t) = a_0(t)\left(\frac{m_e}{2\pi k_B T(t)}\right)^{\frac{3}{2}} \exp\left\{-\frac{m_e v^2}{2k_B T(t)}\right\} \tag{2-2}$$

2.1.2. Single temperature distribution function (non-Maxwellian but modest deviation from thermal equilibrium)

Here we delete the summation over η, but keep a summation over j:

$$f_{\{N_c\}}(v,t) = \left(\frac{m_e}{2\pi k_B T(t)}\right)^{\frac{3}{2}} \exp\left\{-\frac{m_e v^2}{2k_B T(t)}\right\} \sum_{j=0}^{N_c} a_j(t) L_j^{\left(\frac{1}{2}\right)}\left(\frac{m_e v^2}{2k_B T(t)}\right) \tag{2-3}$$

2.1.3. Two-Maxwellian distribution function (non-Maxwellian)

Here, we keep the summation over η, but delete the summation over j:

$\eta = c, h$ and $N_\eta = 0$,

$$f_{\{0,0\}}(v,t) = \sum_{\eta=c,h} a_{\eta 0}(t)\left(\frac{m_e}{2\pi k_B T_\eta(t)}\right)^{\frac{3}{2}} \exp\left\{-\frac{m_e v^2}{2k_B T_\eta(t)}\right\} \tag{2-4}$$

For all the simulations presented in this work, the initial distribution function (at *t*=0) is of this form.

2.1.4. Laguerre electron distribution function with two temperatures (non-Maxwellian)

Here, we keep the summations over η, and j:

$$f_{\{N_c,N_h\}}(v,t) = \sum_{\eta=c,h}\left(\frac{m_e}{2\pi k_B T_\eta(t)}\right)^{\frac{3}{2}} \exp\left\{-\frac{m_e v^2}{2k_B T_\eta(t)}\right\} \sum_{j=0}^{N_\eta} a_{\eta j}(t) L_j^{\left(\frac{1}{2}\right)}\left(\frac{m_e v^2}{2k_B T_\eta(t)}\right) \tag{2-5}$$

2.1.5. Laguerre electron distribution function with three temperatures (non-Maxwellian)

We add an intermediate temperature $\eta = m$, to better represent the intermediate energy electrons

$\eta = c, m, h$ and $N_\eta \neq 0$,

$$f_{\{N_c,N_m,N_h\}}(v,t) = \sum_{\eta=c,m,h} \left(\frac{m_e}{2\pi k_B T_\eta(t)}\right)^{\frac{3}{2}} \exp\left\{-\frac{m_e v^2}{2k_B T_\eta(t)}\right\} \sum_{j=0}^{N_\eta} a_{\eta j}(t) L_j^{\left(\frac{1}{2}\right)}\left(\frac{m_e v^2}{2k_B T_\eta(t)}\right) \quad (2\text{-}6)$$

2.2. Moments of the Laguerre distribution function.

Moments are powerful instruments to obtain overall information about the distribution function by integrating the distribution function on the energy variable. Moment k corresponds to the density multiplied by the average value of velocity to the power $(k-2)$:

$$M_k(t) = n_e < v^{k-2} > (t) = 4\pi \int_0^\infty f(v,t) v^k \, dv \qquad (2\text{-}7)$$

Here, n_e is the total density, k is the number of the moment and $<>$ denotes an average over the distribution function. It may be noted that if $f(v)$ is a Maxwellian of temperature T, the maximum of the integrand in equation (2-7) is at energy $kT/2$. Thus, higher moments sample higher energy regions of the distribution function. Now, we calculate the moments of the Laguerre distribution function. Eq. (2-1) showed the general form of the Laguerre distribution function. Henceforth, it will be written in a more convenient form:

$$F_{\{N_c,N_m,N_h\}}(v,t) = \frac{4}{\sqrt{\pi}} \sum_\eta T_\eta(t)^{-\frac{3}{2}} \exp\left(-\frac{v^2}{T_\eta(t)}\right) \sum_{i=0}^{N_\eta} a_{\eta i}(t) L_i^{\left(\frac{1}{2}\right)}\left(\frac{v^2}{T_\eta(t)}\right) \qquad (2\text{-}8)$$

Here, we scale $T_\eta(t)$ in keV and v^2 in 2 keV/m_e and also we scale $a_{\eta j}(t)$ in such a way that unit density or $a_{\eta 0}(t) = 1$ (see (2-10)), corresponds to 10^{21} cm^{-3}. For convenience, the factor 4π is dropped, *i.e.* it is assumed to be already included in F.

Considering the 2nd equation in section "Orthogonality" of ref. [66], we can write the moments equations for the Laguerre distribution function:

$$M_{\{N_c,N_m,N_h\},k} = \frac{2}{\sqrt{\pi}} \sum_\eta T_\eta(t)^{\left(\frac{k}{2}-1\right)} \sum_{i=0}^{N_\eta} \binom{-\frac{k}{2}+i}{i} a_{\eta i}(t) \, \Gamma\left(\frac{k+1}{2}\right) \qquad (2\text{-}9)$$

Note:

$M_{\{N_c,N_m,N_h\},2}$ depends only on terms $i = 0$

$$M_{\{N_c,N_m,N_h\},2} = \sum_\eta a_{\eta 0}(t) = N_e \text{ (total density)} \qquad (2\text{-}10)$$

And $M_{\{N_c,N_m,N_h\},4}$ depends only on terms $i = 0,1$;

$$M_{\{N_c,N_m,N_h\},4} = \frac{3}{2} \sum_\eta T_\eta(t)(a_{\eta 0}(t) - a_{\eta 1}(t)) = \frac{3}{2} N_e T_e = \epsilon \text{ (total energy density)} \quad (2\text{-}11)$$

And generally, moment $M_{\{N_c,N_m,N_h\},2m+2}$ depends only on terms i=0,1,2,…,m

$$M_{\{N_c,N_m,N_h\},2m+2} = \frac{2}{\sqrt{\pi}} \sum_\eta T_\eta(t)^m \sum_{i=0}^m \binom{-m-1+i}{i} a_{\eta i}(t) \, \Gamma\left(m+\frac{3}{2}\right) \qquad (2\text{-}12)$$

However, $M_{\{N_c,N_m,N_h\},0}$ depends on all of the terms i=0,1,2,...,N$_\eta$.

$$M_{\{N_c,N_m,N_h\},0} = \sum_\eta \frac{2}{T_\eta(t)} \sum_{i=0}^{N_\eta} a_{\eta i}(t) \qquad (2\text{-}13)$$

To simplify the numerical solution of our equations, we define the "normalized moments" $\overline{M}_{\{N_c,N_m,N_h\},k}$,

$$\overline{M}_{\{N_c,N_m,N_h\},k} = \frac{M_{\{N_c,N_m,N_h\},k}}{\Gamma\left(\frac{k+1}{2}\right)}\left(\frac{\sqrt{\pi}}{2}\right) = \sum_\eta T_\eta(t)^{\left(\frac{k}{2}-1\right)}\sum_{i=0}^{N_\eta}\binom{-\frac{k}{2}+i}{i}a_{\eta i}(t) \tag{2-14}$$

In the time evolution of the distribution function we will use these instead of the formal moments (2-9). The reason for doing this is to keep the order of magnitude of the coefficients of the moments about the same, and thus minimize roundoff errors in the computer program which, otherwise, prevent it from converging properly, because the absolute values of the moments increase very rapidly with k.

2.3. **Fitting a Laguerre distribution function by matching the moments**

Equation (2-1) showed the general form of the Laguerre distribution function.

$$F_{\{N_c,N_m,N_h\}}(v,t) = \frac{4}{\sqrt{\pi}}\sum_\eta T_\eta(t)^{-\frac{3}{2}}\exp\left(-\frac{v^2}{T_\eta(t)}\right)\sum_{i=0}^{N_\eta}a_{\eta i}(t)L_i^{\left(\frac{1}{2}\right)}\left(\frac{v^2}{T_\eta(t)}\right) \tag{2-15}$$

In order to construct this Laguerre distribution function, we need to find $\sum_\eta(N_\eta + 2)$ unknowns *i.e.* $T_\eta(t), a_{\eta 0}(t), \dots, a_{\eta N_\eta}(t)$. *e.g.* for a three temperature form we need to find $(N_c + 2) + (N_m + 2) + (N_h + 2)$ unknowns *i.e.*

$T_c(t), a_{c0}(t), \dots, a_{cN_c}(t), T_m(t), a_{m0}(t), \dots, a_{mN_m}(t), T_h(t), a_{h0}(t), \dots, a_{hN_h}(t)$. We match $N_M = \sum_\eta(N_\eta + 2)$ normalized moments of the Laguerre distribution function $\overline{M}_{\{N_c,N_m,N_h\},k}$) to the same number of a given set of normalized moments $\overline{M}_k$ obtained by numerical integration of the "FPI" distribution function We use only even normalized moments here $k = 0,2,4, \dots 2(N_M - 1)$ (We are using only the even moments because then, the moment equation below contains only integral powers of the temperatures, which facilitates the numerical solution. Furthermore, as this implies that the maximum value of k is higher than if we used all the successive moments, it means that we sample higher energy regions of the distribution function. On the other hand, when we tried using successive k values differing by more than 2, we found many glitches at low energy, as the low energy region was then not well sampled.

$$\overline{M}_{\{N_c,N_m,N_h\},k} = \frac{M_k}{\Gamma\left(\frac{k+1}{2}\right)}\left(\frac{\sqrt{\pi}}{2}\right) = \sum_\eta T_\eta(t)^{\left(\frac{k}{2}-1\right)}\sum_{i=0}^{N_\eta}C_{ki}\,a_{\eta i}(t) = \overline{M}_k, \quad k = 0,2,\dots,2(N_M - 1),$$

$$C_{ki} = \binom{-\frac{k}{2}+i}{i} \tag{2-16}$$

This system of equations is linear in the $a_{\eta i}(t)$'s but nonlinear in the $T_\eta(t)$'s. We first seek proper values for the temperatures $T_\eta(t)$'s and then we solve the linear system of equations to find the coefficients $a_{\eta i}(t)$'s. We can thus iterate on the $T_\eta(t)$'s until a satisfactory fit is obtained.

Let us assume here a Laguerre distribution function with s different temperatures, *i.e.* $\eta = 1,2,\dots,s$ and that each temperature has $N_\eta + 1$ terms of generalized Laguerre polynomials. By eliminating the $a_{\eta i}(t)$'s in (2-16), we obtain the s following equations for the temperatures (Appendix A):

$$\sum_{i_1=0}^{N_1+1} \sum_{i_2=0}^{N_2+1} \cdots \sum_{i_s=0}^{N_s+1} \binom{N_1+1}{i_1}(-T_1)^{N_1+1-i_1} \times \binom{N_2+1}{i_2}(-T_2)^{N_2+1-i_2} \times \dots \times$$

$$\binom{N_s+1}{i_s}(-T_s)^{N_s+1-i_s} \times \bar{M}_{\{N_1+1,N_2+1,\dots,N_s+1\},2(l+i_1+i_2+\dots+i_s)} = 0, \ l = 0,1,2,\dots,s-1 \quad (2\text{-}17)$$

By using the Newton-Raphson iteration method, we can find $T_1, T_2, \dots, T_s$ numerically. Of course, we always need a guess fairly close to the answer for each of the temperatures for the iterations to converge. In the time evolution of the distribution function, we use the temperatures from the previous timestep as our guess.

Finally, we can solve the linear set of equations (2-16) to find the $a_{\eta i}(t)$'s.

2.4. **Fitting a reference distribution function ("FPI" simulation results) with a Laguerre distribution function**

Now, we need to study which form of the Laguerre distribution function is suitable to represent the FPI distribution functions initialized with different temperature ratios $\left(\frac{T_c}{T_h}\right)$, and different density ratios $\left(\frac{n_c}{n_h}\right) = \left(\frac{a_{c0}}{a_{h0}}\right)$, at different times.

In each case, we fit the Laguerre distribution function to the FPI distribution function at different timesteps initialized with a two-Maxwellian distribution function at different temperatures (T_c, T_h), which we call the cold and hot temperature respectively.

This fitting is not trivial, even for the single temperature case, because the dependence on the temperature is nonlinear, and we want to optimise the value of T (or the T_η's) as well as those of the a_j's (or the $a_{\eta j}$'s). We match the moments of the fitted function with the moments of the reference *i.e.* "FPI" results by finding the right coefficients and temperatures $(a_{\eta j}, T_\eta)$.

Note:

Low moments are very important in plasma physics (*e.g.* moment 2 and 4 are the total density and the total energy density, respectively). Thus, it is very important that the fitted Laguerre distribution function represent these moments properly, *i.e.* the parts of the distribution function in energy scale that have more contribution to the value of these moments, should be well fitted. Here, before going further, we will assess the effect of a truncation of the distribution function on these two moments. Assuming a single Maxwellian distribution function;

$$F_{\{0\}}(v) = \left(\frac{4}{\sqrt{\pi}}\right) T^{\left(-\frac{3}{2}\right)} a \, e^{\left(-\frac{v^2}{T}\right)}$$

we can write the equations for moments 0, 2 and 4 by considering (2-9).

$$M_0 = 2 \, a \, T^{-1}; \quad M_2 = a; \quad M_4 = \frac{3}{2} a \, T \tag{2-18}$$

We now define the truncated moments.

$$MT_0(E_{max}) = \int_{E_{max}}^{\infty} F_{\{0\}}(v) dv = 2 \, a \, T^{-1} Erfc\left(\sqrt{\frac{e_1}{T}}\right) \tag{2-19}$$

$$MT_2(E_{max}) = \int_{E_{max}}^{\infty} v^2 F_{\{0\}}(v) dv = a\left(\frac{2 \, e^{-\frac{E_{max}}{T}}\sqrt{\frac{E_{max}}{T}}}{\sqrt{\pi}} + Erfc\left(\sqrt{\frac{E_{max}}{T}}\right)\right) \tag{2-20}$$

$$MT_4(E_{max}) = \int_{E_{max}}^{\infty} v^4 F_{\{0\}}(v) dv = a\left(\frac{e^{-\frac{E_{max}}{T}}\sqrt{\frac{E_{max}}{T}}(2E_{max}+3T)}{\sqrt{\pi}} + \frac{3}{2}T \, Erfc\left(\sqrt{\frac{E_{max}}{T}}\right)\right)$$

$$\tag{2-21}$$

Equations (2-19), (2-20) and (2-21) represent the contribution of part of the distribution function with energy higher than E_{max} to moments 0, 2 and 4 respectively. We see on Figure (2.1) that the contribution of the part of the distribution with energy above $15 \, T$ is very small for both density and energy density, and especially for moment k=0, and could be neglected. Hence, it is sufficient for the fitted Laguerre distribution function to represent the distribution function below energy $15T$ well.

Note:

Of course, later in this chapter we will see that by adding more terms of Laguerre polynomials, the fitted function correctly covers higher energy regions. This arbitrarly values (15 T) is the value that we suggest.. Besides, in most of the cases, we are interested in moments lower than 4. For example, the rates of ionization and excitation have the form of moments -1, 0 and 1 with lower limit of the integral at the threshold velocity [67, 68]. So, the contribution of the higher energies are even less than shown on the graphs for these cases.
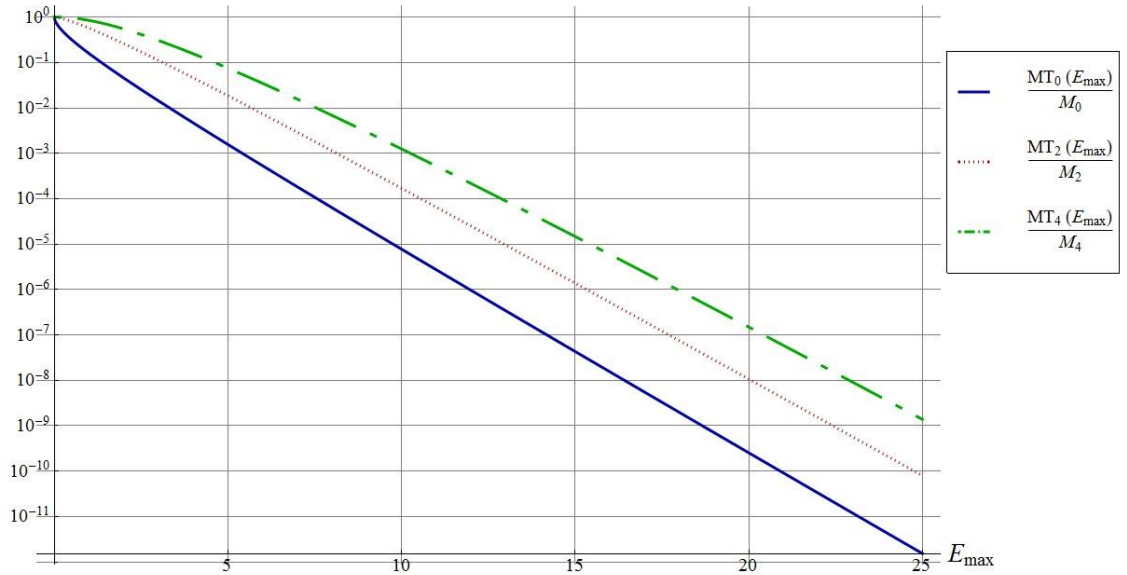
Figure (2.1): Contribution of part of the distribution function with energy above E_{max} to moments 0, 2 (density) and 4 (energy).

In all of the next cases which we simulated, the initial hot temperature is 1 keV, and the total electron density is "1", corresponding to 10^{21} cm^{-3}. The unit of time we use is the collision time for a 1 keV electron in a plasma of this density, *i.e.* about 1.2 picosecond; henceforth, "one collision time" or "one unit time" will correspond to this time interval. It is straightforward to scale the results to other temperatures or densities: The collision time scales as $T_e^{3/2}$ and as $1/n_e$. The important dimensionless parameters of the initialization are the temperature ratio and the density ratio between the hots and colds.

2.4.1. Fitting a single Maxwellian

Of course, a single Maxwellian is not adequate to represent the distribution function at any time step and any temperature ratios.

For example, the result of such a fit to an initial distribution function with a temperature ratio $\left(\frac{T_c}{T_h} = 0.8\right)$ and a density ratio $\left(\frac{n_c}{n_h} = 9\right)$ gave a 10% error at 7 keV and a 100% error at 25 keV and above.

2.4.2. Fitting two-Maxwellians with a single temperature form

To represent a two-Maxwellian distribution by a single temperature Laguerre distribution function, we must first check whether one can express a single Maxwellian by such an expansion, but about a different temperature, and how different these temperatures may be.

Thus, we first express a single Maxwellian with a temperature T by a single temperature form of the Laguerre distribution function with a different temperature T_m.

We first factor the Maxwellian distribution function:

$$f_{\{0\}}(v,t) = a_0(t)\left(\frac{m_e}{2\pi k_B T(t)}\right)^{\frac{3}{2}} \exp\left\{-\frac{m_e v^2}{2k_B T(t)}\right\} =$$

$$a_0(t)\left(\frac{m_e}{2\pi k_B T(t)}\right)^{\frac{3}{2}} \exp\left\{-\frac{m_e v^2}{2k_B T_m(t)}\right\} \underbrace{\exp\left\{\frac{m_e v^2}{2k_B T_m(t)}\left(-\frac{T_m(t)}{T(t)}+1\right)\right\}}_{A} \qquad (2\text{-}22)$$

We now apply the Laguerre expansion for factor A of equation (2-22) (equation 22.9.15 in ref. [53]):

$$e^{\left(\frac{z}{z-1}x\right)} = (1-z)^{\alpha+1}\sum_{n=0}^{\infty} L_n^{(\alpha)}(x)z^n, \qquad |z| < 1 \qquad (2\text{-}23)$$

Substituting:

$$\begin{cases} z \to \dfrac{T_m(t)-T(t)}{T_m(t)} \\ x \to \dfrac{m_e v^2}{2K_B T_m(t)} \\ \alpha \to \dfrac{1}{2} \end{cases} \qquad (2\text{-}24)$$

Equation (2-23) becomes:

$$\exp\left\{\frac{m_e v^2}{2k_B T_m(t)}\left(-\frac{T_m(t)}{T(t)}+1\right)\right\} = \left(\frac{T(t)}{T_m(t)}\right)^{\frac{3}{2}} \sum_{n=0}^{\infty} L_n^{\left(\frac{1}{2}\right)}\left(\frac{m_e v^2}{2k_B T_m(t)}\right)\left(\frac{T_m(t)-T(t)}{T_m(t)}\right)^n,$$

$$|z| = \left|\frac{T_m(t)-T(t)}{T_m(t)}\right| < 1 \qquad (2\text{-}25)$$

And thus, by substituting (2-25) for factor "A" in (2-22):

$$f_{\{0\}}(v,t) \simeq a_0(t)\left(\frac{m_e}{2\pi k_B T_m(t)}\right)^{\frac{3}{2}} \exp\left\{-\frac{m_e v^2}{2k_B T_m(t)}\right\} \times \sum_{n=0}^{n_{max}} L_n^{\left(\frac{1}{2}\right)}\left(\frac{m_e v^2}{2k_B T_m(t)}\right)\left(\frac{T_m(t)-T(t)}{T_m(t)}\right)^n, \quad |z| =$$

$$\left|\frac{T_m(t)-T(t)}{T_m(t)}\right| < 1 \qquad (2\text{-}26)$$

The condition $|z| = \left|\frac{T_m(t)-T(t)}{T_m(t)}\right| < 1$ is not really practical because this expansion converges very slowly for $|z|$ close to 1. So we modify the condition as follows:

$$-0.55 \leq \frac{T_m(t)-T(t)}{T_m(t)} \leq 0.25 \implies 0.65 \leq \frac{T_m(t)}{T(t)} \leq 1.3 \qquad (2\text{-}27)$$

Note:

We have chosen this condition according to the results of an expansion with 9 terms of generalized Laguerre polynomials in (2-26) ($n_{max} = 8$) for different temperature ratios $\left(\frac{T_m(t)}{T(t)}\right)$ in order to obtain less than 10% relative error (compared to the actual single Maxwellian distribution function) below the energy $23\,k_BT$. If we use 17 terms of generalized Laguerre polynomials $n_{max} = 16$, the expansion is valid (less than 10% error) up to energy $54\,k_BT$). The absolute value of z can be larger for negative z because eq. (2.26) is then an alternating sign series, which converges faster.

Figure (2.2) and Figure (2.4) show the results of the expansion with 9 and 17 terms of generalized Laguerre polynomials $n_{max} = 08,\ 16$ with temperatures $(T_m = 0.65\ \text{keV},\ T = 1\ \text{keV},\ a_0 = 1)$ and $(T_m = 1.3\ keV,\ T = 1\ keV,\ a_0 = 1)$ respectively in a Log plot and as a function of energy, while Figure (2.3) and Figure (2.5) show the relative errors of these expansions.
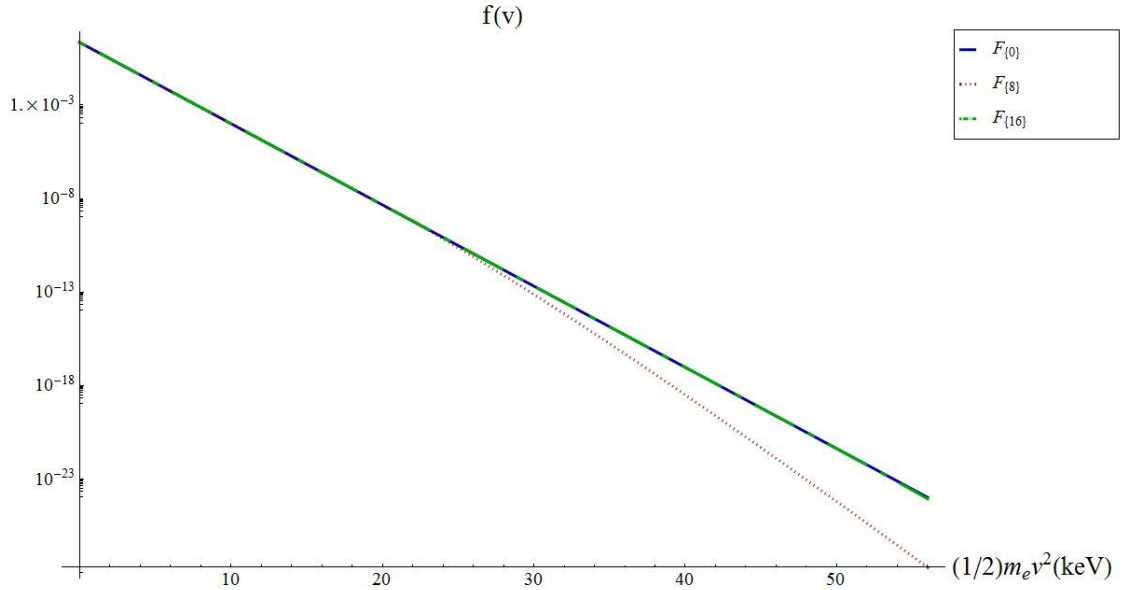
Figure (2.2): Single Maxwellian distribution function $(T = 1\ \text{keV},\ a_0 = 1)$ and a Laguerre expansion distribution function $(T_m = 0.65\ \text{keV},\ a_0 = 1,\ n_{max} = 8,\ 16)$.
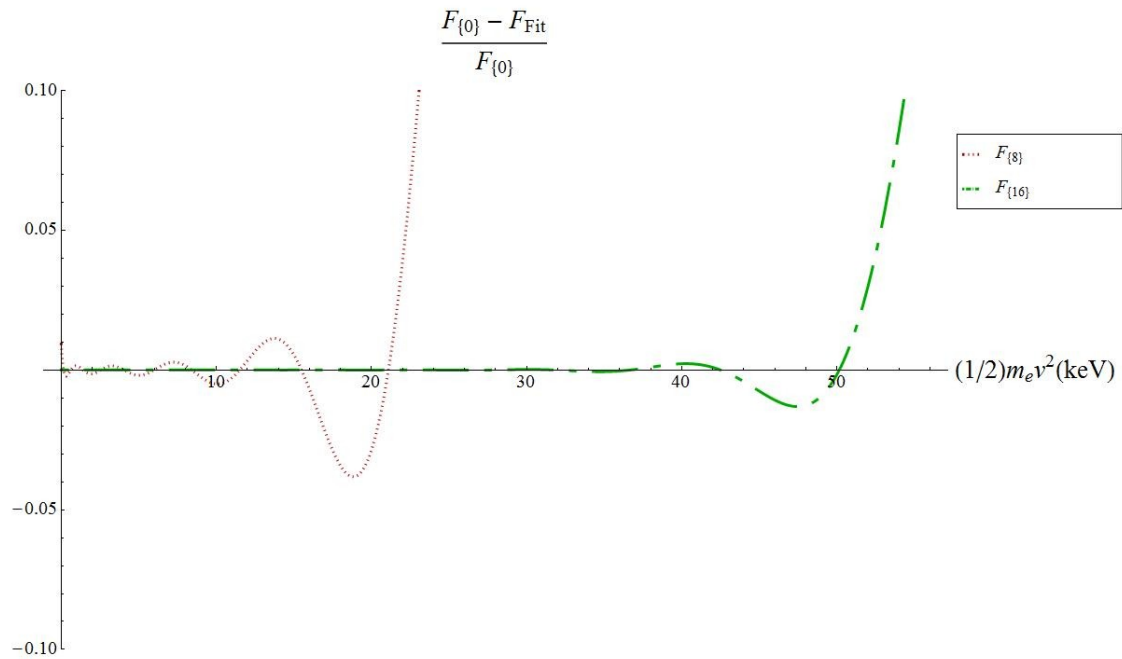
Figure (2.3): Relative error of the expansion illustrated in Figure (2.2).
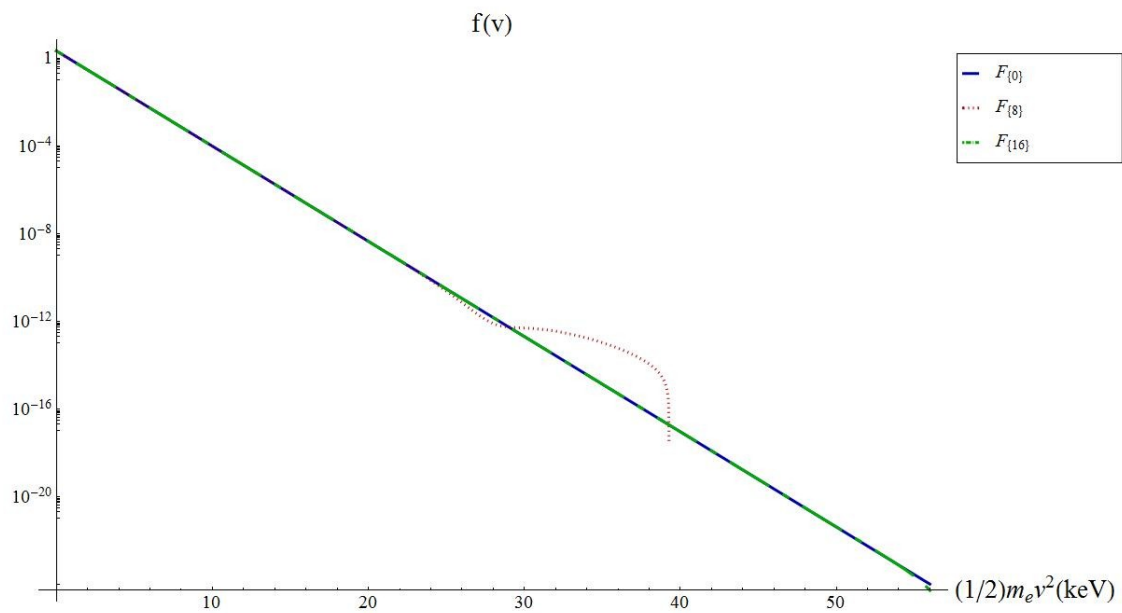
Figure (2.4): Single Maxwellian distribution function ($T = 1\,\text{keV}$, $a_0 = 1$) and a Laguerre expansion distribution function ($T_m = 1.3\text{keV}$, $a_0 = 1$, $n_{max} = 8,\ 16$).
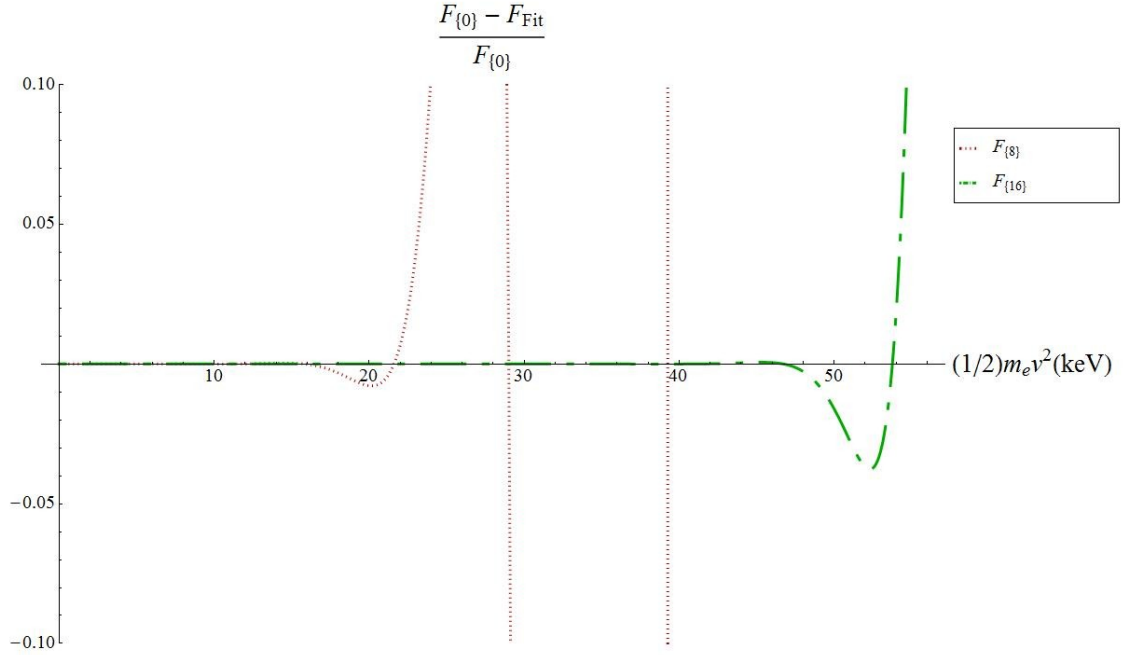
Figure (2.5): Relative error of the expansion illustrated in Figure (2.4).

In the next step, we try to express a two-Maxwellian distribution function with temperatures (T_c, T_h) using a single temperature form of the Laguerre distribution function with a temperature (T_m).

The initial two-Maxwellian distribution function is.

$$f_{\{0,0\}}(v, t = 0) = \sum_{\eta=c,h} a_{\eta 0}(t = 0) \left(\frac{m_e}{2\pi k_B T_\eta(t=0)}\right)^{\frac{3}{2}} \exp\left\{-\frac{m_e v^2}{2 k_B T_\eta(t=0)}\right\} \quad (2\text{-}28)$$

Using, (2-26) we can write (2-28) as:

$$f_{\{0,0\}}(v, 0) \simeq$$

$$\sum_{\eta=c,h} \left\{ a_{\eta 0}(0) \left(\frac{m_e}{2\pi k_B T_m(0)}\right)^{\frac{3}{2}} \exp\left\{-\frac{m_e v^2}{2 k_B T_m(0)}\right\} \times \sum_{n=0}^{n_{max}} L_n^{\left(\frac{1}{2}\right)} \left(\frac{m_e v^2}{2 k_B T_m(0)}\right) \left(\frac{T_m(0) - T_\eta(0)}{T_m(0)}\right)^n \right\}, \quad 0.65 \le$$

$$\frac{T_m(0)}{T_\eta(0)} \le 1.3 \quad (2\text{-}29)$$

Equation (2-29) is in the form of a single temperature distribution function (2-2). But, as we have seen, there is a limitation for using this expression with n_{max}=8. *i.e.*

$$1 \le \frac{T_m(0)}{T_c(0)} \le 1.3 \text{ and } 0.65 \le \frac{T_m(0)}{T_h(0)} \le 1$$

Thus, applying this criterion, we see that the lowest temperature ratio which can be accommodated with 9 terms in the expansion is $\frac{T_c(0)}{T_h(0)} = \frac{0.65}{1.3} = 0.5$, if we use $T_m = 0.65$ as the single temperature for the expansion.

25

Figure (2.6) shows the results of the fits to this initial distribution function at the initial time step with this temperature ratio $\frac{T_c(0)}{T_h(0)} = 0.5$ and density ratio $\frac{a_{c0}}{a_{h0}} = 9$ using a single temperature form of Laguerre distribution function with temperature $T_m = 0.65$ and different numbers of generalized Laguerre polynomials *i.e.* $n_{max} = 0, 4, 8, 16$.
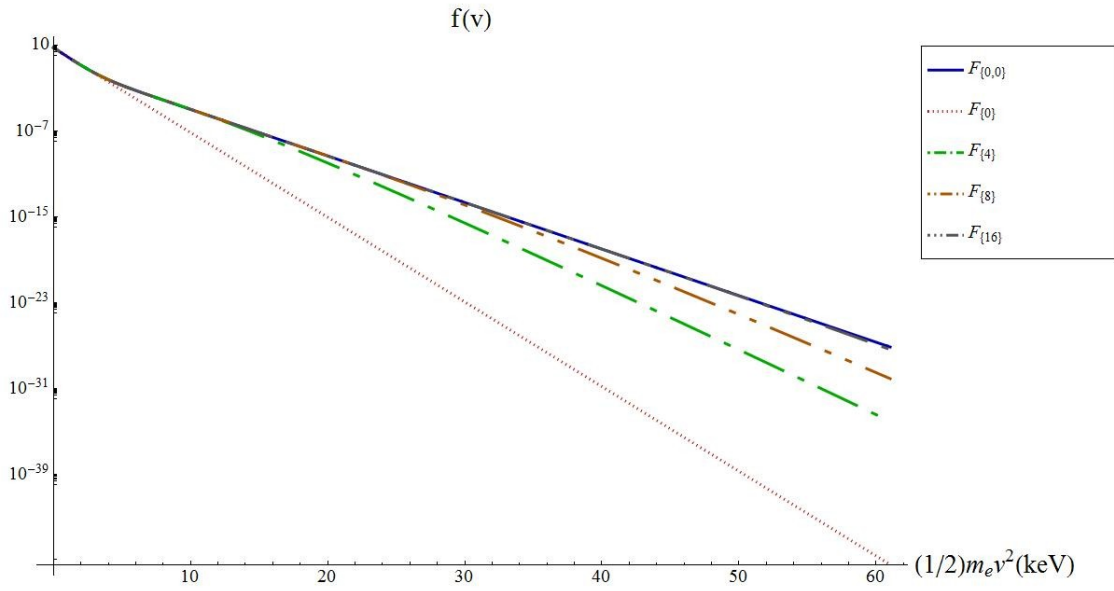
Figure (2.6): Results of the fits of a single temperature form of the Laguerre distribution function with $\left(\frac{T_c(0)}{T_h(0)} = 0.5, \ \frac{a_{c0}(0)}{a_{h0}(0)} = 9, \ T_m = 0.65 \right)$.

Figure (2.7): Relative error of the results of the fits plotted in Figure (2.6).

Figure (2.8): Results of the fits of a single temperature form of the Laguerre distribution function with $\left(\frac{T_c(0)}{T_h(0)} = 0.25, \quad \frac{a_{c0}(0)}{a_{h0}(0)} = 9, \quad T_m = 0.325\right)$.

$$\frac{F_{\{0,0\}} - F_{\text{Fit}}}{F_{\{0,0\}}}$$

Figure (2.9): Relative error of the results of the fits plotted in Figure (2.8).

Comparing Figure (2.6) and Figure (2.7) $\frac{T_c(0)}{T_h(0)} = 0.5$ to Figure (2.8) and Figure (2.9) $\frac{T_c(0)}{T_h(0)} = 0.25$ shows that the fitted Laguerre distribution function with $n_{max} = 8$ can represent the reference distribution function very well for the 2:1 temperature ratio. However, decreasing the temperature ratio $\left(\frac{T_c(0)}{T_h(0)} = 0.25 < 0.5\right)$ reduces the quality of the fitting results for $n_{max} = 8$, but $n_{max} = 16$ still gives good results.

Figure (2.6) and Figure (2.8) were for the initial timestep (2 Maxwellians). However, it is important to verify the possibility of fitting a single, two or three temperature(s) form of the Laguerre distribution function to the reference distribution function in later timesteps *i.e.* the result of the time evolution of the distribution function. In general, since the reference distribution function is not a simple 2 Maxwellians distribution (except for the initial timestep), we cannot use (2-29) any more to find a proper fit. Instead, we use the technique described in sub-section (2.3) *i.e.* fitting a Laguerre distribution function by matching the moments.

2.5. Fitting a Laguerre distribution function to the results obtained from "FPI" for different temperature ratios

2.5.1. Fitting a single temperature form for a 2:1 temperature ratio

Figure (2.10) shows the results of the fits to the "FPI" distribution function at $(t \simeq 1.2 \, psec)$ *i.e.* after one collision time. The initial temperature ratio was $\frac{T_c(0)}{T_h(0)} = 0.5$ and the initial density ratio was $\frac{a_{c0}(0)}{a_{h0}(0)} = 9$. The fits are provided with different numbers of generalized Laguerre polynomials *i.e.* $n_{max} = 0, 4, 8, 16$.
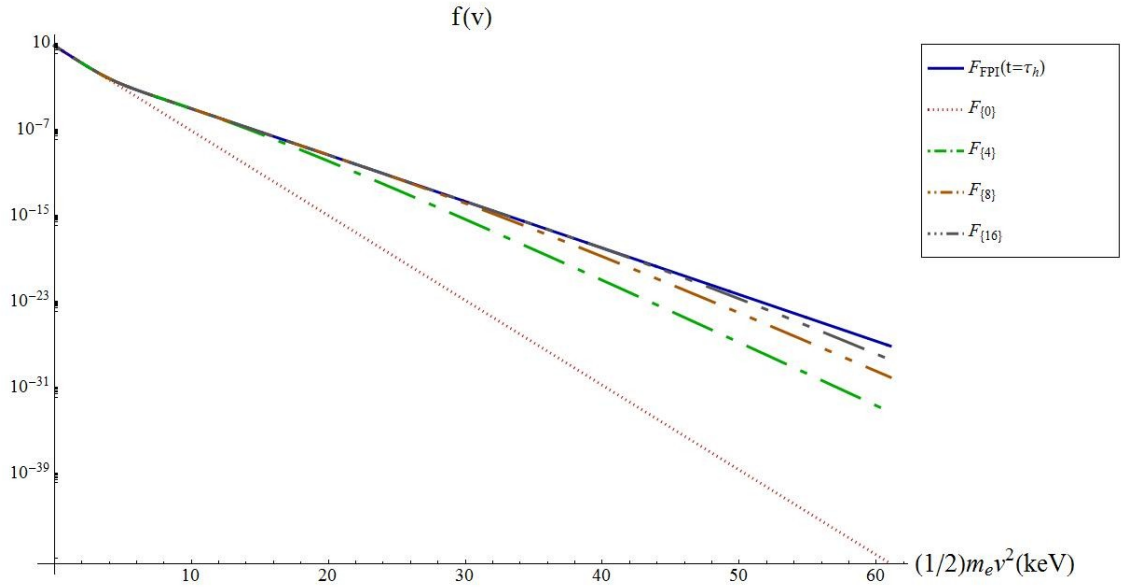
Figure (2.10): Results of the fits of a single temperature form of the Laguerre distribution function at $(t = \tau_h)$ initialized with two Maxwellians $\left(\frac{T_c(0)}{T_h(0)} = 0.5, \ \frac{a_{c0}(0)}{a_{h0}(0)} = 9 \right)$.

$$\frac{F_{\mathrm{FPI}} - F_{\mathrm{Fit}}}{F_{\mathrm{FPI}}}$$
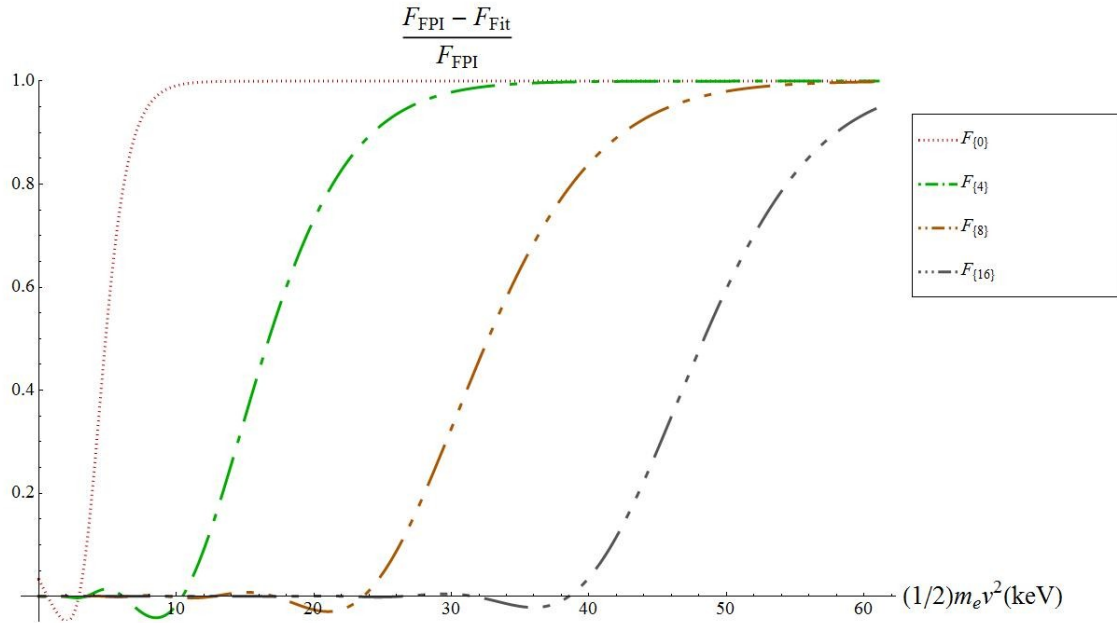
Figure (2.11): Relative error of the results of the fits plotted in Figure (2.10).

In chapter 4 *i.e.* the results of the time evolution of the distribution function, we will see that the quality of the fit improves as time advances. We noted the same thing here, when fitting the results to the "FPI" simulation at many different times (not shown). This is because the cold component's temperature increases, and approaches the reference temperature. So, for all of the cases in this chapter, we check the validity of the fitting method by fitting the Laguerre distribution function after one collision time. Nonetheless, it is clear that expanding about a single Maxwellian is useful only for relatively modest temperature ratios, such as 2:1 or 4:1, and, in the latter case, at the cost of a very large number of terms.

2.5.2. Fitting a two temperature form for a 2:1 temperature ratio

Equation (2-5) showed the form of the two temperature form of the Laguerre distribution function.

There are $\left(2 + (N_c + 1) + (N_h + 1)\right)$ unknowns in the Laguerre distribution function in this form: The two temperatures, $(N_c + 1)$ for the coefficients $a_{cj}(t)$, $(j=0,1,2,...,N_c)$ of the cold temperature and $(N_h + 1)$ for the coefficients $a_{hj}(t)$, $(j=0,1,2,...,N_h)$ of the hot temperature. Hence, we match $\left(2 + (N_c + 1) + (N_h + 1)\right)$ moments $\left(k = 0,2,4,...,2(N_c + N_h + 3)\right)$ of the fitted distribution function to the calculated ones from the FPI distribution function (the method was explained in section 2.3). Figure (2.12) shows the result of the fits to a FPI distribution function

30

after one collision time (for the hot temperature) initialized with a temperature ratio $\left(\frac{T_c(0)}{T_h(0)} = 0.5,\right.$

$\frac{a_{c0}(0)}{a_{h0}(0)} = 9\left.\right)$ using the two temperature form of the Laguerre distribution function (2-5). We vary

N_c, but keep $N_h=0$, because at very high energy, the distribution function is nearly Maxwellian, and multiplying this by a polynomial severely distorts this shape, as the leading term is then this

Maxwellian multiplied by the highest power of v, *i.e.* $v^{2N_h} \exp\left\{-\frac{m_e v^2}{2k_B T_h(t)}\right\}$.
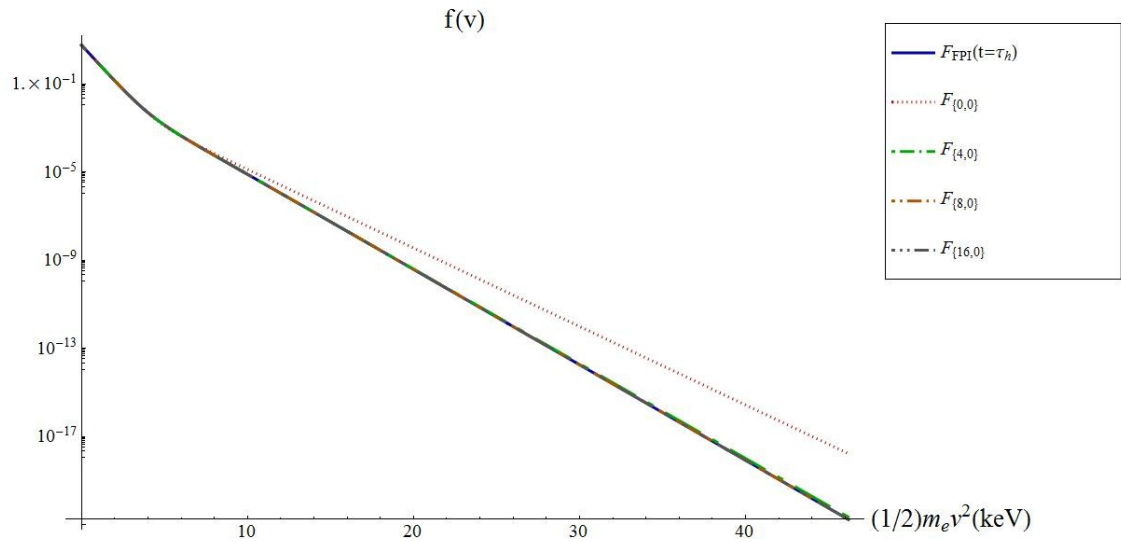
Figure (2.12): Results of the fits of two temperature form of the Laguerre distribution function at $(t = \tau_h)$ initialized with two Maxwellians $\left(\frac{T_c(0)}{T_h(0)} = 0.5, \quad \frac{a_{c0}(0)}{a_{h0}(0)} = 9\right)$.
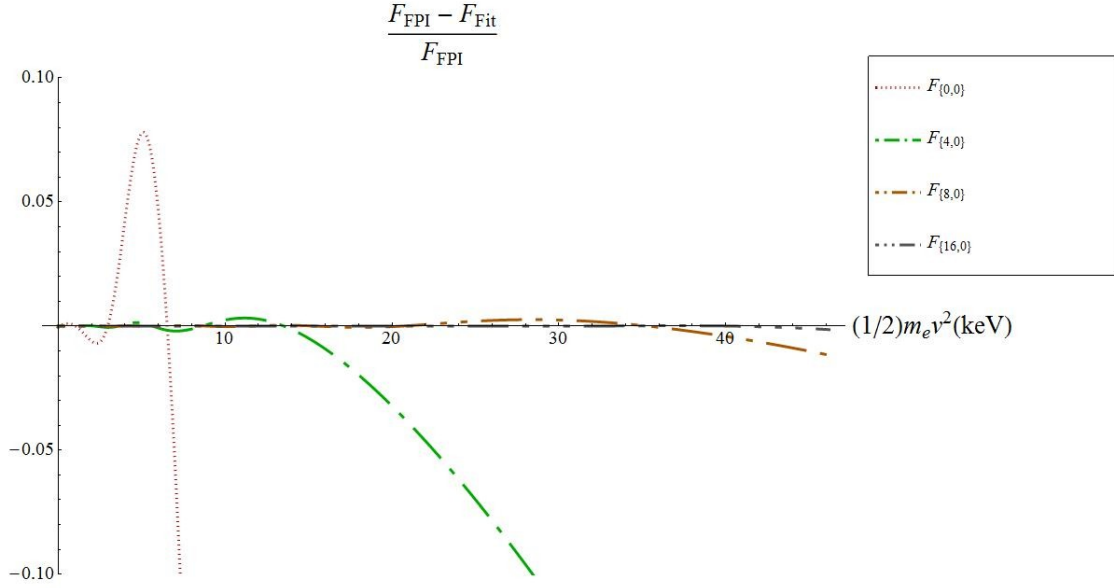
Figure (2.13): Relative error of the results of the fits plotted in Figure (2.12).

Comparing Figure (2.11) and Figure (2.13), we see that we get a much better fit with two temperatures, even if we keep fewer terms: The $N_c=8$ fit here is better than the N=16 fit with a single temperature, and the $N_c=4$ fit is as good as the single temperature fit with N=8.

Obviously, we can see that adding more terms of generalized Laguerre polynomials greatly improves the quality of the fits especially in higher energy regions, while the two-Maxwellian ($F_{\{0,0\}}$, *i.e.* $N_c=N_h=0$) form is very inadequate.

2.5.3. Fitting a single temperature form for a 4:1 temperature ratio

Figure (2.14) shows the result of the fits to a FPI distribution function after one collision time (for the hot temperature) initialized with a temperature ratio $\left(\frac{T_c(0)}{T_h(0)} = 0.25, \frac{a_{c0}(0)}{a_{h0}(0)} = 9\right)$ using the two temperature form of the Laguerre distribution function. Obviously, for this temperature ratio case, we need many terms of Laguerre polynomials in the single temperature form of the Laguerre distribution function to represent the actual one, whereas, in the next subsection we will see that the two temperature form can represent the distribution function with a fewer number of Laguerre terms.
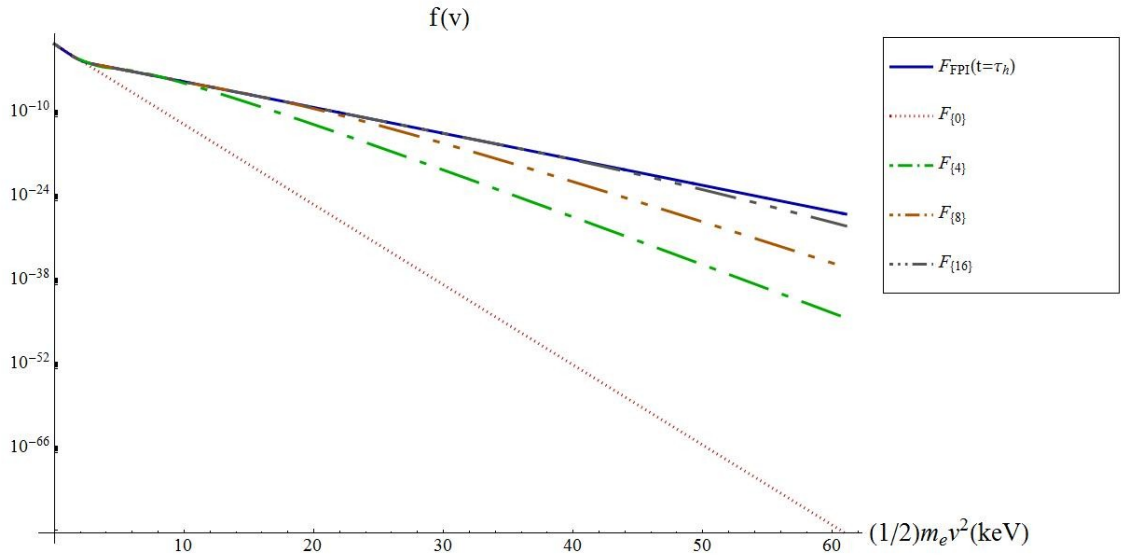
Figure (2.14): Results of the fits of a single temperature form of the Laguerre distribution function at $(t = \tau_h)$ initialized with two Maxwellians $\left(\frac{T_c(0)}{T_h(0)} = 0.25, \; \frac{a_{co}(0)}{a_{ho}(0)} = 9 \right)$.
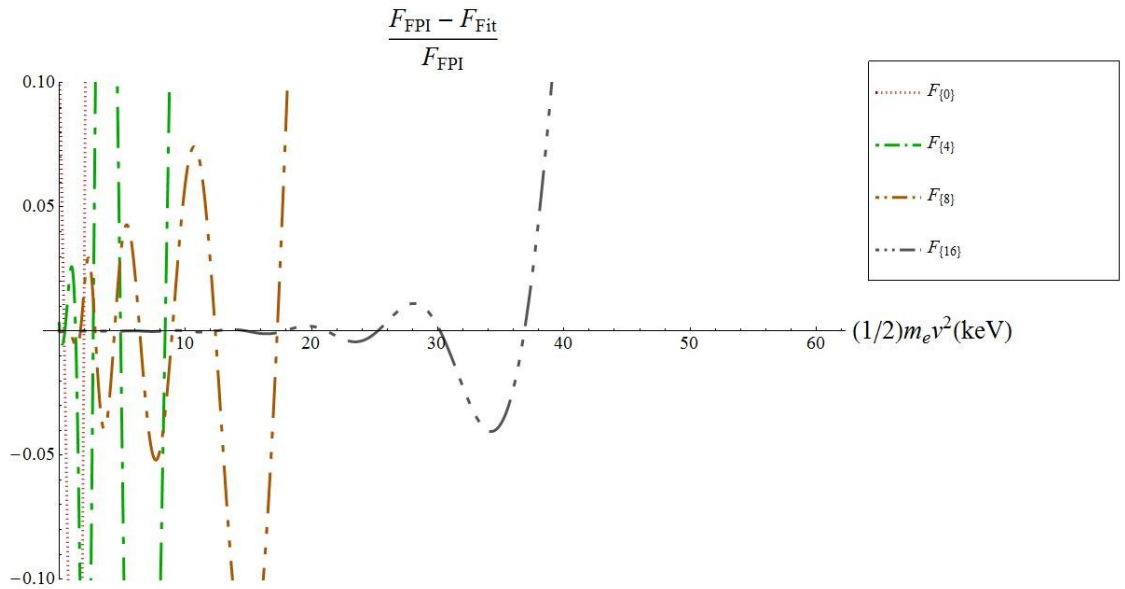
Figure (2.15): error of the results of the fits plotted in Figure (2.14).

Thus, here too, we see that many terms are essential to achieve an adequate representation if we want to use a single temperature, but that the error is somewhat less than for the initial state (compare Fig. 2.9; but note the different vertical scale).

2.5.4. Fitting a two temperature form for a 4:1 temperature ratio

Figure (2.16) shows the result of the fits to a FPI distribution function after one collision time (for the hot temperature) initialized with ratios $\left(\frac{T_c(0)}{T_h(0)} = 0.25, \frac{a_{c0}(0)}{a_{h0}(0)} = 9\right)$ using the two temperature form of the Laguerre distribution function.
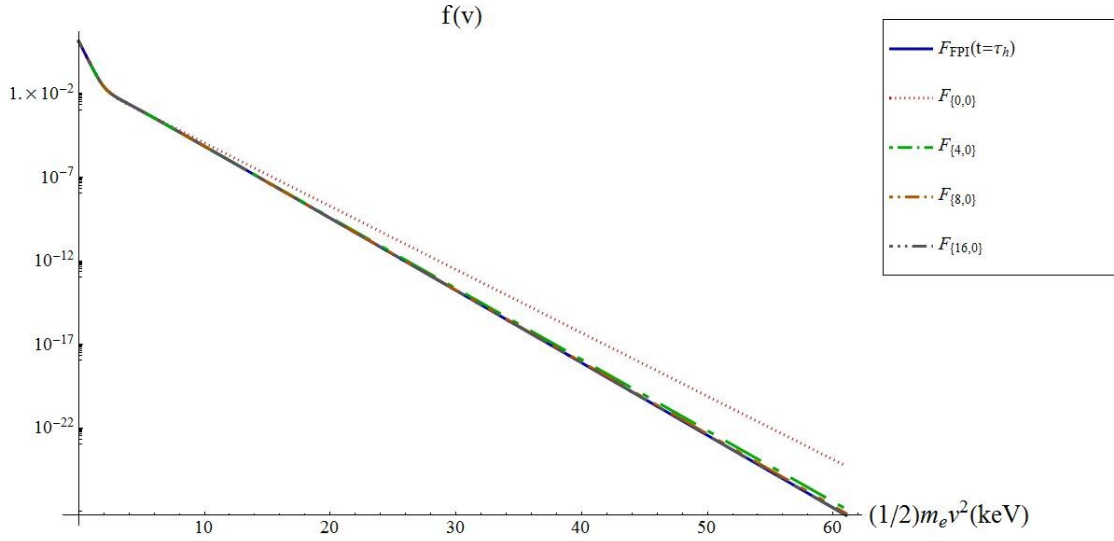
Figure (2.16): Results of the fits of the two temperature form of the Laguerre distribution function $\left(\frac{T_c(t)}{T_h(t)} = 0.25, \frac{a_{c0}}{a_{h0}} = 9, \ t = \tau_{T_h}\right)$.
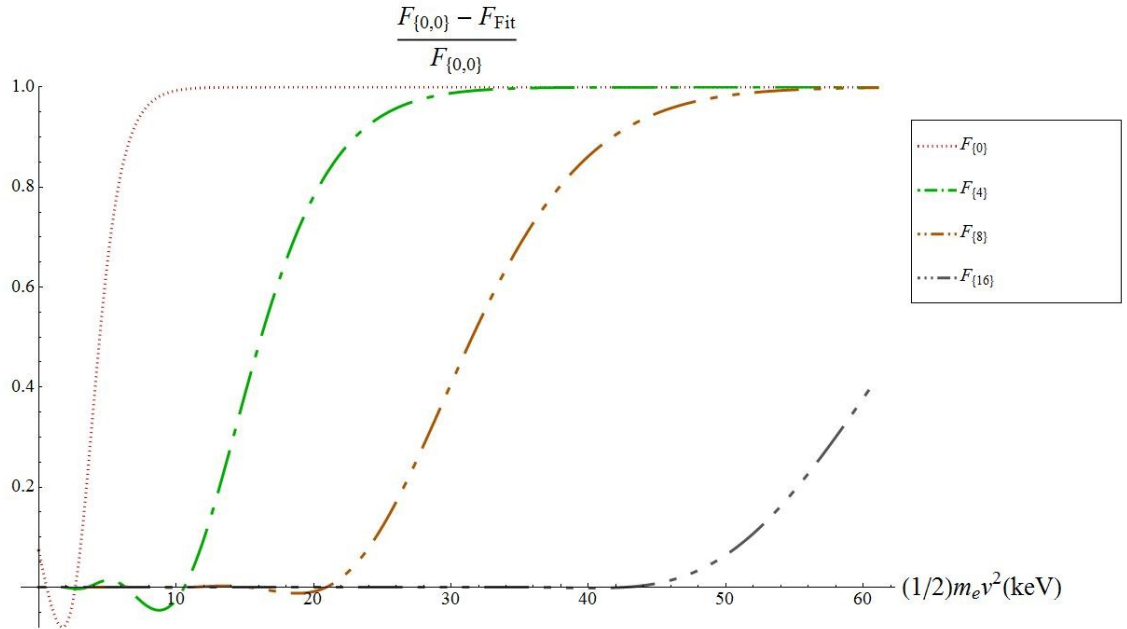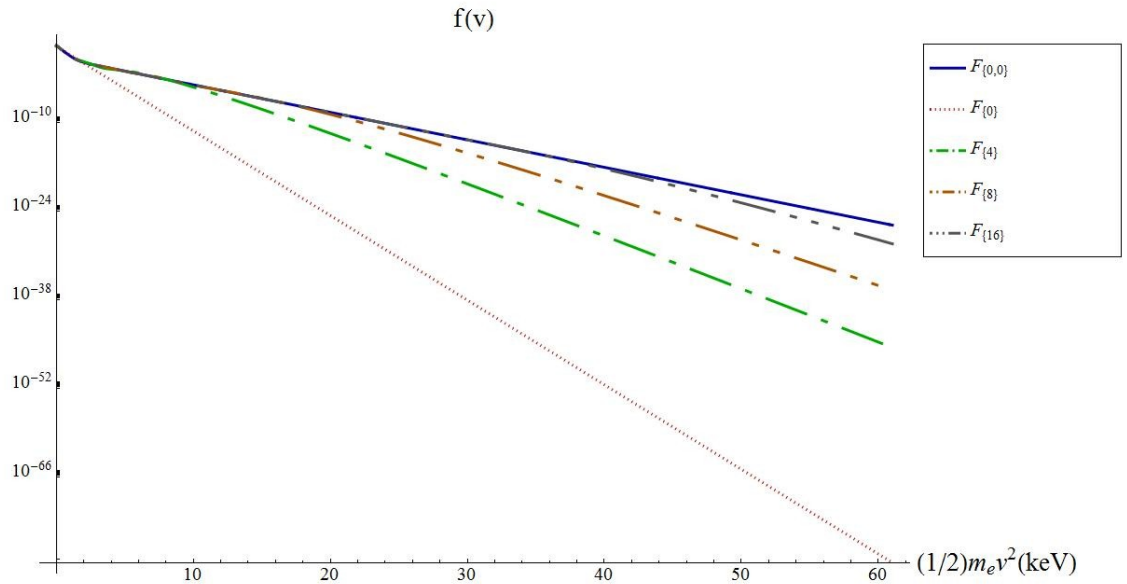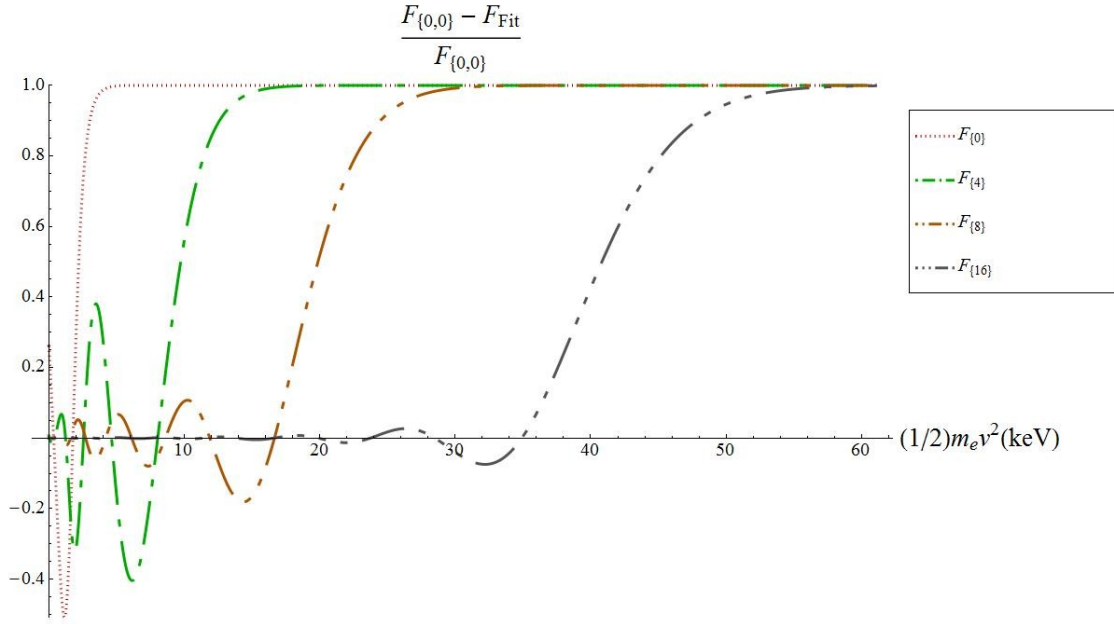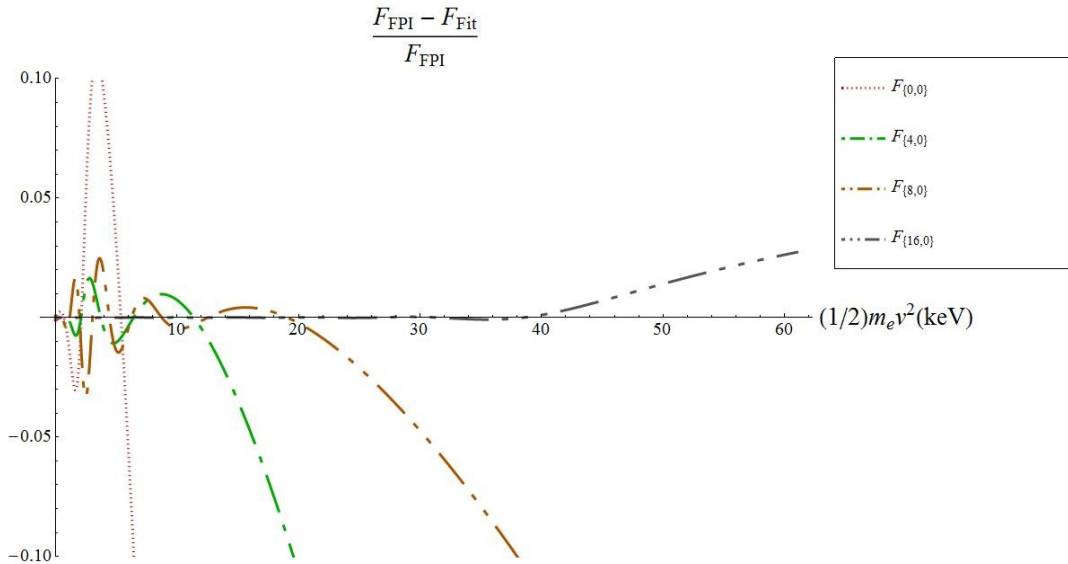

Figure (2.17): Relative error of the results of the fits plotted in Figure (2.16).

Thus, we see that for the initial temperature ratio ¼, a two temperature Laguerre distribution function is adequate, provided that we keep enough Laguerre terms. $N_c \geq 8$, but even $N_c = 4$ would give acceptable results up to almost 20 keV.

2.5.5. Fitting a two temperature form for a 10:1 temperature ratio

Figure (2.18) shows the result of the fits to a FPI distribution function after one collision time (for the hot temperature) initialized with a temperature ratio $\left(\frac{T_c(0)}{T_h(0)} = 0.1, \ \frac{a_{c0}(0)}{a_{h0}(0)} = 9 \right)$ using the two temperature form of the Laguerre distribution function. By comparing the results of the fits with a two temperatures form with a three temperatures form of the Laguerre distribution function (subsection 2.5.6), it will be seen that it is better to use the latter form for this initial temperature ratio.
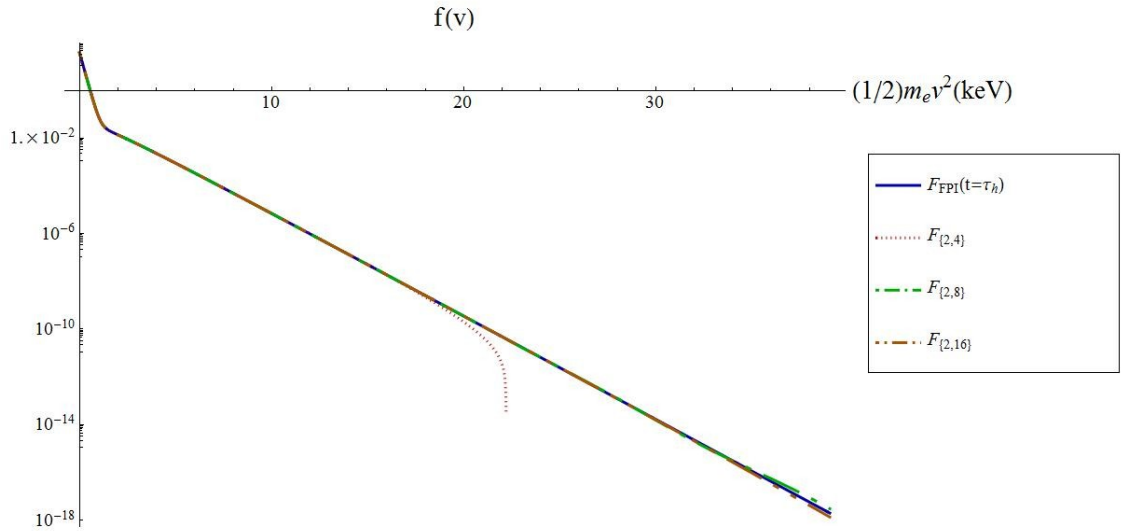
Figure (2.18): Result of the fits of the two temperature form of the Laguerre distribution function $\left(\frac{T_c(t)}{T_h(t)} = 0.1, \ \frac{a_{c0}}{a_{h0}} = 9, \ t = \tau_{T_h} \right)$.
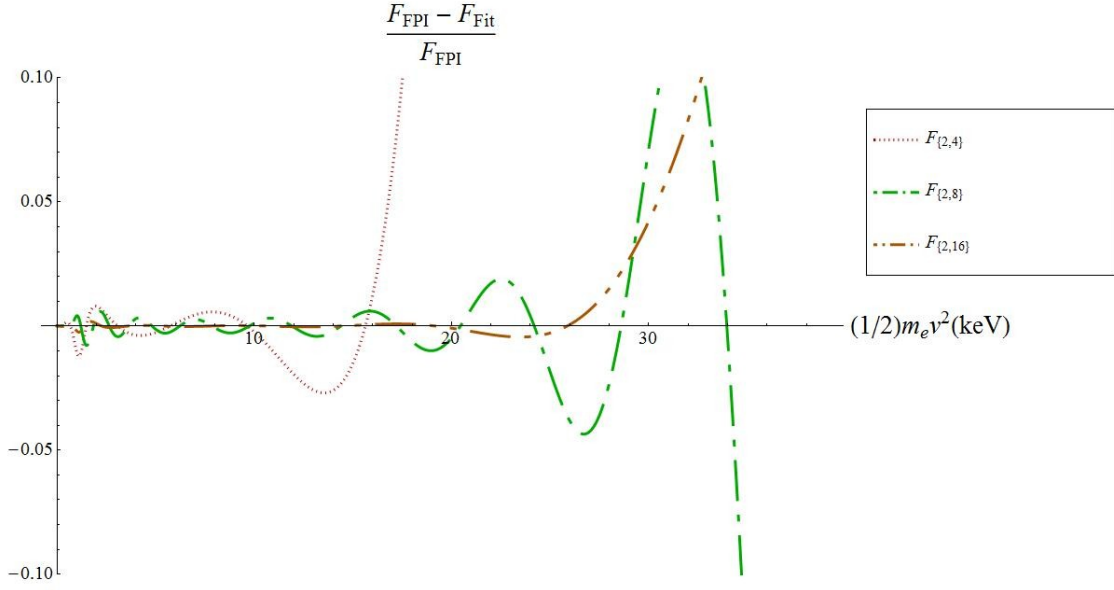
Figure (2.19): Relative error of the results of the fits plotted in Figure (2.18).

2.5.6. Fitting a three temperature form for a 10:1 temperature ratio

A two temperature form of the Laguerre distribution function appears to give fair results for representing the time evolution of the distribution function initialized with very low temperature ratios $\left(\frac{T_c(0)}{T_h(0)} \leq 0.1\right)$. Instead, we use a three temperature form of the Laguerre distribution function (2-6).

There are $\left(3 + (N_c + 1) + (N_m + 1) + (N_h + 1)\right)$ unknowns in the Laguerre distribution function in this form: The three temperatures, $(N_c + 1)$ for the coefficients $a_{cj}(t)$, (j=0,1,2,...,N$_c$) of the cold temperature, $(N_m + 1)$ for the coefficients $a_{mj}(t)$, (j=0,1,2,...,N$_m$) of the medium temperature and $(N_h + 1)$ for the coefficients $a_{hj}(t)$, (j=0,1,2,...,N$_h$) of the hot temperature. Hence, we match $\left(3 + (N_c + 1) + (N_m + 1) + (N_h + 1)\right)$ moments (k=0,2,4,...,2(N$_c$+N$_m$+N$_h$+5) of the fitted distribution function to the calculated ones from the FPI distribution function (using the method explained in section 2.3). Figure (2.20) shows the result of the fits to a FPI distribution function after one collision time (for the hot temperature) initialized with a temperature ratio $\left(\frac{T_c(0)}{T_h(0)} = 0.1, \frac{a_{c0}(0)}{a_{h0}(0)} = 9\right)$ using the three temperature form of the Laguerre distribution function. The quality of the fits are excellent: The error is below 10% all the way up to 80 keV, and even more with more polynomials. For the initial temperature ratios $\frac{T_c(0)}{T_h(0)} \leq 0.1$ the three temperatures form of the Laguerre polynomial is always preferred (see the next few subsections).

36

f(v)
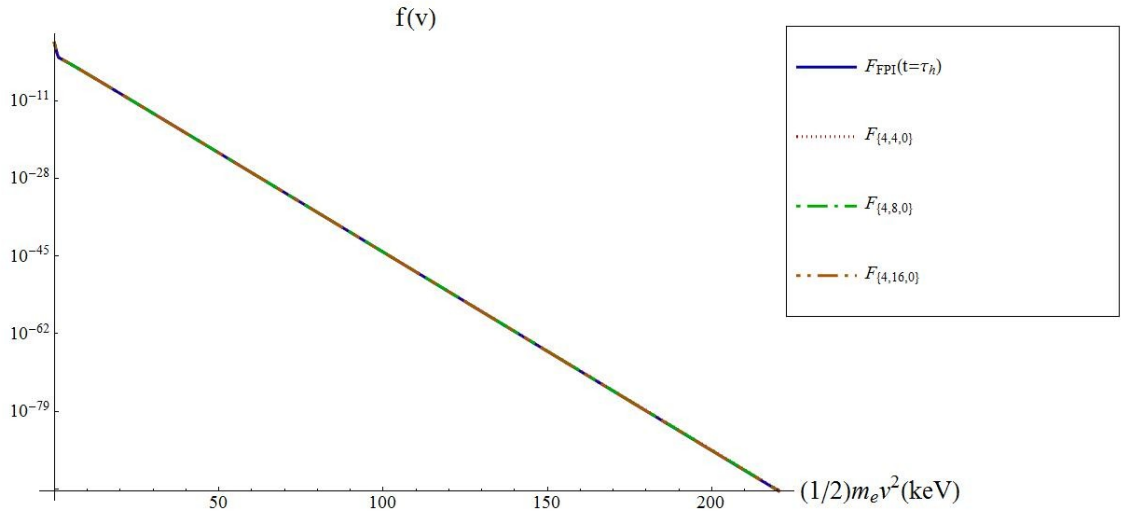
Figure (2.20): Result of the fits of the three temperature form of the Laguerre distribution function $\left(\frac{T_c(0)}{T_h(0)} = 0.1, \frac{a_{c0}(0)}{a_{h0}(0)} = 9, t = \tau_{T_h}\right)$.

$$\frac{F_{\mathrm{FPI}} - F_{\mathrm{Fit}}}{F_{\mathrm{FPI}}}$$
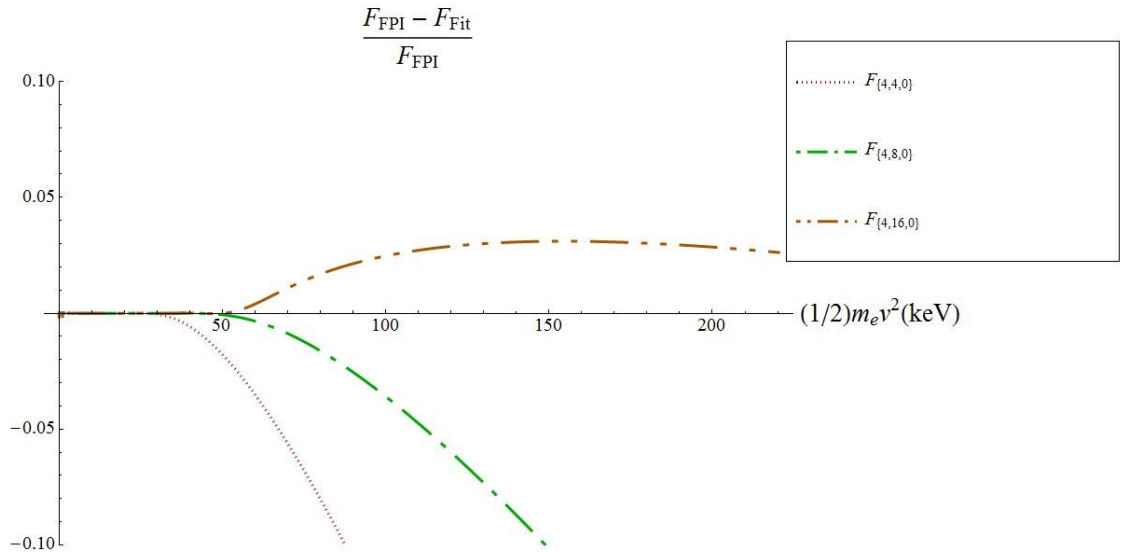
Figure (2.21): Relative error of the results of the fits plotted in Figure (2.20).

2.5.7. Fitting a three temperature form for a 100:1 temperature ratio

Figure (2.22) shows the result of the fits to a FPI distribution function after one collision time (for the hot temperature) initialized with a temperature ratio $\left(\frac{T_c(0)}{T_h(0)} = 0.01, \frac{a_{c0}(0)}{a_{h0}(0)} = 9\right)$ using the

three temperature form of the Laguerre distribution function. We see that the three tempereture form of the Laguerre distribution function is suitable for this initial temperature ratio.
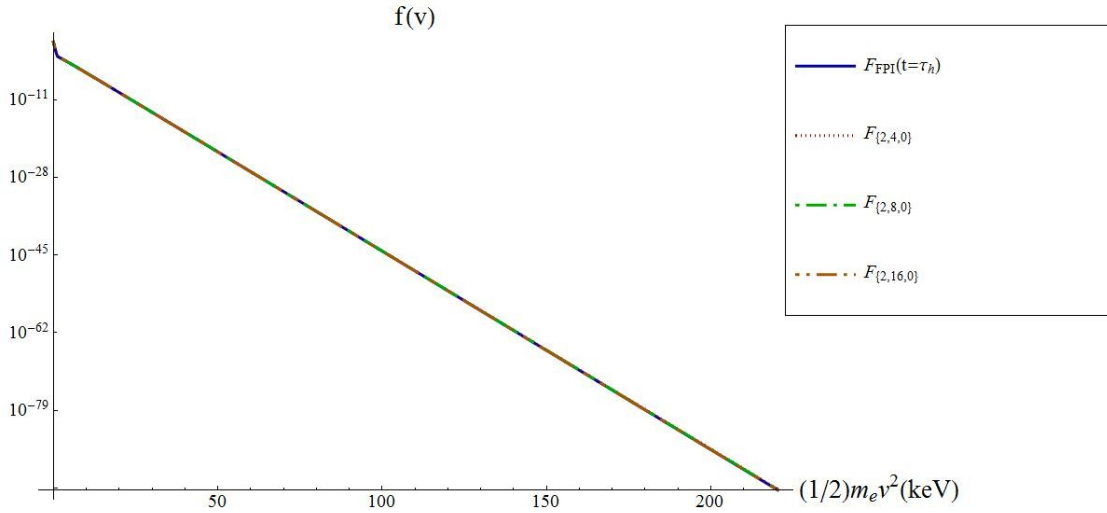
Figure (2.22): Result of the fits of the three temperature form of the Laguerre distribution function $\left(\frac{T_c(0)}{T_h(0)} = 0.01, \frac{a_{co}(0)}{a_{ho}(0)} = 9, t = \tau_{T_h}\right)$.
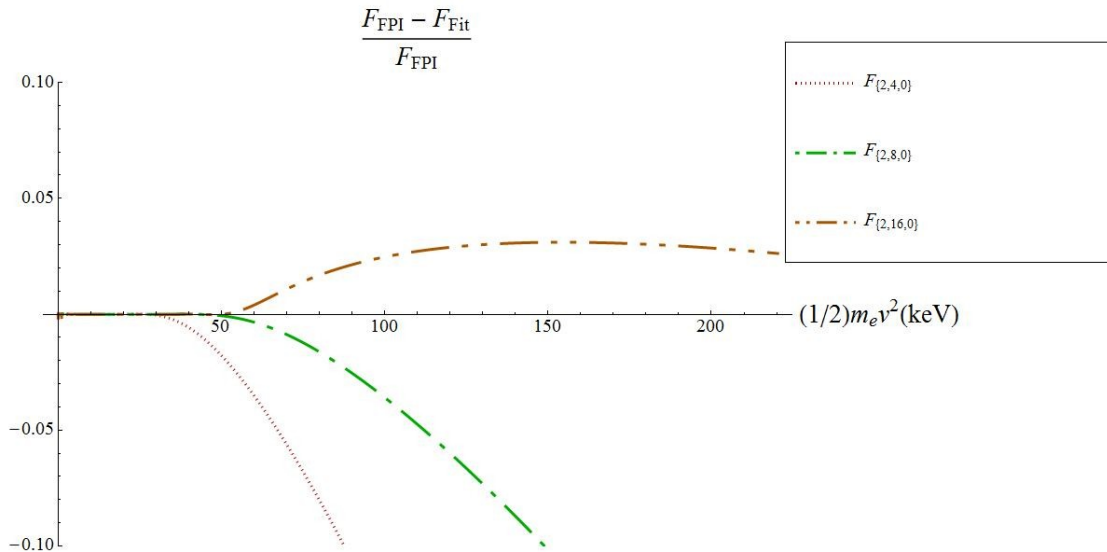
Figure (2.23): Relative error of the results of the fits plotted in Figure (2.22)).

It is clear that the three temperature form provides an excellent fit to the results, up to a very high energy.

2.5.8. Fitting a three temperature form for a 1000:1 temperature ratio

Figure (2.24) shows the result of the fits to a FPI distribution function after half a collision time (for the hot temperature) initialized with a temperature ratio $\left(\frac{T_c(0)}{T_h(0)} = 0.001, \frac{a_{c0}(0)}{a_{h0}(0)} = 9\right)$ using the three temperature form of the Laguerre distribution function, and Figure (2.26) shows the result of the fits for the same temperature ratio after 1 collision time. Same conclusion as subsections 2.5.6 and 2.5.7, here, we also see excellent results by fitting a three temperatures form of the Laguerre distribution function, including the sharp bend at several T_c.
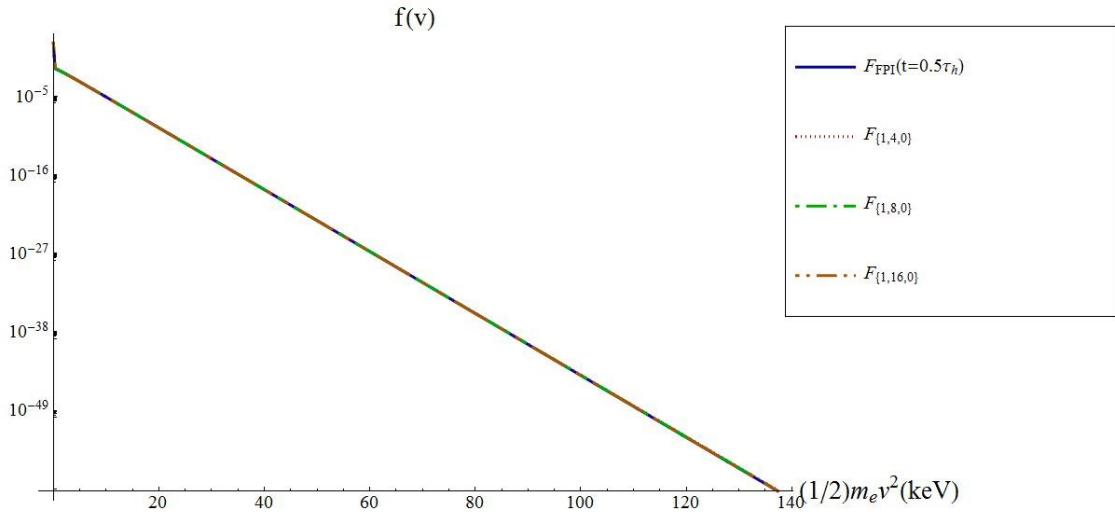
Figure (2.24): Result of the fits of the three temperature form of the Laguerre distribution function $\left(\frac{T_c(0)}{T_h(0)} = 0.001, \ \frac{a_{co}(0)}{a_{ho}(0)} = 9, t = 0.5\tau_{T_h}\right)$.
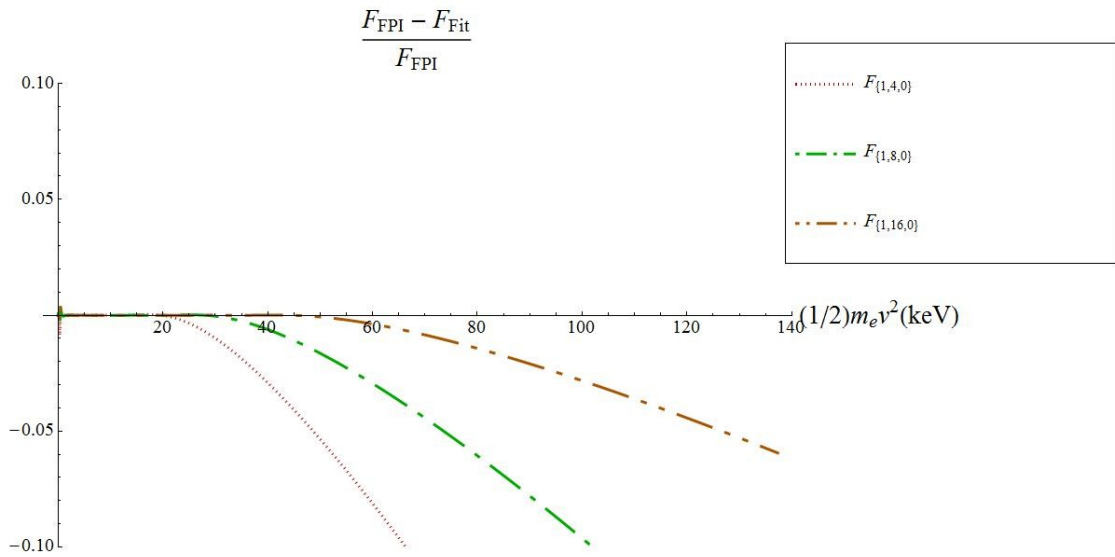
Figure (2.25): Relative error of the results of the fits plotted in Figure (2.24).
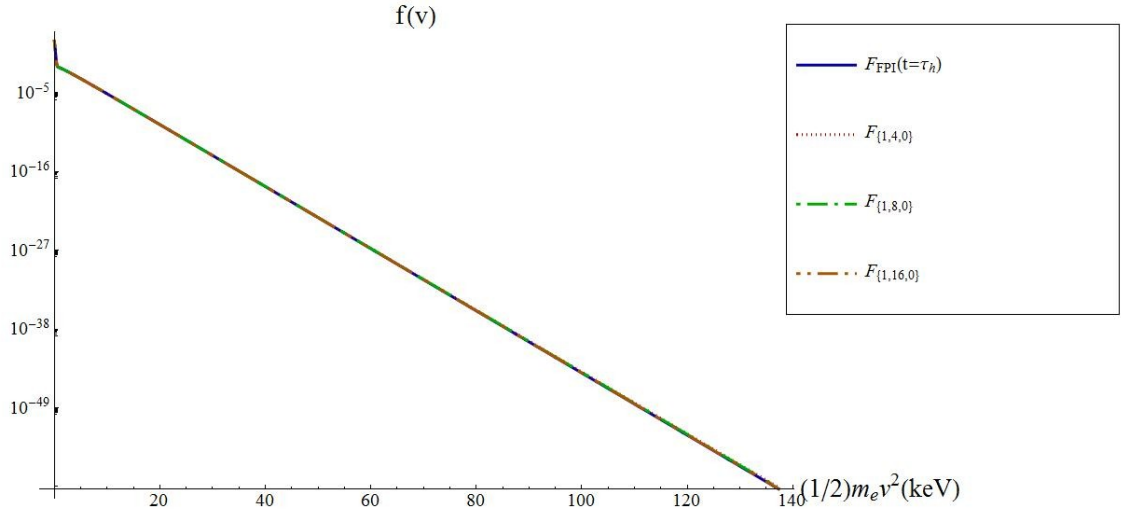
Figure (2.26): Result of the fits of three temperature form of the Laguerre distribution function $\left(\frac{T_c(0)}{T_h(0)} = 0.001, \frac{a_{c0}(0)}{a_{h0}(0)} = 9, t = \tau_{T_h}\right)$.
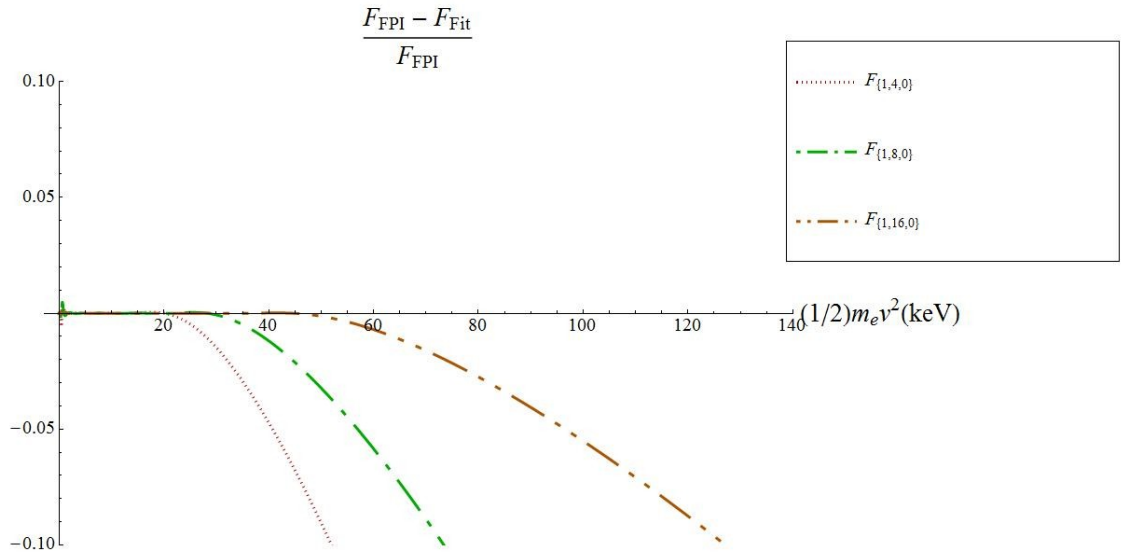
Figure (2.27): Relative error of the results of the fits plotted in Figure (2.26).

Note:

The actual distribution function (*i.e.* "FPI" distribution function) evolves in time. Here as a sample, Figure (2.28) shows the "FPI" distribution function after a half collision time and after one collision time (for hot temperature) as a function of energy in the low energy region. The initial temperature ratio is $\left(\frac{T_c(0)}{T_h(0)} = 0.001\right)$ and the initial density ratio is $\left(\frac{a_{c0}(0)}{a_{h0}(0)} = 9\right)$. Figure

41

(2.29) shows the same plot up to higher energy. On Figure (2.28), we see very well that the cold temperature increases rapidly, and that there is a sharp bend at an energy of several T_c. It is remarkable that this is well reproduced by the Laguerre form. At high energy, we also get an excellent fit.
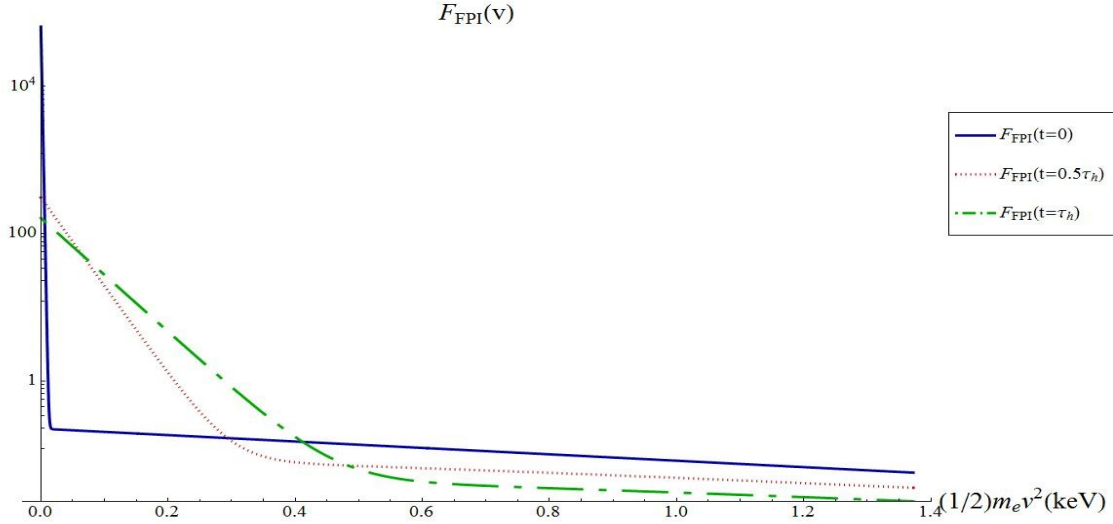
Figure (2.28): "FPI" distribution function at initial state, after a half collision time and after one collision time in the low energy region for the time evolution of the distribution function initialized with $\left(\frac{T_c(0)}{T_h(0)} = 0.001, \frac{a_{c0}(0)}{a_{h0}(0)} = 9\right)$.
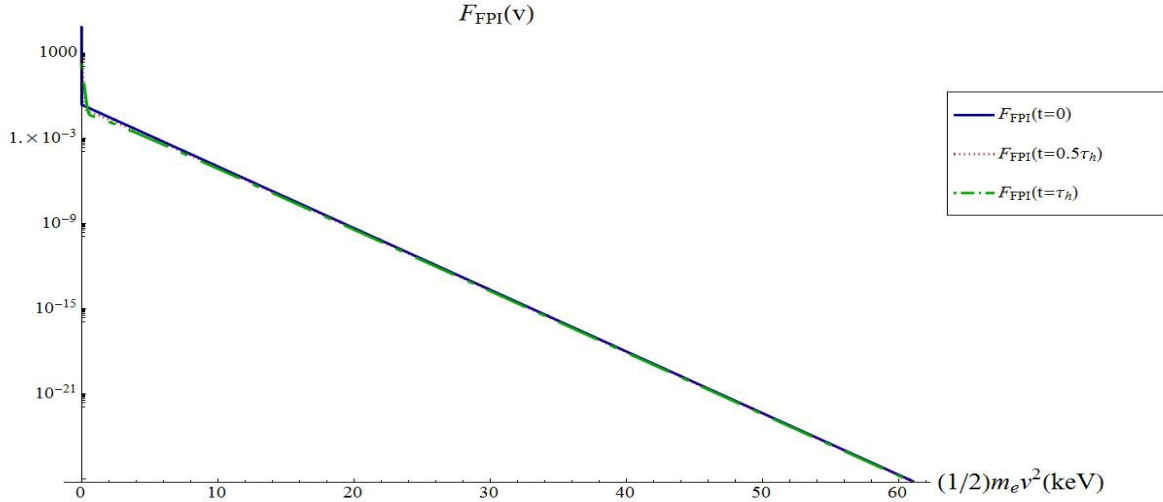
Figure (2.29): "FPI" distribution function at initial state, after a half collision time and after one collision time (hot temperature) in the high energy region for the time evolution of the distribution function initialized with $\left(\frac{T_c(0)}{T_h(0)} = 0.001, \frac{a_{c0}(0)}{a_{h0}(0)} = 9\right)$.

The results show that for low temperature ratios $\left(\frac{T_c(0)}{T_h(0)} \leq 0.1\right)$ a three temperature form of the Laguerre distribution function is a more suitable than a one or two temperature form for representing the time evolution of the distribution function.

To conclude, for simulating the time evolution of the distribution function with any given initial temperature ratio we choose a proper form of the Laguerre distribution function according to:

$$
\begin{cases}
0.5 \leq \dfrac{T_c(0)}{T_h(0)} < 1 & \Rightarrow one\ temperature\ form\ of\ the\ Laguerre\ distribution\ function \\[2mm]
0.1 < \dfrac{T_c(0)}{T_h(0)} < 0.5 & \Rightarrow two\ temperature\ form\ of\ the\ Laguerre\ distribution\ function \\[2mm]
\dfrac{T_c(0)}{T_h(0)} \leq 0.1 & \Rightarrow three\ temperature\ form\ of\ the\ Laguerre\ distribution\ function
\end{cases}
$$

$$(2\text{-}30)$$

Chapter 3

Time evolution of the Laguerre distribution function

The simulation of the time evolution of the Laguerre distribution function is based on five necessary parts.

1- Initializing the distribution function. *i.e.* two-Maxwellian form with given temperatures and densities (for colds and hots).

2- Calculating the moments for a given Laguerre distribution function (for any form of the Laguerre distribution function *i.e.* one, two or three temperatures, if we know the values of the coefficients and temperature(s), we can construct the Laguerre distribution function, and hence, the moments are easily calculated).

3- Choosing a proper form of the Laguerre distribution function by considering the initial temperature ratio $\left(\frac{T_c(0)}{T_{h(0)}}\right)$ according to (2-30). *i.e.* one, two or three temperatures.

4- Calculating the rates of change of the moments due to $e - e$ collisions at any time step for a given Laguerre distribution function. The moments are updated accordingly.

5- Making a proper fit and finding new coefficients and temperature(s) $(a_{\eta i}(t), T_\eta(t))$ of the Laguerre distribution function, so that the updated moments are matched.

3.1. **Initializing the distribution function (two-Maxwellian).**

Equation (2-8) showed the form of a Laguerre distribution function. By substituting $i = 0$, we can get the form of a two Maxwellian distribution function:

$$f_{\{0,0\}}(v, t = 0) = \frac{4}{\sqrt{\pi}} \Sigma_\eta T_\eta(t = 0)^{-\frac{3}{2}} a_{\eta 0}(t = 0) \exp\left(-\frac{v^2}{T_\eta(t=0)}\right) \qquad (3\text{-}1)$$

This distribution evolves in time under the effect of the collision operator. Non-Maxwellian distributions appear in later timesteps and we will try to express them as a Laguerre distribution function in later timesteps.

3.2. $e - e$ **collision operator for a given Laguerre distribution function.**

Equations (1-9) through (1-13) represented the $e - e$ collision operator. Here, we rewrite the equation for the isotropic part of the distribution function $l = 0$:

$$\left(\frac{\partial f_0}{\partial t}\right)_{e-e} = \frac{1}{v^2} \frac{\partial}{\partial v}\left[v^2 \left(D_{\parallel-0}(v)\frac{\partial f_0}{\partial v} + C_0(v)f_0\right)\right] \qquad (3\text{-}2)$$

$$C_0(v) = \frac{4\pi\alpha}{v^2}\int_0^v u^2 f_0(u)\,du \tag{3-3}$$

$$D_{\|-0}(v) = \frac{8\pi\alpha}{3}\left(\int_v^\infty u\,f_0(u)\,du + \left(\frac{1}{v^3}\right)\int_0^v u^4 f_0(u)\,du\right) \tag{3-4}$$

$$\alpha = \frac{4\pi e^4 \mathrm{Ln}\,(\Lambda)}{m_e^4}\ (\mathrm{cgs}) \tag{3-5}$$

For convenience, we can write the genral form of the Laguerre distribution function (equation (2-8)) as a sum of basis functions, each multiplied by its coefficient:

$$\begin{cases} F(v,t) = F_{\{N_c,N_m,N_h\}}(v,t) = \sum_\eta \sum_{i=0}^{N_\eta} a_{\eta i}(t) F_{\eta i}(v,t) \\ \text{where } F_{\eta i}(v,t) = \frac{4}{\sqrt{\pi}} T_\eta(t)^{-\frac{3}{2}} \exp\left(-\frac{v^2}{T_\eta(t)}\right) L_i^{\left(\frac{1}{2}\right)}\left(\frac{v^2}{T_\eta(t)}\right) \end{cases} \tag{3-6}$$

Rewriting the collision operator for the Laguerre distribution function as a sum of all possible collisions between these basis functions (in the spherical Rosenbluth potentials approximation [6]), and remembering that the electron-electron collision operator is bilinear in the distribution function, we get:

$$\left(\frac{\partial F(v,t)}{\partial t}\right)_{e-e} = \sum_\eta \sum_{p=0}^{N_\eta} \sum_\zeta \sum_{q=0}^{N_\zeta} a_{\zeta q}(t) a_{\eta p}(t) Coll\{F_{\zeta q}(v,t), F_{\eta p}(v,t)\} \tag{3-7}$$

$$\begin{cases} Coll\{F_{\zeta q}(v,t), F_{\eta p}(v,t)\} \overset{\text{def}}{=} \frac{1}{v^2}\frac{\partial}{\partial v}\left[v^2\left(D_{\eta p}(v,t)\frac{\partial F_{\zeta q}(v,t)}{\partial v} + C_{\eta p}(v,t) F_{\zeta q}(v,t)\right)\right] \\ C_{\eta p}(v,t) \overset{\text{def}}{=} \frac{4\pi\alpha}{v^2}\int_0^v u^2 F_{\eta p}(u,t)\,du \\ D_{\eta p}(v,t) \overset{\text{def}}{=} \frac{4\pi\alpha}{3}\left(\int_v^\infty u\,F_{\eta p}(u,t)\,du + \left(\frac{1}{v^3}\right)\int_0^v u^4 F_{\eta p}(u,t)\,du\right) \end{cases} \tag{3-8}$$

To shorten the notation, we write $C_{\eta p}(v,t)$ and $D_{\eta p}(v,t)$ instead of $C_{0,\eta p}(v,t)$ and $D_{\|-0,\eta p}(v,t)$.

After some lengthy algebra, we obtain the following expressions for $C_{\eta p}(v,t)$ and $D_{\eta p}(v,t)$. The steps to obtain these expressions from eq. (3.8) are explained in Appendix B.

$$C_{\eta p}(v,t) = \begin{cases} 8\sqrt{\pi}\,\alpha\left(\frac{\sqrt{\pi}}{2v^2}\,\mathrm{Erf}\left(\sqrt{\frac{v^2}{T_\eta(t)}}\right) - T_\eta(t)^{-\frac{1}{2}}\frac{e^{-\frac{v^2}{T_\eta(t)}}}{v}\right), & p = 0 \\ \left(\frac{8\sqrt{\pi}\,\alpha}{p}\right) T_\eta(t)^{-\frac{3}{2}} v\, e^{-\frac{v^2}{T_\eta(t)}} L_{p-1}^{\left(\frac{3}{2}\right)}\left(\frac{v^2}{T_\eta(t)}\right), & p \geq 1 \end{cases} \tag{3-9}$$

$$D_{\eta 0}(v,t) = 4\sqrt{\pi}\alpha\,T_\eta(t)^{-\frac{1}{2}}\left(-\frac{T_\eta(t)}{v^2}\,e^{-\frac{v^2}{T_\eta(t)}} + \frac{\sqrt{\pi}}{2}\left(\frac{T_\eta(t)}{v^2}\right)^{\frac{3}{2}} Erf\left(\sqrt{\frac{v^2}{T_\eta(t)}}\right)\right),\ p = 0 \tag{3-10}$$

$$D_{\eta 1}(v,t) =$$

$$4\sqrt{\pi}\alpha\, T_\eta(t)^{-\frac{1}{2}}\left(\left(\frac{T_\eta(t)}{v^2}+1\right)e^{-\frac{v^2}{T_\eta(t)}}-\frac{\sqrt{\pi}}{2}\left(\frac{T_\eta(t)}{v^2}\right)^{\frac{3}{2}}Erf\left(\sqrt{\frac{v^2}{T_\eta(t)}}\right)\right),\ p=1 \qquad (3\text{-}11)$$

$$D_{\eta p}(v,t)=\frac{8\sqrt{\pi}\alpha}{3}T_\eta(t)^{-\frac{1}{2}}\left(e^{-\frac{v^2}{T_\eta(t)}}L_p^{\left(-\frac{1}{2}\right)}\left(\frac{v^2}{T_\eta(t)}\right)+\frac{v^2}{T_\eta(t)}\left(\frac{1}{p(p-1)}\right)\left(p\,L_{p-1}^{\left(\frac{3}{2}\right)}\left(\frac{v^2}{T_\eta(t)}\right)e^{-\frac{v^2}{T_\eta(t)}}-\right.\right.$$

$$\left.\left.L_{p-1}^{\left(\frac{5}{2}\right)}\left(\frac{v^2}{T_\eta(t)}\right)e^{-\frac{v^2}{T_\eta(t)}}\right)\right),\ p\geq 2 \qquad (3\text{-}12)$$

We now calculate the $Coll\{F_{\zeta q}(v,t),F_{\eta p}(v,t)\}$ term in (3-8) for these three different situations $(p=0,\ p=1,\ p\geq 2)$ (see Appendix B). We obtain:

$$\left(\frac{\partial F(v,t)}{\partial t}\right)_{e-e}=\sum_\eta\sum_{p=0}^{N_\eta}\sum_\zeta\sum_{q=0}^{N_\zeta}a_{\zeta q}(t)a_{\eta p}(t)Coll\{F_{\zeta q}(\gamma_{\zeta\eta}x_\eta),F_{\eta p}(x_\eta)\} \qquad (3\text{-}13)$$

$$Coll\{F_{\zeta q}(\gamma_{\zeta\eta}x_\eta),F_{\eta 0}(x_\eta)\}=$$

$$-Co_{\zeta q\eta 0}e^{-\left((\gamma_{\zeta\eta}+1)x_\eta\right)}\left(-\left(\frac{\sqrt{\pi}}{2}\right)\gamma_{\zeta\eta}e^{x_\eta}\left(\frac{Erf(\sqrt{x_\eta})}{\sqrt{x_\eta}}\right)\left(-L_q^{\left(\frac{3}{2}\right)}(\gamma_{\zeta\eta}x_\eta)+\gamma_{\zeta\eta}L_q^{\left(\frac{5}{2}\right)}(\gamma_{\zeta\eta}x_\eta)\right)+\right.$$

$$\left.\left(-L_q^{\left(\frac{1}{2}\right)}(\gamma_{\zeta\eta}x_\eta)+\gamma_{\zeta\eta}{}^2L_q^{\left(\frac{5}{2}\right)}(\gamma_{\zeta\eta}x_\eta)\right)\right),\ p=0 \qquad (3\text{-}14)$$

$$Coll\{F_{\zeta q}(\gamma_{\zeta\eta}x_\eta),F_{\eta 1}(x_\eta)\}=-Co_{\zeta q\eta 1}e^{-\left((\gamma_{\zeta\eta}+1)x_\eta\right)}\left(L_q^{\left(\frac{1}{2}\right)}(\gamma_{\zeta\eta}x_\eta)\left(-\frac{3}{2}+x_\eta\right)+\right.$$

$$\left.\left(\frac{1}{2}\right)\gamma_{\zeta\eta}L_q^{\left(\frac{3}{2}\right)}(\gamma_{\zeta\eta}x_\eta)+\gamma_{\zeta\eta}{}^2L_q^{\left(\frac{5}{2}\right)}(\gamma_{\zeta\eta}x_\eta)\left(\left(\frac{\sqrt{\pi}}{2}\right)e^{x_\eta}\left(\frac{Erf[\sqrt{x_\eta}]}{\sqrt{x_\eta}}\right)-(x_\eta+1)\right)\right),\ p=1\quad(3\text{-}15)$$

$$Coll\{F_{\zeta q}(\gamma_{\zeta\eta}x_\eta),F_{\eta p}(x_\eta)\}=$$

$$Co_{\zeta q\eta p}\,e^{-\left((\gamma_{\zeta\eta}+1)x_\eta\right)}\left(L_q^{\left(\frac{1}{2}\right)}(x_\eta)L_q^{\left(\frac{1}{2}\right)}(\gamma_{\zeta\eta}x_\eta)+\left(\frac{1}{p-1}\right)\gamma_{\zeta\eta}^2x_\eta L_{p-1}^{\left(\frac{1}{2}\right)}(x_\eta)L_q^{\left(\frac{5}{2}\right)}(\gamma_{\zeta\eta}x_\eta)-\right.$$

$$\left.\left(\frac{1}{p(p-1)}\right)\gamma_{\zeta\eta}^2x_\eta L_{p-1}^{\left(\frac{3}{2}\right)}(x_\eta)L_q^{\left(\frac{5}{2}\right)}(\gamma_{\zeta\eta}x_\eta)-\left(\frac{1}{2}\right)\left(\frac{1}{p}\right)\gamma_{\zeta\eta}L_{p-1}^{\left(\frac{1}{2}\right)}(x_\eta)L_q^{\left(\frac{3}{2}\right)}(\gamma_{\zeta\eta}x_\eta)\right),\ p\geq 2\quad(3\text{-}16)$$

Where for all three cases we have:

$$\begin{cases} Co_{\zeta q \eta p} = 64\,\alpha\,T_\zeta(t)^{-\frac{3}{2}}T_\eta(t)^{-\frac{3}{2}} \\ x_\eta = \dfrac{v^2}{T_\eta(t)} \\ x_\zeta = \dfrac{v^2}{T_\zeta(t)} = \gamma_{\zeta\eta}x_\eta \\ \gamma_{\zeta\eta} = \left(\dfrac{T_\eta(t)}{T_\zeta(t)}\right) \\ \mathcal{F}_{\eta p}(x_\eta) = F_{\eta p}(v,t) \\ \mathcal{F}_{\zeta q}(x_\zeta) = F_{\zeta q}(v,t) = \mathcal{F}_{\eta p}(\gamma_{\zeta\eta}x_\eta) \end{cases} \qquad (3\text{-}17)$$

3.3. Rates of change of the moments due to $e-e$ collisions for a given Laguerre distribution function.

By combining the above equations, the rates of change of the moments due to $e-e$ collisions for a Laguerre distribution function $F(v,t)$ are therefore given by:

$$\left(\frac{\partial M_k}{\partial t}\right)_{e-e} = \int_0^\infty v^k \left(\frac{\partial F(v,t)}{\partial t}\right)_{e-e} dv =$$

$$\sum_\eta \sum_{p=0}^{N_\eta} \sum_\zeta \sum_{q=0}^{N_\zeta} a_{\zeta q}(t)a_{\eta p}(t) \int_0^\infty v^k Coll\{F_{\zeta q}(v,t), F_{\eta p}(v,t)\}dv =$$

$$\sum_\eta \sum_{p=0}^{N_\eta} \sum_\zeta \sum_{q=0}^{N_\zeta} a_{\zeta q}(t)a_{\eta p}(t)\xi_{k\zeta q \eta p}(T_\zeta, T_\eta) \qquad (3\text{-}18)$$

where we define $\xi_{k\zeta q \eta p}(T_\zeta, T_\eta)$ as:

$$\xi_{k\zeta q \eta p}(T_\zeta, T_\eta) = \int_0^\infty v^k Coll\{F_{\zeta q}(v,t), F_{\eta p}(v,t)\}dv =$$

$$\left(\frac{1}{2}\right)T_\eta(t)^{\frac{k+1}{2}}\int_0^\infty x_\eta^{\frac{k-1}{2}}Coll\{\mathcal{F}_{\zeta q}(\gamma_{\zeta\eta}x_\eta), \mathcal{F}_{\eta p}(x_\eta)\}dx_\eta \qquad (3\text{-}19)$$

Considering (3-14), (3-15), (3-16), (3-17) and (3-19), we can write:

$$\xi_{k\zeta q\eta 0}(T_\zeta, T_\eta) =$$

$$-\left(\frac{\sqrt{\pi}}{4}\right)Co_{\zeta q\eta 0}\gamma_{\zeta\eta}T_\eta(t)^{\frac{k+1}{2}}S1_{\zeta\eta q\left(\frac{3}{2}\right)\left(\frac{k}{2}-1\right)} + \left(\frac{\sqrt{\pi}}{4}\right)Co_{\zeta q\eta 0}\gamma_{\zeta\eta}^2 T_\eta(t)^{\frac{k+1}{2}}S1_{\zeta\eta q\left(\frac{5}{2}\right)\left(\frac{k}{2}-1\right)} +$$

$$\left(\frac{1}{2}\right)Co_{\zeta q\eta 0}T_\eta(t)^{\frac{k+1}{2}}S2_{\zeta\eta q0\left(\frac{1}{2}\right)\left(\frac{1}{2}\right)\left(\frac{k-1}{2}\right)} - \left(\frac{1}{2}\right)Co_{\zeta q\eta 0}\gamma_{\zeta\eta}^2 T_\eta(t)^{\frac{k+1}{2}}S2_{\zeta\eta q0\left(\frac{5}{2}\right)\left(\frac{1}{2}\right)\left(\frac{k-1}{2}\right)}, \quad p=0 \quad (3\text{-}20)$$

$$\xi_{k\zeta q\eta 1}(T_\zeta, T_\eta) =$$

$$-\left(\frac{1}{4}\right)Co_{\zeta q\eta 1}\gamma_{\zeta\eta}T_\eta(t)^{\frac{k+1}{2}}S2_{\zeta\eta q0\left(\frac{3}{2}\right)\left(\frac{1}{2}\right)\left(\frac{k-1}{2}\right)} + \left(\frac{3}{4}\right)Co_{\zeta q\eta 1}T_\eta(t)^{\frac{k+1}{2}}S2_{\zeta\eta q0\left(\frac{1}{2}\right)\left(\frac{1}{2}\right)\left(\frac{k-1}{2}\right)} -$$

$$\left(\frac{1}{2}\right)Co_{\zeta q\eta 1}T_\eta(t)^{\frac{k+1}{2}}S2_{\zeta\eta q0\left(\frac{1}{2}\right)\left(\frac{1}{2}\right)\left(\frac{k+1}{2}\right)} - \left(\frac{\sqrt{\pi}}{4}\right)Co_{\zeta q\eta 1}\gamma_{\zeta\eta}^2 T_\eta(t)^{\frac{k+1}{2}}S1_{\zeta\eta q\left(\frac{5}{2}\right)\left(\frac{k}{2}-1\right)} +$$

$$\left(\frac{1}{2}\right)Co_{\zeta q\eta 1}\gamma_{\zeta\eta}^2 T_\eta(t)^{\frac{k+1}{2}}S2_{\zeta\eta q0\left(\frac{5}{2}\right)\left(\frac{1}{2}\right)\left(\frac{k+1}{2}\right)} + \left(\frac{1}{2}\right)Co_{\zeta q\eta 1}\gamma_{\zeta\eta}^2 T_\eta(t)^{\frac{k+1}{2}}S2_{\zeta\eta q0\left(\frac{5}{2}\right)\left(\frac{1}{2}\right)\left(\frac{k-1}{2}\right)}, \quad p=1$$

$$(3\text{-}21)$$

$$\xi_{k\zeta q\eta p}(T_\zeta, T_\eta) =$$

$$\left(\tfrac{1}{2}\right)Co_{\zeta q\eta p}T_\eta(t)^{\frac{k+1}{2}}S2_{\zeta\eta qp\left(\frac{1}{2}\right)\left(\frac{1}{2}\right)\left(\frac{k-1}{2}\right)} + \left(\tfrac{1}{2}\right)\left(\tfrac{1}{p-1}\right)Co_{\zeta q\eta p}\gamma_{\zeta\eta}^2 T_\eta(t)^{\frac{k+1}{2}}S2_{\zeta\eta q(p-1)\left(\frac{5}{2}\right)\left(\frac{1}{2}\right)\left(\frac{k+1}{2}\right)} -$$

$$\left(\tfrac{1}{2}\right)\left(\tfrac{1}{p(p-1)}\right)Co_{\zeta q\eta p}\gamma_{\zeta\eta}^2 T_\eta(t)^{\frac{k+1}{2}}S2_{\zeta\eta q(p-1)\left(\frac{5}{2}\right)\left(\frac{3}{2}\right)\left(\frac{k+1}{2}\right)} -$$

$$\left(\tfrac{1}{4}\right)\left(\tfrac{1}{p}\right)Co_{\zeta q\eta p}\gamma_{\zeta\eta}T_\eta(t)^{\frac{k+1}{2}}S2_{\zeta\eta q(p-1)\left(\frac{3}{2}\right)\left(\frac{1}{2}\right)\left(\frac{k-1}{2}\right)}, \quad p \geq 2 \qquad (3\text{-}22)$$

We recall that in our work we always use even moments, *i.e.* k is an even integer larger than or equal to 0 $\left(\frac{k}{2}\epsilon\mathbb{Z}^+\right)$.

$S1_{\zeta\eta n\alpha_1 i}$ and $S2_{\zeta\eta n m\alpha_1\alpha_2 h}$ are given by the formulas below:

$$S1_{\zeta\eta n\alpha_1 i} = \int_0^\infty x_\eta{}^i Erf\left[\sqrt{x_\eta}\right]e^{-(\gamma_{\zeta\eta}x_\eta)}L_n^{(\alpha_1)}(\gamma_{\zeta\eta}x_\eta)dx_\eta, \ i \in \mathbb{Z} \geq -1 \qquad (3\text{-}23)$$

$$S2_{\zeta\eta n m\alpha_1\alpha_2 h} = \int_0^\infty x_\eta{}^h e^{-\left((\gamma_{\zeta\eta}+1)x_\eta\right)}L_n^{(\alpha_1)}(\gamma_{\zeta\eta}x_\eta)L_m^{(\alpha_2)}(x_\eta)dx_\eta, \ \left(h+\tfrac{1}{2}\right) \in \mathbb{Z}^+ \quad (3\text{-}24)$$

Hence, by solving the integrals (3-23) and (3-24), we can calculate the rates of change of the moments.

By expanding the generalized Laguerre polynomials (3-23) becomes:

$$S1_{\zeta\eta n\alpha_1 i} = \sum_{w=0}^n \frac{(-1^w)}{w!}\binom{n+\alpha_1}{n-w}\gamma_{\zeta\eta}^w \overline{S1}_{\zeta\eta n\alpha_1(i+w)}, \qquad i \in \mathbb{Z} \geq -1, \qquad w \in \mathbb{Z}^+$$

$$\overline{S1}_{\zeta\eta n\alpha_1 j} = \int_0^\infty x_\eta{}^j Erf\left[\sqrt{x_\eta}\right]e^{-(\gamma_{\zeta\eta}x_\eta)}dx_\eta, \ j \in \mathbb{Z} \geq -1 \qquad (3\text{-}25)$$

For $(j = -1)$, using the Taylor expansion series for both the error function and the exponential function in equation (3-25) leads to the result below:

$$\overline{S1}_{\zeta\eta n\alpha_1(-1)} = Ln\left[\sqrt{\tfrac{1}{\gamma_{\zeta\eta}}} + \sqrt{\tfrac{1}{\gamma_{\zeta\eta}}+1}\right] = 2\,ArcSinh\left[\sqrt{\tfrac{1}{\gamma_{\zeta\eta}}}\right], \ j = -1 \qquad (3\text{-}26)$$

And for $(j \geq 0)$, by integrating by parts we have,

$$\overline{S1}_{\zeta\eta n\alpha_1 j} = \left(\tfrac{1}{\sqrt{\pi}}\right)\left(\tfrac{1}{\gamma_{\zeta\eta}}\right)\left(\tfrac{1}{\gamma_{\zeta\eta}+1}\right)^{j+\frac{1}{2}}\Gamma\left[j+\tfrac{1}{2}\right] + \left(\tfrac{j}{\gamma_{\zeta\eta}}\right)\overline{S1}_{\zeta\eta n\alpha_1(j-1)}, \ j \geq 0 \qquad (3\text{-}27)$$

Equation (3-27) is a recurrence relation to calculate $\left(\overline{S1}_{\zeta\eta n\alpha_1 j}\right)$.

Now, for (3-24), by expanding the generalized Laguerre polynomials we get:

$$S2_{\zeta\eta n m\alpha_1\alpha_2 h} = \sum_{i=0}^n \sum_{j=0}^m \frac{(-1)^{i+j}}{i!j!}\binom{n+\alpha_1}{n-i}\binom{m+\alpha_2}{m-j}\gamma_{\zeta\eta}^i\left(\tfrac{1}{1+\gamma_{\zeta\eta}}\right)^{h+i+j+1}\Gamma[h+i+j+1],$$

$$\left(h+\tfrac{1}{2}\right) \in \mathbb{Z}^+ \qquad (3\text{-}28)$$

3.4. **Time evolution of the moments**

In the time evolution of the moments (as a result of the time evolution of the distribution function), we use the 1st order approximation in the time-dependence for the moments and we neglect the 2nd, 3rd,.., *etc.* order terms. Expanding M_k at time t_n, one obtains:

$$M_k^{t_{n+1}} = M_k^{t_n} + \left(\frac{\partial M_k}{\partial t}\right)_{e-e}^{t_n} \Delta t + \underbrace{\frac{1}{2}\left(\frac{\partial^2 M_k}{\partial t^2}\right)_{e-e}^{t_n} \Delta t^2 + \cdots}_{\simeq 0} \tag{3-29}$$

This is true only if we keep Δt sufficiently small:

$$\frac{1}{2}\left(\frac{\partial^2 M_k}{\partial t^2}\right)_{e-e}^{t_n} \Delta t^2 \ll \left(\frac{\partial M_k}{\partial t}\right)_{e-e}^{t_n} \Delta t \Rightarrow \Delta t \ll 2 \frac{\left(\frac{\partial M_k}{\partial t}\right)_{e-e}^{t_n}}{\left(\frac{\partial^2 M_k}{\partial t^2}\right)_{e-e}^{t_n}} \tag{3-30}$$

To summarize, at each time we can calculate the moments for the next time analytically, by using equations 3-18 through 3-30, and by applying the fitting procedure described in chapter 2, we get the updated temperatures and coefficients.

Chapter 4

Numerical results for the time evolution of the distribution function

We are now able to simulate the time evolution of the distribution function based on the procedure explained in the previous chapter which is illustrated and summarized in Figure (4.1).

In this chapter, we provide the numerical results of the time evolution of the Laguerre distribution function initialized with a two-Maxwellian distribution function with different temperature and density ratios. Table (4.1) is the list of the processed cases. For most of the cases, the code represented the time evolution of the distribution function well. But for seven cases of this table (*i.e.* cases number 9, 10, 22, 23, 28, 37 and 47 in Table (4.1)) it crashed and could not process the time evolution of the distribution function after a certain time. The main reason for this sort of crash is choosing inappropriate numbers of generalized Laguerre polynomials for one or more populations (cold, medium or/and hot). Even if we satisfy $\sum_\eta (N_\eta + 2)$ moment equations for each case at any single timestep, it does not necessarily mean that we can reproduce the time evolution of the distribution function for any arbitrary number of Laguerre terms. We need to choose properly the number of Laguerre terms for each population (*i.e.* cold, medium and hot) by considering the structure of the distribution function. For example, for the time evolution of the distribution function for initial temperature ratio 2:1 we cannot use the 2 temperature form of the Laguerre distribution function with $(N_c > 7)$ (*i.e.* cases number 9 and 10 in Table (4.1) because the contribution of the cold component to the high moments is negligible (due to the $T_c^{(\frac{k}{2}-1)}$ factor) compared to that of the hot component ($T_h^{(\frac{k}{2}-1)}$ factor), and the system of equations then becomes, in effect, overdetermined for the coefficients for the hot component, and underdetermined for the coefficients of the cold component. Thus, using 8 or more Laguerre terms for the colds causes a very early crash in the process of the time evolution of the distribution function. It has not yet been possible to find a robust procedure to always avoid such crashes, but when it happens early, the code was programmed to restart with a different number of terms in the Laguerre expansion, until a set was found which produced appropriate results. This is why the number of terms differs for different temperature ratios.

1 Initialize the distribution function *i.e.* two Maxwellians

2 Calculate the moments (section 2.2) $M_k(t_n = 0)$, $n = 0$

3 Select the proper form of the Laguerre distribution function (one, two or three temperatures) (equation (2-30))

4 Calculate the rates of change of the moments (section 3.3) $\dfrac{\partial M_k(t_n)}{\partial t}$

5 Advance time $t_{n+1} = t_n + \Delta t$

6 Update moments for the new timestep (section 3.4) $M_k(t_{n+1}) = M_k(t_n) + \dfrac{\partial M_k(t_n)}{\partial t}\Delta t$

7 Update the coefficients and temperature(s) of the Laguerre distribution function by fitting to the new moments (section 2.3) $\left(a_{\eta i}(t_{n+1}), T_\eta(t_{n+1})\right)$

8 Prepare for the next timestep $n = n + 1$

Figure (4.1): Procedure for simulating the time evolution of the Laguerre distribution function.

No.	$\frac{T_c}{T_h}$	$\frac{a_{c0}}{a_{h0}}$	N_T	N_c	N_m	N_h	$\frac{t_L}{\tau}$	Energy of the 10% error							
								$\frac{t}{\tau}=\frac{1}{2}$	1	5	10	38	48	91	100
1	1/2	1/1	1	06	Na	Na	10	17.31	18.57	13.16	14.55				
2		9/1		04	Na	Na	10	11.66	10.87	10.28	9.257				
3			1	06	Na	Na	10	16.35	16.42	18.95	15.69				
4*				08	Na	Na	10	22.12	22.17	20.35	26.03				
5				16	Na	Na	10	18.07	13.74	16.36	15.57				
6				04	Na	00	10	37.84	22.34	16.13	17.95				
7				05	Na	00	10	43.47	30.27	17.94	16.38				
8**			2	07	Na	00	100	50.60	34.81	20.96	19.39	18.15	17.54	20.68	21.57
9				08	Na	00	0								
10				16	Na	00	0								
11	1/4	1/1	1	09	Na	Na	10	14.97	22.92	19.34	23.72				
12		9/1		04	Na	Na	10	1.214	1.950	3.138	4.527				
13			1	08	Na	Na	10	9.063	8.886	7.720	6.979				
14*				16	Na	Na	10	37.03	37.01	35.71	34.64				
15				04	Na	00	10	29.01	19.56	12.35	6.938				
16				07	Na	00	10	51.90	40.71	25.74	22.46				
17**			2	11	Na	00	100	123.8	108.3	42.02	36.26	28.28	26.94	12.57	14.80
18				16	Na	00	10	20.18	15.98	13.17	13.08				
19			3	06	02	00	10	112.0	81.02	60.31	50.47				
20				08	02	00	10	130.1	93.75	69.87	126.6				
21	1/10	9/1		02	Na	04	10	13.43	10.36	7.453	9.661				
22			2	02	Na	08	1.8	0.64	0.91						
23				02	Na	16	2.6	40.44	28.38						
24				02	04	00	10	62.75	46.81	32.26	29.77				
25				04	04	00	10	98.20	73.66	51.78	47.68				
26**			3	04	06	00	100	122.4	88.29	56.67	52.65	47.99	46.39	40.38	40.74
27				04	08	00	10	134.3	97.88	60.31	1.821				
28				04	16	00	0								
29		99/1	3	02	04	00	10	65.78	49.22	33.67	30.95				
30*				02	08	00	10	100.0	73.31	47.49	43.00				

Legend	
	Code was not run for this interval
	Code is not converging for this interval
N_T	Number of temperatures
t_L	Last produced timestep
τ	Collision time (hot)
*	For these cases 4 figures are provided
**	For these cases 6 figures are provided

No.	$\frac{T_c}{T_h}$	$\frac{a_{c0}}{a_{h0}}$	N_T	Nc	Nm	Nh	$\frac{t_L}{\tau}$	Energy of the 10% error							
								$\frac{t}{\tau}=0.5$	1	5	10	38	48	91	100
31				02	04	00	10	68.38	51.02	33.47	30.63				
32	1/30	9/1	3	02	08	00	10	103.1	74.18	47.37	42.95				
33				02	10	00	10	121.3	86.79	54.44	49.59				
34				01	04	00	10	60.44	44.96	29.05	26.20				
35		967/33	3	02	04	00	10	75.44	59.24	40.89	37.21				
36**	1/100			02	08	00	48	121.3	88.50	54.84	51.94	48.03	0.724		
37				02	16	00	0.9	42.00							
38		9968/32	3	00	04	00	10	51.58	37.26	23.44	20.94				
39*				00	08	00	10	91.96	64.08	37.64	33.12				
40				01	02	00	10	39.32	30.05	20.38	18.59				
41	1/300	9/1	3	01	04	00	10	54.58	40.13	26.78	24.39				
42				02	08	00	10	110.6	78.50	48.24	43.47				
43				01	04	00	10	55.03	40.37	26.82	24.41				
44*				02	06	00	10	91.14	66.98	41.54	37.58				
45	1/1000	9/1	3	01	08	00	10	87.24	62.87	38.13	1.479				
46**				02	08	00	91	111.2	78.95	48.35	43.54	37.11	35.48	27.80	
47				01	16	00	6.4	155.2	106.8	0.785					

Legend	
	Code was not run for this interval
	Code is not converging for this interval
N_T	Number of temperatures
t_L	Last produced timestep
τ	Collision time (hot)
*	For these cases 4 figures are provided
**	For these cases 6 figures are provided

Table (4.1): The initial temperature and density ratios (characterizing the initial two-Maxwellian distribution functions) used for each set of the results (*i.e.* time evolution of the Laguerre distribution function), and quality of the results, as indicated by the energy at which the difference compared to the results obtained from the "FPI" finite difference electron kinetic code reached 10%.

In order to illustrate some of the results, ten (10) of the cases of Table (4.1) are selected (*i.e.* cases number 4, 8, 14, 17, 26, 30, 36, 39, 44 and 46 denoted by (*) and (**)). For each case, four figures are presented as follows:

1- The Laguerre distribution function as a function of energy at different times.

2- The relative error of each plot illustrated in the first figure. The reference distribution function is the one obtained from the "FPI" code at the same physical time.

3- The time evolution of the temperatures (T_η's).

4- The time evolution of some of the coefficients ($a_{\eta i}$'s).

For 5 of these cases (*i.e.* cases number 8, 17, 26, 36 and 46 denoted by (**)), we also have added two extra figures:

5- The time evolution of the moments ($M_{\{N_c,N_m,N_h\},k}(t)$ calculated by using equation (2-9)).

6- The time evolution of the relative deviation of the moments from their ultimate value. The distribution function ultimately tends toward a single Maxwellian with the density ($N_e = M_{\{N_c,N_m,N_h\},2}$, equation (2-10)) and the temperature ($T_e = \left(\frac{2}{3}\right)\frac{M_{\{N_c,N_m,N_h\},4}}{N_e}$, equation (2-11)). Hence, the ultimate value of each moment is the same moment of that single Maxwellian distribution function as given by taking only one term in (2-9) $M_{\{0\},k} = \frac{2}{\sqrt{\pi}}N_e T_e^{(k-1)/2}\Gamma\left(\frac{k+1}{2}\right)$, and the normalized moment's ultimate values are the same, without the factor $\frac{2}{\sqrt{\pi}}\Gamma\left(\frac{k+1}{2}\right)$, *i.e.* $N_e T_e^{(k-1)/2}$.

Note:

For most cases, we ran the code for 10 collision times, except for those denoted by (**), which we ran for 100 collision time $\left(\frac{t}{\tau} = 100\right)$ to study the limitation of the time evolution of the Laguerre distribution function. As will be seen later, it is at the later times that the evolution of the moments is particularly instructive, and explains why the code crashed in some cases: For cases 36 and 46 in Table (4.1), the code crashed at 48 and 91 collision time respectively. By considering the last figure in each case, most of the moments are very close to the moments of a single Maxwellian at the time of the crash. Hence, most of the coefficients except a_{c0} and a_{c1} are small and the code fails to provide a fit and update the coefficients because of the over determination of the linear set of equations at these late times.

4.1. Time evolution of the Laguerre distribution function for a 1:2 initial temperature ratio $\left(\frac{T_c(t=0)}{T_h(t=0)} = \frac{1}{2}\right)$

4.1.1. Single temperature form of the Laguerre distribution function ($N = 08$); 9:1 initial density ratio $\left(\frac{a_{c0}(t=0)}{a_{h0}(t=0)} = 9\right)$ (case no. 4 in Table (4.1))

Figure (4.2) shows the time evolution of a single temperature form of the Laguerre distribution function ($N = 08$) for an initial two-Maxwellian distribution $\left(\frac{T_c(t=0)}{T_h(t=0)} = \frac{1}{2}, \frac{a_{c0}(t=0)}{a_{h0}(t=0)} = 9\right)$. As we expected, according to the fits in sub-section 2.5.1, a single temperature form of the Laguerre distribution function is suitable for representing the time evolution of the distribution function in this situation. Figure (4.3) shows the relative errors of the results of the time evolution of the distribution function compared to "FPI" at the same times $\left(\frac{t}{\tau} = 0.5, 1, 5, 10\right)$. In this case, we have ($N + 2 = 10$) unknowns in the Laguerre distribution function *i.e.* $a_0(t), a_1(t), \dots, a_8(t), T$. We therefore need to calculate the time evolution of 10 moments $(M_{\{N_c,N_m,N_h\},0}, M_{\{N_c,N_m,N_h\},2}, \dots, M_{\{N_c,N_m,N_h\},18})$ to find the right coefficients and temperature at each timestep using the fitting method described in section 2.4.

Figure (4.4) shows the time evolution of the coefficients of the Laguerre distribution function. Since, this is a single temperature case. $a_0(t)$ is always equal to 1 to conserve the density:

$$M_{\{N_c,N_m,N_h\},2} = a_0(t) = a_{c0}(0) + a_{h0}(0) = N_e = 1 \tag{4-1}$$

and $a_0(t)$, $a_1(t)$ and $T(t)$ are responsible for conservation of the energy:

$$M_{\{N_c,N_m,N_h\},4} = \frac{3}{2}\big(a_0(t)T(t) - a_1(t)T(t)\big) = \frac{3}{2}\big(a_{c0}(0)T_c(0) + a_{h0}(0)T_h(0)\big) = 0.825 \Rightarrow$$

$$a_1(t) = 1 - \frac{0.55}{T(t)} \text{ and } T(t) = \frac{0.55}{1 - a_1(t)} \tag{4-2}$$

Due to this simple relation between $T(t)$ and $a_1(t)$, we have not made a separate plot for $T(t)$ for this case. At each timestep, the values of the coefficients and the temperature change in order to satisfy the time evolution of the moments. We note that the coefficients other than a_0 evolve very quickly at the beginning (at t=0, they were all 0, except a_0), and slowly thereafter, and also that their absolute values are considerably smaller than a_0.

Figure (4.2): Time evolution of a single temperature form of the Laguerre distribution function $\left(N = 08, \frac{T_c(t=0)}{T_h(t=0)} = \frac{1}{2}, \frac{a_{c0}(t=0)}{a_{h0}(t=0)} = 9\right)$.

Figure (4.3): Relative error of the time evolution of a single temperature form of the Laguerre distribution function $\left(N = 08, \frac{T_c(t=0)}{T_h(t=0)} = \frac{1}{2}, \frac{a_{c0}(t=0)}{a_{h0}(t=0)} = 9\right)$.

Figure (4.4): Time evolution of the coefficients of the Laguerre distribution function $\left(N = 08, \frac{T_c(t=0)}{T_h(t=0)} = \frac{1}{2}, \frac{a_{c0}(t=0)}{a_{h0}(t=0)} = 9\right)$.

4.1.2. A two temperature form of the Laguerre distribution function ($N_c = 07, N_h = 00$); 9:1 initial density ratio $\left(\frac{a_{c0}(t=0)}{a_{h0}(t=0)} = 9\right)$ (case no. 8 in Table (4.1))

Figure (4.5) shows the time evolution of a two temperature form of the Laguerre distribution function ($N_c = 07$, $N_h = 00$) for an initial two-Maxwellian distribution $\left(\frac{T_c(t=0)}{T_h(t=0)} = \frac{1}{2}, \frac{a_{c0}(t=0)}{a_{h0}(t=0)} = 9\right)$. For this case, we run the code for a longer time. Figure (4.6) shows the relative errors of the results of the time evolution of the distribution function compared to "FPI" at different times $\left(\frac{t}{\tau} = 1, 2, 5, 10, 20, 50, 100\right)$. In this case, we have ($N_c + N_h + 4 = 11$) unknowns in the Laguerre distribution function *i.e.* $a_{c0}(t), a_{c1}(t), \dots, a_{c7}(t), a_{h0}(t), T_c, T_h$. We need to calculate the time evolution of 11 moments ($M_{\{N_c,N_m,N_h\},0}, M_{\{N_c,N_m,N_h\},2}, \dots, M_{\{N_c,N_m,N_h\},20}$) to find the right coefficients and temperatures at each time using the fitting method described in section 2.3.

Figure (4.7) shows the time evolution of the two temperatures. Eventually, after many collision times, $T_c(t)$ tends towards the equilibrium temperature ($T_e = 0.55$). Although, $T_h(t)$ increases gradually and after 100 collision time reaches ($T_h(100\tau_h) \simeq 1.9\text{keV}$), most of the total energy density is in the cold electrons (mostly the $a_{c0}(t)$ term) because a_{h0} is extremely small.

$T_c(100\tau_h) \simeq 0.5284, \qquad T_h(100\tau_h) \simeq 1.893$

$$a_{c0}(100\tau_h) \simeq 1, \qquad a_{c1}(100\tau_h) \simeq -0.04085$$

$$a_{h0}(100\tau_h) \simeq 3.401 \times 10^{-12}$$

$$M_4(0) = \frac{3}{2}N_e T_e = 0.825$$

$$M_{4c0}(100\tau_h) = \frac{3}{2}a_{c0}(100\tau_h)T_c(100\tau_h) \simeq 0.7926$$

$$M_{4c1}(100\tau_h) = -\frac{3}{2}a_{c1}(100\tau_h)T_c(100\tau_h) \simeq 0.0324$$

$$M_{4h0}(100\tau_h) = \frac{3}{2}a_{h0}(100\tau_h)T_h(100\tau_h) \simeq 9.655 * 10^{-12}$$

Although the hot population (*i.e.* $a_{h0}(t)$) diminishes very fast, the electron distribution still remains non-Maxwellian with significant Laguerre terms of order higher than 0 (*i.e.* $a_{c1}, a_{c2}, ...$) even at very late physical times, after many collisions.

Figure (4.8) shows the time evolution of the coefficients of the Laguerre distribution function. All of the coefficients gradually diminish during the time evolution of the Laguerre distribution function except $a_{c0}(t)$. The rapid decrease of $a_{h0}(t)$ is particularly noteworthy. The evolution of the two temperatures might seem, at first sight, to contradict the conservation of energy, but it can be noticed, first, that the density of the hot component $a_{h0}(t)$ decreases gradually to very small values, and also that the absolute value of the term $a_{c1}(t)$, which contributes to the energy density (see (2-11)), decreases gradually.

Figure (4.9) shows the time evolution of the moments of the Laguerre distribution function. Of course, moments 2 and 4 are always constant due to the density and energy conservation. The other moments are tending toward the moments of a single Maxwellian, *i.e.* the ultimate solution of the distribution function at $t \to \infty$. Figure (4.10) shows the deviation of the moments from the moments of this single Maxwellian. In this case, since the initial temperatures are relatively close $\left(\frac{T_c(0)}{T_h(0)} = \frac{1}{2}\right)$, we have a fast relaxation of hot electrons and the moments get close to their ultimate value very fast (*i.e.* moments of a single Maxwellian).

It may be noticed, here and in the following such graphs, that the deviation of moments $k=2$ and $k=4$ is minute, of the order of 10^{-13} or less. This is to be expected, because these are the two conserved quantities, the particle and energy densities: N_e and 3/2 $N_e T$, and deviations are due to round-off errors only. For the other moments, the higher moments relax more slowly to their ultimate value, because the relaxation of faster electrons is slower than that of the lower energy ones. Therefore, it is moment $k=0$ which approaches its ultimate value first.
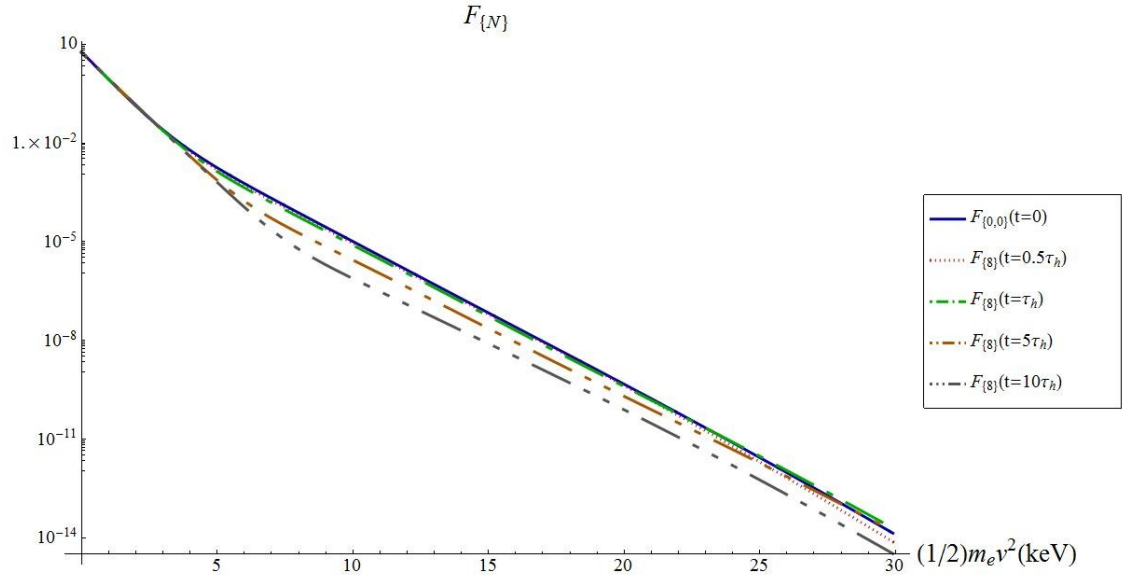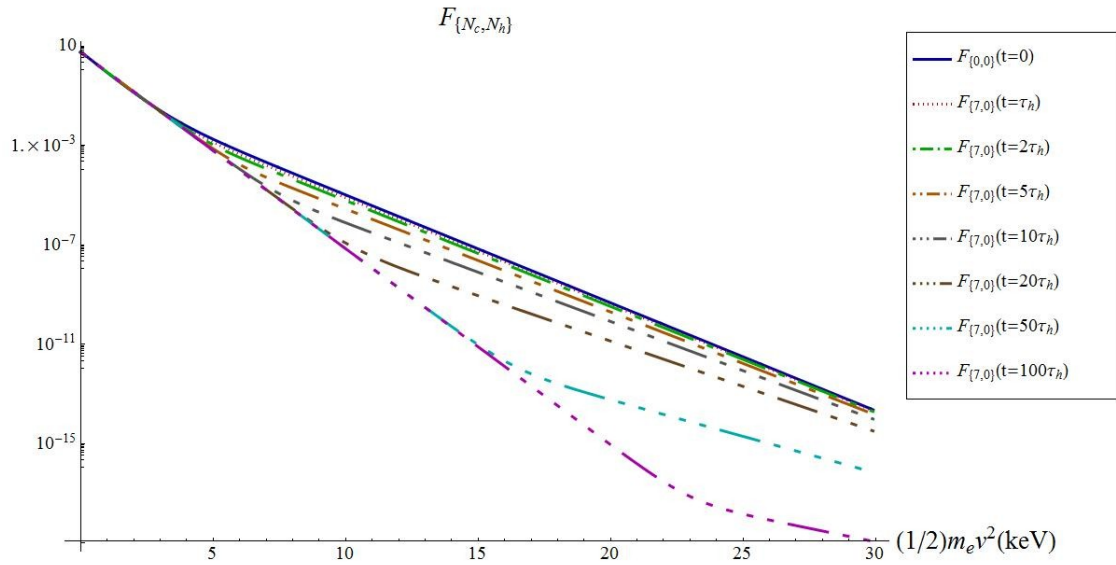
Figure (4.5): Time evolution of a two temperature form of the Laguerre distribution function ($N_c = 07, N_h = 00, \frac{T_c(t=0)}{T_h(t=0)} = \frac{1}{2}, \frac{a_{c0}(t=0)}{a_{h0}(t=0)} = 9$).
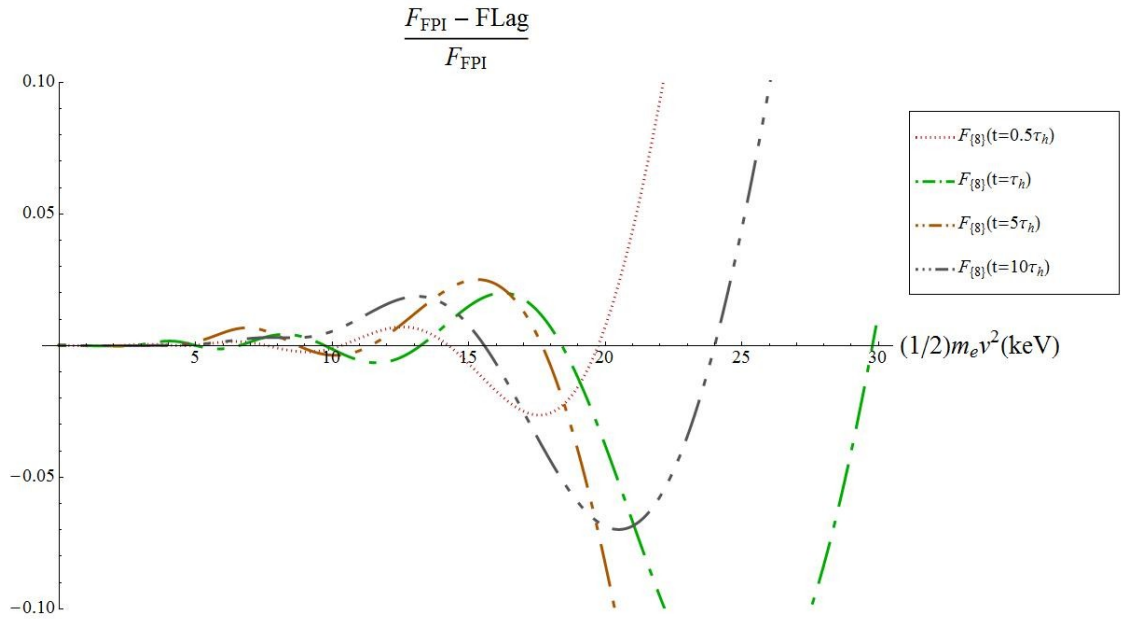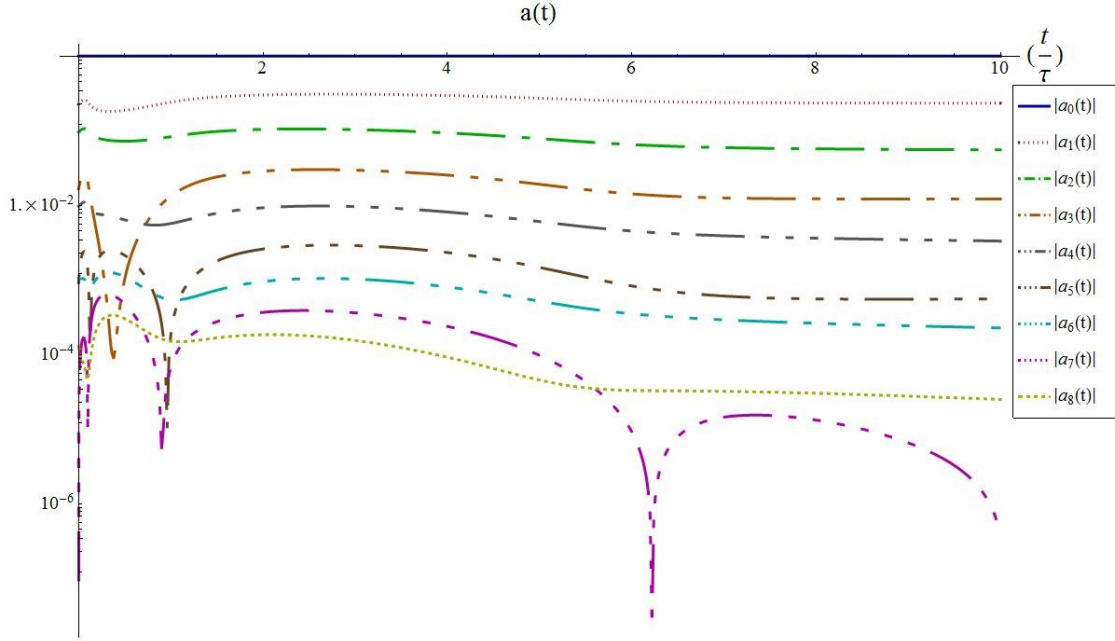

Figure (4.6): Relative error of the time evolution of a two temperature form of the Laguerre distribution function ($N_c = 07, N_h = 00, \frac{T_c(t=0)}{T_h(t=0)} = \frac{1}{2}, \frac{a_{c0}(t=0)}{a_{h0}(t=0)} = 9$).

Figure (4.7): Time evolution of the temperatures of the Laguerre distribution function ($N_c = 07, N_h = 00, \frac{T_c(t=0)}{T_h(t=0)} = \frac{1}{2}, \frac{a_{c0}(t=0)}{a_{h0}(t=0)} = 9$).
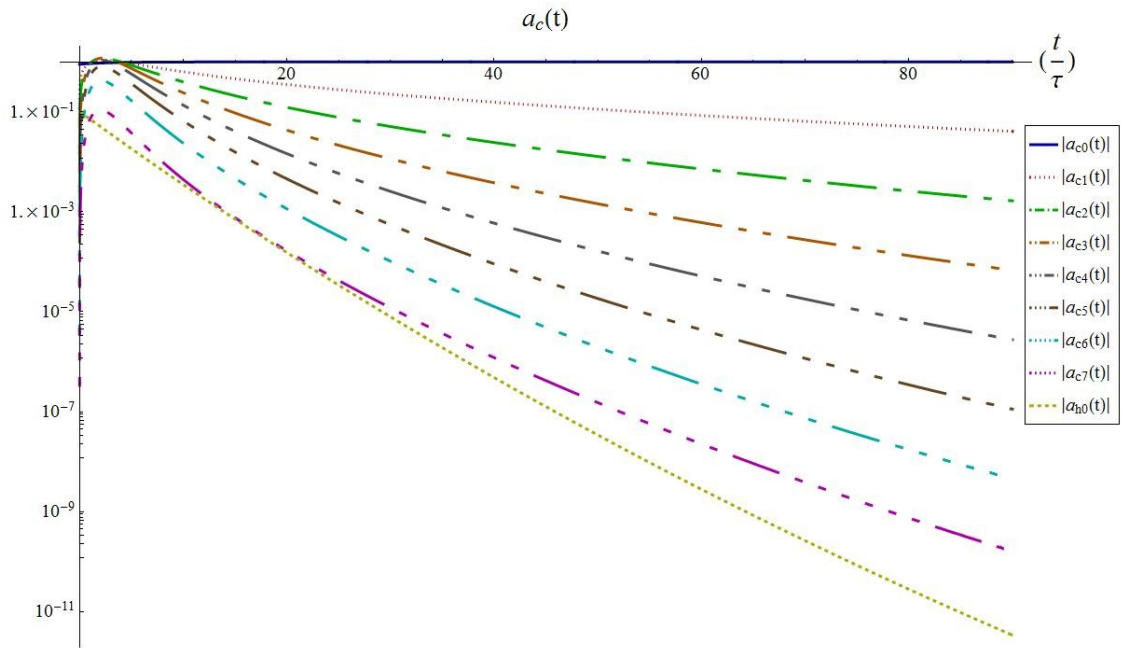
Figure (4.8): Time evolution of the coefficients (cold and hot) of the Laguerre distribution function ($N_c = 07, N_h = 00, \frac{T_c(t=0)}{T_h(t=0)} = \frac{1}{2}, \frac{a_{c0}(t=0)}{a_{h0}(t=0)} = 9$).

Figure (4.9): Time evolution of the moments of the Laguerre distribution function ($N_c = 07, N_h = 00, \frac{T_c(t=0)}{T_h(t=0)} = \frac{1}{2}, \frac{a_{c0}(t=0)}{a_{h0}(t=0)} = 9$).

Figure (4.10): Time evolution of the deviation of the moments of the Laguerre distribution function from the moments of a single Maxwellian $\left(N_c = 07, \ N_h = 00, \ \frac{T_c(t=0)}{T_h(t=0)} = \frac{1}{2}, \ \frac{a_{c0}(t=0)}{a_{h0}(t=0)} = 9 \right)$.

4.2. Time evolution of the Laguerre distribution function for a 1:4 initial temperature ratio $\left(\frac{T_c(t=0)}{T_h(t=0)} = \frac{1}{4}\right)$

4.2.1. A single temperature form of the Laguerre distribution function ($N = 16$); 9:1 initial density ratio $\left(\frac{a_{c0}(t=0)}{a_{h0}(t=0)} = 9\right)$ (case no. 14 in Table (4.1))

Figure (4.11) shows the time evolution of a single temperature form of the Laguerre distribution function ($N = 16$) for an initial two-Maxwellian distribution $\left(\frac{T_c(t=0)}{T_h(t=0)} = \frac{1}{4}\right)$, $\frac{a_{c0}(t=0)}{a_{h0}(t=0)} = 9$). As we expected according to the fits in sub-section 2.5.3, a single temperature form of the Laguerre distribution function with many Laguerre terms can represent the time evolution of the distribution function in this situation. Figure (4.12) shows the relative errors of the results of the time evolution of the distribution function compared to "FPI" at different times $\left(\frac{t}{\tau} = 0.5, 1, 5, 10\right)$. In this case, we have ($N + 2 = 18$) unknowns in the Laguerre distribution function, i.e. $a_{c0}(t), a_{c1}(t), \dots, a_{c16}(t), T_c(t)$. We need to calculate the time evolution of 18 moments $\left(M_{\{N_c,N_m,N_h\},0}, M_{\{N_c,N_m,N_h\},2}, \dots, M_{\{N_c,N_m,N_h\},34}\right)$ to find the right coefficients and the temperature at each timestep using the fitting method described in section 2.3.

Figure (4.13) shows the time evolution of the coefficients of the Laguerre distribution function. Since this is a single temperature case, $a_0(t)$ is always equal to 1 to conserve the density:

$$M_2(t) = a_0(t) = a_{c0}(0) + a_{h0}(0) = N_e = 1 \tag{4-3}$$

and $a_0(t)$, $a_1(t)$ and $T(t)$ are responsible for conservation of the energy:

$$M_4(t) = \frac{3}{2}\left(a_0(t)T(t) - a_1(t)T(t)\right) = \frac{3}{2}\left(a_{c0}(0)T_c(0) + a_{h0}(0)T_h(0)\right) = 0.4875 \Rightarrow$$

$$a_1(t) = 1 - \frac{0.325}{T(t)} \text{ and } T(t) = \frac{0.325}{1 - a_1(t)} \tag{4-4}$$

Due to this simple relation between $T(t)$ and $a_1(t)$, we have not made a separate plot for $T(t)$ for this case.

At each timestep, the values of the coefficients and the temperature change in order to satisfy the time evolution of the moments.

Figure (4.11): Time evolution of a single temperature form of the Laguerre distribution function ($N = 16, \frac{T_c(t=0)}{T_h(t=0)} = \frac{1}{4}, \frac{a_{c0}(t=0)}{a_{h0}(t=0)} = 9$).

Figure (4.12): Relative error of the time evolution of a single temperature form of the Laguerre distribution function ($N = 16, \frac{T_c(t=0)}{T_h(t=0)} = \frac{1}{4}, \frac{a_{c0}(t=0)}{a_{h0}(t=0)} = 9$).

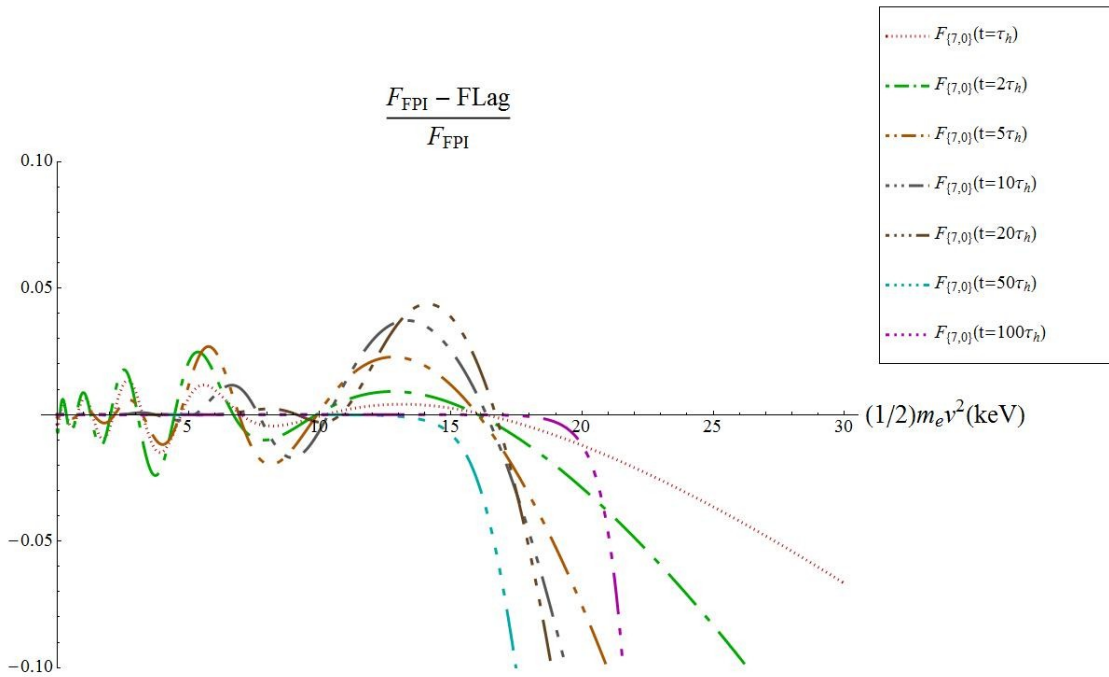Figure (4.13): Time evolution of the coefficients of the Laguerre distribution function ($N = 16, \frac{T_c(t=0)}{T_h(t=0)} = \frac{1}{4}, \frac{a_{c0}(t=0)}{a_{h0}(t=0)} = 9$).

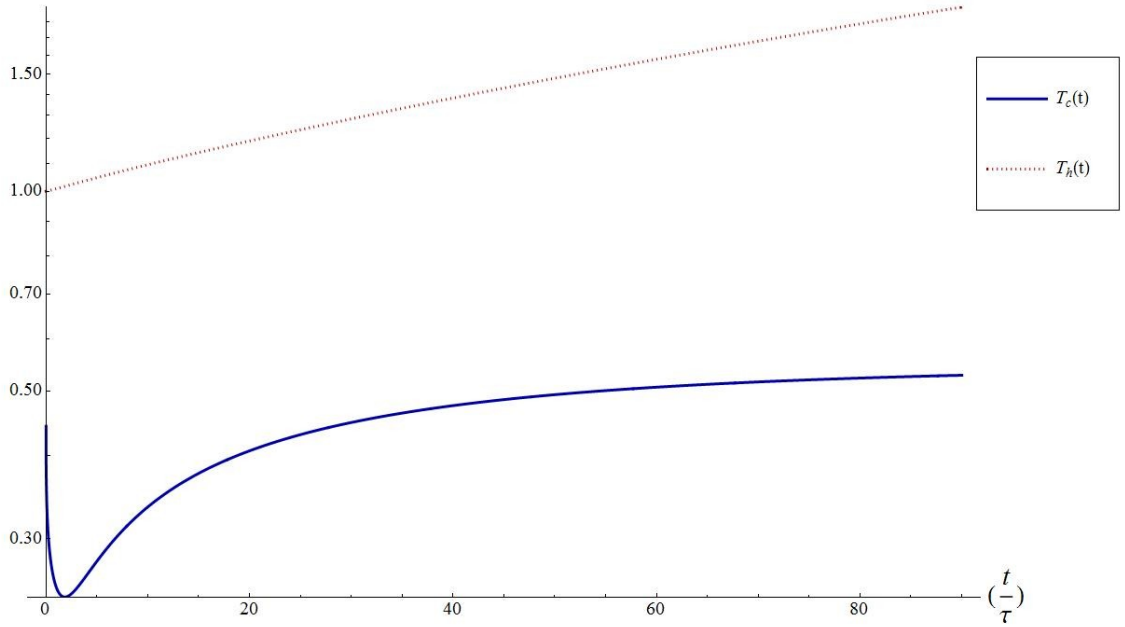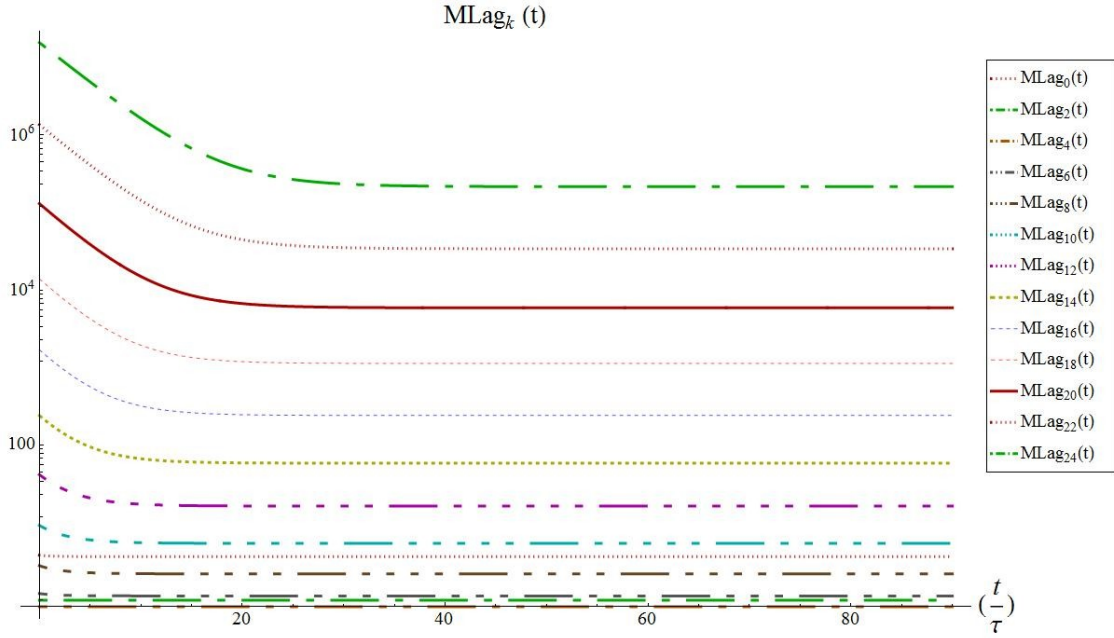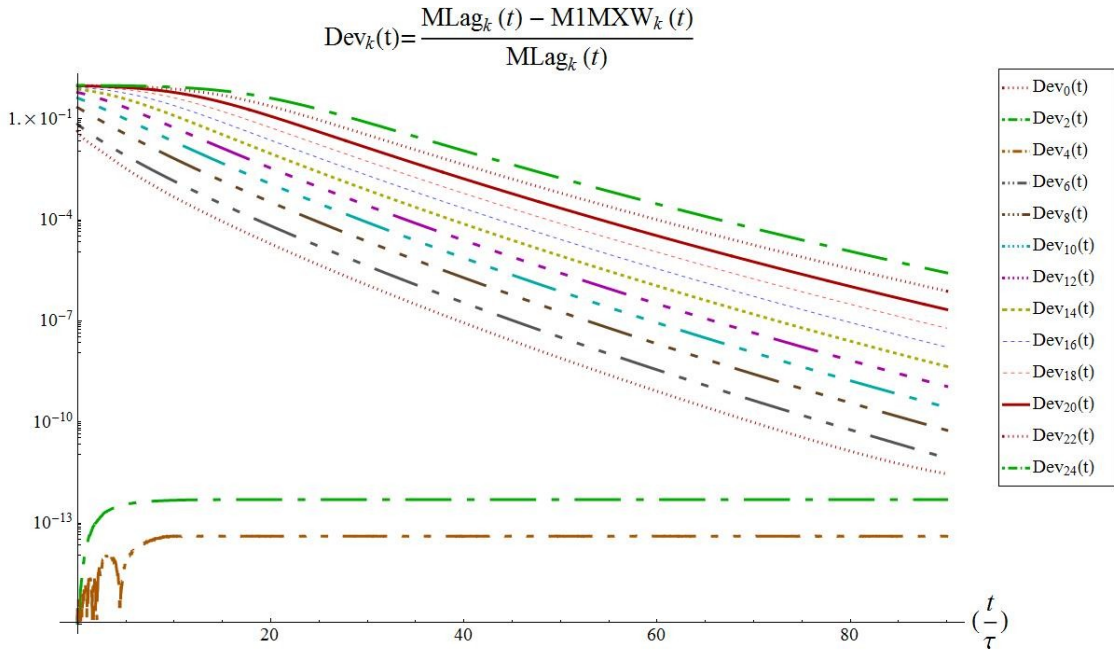### 4.2.2. A two temperature form of the Laguerre distribution function ($N_c = 11, N_h = 00$); 9:1 initial density ratio $\left(\frac{a_{c0}(t=0)}{a_{h0}(t=0)} = 9\right)$ (case no. 17 in Table (4.1))

Figure (4.14) shows the time evolution of a two temperature form of the Laguerre distribution function ($N_c = 11$, $N_h = 00$) for an initial two-Maxwellian distribution $\left(\frac{T_c(t=0)}{T_h(t=0)} = \frac{1}{4}, \frac{a_{c0}(t=0)}{a_{h0}(t=0)} = 9\right)$. For this case, we run the code for a longer time. Figure (4.15) shows the relative errors of the results of the time evolution of the distribution function compared to "FPI" at different times $\left(\frac{t}{\tau} = 1, 2, 5, 10, 20, 50, 100\right)$. In this case, we have ($N_c + N_h + 4 = 15$) unknowns in the Laguerre distribution function *i.e.* $a_{c0}(t), a_{c1}(t), \dots, a_{c11}(t), a_{h0}(t), T_c, T_h$. We need to calculate the time evolution of 15 moments ($M_{\{N_c, N_m, N_h\},0}, M_{\{N_c, N_m, N_h\},2}, \dots, M_{\{N_c, N_m, N_h\},28}$) to find the right coefficients and temperatures at each times using the fitting method described in section 2.3.

Figure (4.16) shows the time evolution of the two temperatures. Eventually, $T_c(t)$ after many collision times tends toward the equilibrium temperature ($T_e = 0.325$). Although, $T_h(t)$ increases gradually and after 100 collision time reaches ($T_h(100\tau_h) \simeq 1.9$keV), almost all of the energy density is in cold electrons (mostly the $a_{c0}(t)$ term), because $a_{h0}(t)$ is extremely small:

65

$$T_c(100\tau_h) \simeq 0.3778, \qquad T_h(100\tau_h) \simeq 1.559$$

$$a_{c0}(100\tau_h) = 1 - a_{h0}(100\tau_h) \simeq 1, \qquad a_{c1}(100\tau_h) \simeq 0.1397$$

$$a_{h0}(100\tau_h) \simeq 3.805 \times 10^{-13}$$

$$M_4(0) = \frac{3}{2}N_e T_e = 0.4875$$

$$M_{4c0}(100\tau_h) = \frac{3}{2}a_{c0}(100\tau_h)T_c(100\tau_h) \simeq 0.5666$$

$$M_{4c1}(100\tau_h) = -\frac{3}{2}a_{c1}(100\tau_h)T_c(100\tau_h) \simeq -0.07914$$

$$M_{4h0}(100\tau_h) = \frac{3}{2}a_{h0}(100\tau_h)T_h(100\tau_h) \simeq 8.9 * 10^{-13}$$

During the time evolution of the Laguerre distribution function, the hot population diminishes very fast (*i.e.* $a_{h0}(t)$), but still the distribution remains non-Maxwellian due to higher orders of the cold Laguerre terms (*i.e.* $a_{c1}, a_{c2}, ...$), even at very late physical time and after many collision times.

Figure (4.17) shows the time evolution of the coefficients of the Laguerre distribution function. All of the coefficients gradually diminish during the time evolution of the Laguerre distribution function except $a_{c0}(t)$. The rapid decrease of $a_{h0}(t)$ is evident in this figure.

Figure (4.18) shows the time evolution of the moments of the Laguerre distribution function. Of course, moments 2 and 4 are always constant due to the density and energy conservation. The other moments are tending toward the moments of a single Maxwellian *i.e.* the ultimate solution of the distribution function at $t \to \infty$ (Figure (4.19) shows the deviation of the moments from the moments of a single Maxwellian). In this case, since the initial temperatures are not very different $\left(\frac{T_c(0)}{T_h(0)} = \frac{1}{4}\right)$, the moments get close to their ultimate values (*i.e.* moments of a single Maxwellian) rather fast.
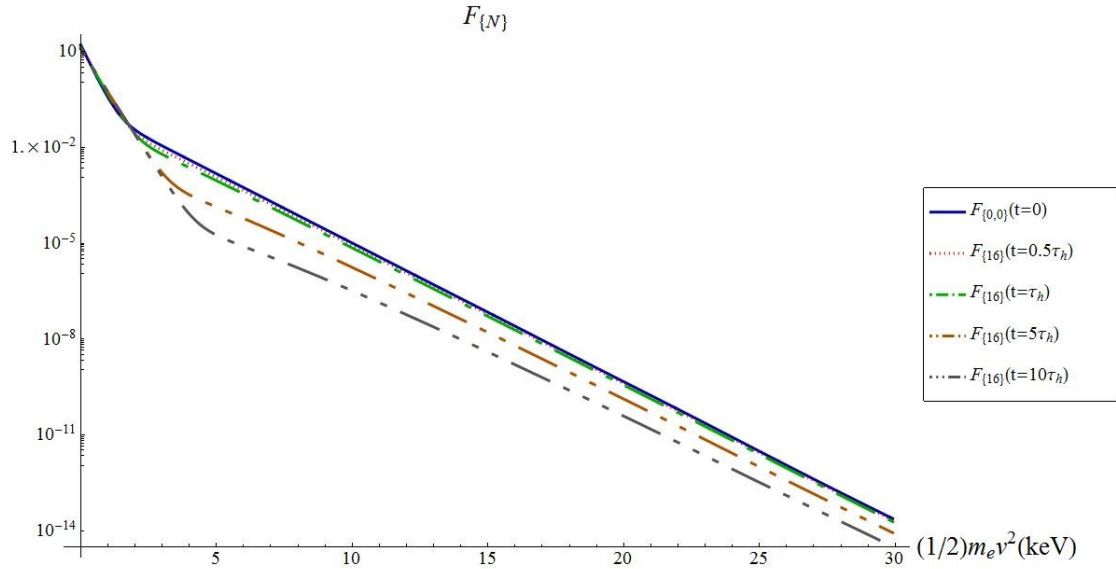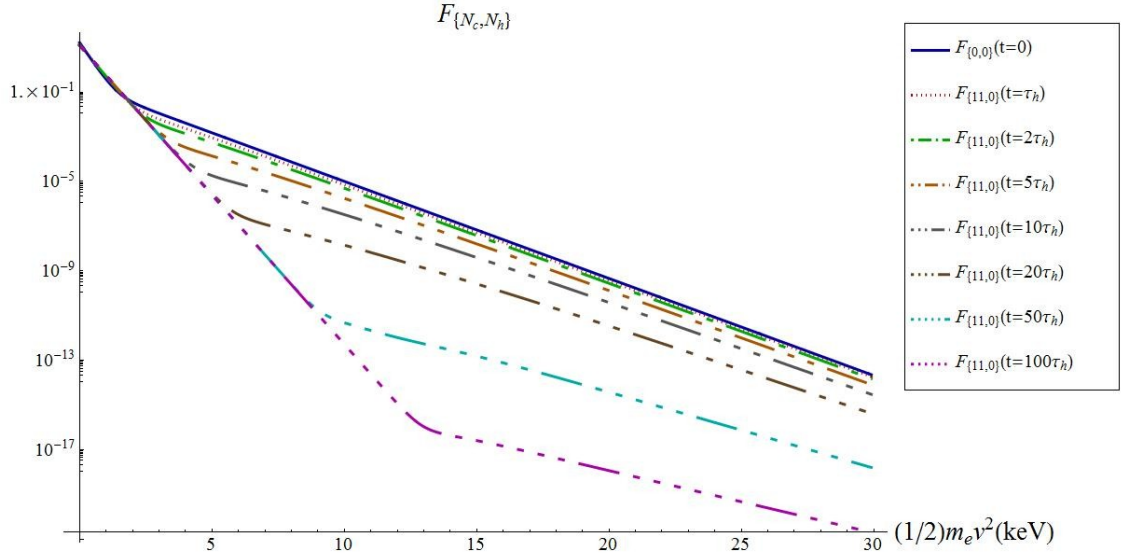
Figure (4.14): Time evolution of a two temperature form of the Laguerre distribution function $(N_c = 11, N_h = 00, \frac{T_c(t=0)}{T_h(t=0)} = \frac{1}{4}, \frac{a_{c0}(t=0)}{a_{h0}(t=0)} = 9)$.

Figure (4.15): Relative error of the time evolution of a two temperature form of the Laguerre distribution function $\left(N_c = 11, N_h = 00, \frac{T_c(t=0)}{T_h(t=0)} = \frac{1}{4}, \frac{a_{c0}(t=0)}{a_{h0}(t=0)} = 9\right)$.
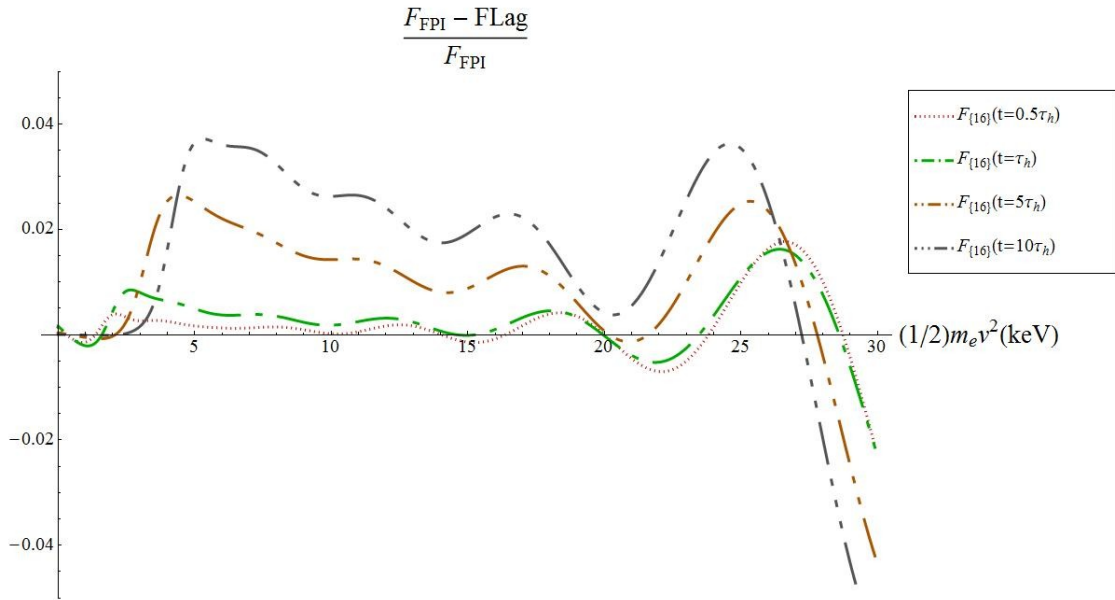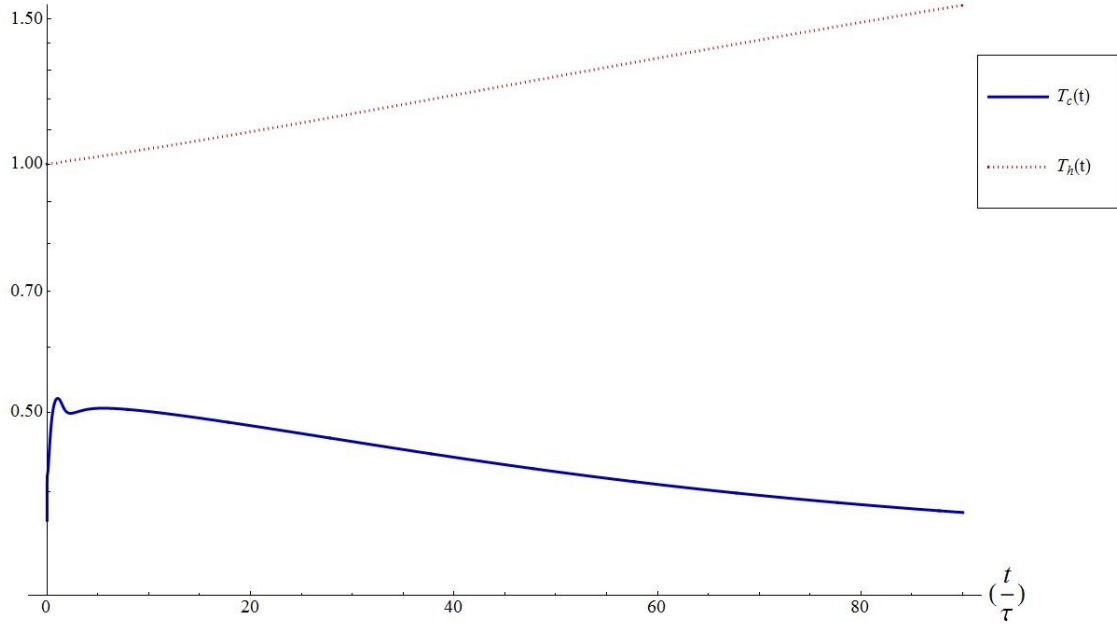
Figure (4.16): Time evolution of the temperatures of the Laguerre distribution function $(N_c = 11, N_h = 00, \frac{T_c(t=0)}{T_h(t=0)} = \frac{1}{4}, \frac{a_{c0}(t=0)}{a_{h0}(t=0)} = 9)$.
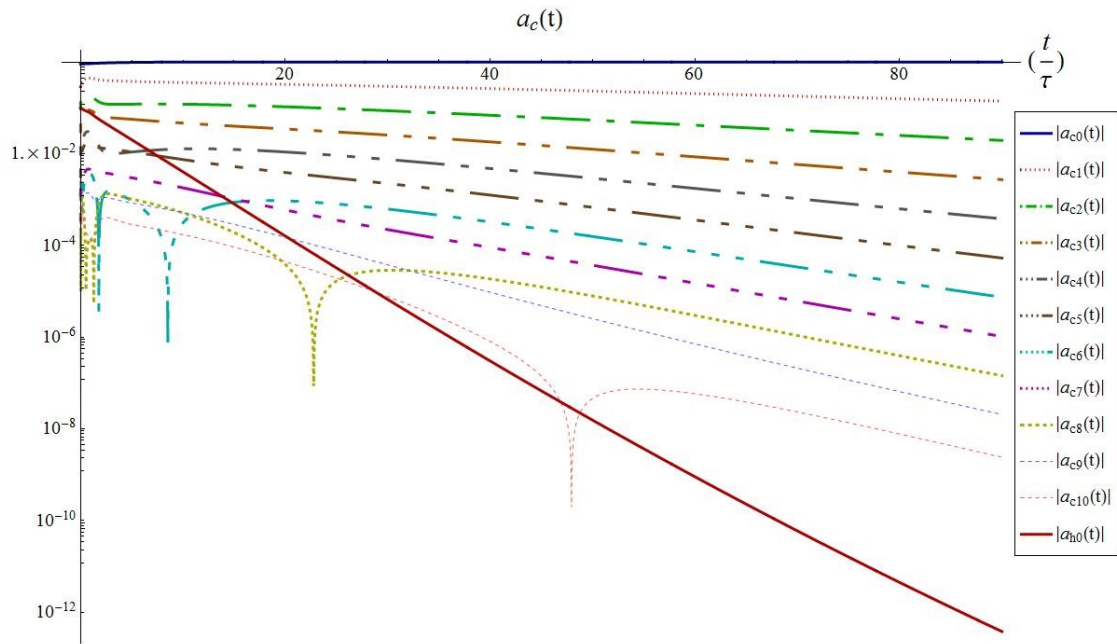
Figure (4.17): Time evolution of the coefficients (cold and hot) of the Laguerre distribution function $(N_c = 11, N_h = 00, \frac{T_c(t=0)}{T_h(t=0)} = \frac{1}{4}, \frac{a_{c0}(t=0)}{a_{h0}(t=0)} = 9)$.
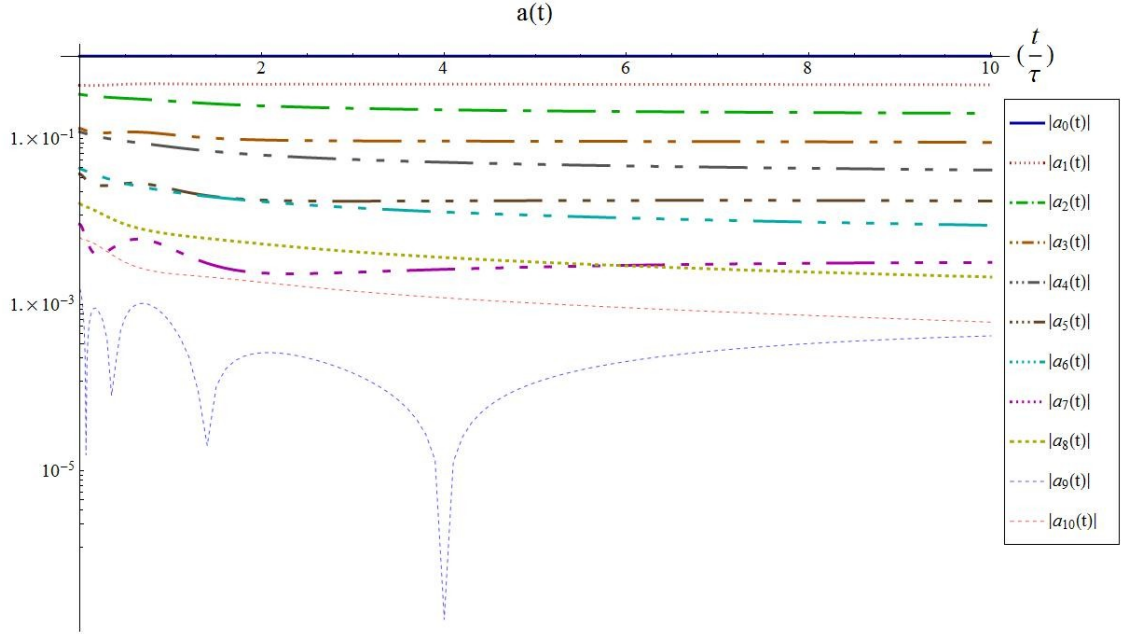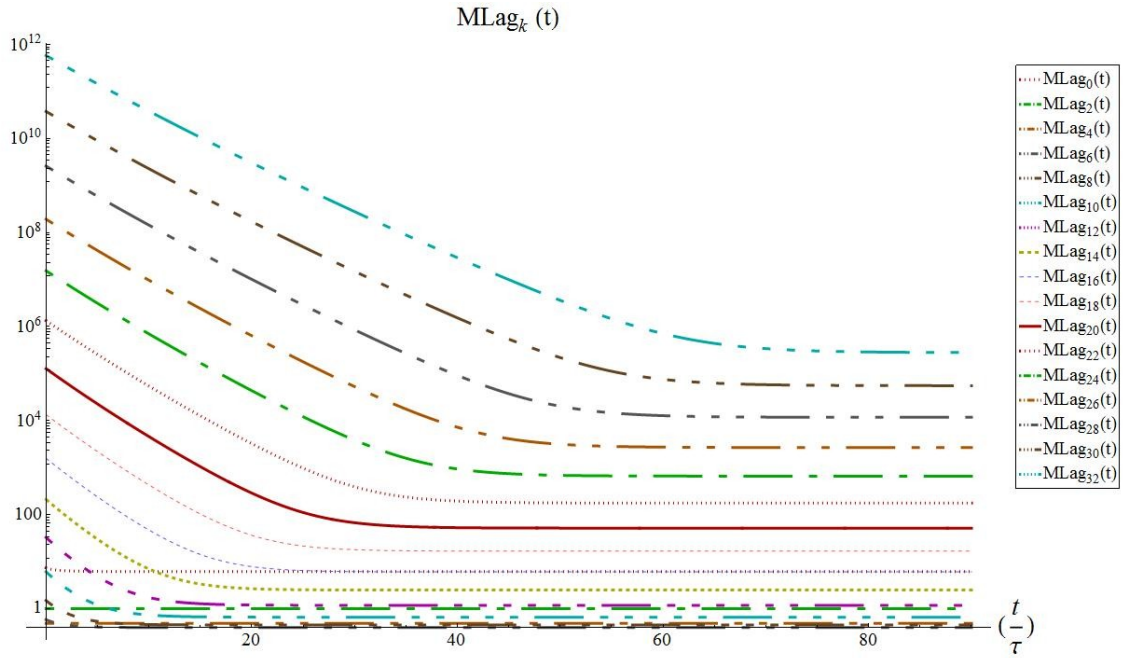
Figure (4.18): Time evolution of the moments of the Laguerre distribution function ($N_c = 11, N_h = 00, \frac{T_c(t=0)}{T_h(t=0)} = \frac{1}{4}, \frac{a_{c0}(t=0)}{a_{h0}(t=0)} = 9$).

Figure (4.19): Time evolution of the deviation of the moments of the Laguerre distribution function from the moments of a single Maxwellian $\left(N_c = 11, N_h = 00, \frac{T_c(t=0)}{T_h(t=0)} = \frac{1}{4}, \frac{a_{c0}(t=0)}{a_{h0}(t=0)} = 9\right)$.

4.3. Time evolution of the Laguerre distribution function for a 1:10 initial temperature ratio $\left(\frac{T_c(t=0)}{T_h(t=0)} = \frac{1}{10} \right)$

We now show the results of two simulations with the same 1:10 initial temperature ratio, but with different initial density ratios. Both used a three temperature form.

4.3.1. A three temperature form of the Laguerre distribution function ($N_c = 04, N_m = 06, N_h = 00$); 9:1 initial density ratio $\left(\frac{a_{c0}(t=0)}{a_{h0}(t=0)} = 9 \right)$ (case no. 26 in Table (4.1))

Figure (4.20) shows the time evolution of a three temperature form of the Laguerre distribution function ($N_c = 04$, $N_m = 06$, $N_h = 00$) for an initial two-Maxwellian distribution $\left(\frac{T_c(t=0)}{T_h(t=0)} = \frac{1}{10}, \frac{a_{c0}(t=0)}{a_{h0}(t=0)} = 9 \right)$. For this case, we ran the code for a longer time. For each initial temperature ratio we studied the time evolution of the distribution function for a longer time with one particular form of the Laguerre distribution function to gain more insight into the long term evolution of the moments and of the temperatures and coefficients. Figure (4.21) shows the relative errors of the results of the time evolution of the distribution function compared to "FPI" at the same times $\left(\frac{t}{\tau} = 1, 2, 5, 10, 20, 50, 100 \right)$. In this case, we have ($N_c + N_m + N_h + 6 = 16$) unknowns in the Laguerre distribution function i.e. $a_{c0}(t), a_{c1}(t), \ldots, a_{c4}(t), a_{m0}(t), a_{m1}(t), \ldots,$

$a_{m6}(t), a_{h0}(t), T_c, T_m, T_h$. We need to calculate the time evolution of 16 moments $(M_{\{N_c,N_m,N_h\},0}, M_{\{N_c,N_m,N_h\},2}, \ldots, M_{\{N_c,N_m,N_h\},30})$ to find the right coefficients and temperatures at each timestep using the fitting method described in section 2.3.

Figure (4.22) shows the time evolution of the three temperatures. Eventually, $T_c(t)$ tends toward the equilibrium temperature ($T_e = 0.19$). Although, $T_h(t)$ increases rapidly and after 100 collision time reaches ($T_h(100\tau_h) \simeq 24 \text{ keV}$), most of the total energy density is in cold electrons (mostly the $a_{c0}(t)$ term) because a_{h0} and a_{m0} are extremely small.

$T_c(100\tau_h) \simeq 0.1904, \quad T_m(100\tau_h) \simeq 1.015, \quad T_h(100\tau_h) \simeq 24.00$

$a_{c0}(100\tau_h) \simeq 1, \quad a_{c1}(100\tau_h) \simeq 1.918 * 10^{-3}$

$a_{m0}(100\tau_h) \simeq 1.970 * 10^{-14}, \quad a_{m1}(100\tau_h) \simeq -2.328 * 10^{-14}$

$a_{h0}(100\tau_h) \simeq 5.968 \times 10^{-35}$

$M_4(0) = \frac{3}{2} N_e T_e = 0.285$

$M_{4c0}(100\tau_h) = \frac{3}{2} a_{c0}(100\tau_h) T_c(100\tau_h) \simeq 0.285548$

$$M_{4c1}(100\tau_h) = -\frac{3}{2}a_{c1}(100\tau_h)T_c(100\tau_h) \simeq -5.48 * 10^{-4}$$

$$M_{4m0}(100\tau_h) = \frac{3}{2}a_{m0}(100\tau_h)T_m(100\tau_h) \simeq 3 * 10^{-14}$$

$$M_{4m1}(100\tau_h) = -\frac{3}{2}a_{m1}(100\tau_h)T_m(100\tau_h) \simeq 3.545 * 10^{-14}$$

$$M_{4h0}(100\tau_h) = \frac{3}{2}a_{h0}(100\tau_h)T_h(100\tau_h) \simeq 2.149 * 10^{-33}$$

During the time evolution of the Laguerre distribution function the hot and medium populations diminish fast (*i.e.* $a_{m0}(t), a_{m1}(t), ..., a_{h0}(t)$), but the electron distribution still remains non-Maxwellian due to the higher order cold Laguerre terms (*i.e.* $a_{c1}, a_{c2}, ...$), even at very late physical time and after many collisions.

Figure (4.23) and Figure (4.24) show the time evolution of the coefficients of the Laguerre distribution function. All of the coefficients gradually diminish during the time evolution of the Laguerre distribution function except $a_{c0}(t)$. The rapid decrease of $a_{h0}(t)$ is particularly evident. At certain times, strong oscillations of the coefficients appear (e.g at t=38 on Fig. (4.23), accompanied by very low amplitude oscillations of the temperatures on Fig. (4.22)), but these coefficients are then at sufficiently low values that this does not appreciably affect the distribution function.

Figure (4.25) shows the time evolution of the moments of the Laguerre distribution function. Of course, moments 2 and 4 are always constant due to the density and energy conservation. The other moments are tending toward the moments of a single Maxwellian *i.e.* the ultimate solution of the distribution function at $t \to \infty$ (Figure (4.26) shows the deviation of the moments from the moments of a single Maxwellian). In this case, since the initial temperatures are moderately close $\left(\frac{T_c(0)}{T_h(0)} = \frac{1}{10}\right)$, the moments get close to their ultimate value (*i.e.* moments of a single Maxwellian) relatively fast but of course the process is still slower than the previous cases with a higher initial temperature ratios.

The rate of decrease of the higher moments is approximately independent of the initial temperature ratio, as it is due to the slowing down of the fast electrons (whose initial temperature is 1 in all cases) colliding with the much slower ones of the cold component of the distribution function, and this slowing down rate is approximately independent of the cold temperature, provided it is considerably less than the hot one. However, for very lower temperature ratios, since the ultimate single temperature is lower, the high order moments have lower values (because of the $T^{\frac{k}{2}-1}$ factor), and it therefore takes more slowing down times to reach this lower

value.

Figure (4.20): Time evolution of a three temperature form of the Laguerre distribution function $(N_c = 04, N_m = 06, N_h = 00, \frac{T_c(t=0)}{T_h(t=0)} = \frac{1}{10}, \frac{a_{c0}(t=0)}{a_{h0}(t=0)} = 9)$.
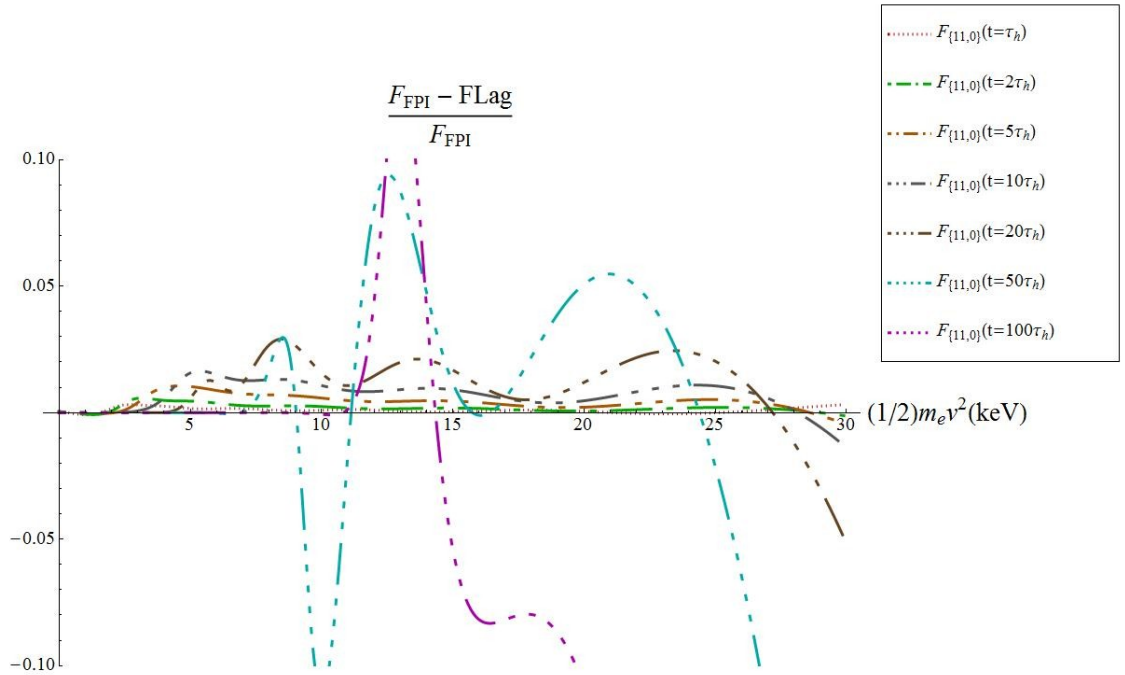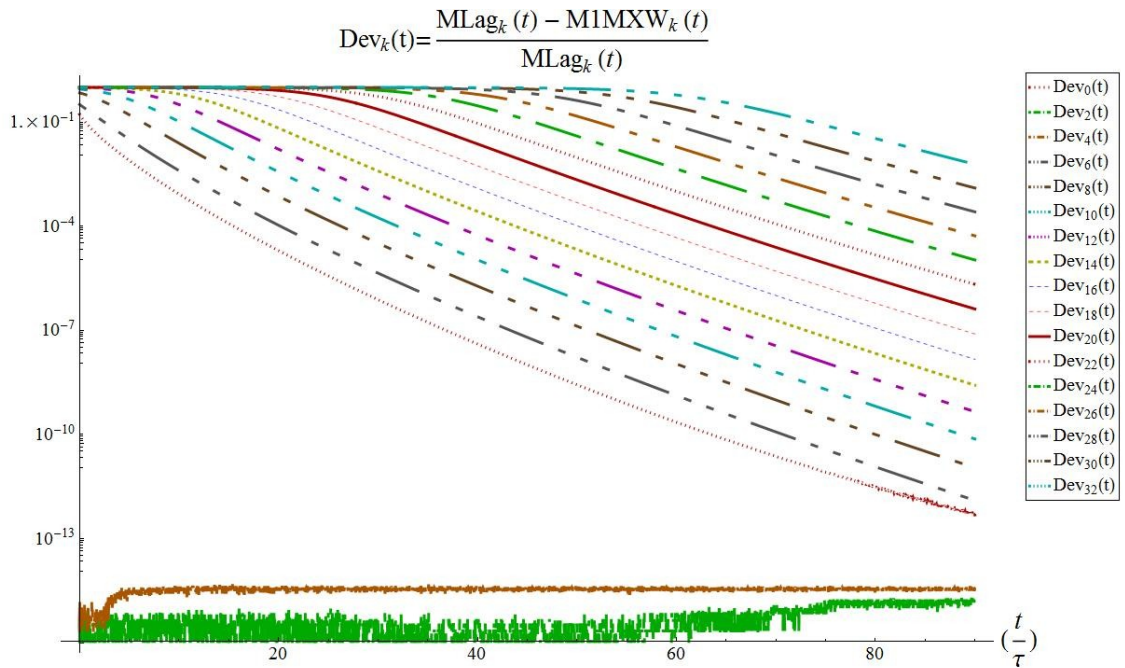

Figure (4.21): Relative error of the time evolution of a three temperature form of the Laguerre distribution function $(N_c = 04, N_m = 06, N_h = 00, \frac{T_c(t=0)}{T_h(t=0)} = \frac{1}{10}, \frac{a_{c0}(t=0)}{a_{h0}(t=0)} = 9)$.

72

Figure (4.22): Time evolution of the temperatures of the Laguerre distribution function $\left(N_c = 04, N_m = 06, N_h = 00, \frac{T_c(t=0)}{T_h(t=0)} = \frac{1}{10}, \frac{a_{c0}(t=0)}{a_{h0}(t=0)} = 9\right)$.

Figure (4.23): Time evolution of the coefficients (cold and hot) of the Laguerre distribution function $\left(N_c = 04, N_m = 06, N_h = 00, \frac{T_c(t=0)}{T_h(t=0)} = \frac{1}{10}, \frac{a_{c0}(t=0)}{a_{h0}(t=0)} = 9\right)$.

73

Figure (4.24): Time evolution of the coefficients (medium) of the Laguerre distribution function$\left(N_c = 04, N_m = 06, N_h = 00, \frac{T_c(t=0)}{T_h(t=0)} = \frac{1}{10}, \frac{a_{c0}(t=0)}{a_{h0}(t=0)} = 9\right)$.

Figure (4.25): Time evolution of the moments of the Laguerre distribution function$\left(N_c = 04, N_m = 06, N_h = 00, \frac{T_c(t=0)}{T_h(t=0)} = \frac{1}{10}, \frac{a_{c0}(t=0)}{a_{h0}(t=0)} = 9\right)$.

$$\mathrm{Dev}_k(t) = \frac{\mathrm{MLag}_k(t) - \mathrm{M1MXW}_k(t)}{\mathrm{MLag}_k(t)}$$

Figure (4.26): Time evolution of the deviation of the moments of the Laguerre distribution function from the moments of a single Maxwellian $\left(N_c = 04, N_m = 06, N_h = 00, \frac{T_c(t=0)}{T_h(t=0)} = \frac{1}{10}, \frac{a_{c0}(t=0)}{a_{h0}(t=0)} = 9\right)$.

4.3.2. A three temperature form of the Laguerre distribution function ($N_c = 02, N_m = 08, N_h = 00$); 99:1 initial density ratio $\left(\frac{a_{c0}(t=0)}{a_{h0}(t=0)} = 99\right)$ (case no. 30 in Table (4.1))

Figure (4.27) shows the time evolution of a three temperature form of the Laguerre distribution function ($N_c = 02$, $N_m = 08$, $N_h = 00$) for an initial two-Maxwellian distribution $\left(\frac{T_c(t=0)}{T_h(t=0)} = \frac{1}{10}, \frac{a_{c0}(t=0)}{a_{h0}(t=0)} = 99\right)$. As we expected, according to the fits in sub-section 2.5.1, a three temperature form of the Laguerre distribution function is suitable for representing the time evolution of the distribution function in this situation. Figure (4.28) shows the relative errors of the results of the time evolution of the distribution function compared to "FPI" at different times $\left(\frac{t}{\tau} = 0.5, 1, 5, 10\right)$. The relative error is less than 2% below energy 30 keV. In this case, we have ($N_c + N_m + N_h + 6 = 16$) unknowns in the Laguerre distribution function

i.e. $a_{c0}(t), a_{c1}(t), a_{c2}(t),\ a_{m0}(t), a_{m1}(t), \dots, a_{m8}(t), a_{h0}(t), T_c, T_m, T_h$. We need to calculate the time evolution of 16 moments ($M_{\{N_c,N_m,N_h\},0}, M_{\{N_c,N_m,N_h\},2}, \dots, M_{\{N_c,N_m,N_h\},30}$) to find the right coefficients and temperatures at each timestep using the fitting method described in section 2.3.

75

Figure (4.29) shows the time evolution of the three temperatures. Eventually, $T_c(t)$ tends toward the equilibrium temperature $T_e = 0.109$.

Figure (4.30) and Figure (4.31) show the time evolution of the coefficients of the Laguerre distribution function. As before, all of the coefficients gradually diminish during the time evolution of the Laguerre distribution function except $a_{c0}(t)$, reflecting the fact that the distribution function is gradually evolving toward a single Maxwellian.

Figure (4.27): Time evolution of a three temperature form of the Laguerre distribution function $(N_c = 02, N_m = 08, N_h = 00, \frac{T_c(t=0)}{T_h(t=0)} = \frac{1}{10}, \frac{a_{c0}(t=0)}{a_{h0}(t=0)} = 99)$.
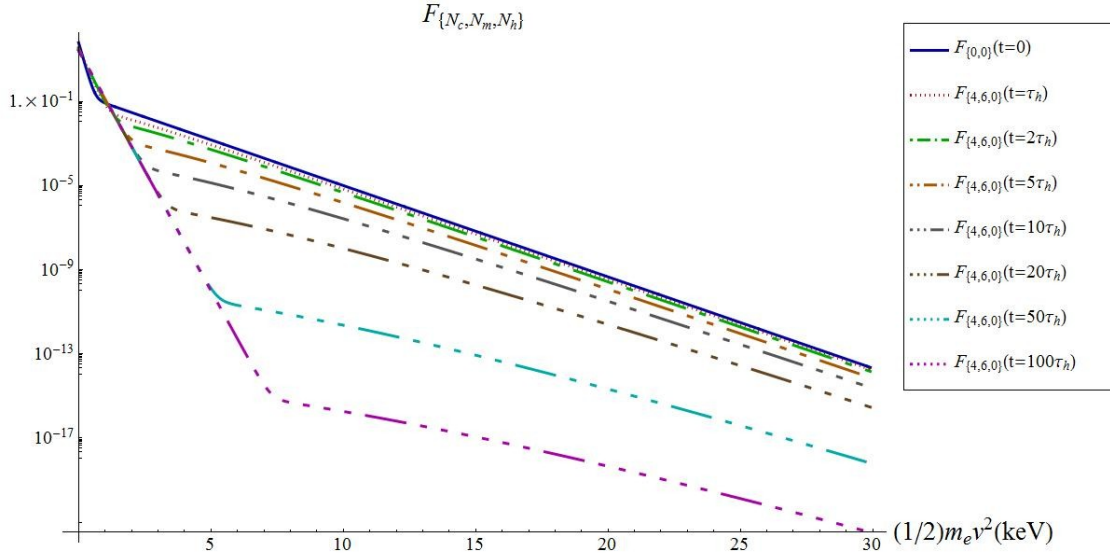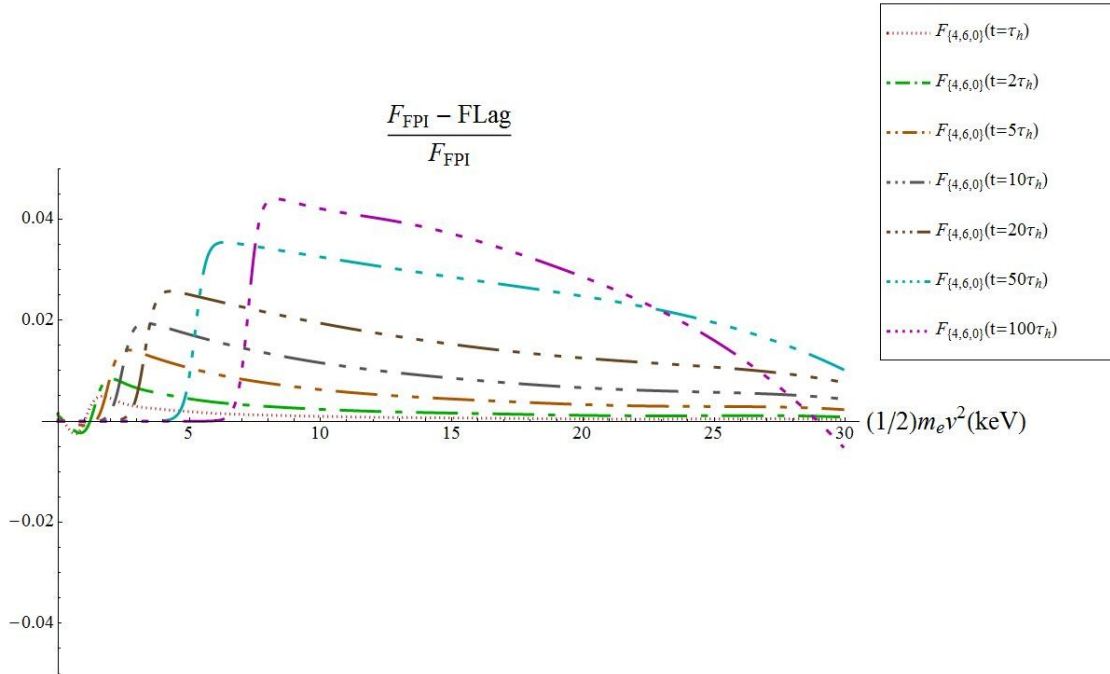
Figure (4.28): Relative error of the time evolution of a three temperature form of the Laguerre distribution function ($N_c = 02, N_m = 08, N_h = 00, \frac{T_c(t=0)}{T_h(t=0)} = \frac{1}{10}, \frac{a_{c0}(t=0)}{a_{h0}(t=0)} = 99$).
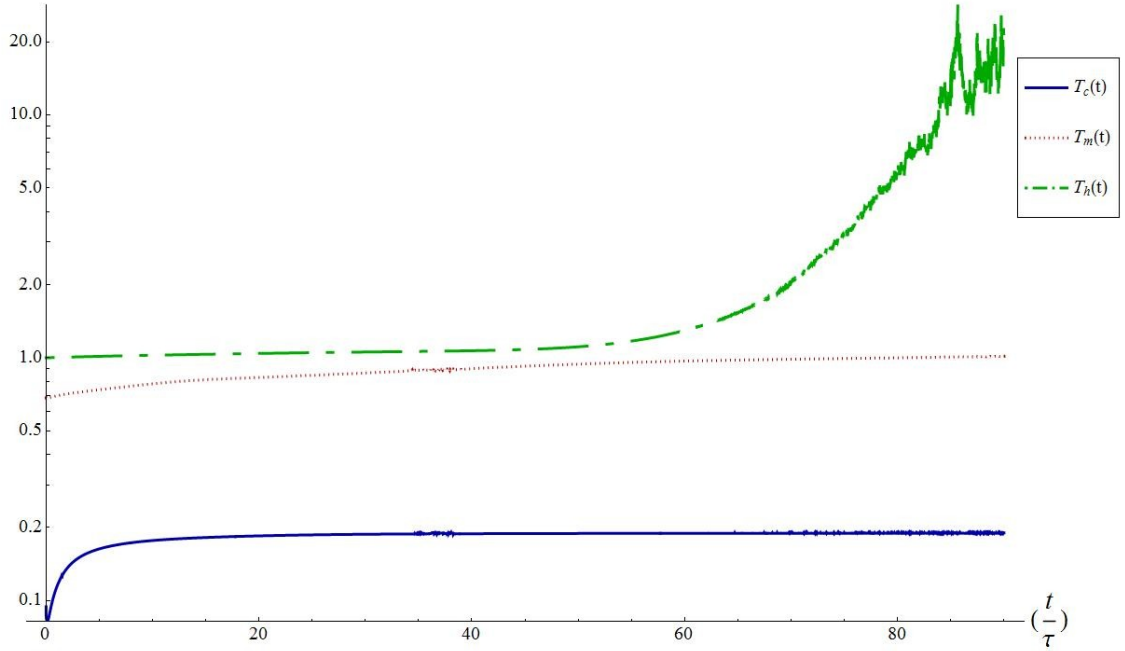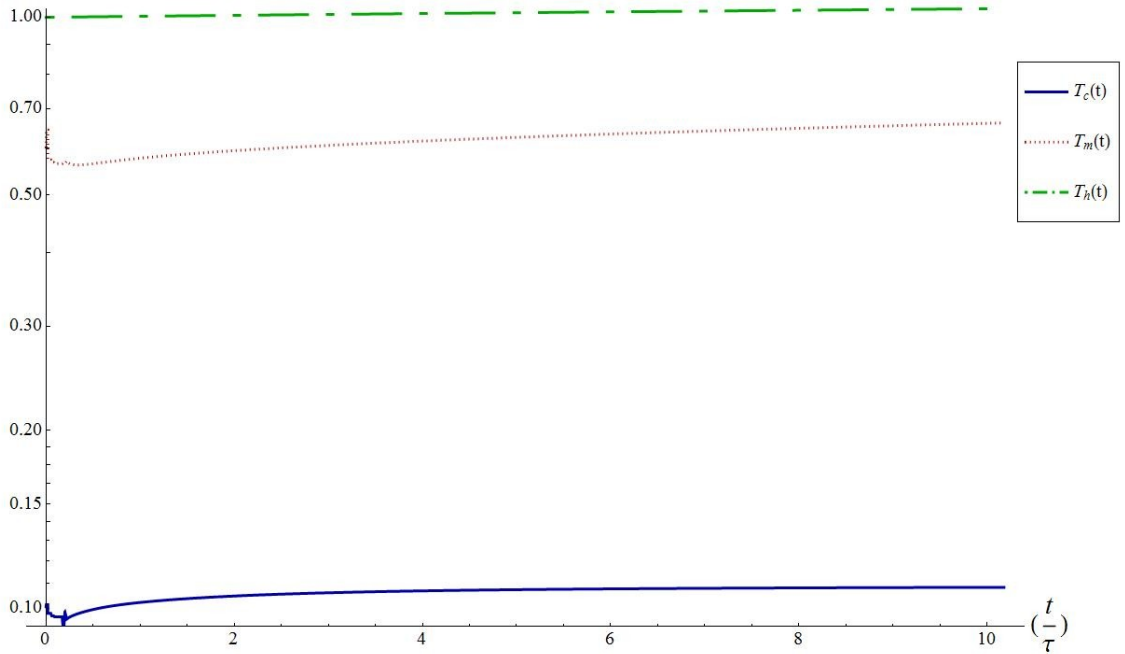

Figure (4.29): Time evolution of the temperatures of the Laguerre distribution function ($N_c = 02, N_m = 08, N_h = 00, \frac{T_c(t=0)}{T_h(t=0)} = \frac{1}{10}, \frac{a_{c0}(t=0)}{a_{h0}(t=0)} = 99$).

Figure (4.30): Time evolution of the coefficients (cold and hot) of the Laguerre distribution function ($N_c = 02, N_m = 08, N_h = 00, \frac{T_c(t=0)}{T_h(t=0)} = \frac{1}{10}, \frac{a_{c0}(t=0)}{a_{h0}(t=0)} = 99$).

Figure (4.31): Time evolution of the coefficients (medium) of the Laguerre distribution function ($N_c = 02, N_m = 08, N_h = 00, \frac{T_c(t=0)}{T_h(t=0)} = \frac{1}{10}, \frac{a_{c0}(t=0)}{a_{h0}(t=0)} = 99$).
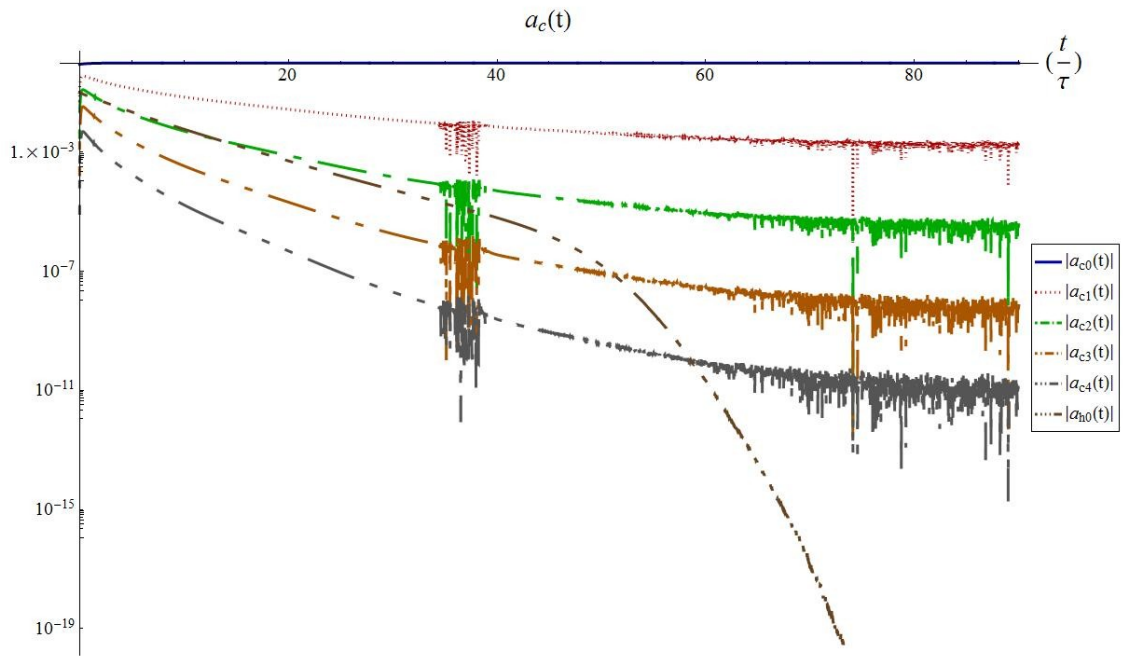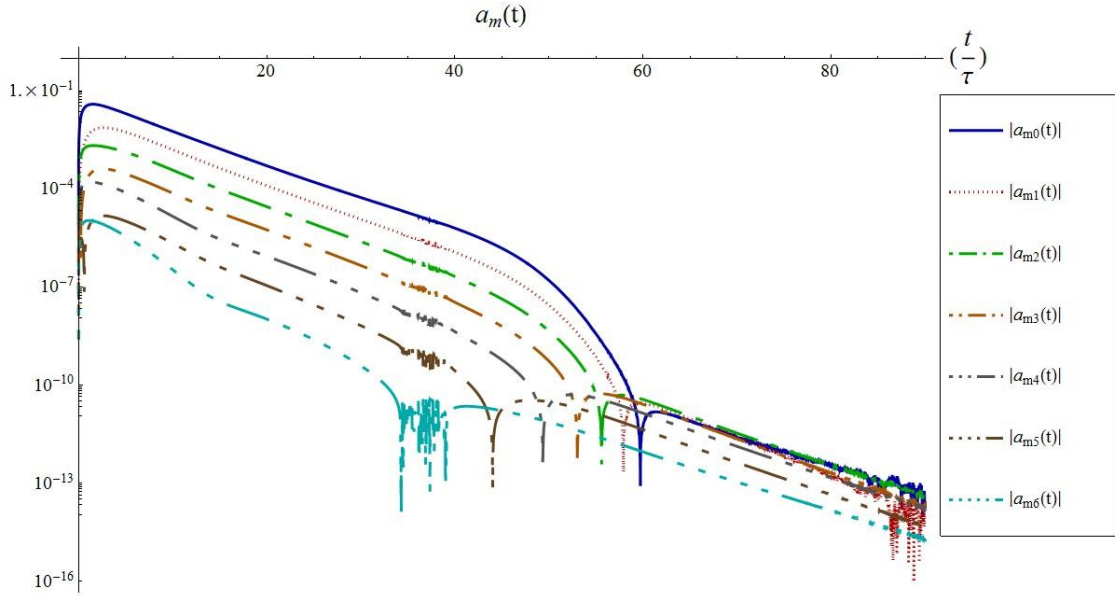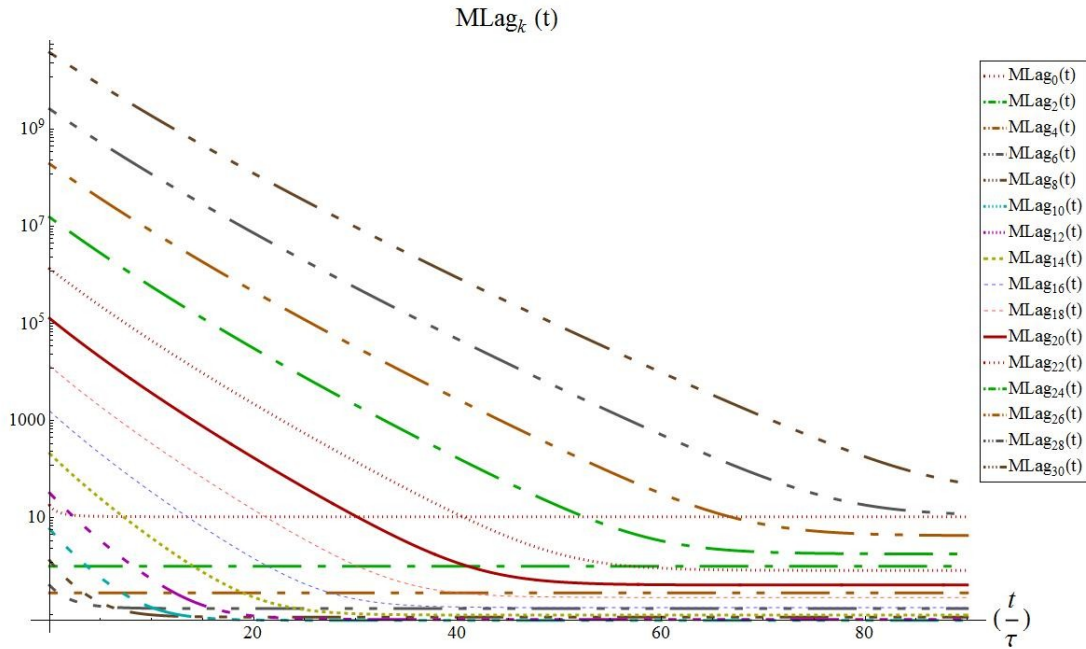
4.4. Time evolution of the Laguerre distribution function for a 1:100 initial temperature ratio $\left(\frac{T_c(t=0)}{T_h(t=0)} = \frac{1}{100}\right)$

4.4.1. A three temperature form of the Laguerre distribution function ($N_c = 00, N_m = 08, N_h = 00$); 9968:32 initial density ratio $\left(\frac{a_{c0}(t=0)}{a_{h0}(t=0)} = \frac{9968}{32}\right)$ (case no. 39 in Table (4.1))

Figure (4.32) shows the time evolution of a three temperature form of the Laguerre distribution function ($N_c = 00$, $N_m = 08$, $N_h = 00$) for an initial two-Maxwellian distribution $\left(\frac{T_c(t=0)}{T_h(t=0)} = \frac{1}{100}, \frac{a_{c0}(t=0)}{a_{h0}(t=0)} = \frac{9968}{32}\right)$. As we expected according to the fits in sub-section 2.5.1, a three temperature form of the Laguerre distribution function is suitable for representing the time evolution of the distribution function in this situation. Figure (4.33) shows the relative errors of the results of the time evolution of the distribution function compared to "FPI" at different times $\left(\frac{t}{\tau} = 0.5, 1, 5, 10\right)$. The relative error is considerably decreased compared to the previous result *i.e.* higher initial temperature ratios $\frac{T_c(0)}{T_h(0)}$. In this case, we have ($N_c + N_m + N_h + 6 = 14$) unknowns in the Laguerre distribution function

i.e. $a_{c0}(t), a_{m0}(t), a_{m1}(t), \dots, a_{m8}(t), a_{h0}(t), T_c, T_m, T_h$. We need to calculate the time evolution of 14 moments ($M_{\{N_c,N_m,N_h\},0}, M_{\{N_c,N_m,N_h\},2}, \dots, M_{\{N_c,N_m,N_h\},26}$) to find the right coefficients and temperatures at each timestep using the fitting method described in section 2.3.

Figure (4.34) shows the time evolution of the three temperatures. Eventually, $T_c(t)$ tends toward the equilibrium temperature $T_e = 0.013168$.

Figure (4.35) and Figure (4.36) show the time evolution of the coefficients of the Laguerre distribution function. As before, all of the coefficients gradually diminish during the time evolution of the Laguerre distribution function except $a_{c0}(t)$ as the plasma evolves toward a single Maxwellian.

Figure (4.32): Time evolution of a three temperature form of the Laguerre distribution function $\left(N_c = 00, N_m = 08, N_h = 00, \frac{T_c(t=0)}{T_h(t=0)} = \frac{1}{100}, \frac{a_{c0}(t=0)}{a_{h0}(t=0)} = \frac{9968}{32}\right)$.
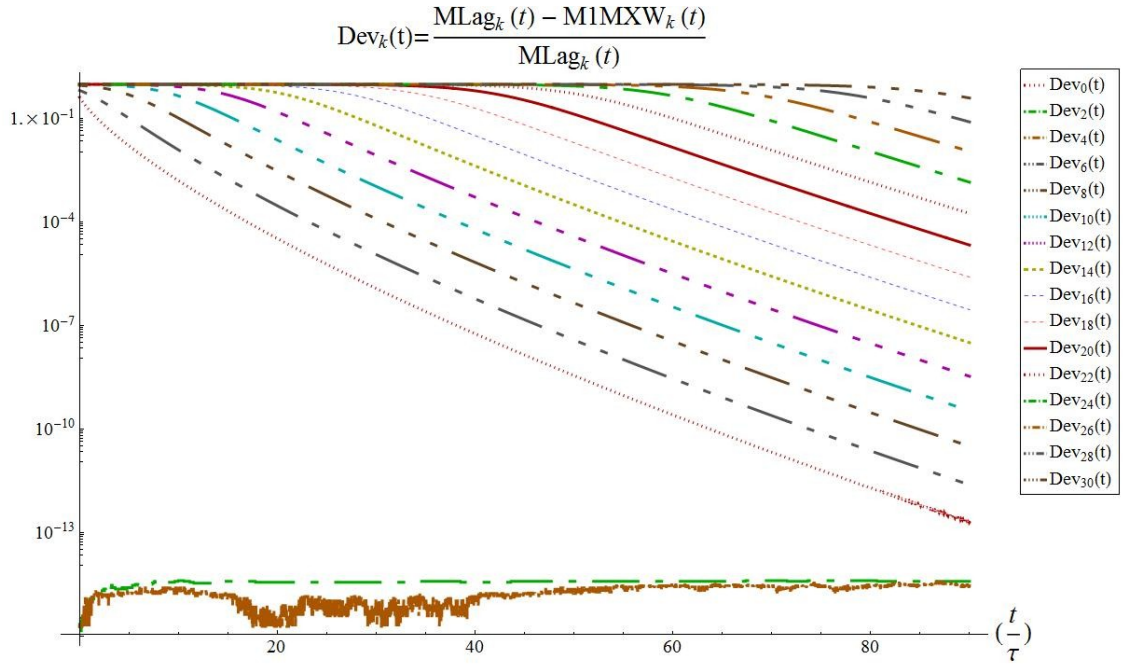

Figure (4.33): Relative error of the time evolution of a three temperature form of the Laguerre distribution function $\left(N_c = 00, N_m = 08, N_h = 00, \frac{T_c(t=0)}{T_h(t=0)} = \frac{1}{100}, \frac{a_{c0}(t=0)}{a_{h0}(t=0)} = \frac{9968}{32}\right)$.

Figure (4.34): Time evolution of the temperatures of the Laguerre distribution function $\left(N_c = 00, N_m = 08, N_h = 00, \frac{T_c(t=0)}{T_h(t=0)} = \frac{1}{100}, \frac{a_{c0}(t=0)}{a_{h0}(t=0)} = \frac{9968}{32}\right)$.

Figure (4.35): Time evolution of the coefficients (cold and hot) of the Laguerre distribution function $\left(N_c = 00, N_m = 08, N_h = 00, \frac{T_c(t=0)}{T_h(t=0)} = \frac{1}{100}, \frac{a_{c0}(t=0)}{a_{h0}(t=0)} = \frac{9968}{32}\right)$.

Figure (4.36): Time evolution of the coefficients (medium) of the Laguerre distribution function $\left(N_c = 00, N_m = 08, N_h = 00, \frac{T_c(t=0)}{T_h(t=0)} = \frac{1}{100}, \frac{a_{c0}(t=0)}{a_{h0}(t=0)} = \frac{9968}{32}\right)$.

4.4.2. A three temperature form of the Laguerre distribution function ($N_c = 00, N_m = 08, N_h = 00$); 967:33 initial density ratio $\left(\frac{a_{c0}(t=0)}{a_{h0}(t=0)} = \frac{967}{33}\right)$ (case no. 36 in Table (4.1))
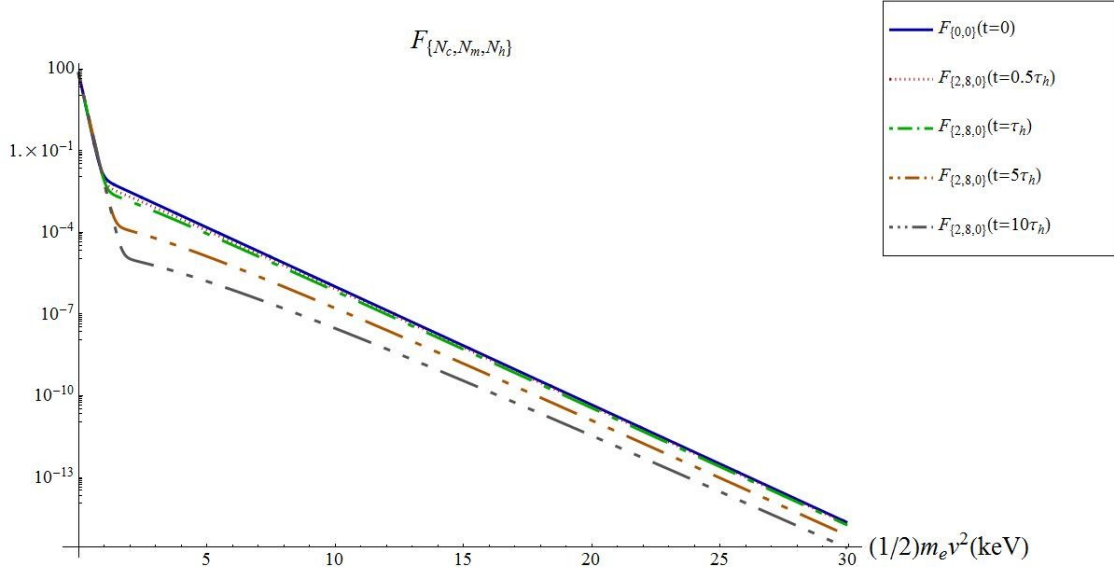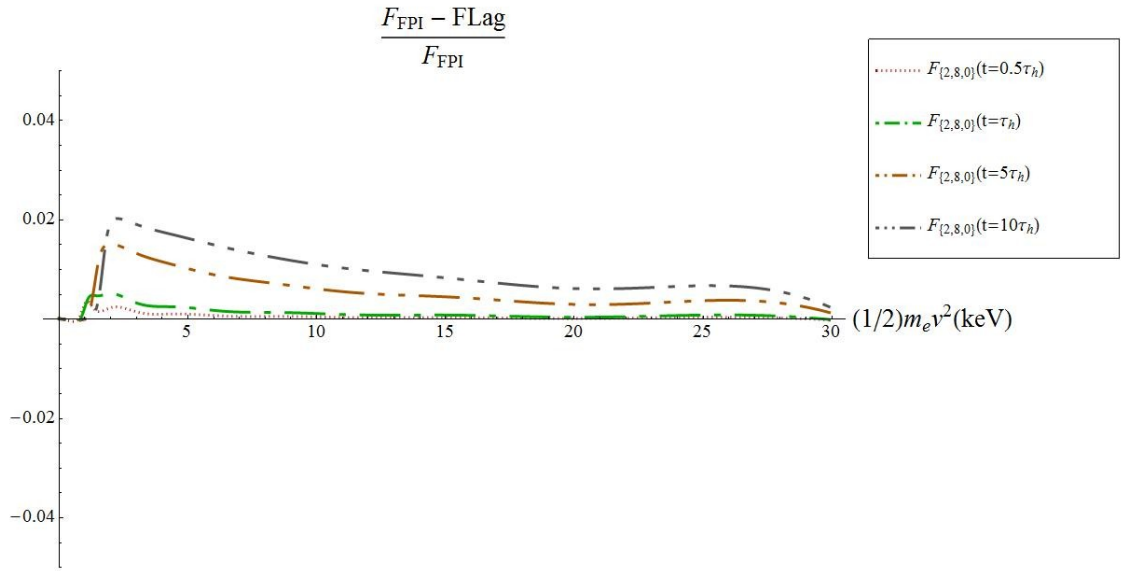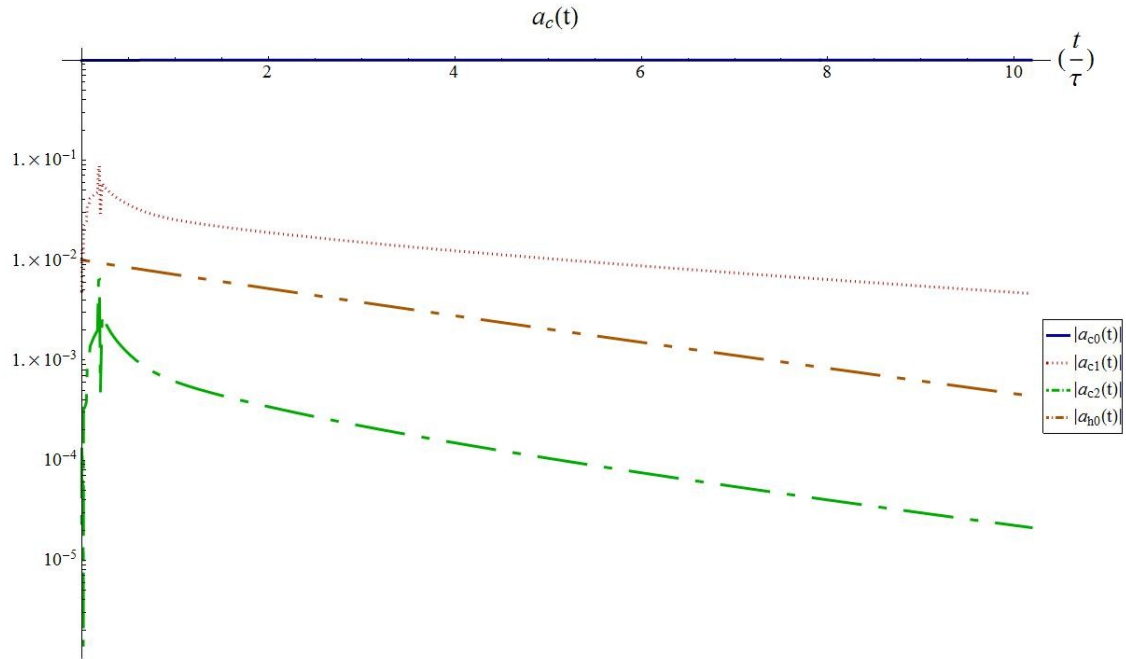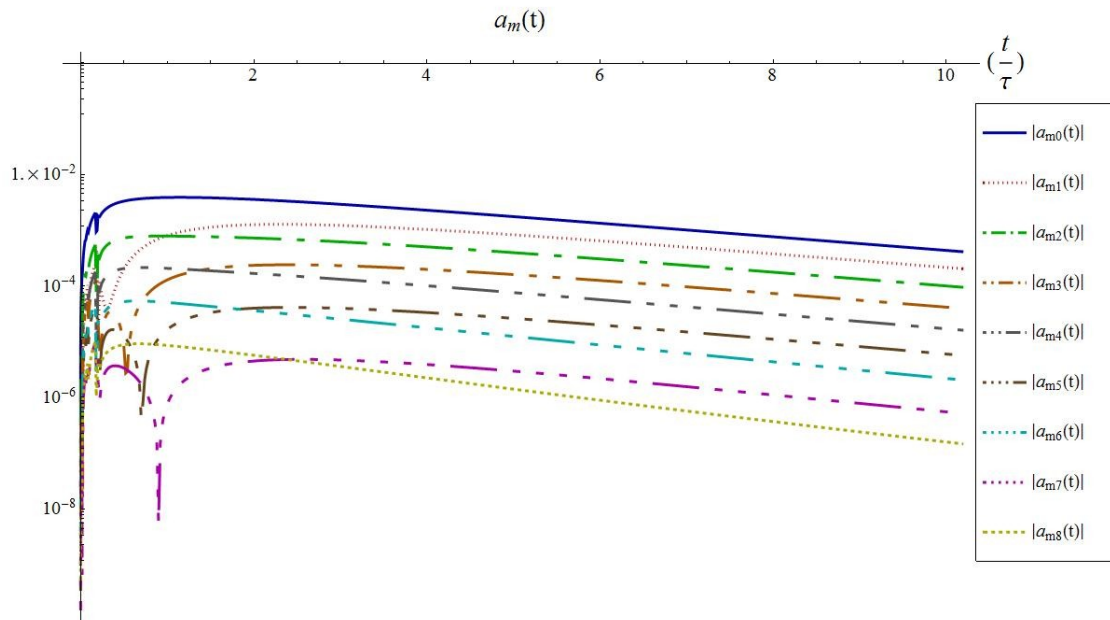
Figure (4.37) shows the time evolution of a three temperature form of the Laguerre distribution function ($N_c = 00$, $N_m = 08$, $N_h = 00$) for an initial two-Maxwellian distribution $\left(\frac{T_c(t=0)}{T_h(t=0)} = \frac{1}{100}, \frac{a_{c0}(t=0)}{a_{h0}(t=0)} = \frac{967}{33}\right)$. For this case, we ran the code for a longer time. Figure (4.38) shows the relative errors of the results of the time evolution of the distribution function compared to "FPI" at different times $\left(\frac{t}{\tau} = 1, 2, 5, 10, 20, 50\right)$. In this case, we have $(N_c + N_m + N_h + 6 = 14)$ unknowns in the Laguerre distribution function i.e. $a_{c0}(t), a_{m0}(t), a_{m1}(t), ...,$

$a_{m8}(t), a_{h0}(t), T_c, T_m, T_h$. We need to calculate the time evolution of 14 moments $(M_{\{N_c,N_m,N_h\},0}, M_{\{N_c,N_m,N_h\},2}, ..., M_{\{N_c,N_m,N_h\},26})$ to find the right coefficients and temperatures at each time using the fitting method described in section 2.3.

Note: After 50 collision time $(\frac{t}{\tau} > 50)$ the code cannot compute the time evolution of the Laguerre distribution function because most of the low moments are extremely close to their ultimate values (moments of a single Maxwellian) and the fitting method is not able to provide a proper fit after this time (over determined). It would be possible to make the code switch

automatically to a single Maxwellian when the moments are sufficiently close to their ultimate value, but this is not entirely satisfactory, as it would completely eliminate the remaining fast electrons. It would be better to develop a perturbation type of model for the fast electron population when it becomes become very small, but we have not had time to develop this.

Figure (4.39) shows the time evolution of the three temperatures. Eventually, $T_c(t)$ after many collision times tends toward the equilibrium temperature $(T_e = 0.04168)$. Although, $T_h(t)$ increases slightly and reaches $T_h(50\tau_h) \simeq 1.1 keV$, after 50 collision times, most of the total energy density is in cold electrons (mostly the $a_{c0}(t)$ term) because a_{h0}, a_{m0} and a_{m1} are very small.

$$T_c(50\tau_h) \simeq 4.277 * 10^{-2}, \qquad T_m(50\tau_h) \simeq 0.6159, \qquad T_h(50\tau_h) \simeq 1.136$$

$$a_{c0}(50\tau_h) \simeq 1$$

$$a_{m0}(50\tau_h) \simeq -5.315 * 10^{-7}, \qquad a_{m1}(50\tau_h) \simeq 3.757 * 10^{-7}$$

$$a_{h0}(50\tau_h) \simeq 5.058 * 10^{-7}$$

$$M_4(0) = \frac{3}{2} N_e T_e = 0.0641511$$

$$M_{4c0}(50\tau_h) = \frac{3}{2} a_{c0}(50\tau_h) T_c(50\tau_h) \simeq 0.0641511$$

$$M_{4m0}(50\tau_h) = \frac{3}{2} a_{m0}(50\tau_h) T_m(50\tau_h) \simeq -4.91 * 10^{-7}$$

$$M_{4m1}(50\tau_h) = -\frac{3}{2} a_{m1}(50\tau_h) T_m(50\tau_h) \simeq -3.47 * 10^{-7}$$

$$M_{4h0}(50\tau_h) = \frac{3}{2} a_{h0}(50\tau_h) T_h(50\tau_h) \simeq 8.62 * 10^{-7}$$

During the time evolution of the Laguerre distribution function, the hot and medium populations diminish (*i.e.* $|a_{m0}(t)|, |a_{m1}(t)|, ..., a_{h0}(t)$), and become part of the cold electrons.

Figure (4.40) and Figure (4.41) show the time evolution of the coefficients of the Laguerre distribution function. All of the coefficients gradually diminish during the time evolution of the Laguerre distribution function except $a_{c0}(t)$. The rapid decrease of $a_{h0}(t)$ is evident.

Figure (4.42) shows the time evolution of the moments of the Laguerre distribution function. Of course, moments 2 and 4 are always constant due to the density and energy conservation. The other moments are tending toward the moments of a single Maxwellian *i.e.* the ultimate solution of the distribution function at $t \to \infty$. Figure (4.43) shows the deviation of the moments from the moments of a single Maxwellian. In this case, since the initial temperature ratio is small $\left(\frac{T_c(0)}{T_h(0)} = \frac{1}{100}\right)$, it takes longer for the moments to get close to their ultimate value (*i.e.* moments of a single Maxwellian).
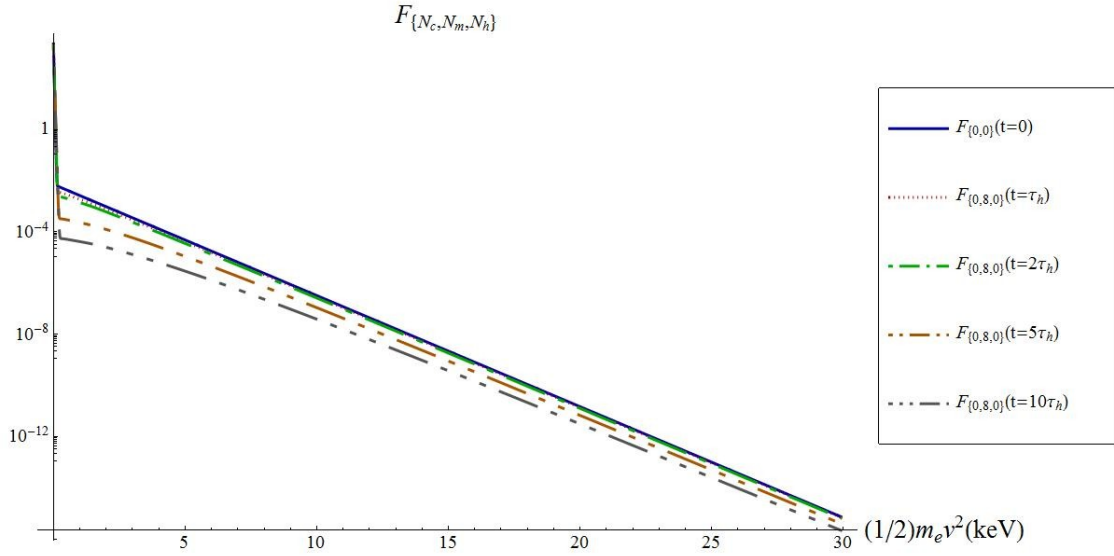
Figure (4.37): Time evolution of a three temperature form of the Laguerre distribution function $\left(N_c = 02, N_m = 08, N_h = 00, \frac{T_c(t=0)}{T_h(t=0)} = \frac{1}{100}, \frac{a_{c0}(t=0)}{a_{h0}(t=0)} = \frac{967}{33} \right)$.
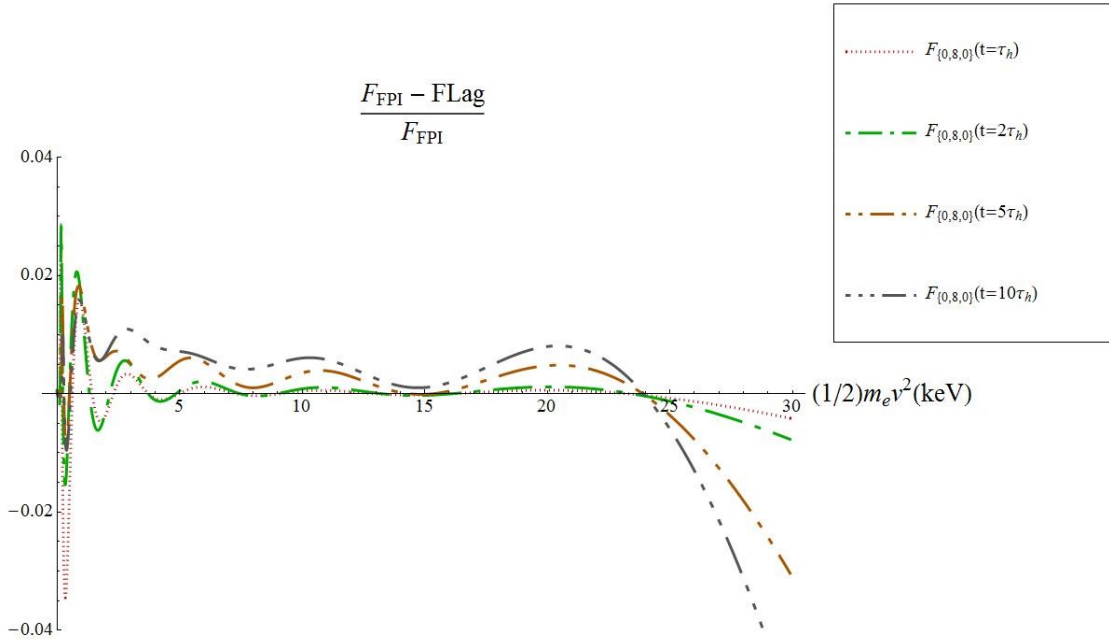

Figure (4.38): Relative error of the time evolution of a three temperature form of the Laguerre distribution function $\left(N_c = 02, N_m = 08, N_h = 00, \frac{T_c(t=0)}{T_h(t=0)} = \frac{1}{100}, \frac{a_{c0}(t=0)}{a_{h0}(t=0)} = \frac{967}{33} \right)$.
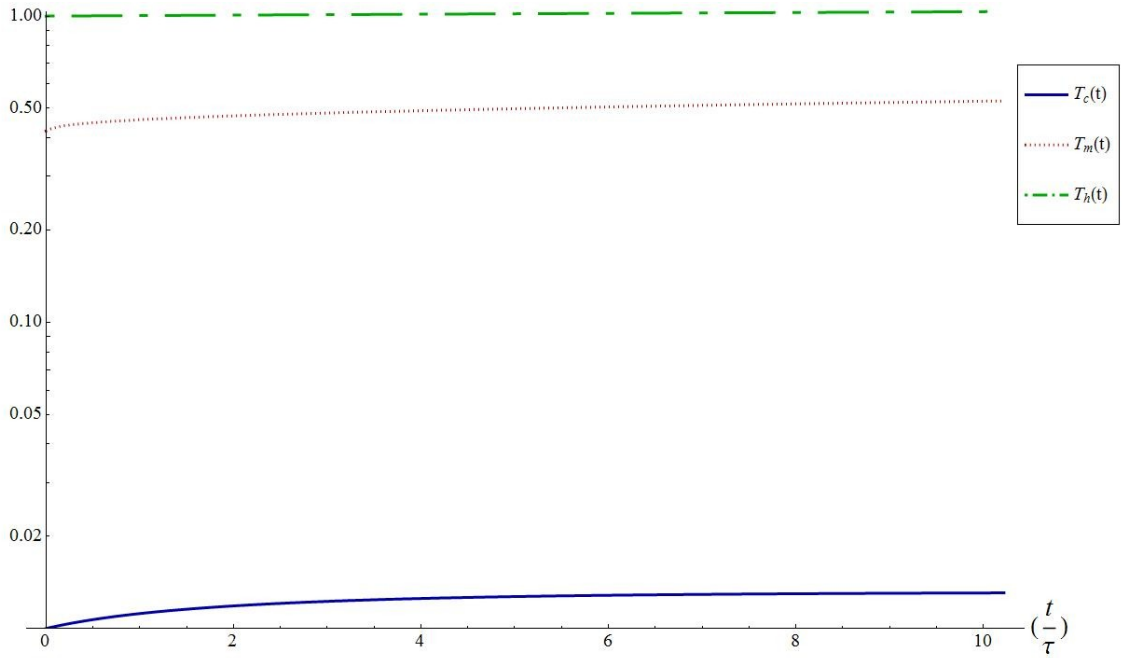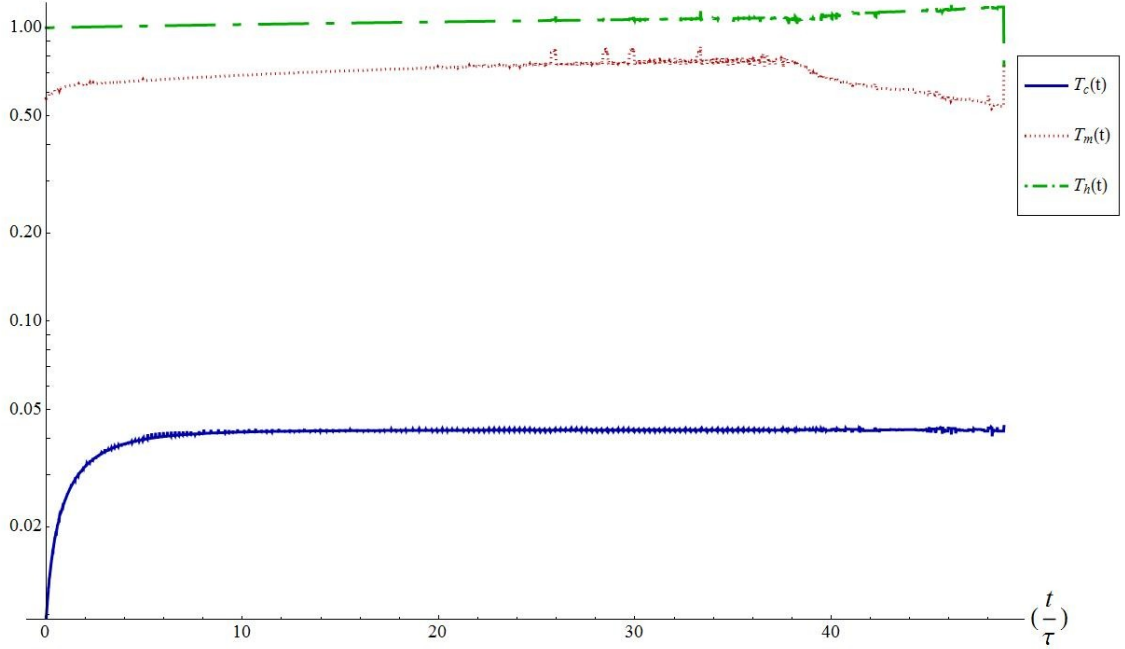
Figure (4.39): Time evolution of the temperatures of the Laguerre distribution function $\left(N_c = 02, N_m = 08, N_h = 00, \frac{T_c(t=0)}{T_h(t=0)} = \frac{1}{100}, \frac{a_{c0}(t=0)}{a_{h0}(t=0)} = \frac{967}{33}\right)$.
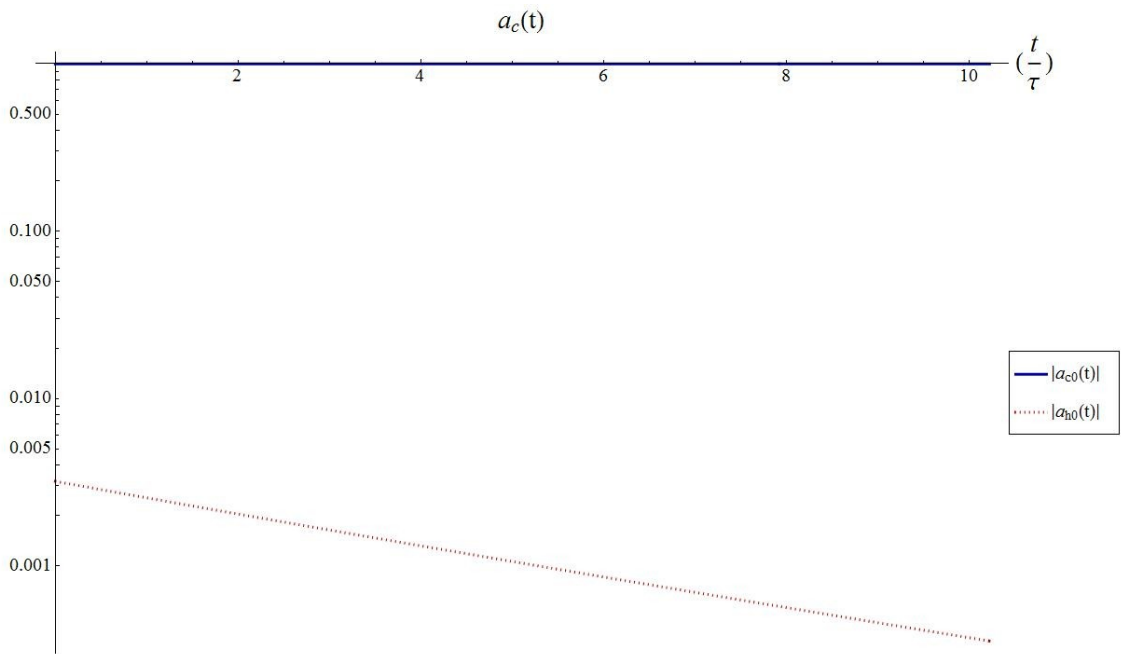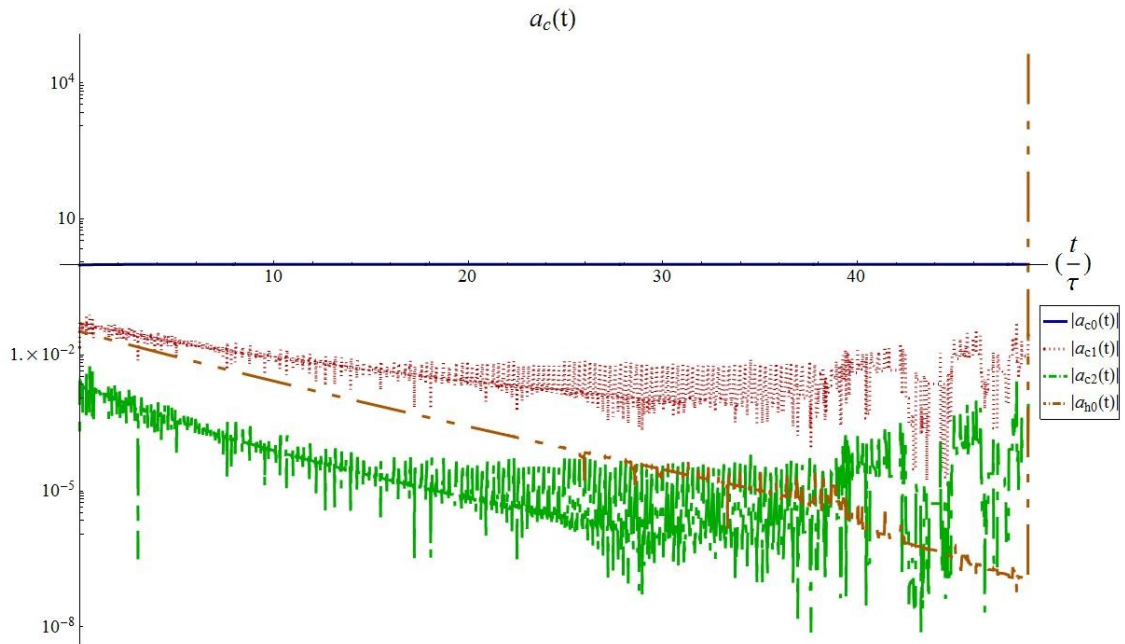

Figure (4.40): Time evolution of the coefficients (cold and hot) of the Laguerre distribution function $\left(N_c = 02, N_m = 08, N_h = 00, \frac{T_c(t=0)}{T_h(t=0)} = \frac{1}{100}, \frac{a_{c0}(t=0)}{a_{h0}(t=0)} = \frac{967}{33}\right)$.
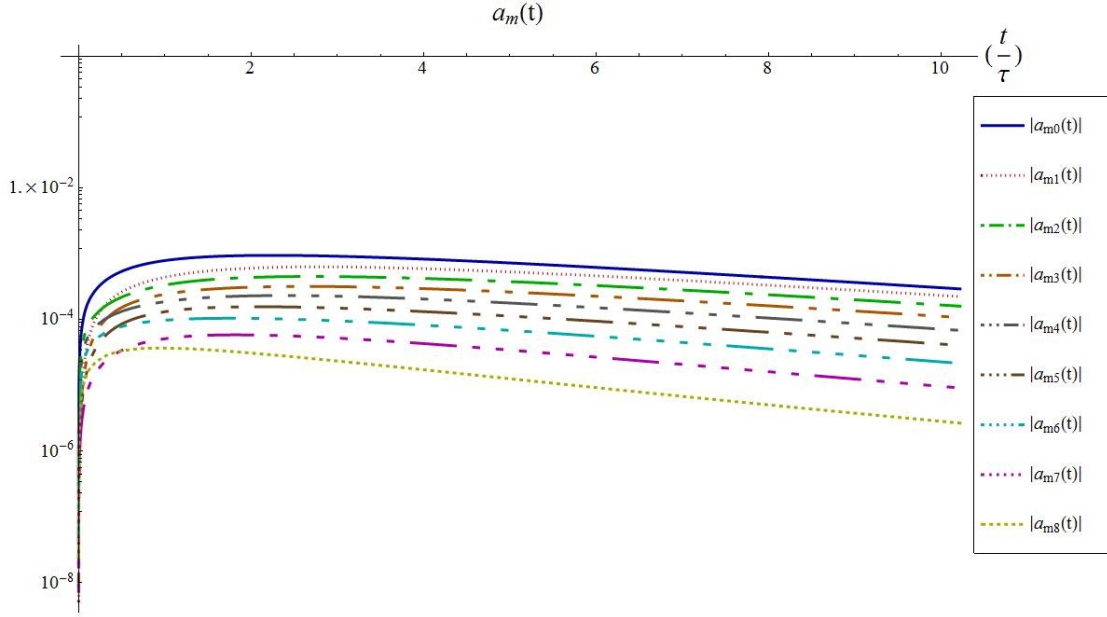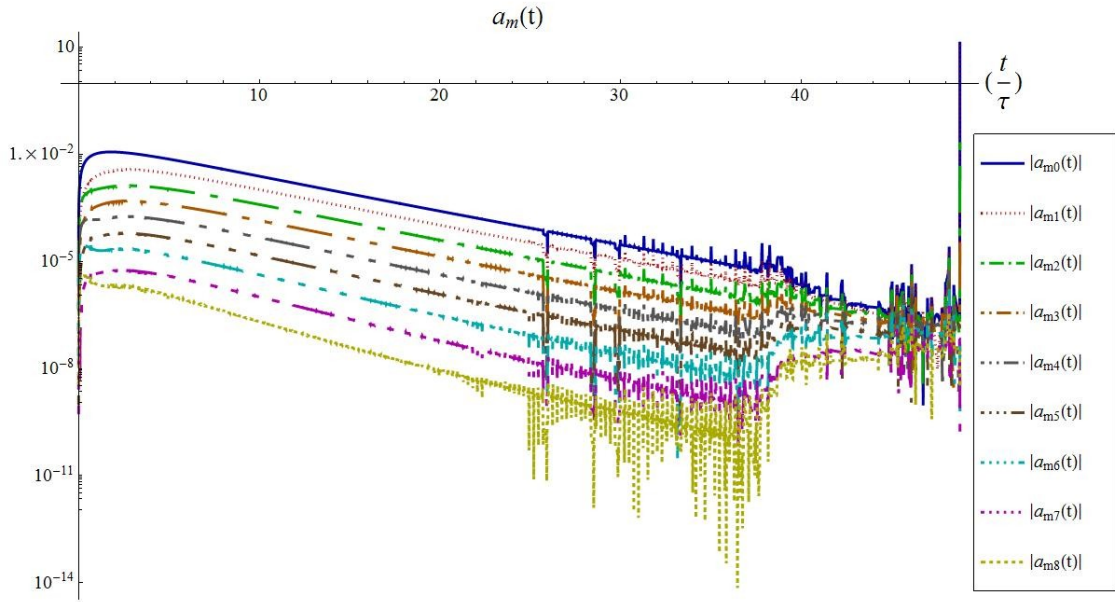
Figure (4.41): Time evolution of the coefficients (medium) of the Laguerre distribution function $\left(N_c = 02, N_m = 08, N_h = 00, \frac{T_c(t=0)}{T_h(t=0)} = \frac{1}{100}, \frac{a_{c0}(t=0)}{a_{h0}(t=0)} = \frac{967}{33}\right)$.
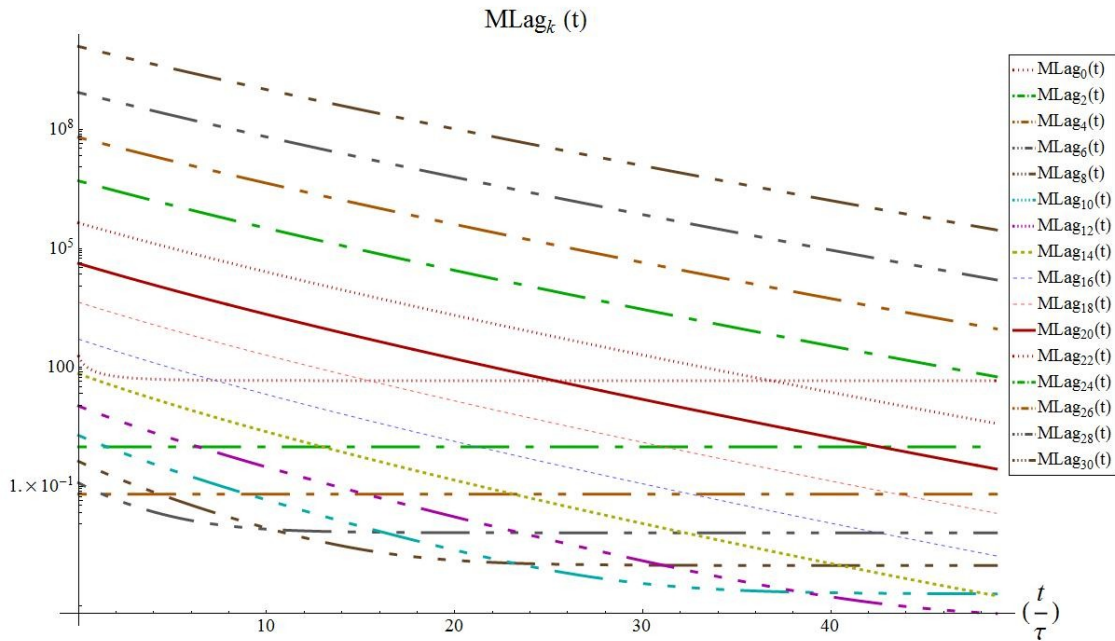
Figure (4.42): Time evolution of the moments of the Laguerre distribution function $\left(N_c = 02, N_m = 08, N_h = 00, \frac{T_c(t=0)}{T_h(t=0)} = \frac{1}{100}, \frac{a_{c0}(t=0)}{a_{h0}(t=0)} = \frac{967}{33}\right)$

$$\text{Dev}_k(t) = \frac{\text{MLag}_k(t) - \text{M1MXW}_k(t)}{\text{MLag}_k(t)}$$
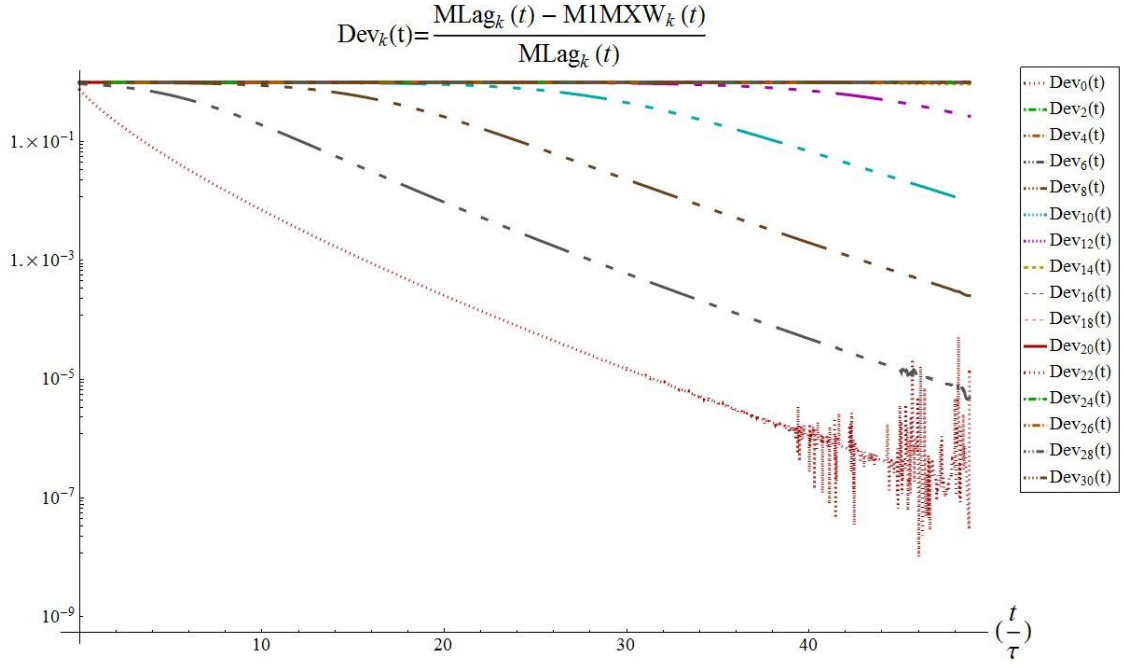
Figure (4.43): Time evolution of the deviation of the moments of the Laguerre distribution function from the moments of a single Maxwellian $\left(N_c = 02, N_m = 08, N_h = 00, \frac{T_c(t=0)}{T_h(t=0)} = \frac{1}{100}, \frac{a_{c0}(t=0)}{a_{h0}(t=0)} = \frac{967}{33} \right)$.

4.5. Time evolution of the Laguerre distribution function for a 1:1000 initial temperature ratio $\left(\frac{T_c(t=0)}{T_h(t=0)} = \frac{1}{1000} \right)$

4.5.1. A three temperature form of the Laguerre distribution function ($N_c = 02, N_m = 06, N_h = 00$); 9:1 initial density ratio $\left(\frac{a_{c0}(t=0)}{a_{h0}(t=0)} = 9 \right)$ (case no. 44 in Table (4.1))

Figure (4.44) shows the time evolution of a three temperature form of the Laguerre distribution function ($N_c = 02$, $N_m = 06$, $N_h = 00$) for an initial two-Maxwellian distribution $\left(\frac{T_c(t=0)}{T_h(t=0)} = \frac{1}{1000}, \frac{a_{c0}(t=0)}{a_{h0}(t=0)} = 9 \right)$. As we expected according to the fits in sub-section 2.5.8, a three temperature form of the Laguerre distribution function is suitable for representing the time evolution of the distribution function in this section. Figure (4.45) shows the relative errors of the results of the time evolution of the distribution function compared to "FPI" at different times $\left(\frac{t}{\tau} = 0.5, 1, 5, 10 \right)$. The relative error is less than 2% below energy 30 keV. In this case, we have ($N_c + N_m + N_h + 6 = 14$) unknowns in the Laguerre distribution function i.e. $a_{c0}(t), a_{c1}(t),$

87

$a_{c2}(t), a_{m0}(t), a_{m1}(t), \ldots, a_{m6}(t), a_{h0}(t), T_c, T_m, T_h$. We need to calculate the time evolution of 14 moments $(M_{\{N_c,N_m,N_h\},0}, M_{\{N_c,N_m,N_h\},2}, \ldots, M_{\{N_c,N_m,N_h\},26})$ to find the right coefficients and temperatures at each time using the fitting method described in section 2.3.

Figure (4.46) shows the time evolution of the three temperatures. Eventually, after many collision times, $T_c(t)$ tends toward the equilibrium temperature $T_e = 0.1009$.

Figure (4.47) and Figure (4.48) show the time evolution of the coefficients of the Laguerre distribution function. As before, all of the coefficients gradually diminish during the time evolution of the Laguerre distribution function except $a_{c0}(t)$, as the distribution function gradually relaxes toward a single Maxwellian at this equilibrium temperature.

Figure (4.44): Time evolution of a three temperature form of the Laguerre distribution function $(N_c = 02, N_m = 06, N_h = 00, \frac{T_c(t=0)}{T_h(t=0)} = \frac{1}{1000}, \frac{a_{c0}(t=0)}{a_{h0}(t=0)} = 9)$.

Figure (4.45): Relative error of the time evolution of a three temperature form of the Laguerre distribution function $(N_c = 02, N_m = 06, N_h = 00, \frac{T_c(t=0)}{T_h(t=0)} = \frac{1}{1000}, \frac{a_{c0}(t=0)}{a_{h0}(t=0)} = 9)$.

Figure (4.46): Time evolution of the temperatures of the Laguerre distribution function $(N_c = 02, N_m = 06, N_h = 00, \frac{T_c(t=0)}{T_h(t=0)} = \frac{1}{1000}, \frac{a_{c0}(t=0)}{a_{h0}(t=0)} = 9)$.

Figure (4.47): Time evolution of the coefficients (cold and hot) of the Laguerre distribution function $(N_c = 02, N_m = 06, N_h = 00, \frac{T_c(t=0)}{T_h(t=0)} = \frac{1}{1000}, \frac{a_{c0}(t=0)}{a_{h0}(t=0)} = 9)$.
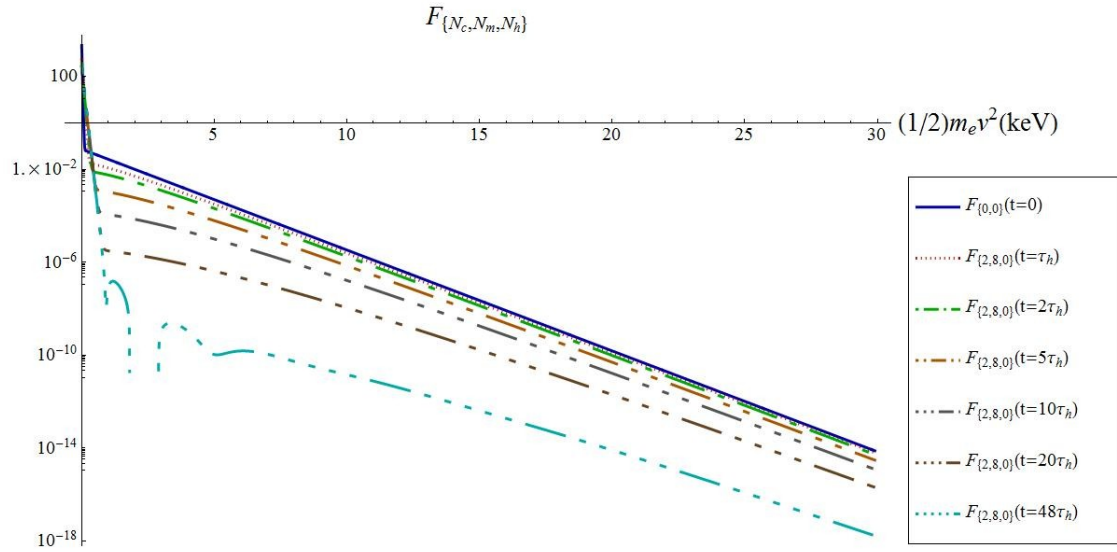
90

Figure (4.48): Time evolution of the coefficients (medium) of the Laguerre distribution function ($N_c = 02, N_m = 06, N_h = 00, \frac{T_c(t=0)}{T_h(t=0)} = \frac{1}{1000}, \frac{a_{c0}(t=0)}{a_{h0}(t=0)} = 9$).

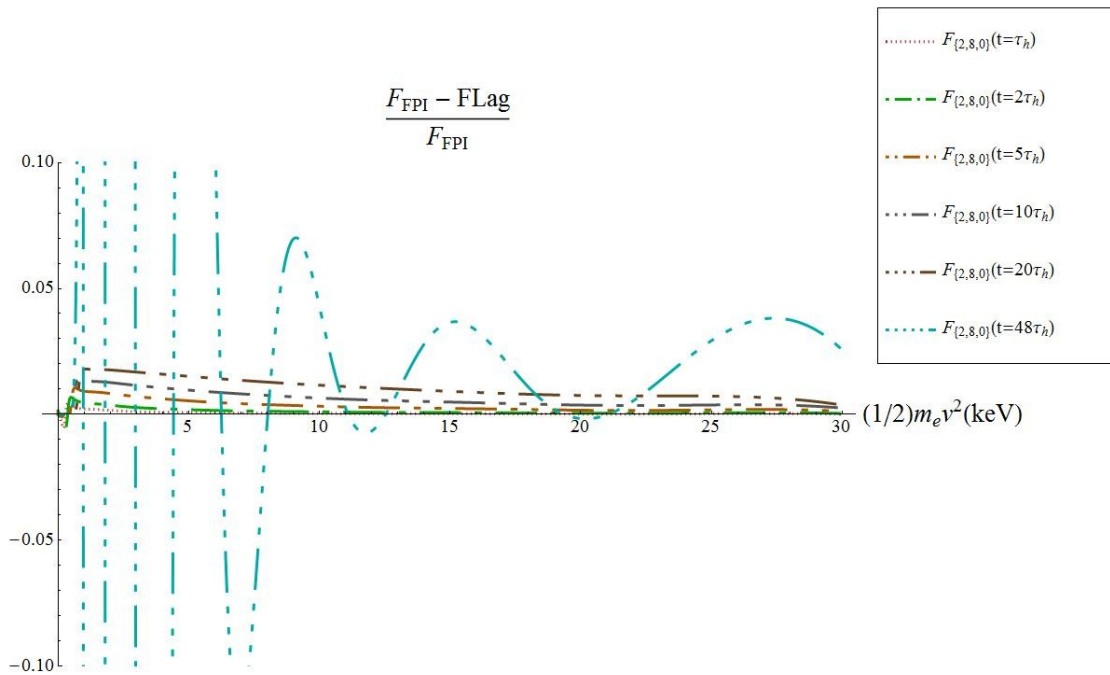### 4.5.2. A three temperature form of the Laguerre distribution function ($N_c = 02, N_m = 08, N_h = 00$); 9:1 initial density ratio $\left(\frac{a_{c0}(t=0)}{a_{h0}(t=0)} = 9\right)$ (case no. 46 in Table (4.1))

Figure (4.49) shows the time evolution of a three temperature form of the Laguerre distribution function ($N_c = 02$, $N_m = 08$, $N_h = 00$) for an initial two-Maxwellian distribution $\left(\frac{T_c(t=0)}{T_h(t=0)} = \frac{1}{1000}, \frac{a_{c0}(t=0)}{a_{h0}(t=0)} = 9\right)$. For this case, we ran the code for a longer time. Figure (4.50) shows the relative errors of the results of the time evolution of the distribution function compared to "FPI" at different times $\left(\frac{t}{\tau} = 1, 2, 5, 10, 20, 50, 100\right)$. In this case, we have ($N_c + N_m + N_h + 6 = 16$) unknowns in the Laguerre distribution function i.e. $a_{c0}(t), a_{c1}(t), a_{c2}(t), a_{m0}(t),$

$a_{m1}(t), \ldots, a_{m8}(t), a_{h0}(t), T_c, T_m, T_h$. We need to calculate the time evolution of 16 moments $(M_{\{N_c, N_m, N_h\}, 0}, M_{\{N_c, N_m, N_h\}, 2}, \ldots, M_{\{N_c, N_m, N_h\}, 30})$ to find the right coefficients and temperatures at each timestep using the fitting method described in section 2.3.

Figure (4.51) shows the time evolution of the three temperatures. Eventually, after many collision times, $T_c(t)$ tends toward the equilibrium temperature ($T_e = 0.1009$). Although, $T_h(t)$ increases slightly and after 100 collision time reaches ($T_h(100\tau_h) \simeq 1.2 KeV$), most of the total

energy density is in the cold electrons (mostly the $a_{c0}(t)$ term) because a_{h0}, a_{m0} and a_{m1} are extremely small.

$$T_c(100\tau_h) \simeq 0.1009, \qquad T_m(100\tau_h) \simeq 0.9148, \qquad T_h(100\tau_h) \simeq 1.209$$

$$a_{c0}(100\tau_h) \simeq 1, \qquad a_{c1}(100\tau_h) \simeq -1.2 * 10^{-5}$$

$$a_{m0}(100\tau_h) \simeq -4.063 * 10^{-11}, \qquad a_{m1}(100\tau_h) \simeq 1.297 * 10^{-11}$$

$$a_{h0}(100\tau_h) \simeq 4.068 * 10^{-11}$$

$$M_4(0) = \frac{3}{2} N_e T_e = 0.15135$$

$$M_{4c0}(100\tau_h) = \frac{3}{2} a_{c0}(100\tau_h) T_c(100\tau_h) \simeq 0.151348$$

$$M_{4c1}(100\tau_h) = -\frac{3}{2} a_{c1}(100\tau_h) T_c(100\tau_h) \simeq 1.870 * 10^{-6}$$

$$M_{4m0}(100\tau_h) = \frac{3}{2} a_{m0}(100\tau_h) T_m(100\tau_h) \simeq -5.575 * 10^{-11}$$

$$M_{4m1}(100\tau_h) = -\frac{3}{2} a_{m1}(100\tau_h) T_m(100\tau_h) \simeq -1.7802 * 10^{-11}$$

$$M_{4h0}(100\tau_h) = \frac{3}{2} a_{h0}(100\tau_h) T_h(100\tau_h) \simeq 7.376 * 10^{-11}$$

During the time evolution of the Laguerre distribution function the hot and medium population diminish (*i.e.* $a_{m0}(t), a_{m1}(t), a_{m2}(t), a_{h0}(t)$).

Figure (4.52) and Figure (4.53) show the time evolution of the coefficients of the Laguerre distribution function. All of the coefficients gradually diminish during the time evolution of the Laguerre distribution function except $a_{c0}(t)$. The rapid decrease of $a_{h0}(t)$ is particularly noteworthy.

Figure (4.54) shows the time evolution of the moments of the Laguerre distribution function. Of course, moments 2 and 4 are always constant due to the density and energy conservation. The other moments are tending toward the moments of a single Maxwellian *i.e.* the ultimate solution of the distribution function at $t \to \infty$. Figure (4.55) shows the deviation of the moments from the moments of a single Maxwellian. In this case, since the initial temperature ratio is small $\left(\frac{T_c(0)}{T_h(0)} = \frac{1}{1000}\right)$, the moments get close to their ultimate value slowly (*i.e.* moments of a single Maxwellian) and after 100 collision time most of the moments have not relaxed yet.

Note:

Obviously, the process of relaxation of the moments takes longer for a lower initial temperature ratio $\frac{T_c(0)}{T_h(0)}$ (by comparing Figure (4.10), Figure (4.19), Figure (4.26), Figure (4.43) and Figure (4.55)).

In Figure (4.49), we have shown the local temperatures (from the slope of the distribution function) in different energy regions for the Laguerre distribution function at the latest physical time ($F_{\{2,8,0\}}(100\tau_h)$) using three lines. These lines indicate that during the time evolution the relaxation of the medium energy electrons is faster than for the high energy electrons, consequently, after many collisions, the local temperature of the medium energy part of the distribution function increases and it becomes even larger than the local temperature of the high energy region of the distribution function. This temperature of the intermediate energy electrons must not be confused with T_m, the intermediate temperature used in the three temperature form of the Laguerre distribution, which is lower than T_h. The local temperature of the low energy region is very near the temperature of the ultimate single Maxwellian at $t \to \infty$.
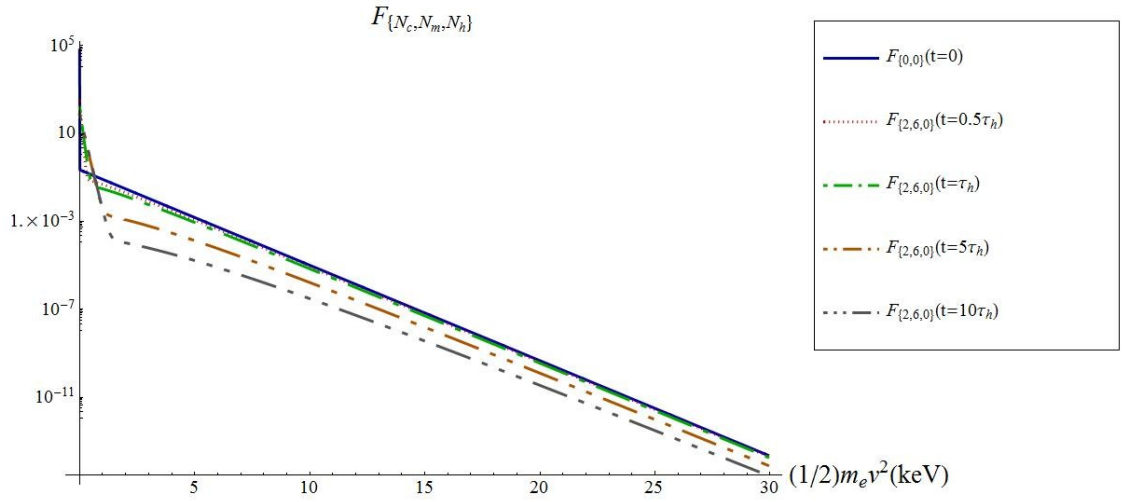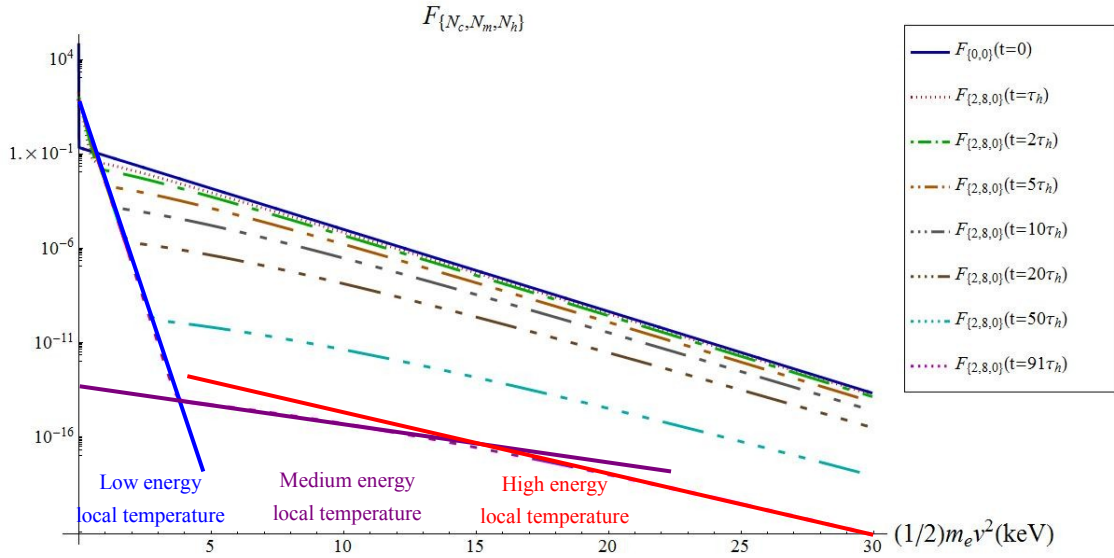
Figure (4.49): Time evolution of a three temperature form of the Laguerre distribution function ($N_c = 02, N_m = 08, N_h = 00, \frac{T_c(t=0)}{T_h(t=0)} = \frac{1}{1000}, \frac{a_{c0}(t=0)}{a_{h0}(t=0)} = 9$).
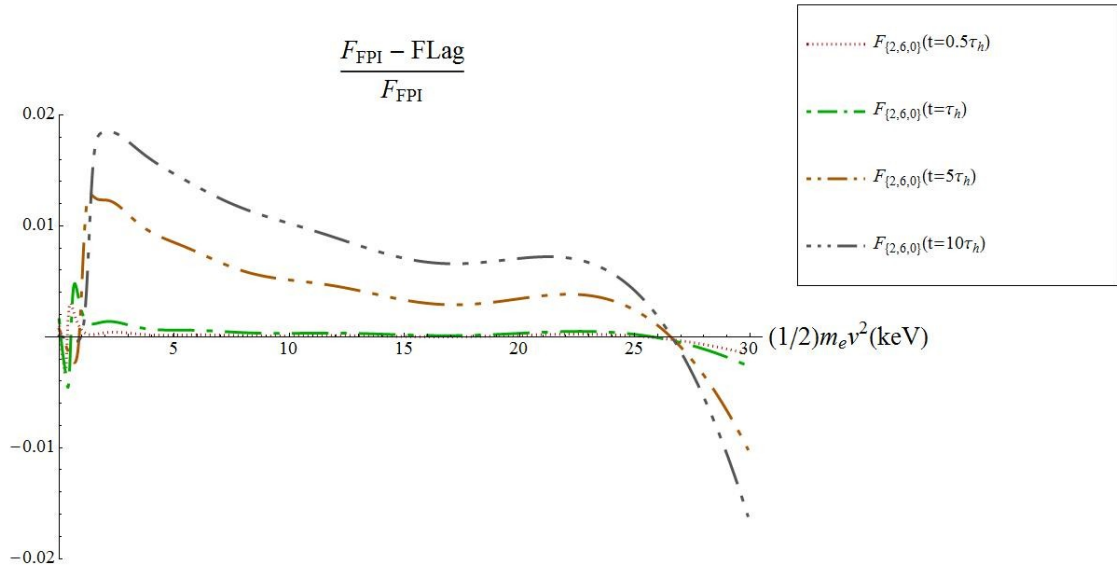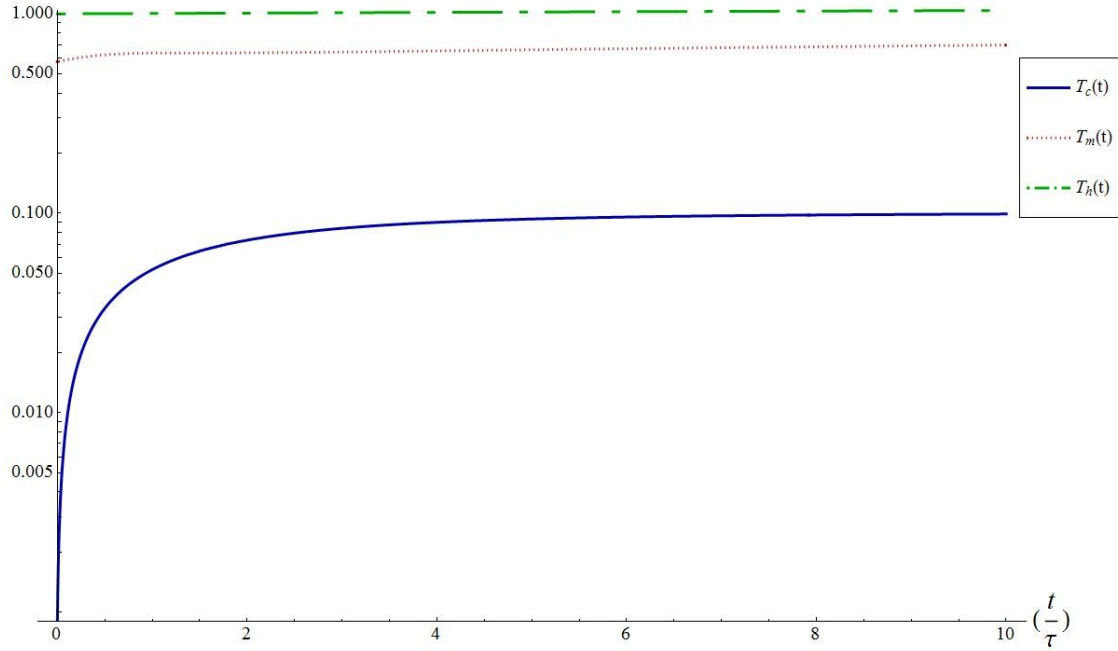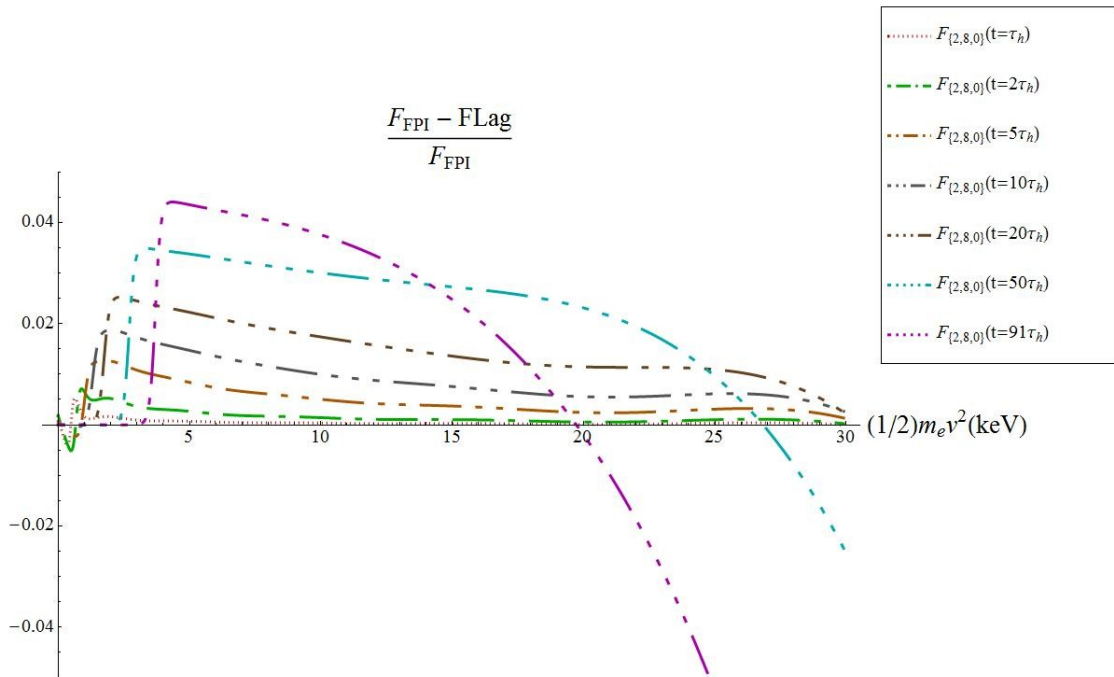

Figure (4.50): Relative error of the time evolution of a three temperature form of the Laguerre distribution function ($N_c = 02, N_m = 08, N_h = 00, \frac{T_c(t=0)}{T_h(t=0)} = \frac{1}{1000}, \frac{a_{c0}(t=0)}{a_{h0}(t=0)} = 9$).
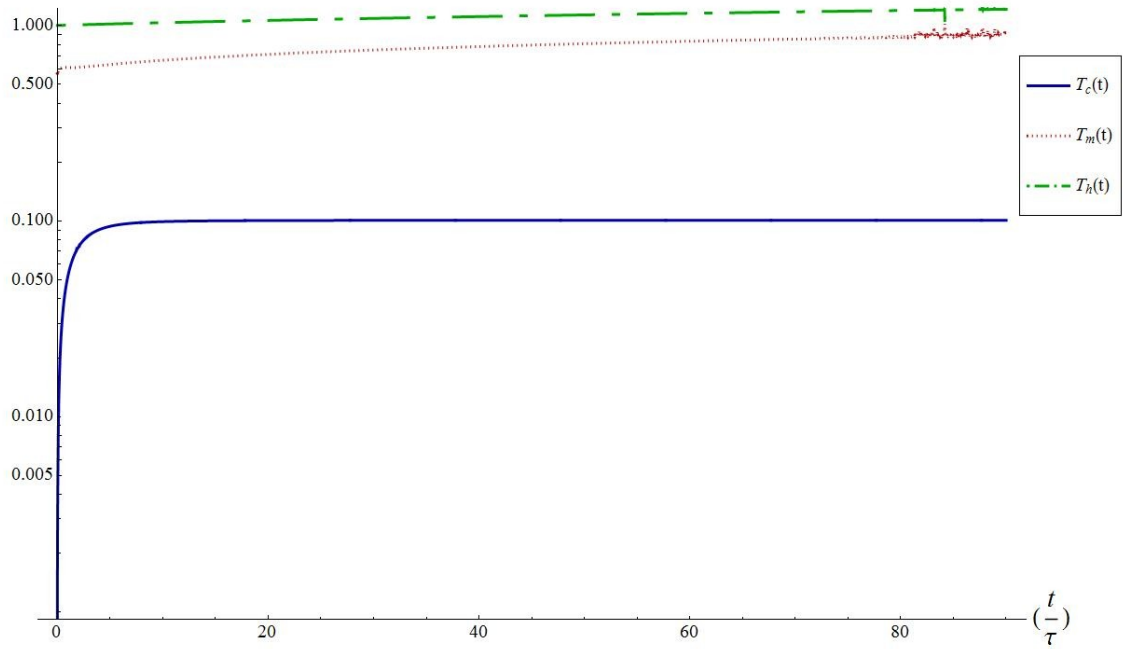
Figure (4.51): Time evolution of the temperatures of the Laguerre distribution function ($N_c = 02, N_m = 08, N_h = 00, \frac{T_c(t=0)}{T_h(t=0)} = \frac{1}{1000}, \frac{a_{c0}(t=0)}{a_{h0}(t=0)} = 9$).
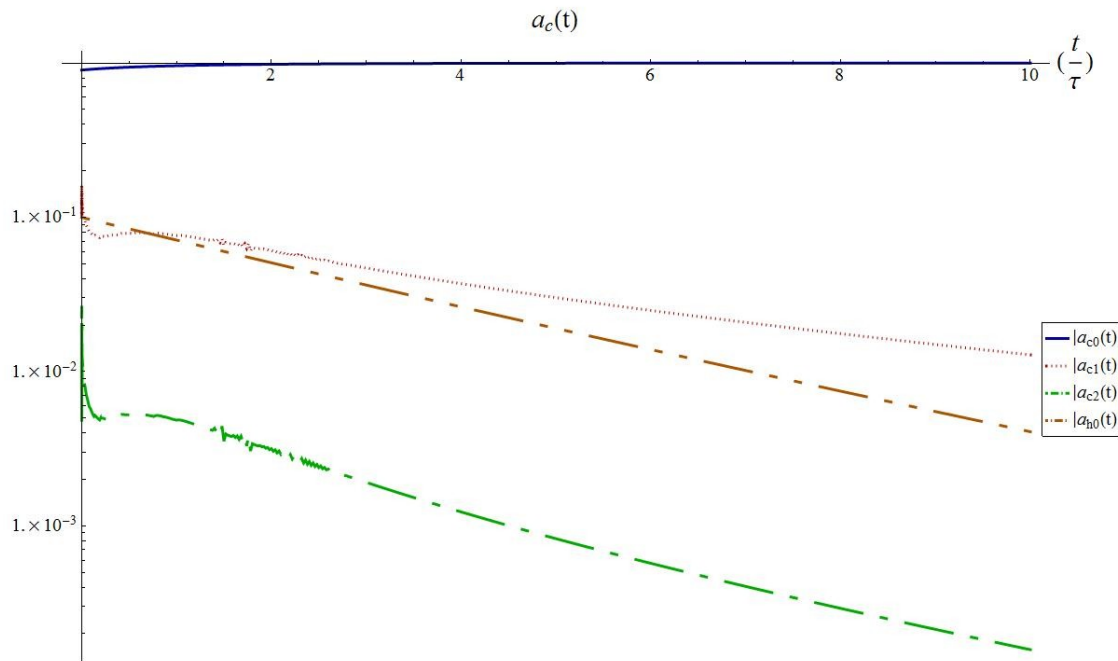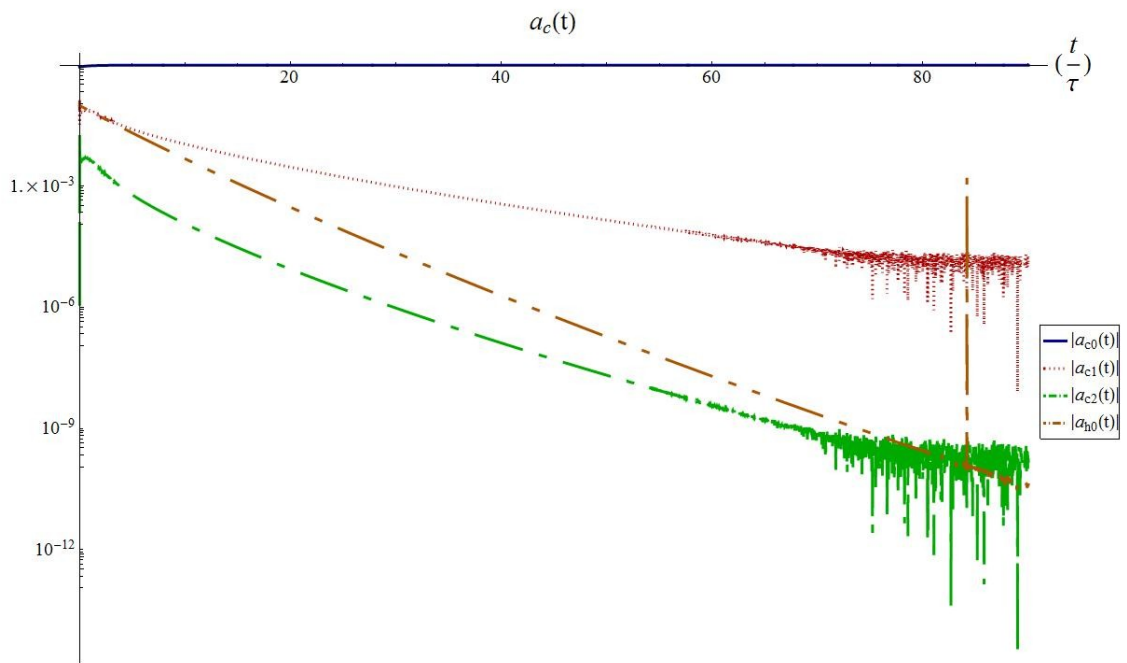

Figure (4.52): Time evolution of the coefficients (cold and hot) of the Laguerre distribution function ($N_c = 02, N_m = 08, N_h = 00, \frac{T_c(t=0)}{T_h(t=0)} = \frac{1}{1000}, \frac{a_{c0}(t=0)}{a_{h0}(t=0)} = 9$).
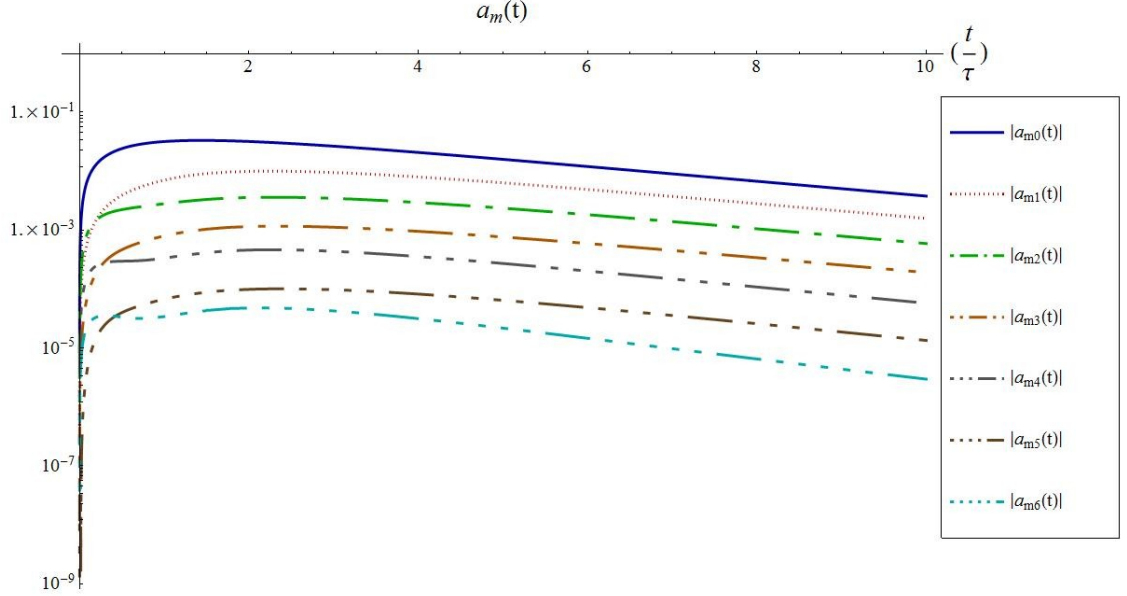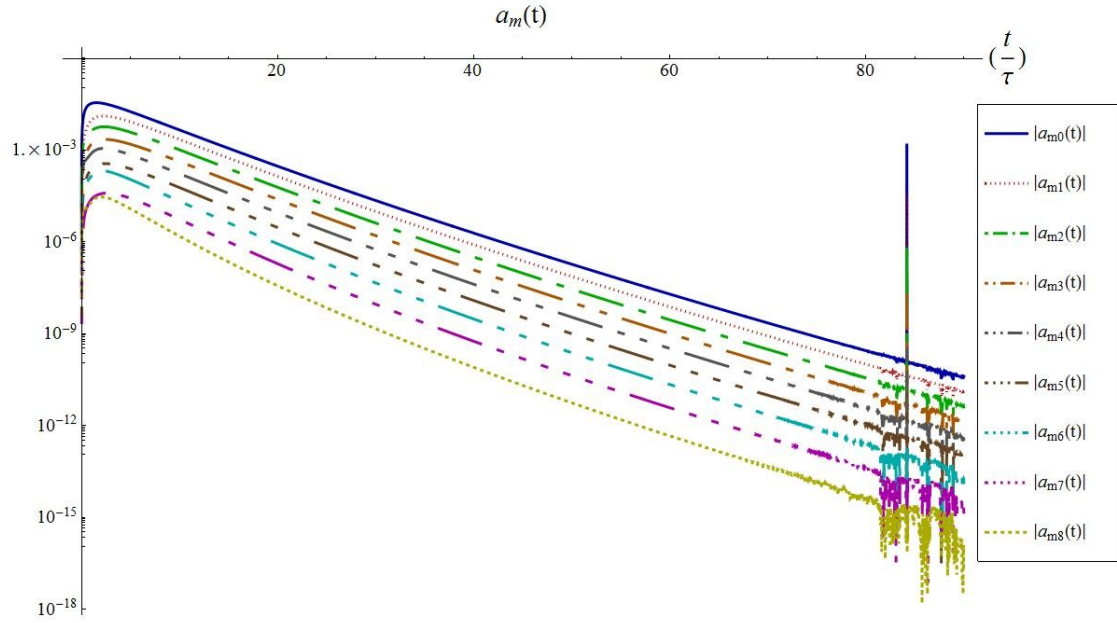
Figure (4.53): Time evolution of the coefficients (medium) of the Laguerre distribution function ($N_c = 02, N_m = 08, N_h = 00, \frac{T_c(t=0)}{T_h(t=0)} = \frac{1}{1000}, \frac{a_{c0}(t=0)}{a_{h0}(t=0)} = 9$).
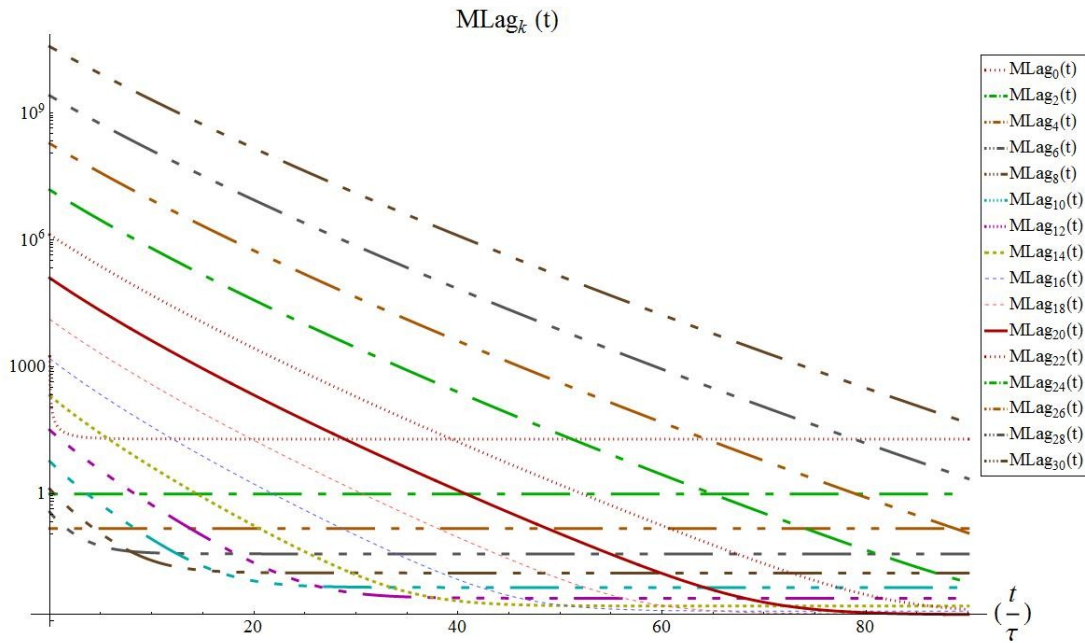
Figure (4.54): Time evolution of the moments of the Laguerre distribution function ($N_c = 02, N_m = 08, N_h = 00, \frac{T_c(t=0)}{T_h(t=0)} = \frac{1}{1000}, \frac{a_{c0}(t=0)}{a_{h0}(t=0)} = 9$).

$$\text{Dev}_k(t) = \frac{\text{MLag}_k(t) - \text{M1MXW}_k(t)}{\text{MLag}_k(t)}$$
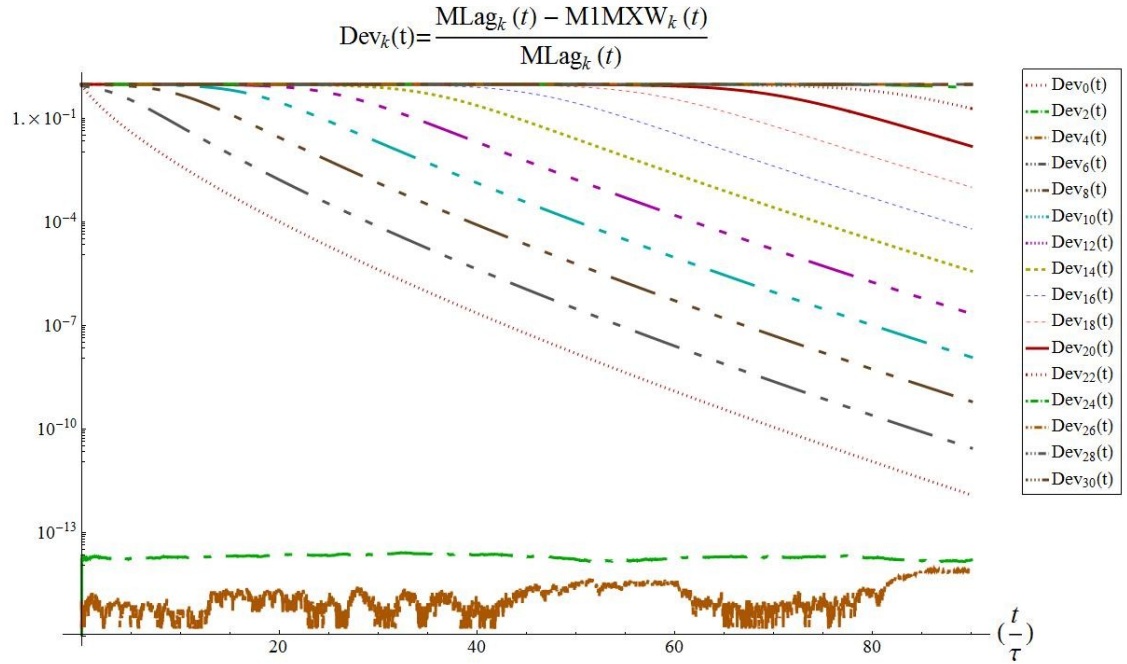
Figure (4.55): Time evolution of the deviation of the moments of the Laguerre distribution function from the moments of a single Maxwellian ($N_c = 02, N_m = 08, N_h = 00, \frac{T_c(t=0)}{T_h(t=0)} = \frac{1}{1000}, \frac{a_{c0}(t=0)}{a_{h0}(t=0)} = 9$).

In summary, for all of the cases provided in this chapter, we can see an elbow in the plots of the distribution function as a function of energy. Obviously, the energy of the joint of this elbow is decreasing when we decrease the initial temperature ratio T_c/T_h. This energy is important to us because, beyond this energy the distribution function is dominated by the hots, whereas, the lower energy part is dominated by the colds. Qualitatively, this describes how we should choose the number of terms for each population (cold, medium, hot). When the temperature ratio is high (*i.e.* subsections 4.1 and 4.2), the energy of the joint is at higher energies, thus we need to choose more cold Laguerre terms. For lower temperature cases (*i.e.* subsections 4.3 through 4.5) the energy of the elbow is at relatively lower energies and we need to choose more medium Laguerre terms instead.

Also, by looking more closely at the time evolution of the distribution function for each case, we can see that the energy of the joint also increases in time. This describes the relaxation of the hots on the cold component of the distribution function. This phenomenon is also observable in the plots of the time evolution of the moments, where the moments are tending toward the moments of the ultimate equilibrium Maxwellian solution of the time evolution of the distribution function. This process is slower when the initial temperature ratio is lower (*i.e.* $T_c/T_h < 0.1$) and

describes the reason why the coefficients of the Laguerre terms (exept a_{c0}) are diminishing more slowly in time for the cases initialized with lower temperature ratios.

In this chapter we provided the time evolution of the distribution function for different initial temperature ratios. We also, compared the results to the results obtained from "FPI" code. In all of the cases, by using less than 15 terms of the Laguerre polynomials, we can provide the time evolution of the distribution function for energy below 15 times T_h with relative error less than 10% (we also see that by adding more terms we can improve the accuracy of results up to higher energies).

As a result, in very low initial temperature ratios cases (*e.g.* $\frac{T_c}{T_h} < 0.01$) where, we need many points in the finite velocity grid in the "FPI" code (*e.g.* 19000 points), nevertheless, we can treat the time evolution of the distribution function by using just 15 moment equations of the Laguerre distribution function. In order to compare the computational time of the "FPI" with the Laguerre code, we ran both codes for the time evolution of the distribution function of a typical case initialized with a two-Maxwellians with temperature ratio 1000:1 for the duration of 10 collision times (of the hot temperature). Although far less effort was made to optimize it than for "FPI", the Laguerre code finished the process in 4:20 minutes and "FPI" in 30 minutes.

Chapter 5

Conclusion

The Vlasov-Fokker-Planck equation describes the effect of an electro-magnetic field and spatial gradients inside the plasma, using the equations of motion and considering the continuity equation in phase space (1-2). Without the presence of the magnetic field (except possibly along axis $\hat{x}$) and assuming azimutal symmetry about the axis $\hat{x}$ (the direction of the electric field or the gradients) one can reduce the 6 phase-space dimensions of the distribution function to just 3 (x, v, μ) ((1-3) and (1-4)). Further, by expanding the angular dependence μ in terms of the Legendre polynomials ((1-5) and (1-6)), finally, we can rewrite the Vlasov-Fokker-Planck equation as a set of coupled equations in (x,v) (1-7). A finite difference grid on x is the best way to simulate the time evolution of the distribution function in different positions. But we first need to solve the collision terms on the right hand side of this equation. One solution is using another finite difference grid in v. The "FPI" code [16, 37] is based on this technique, and the results produced by this code are very close to the results obtained experimentally [37, 58]. The only issue about using this code is that it is time consuming specially for the high temperature ratios where we need a higher resolution on the energy grid to cover the perturbations in low energy region. In this present work, we have introduced the multi-temperature Laguerre distribution function (see equation (1-14)). We suggest replacing the finite difference grid on v with the multi-temperature Laguerre distribution function. In many cases, it is useful to have an analytic form (Laguerre distribution function) for the distribution function instead of a set of values on a velocity or energy grid. For example, we can calculate the rates of ionization and excitation analytically, instead of doing a numerical integration on a velocity or energy grid. This is another advantage of using the Laguerre distribution function.

In this work, we have only provided the time evolution of the isotropic part of the electron distribution function for the *e-e* collisions. This is the most complicated part of the Vlasov-Fokker-Planck equation, as all other parts are linear. We first showed, in chapter 2, that it is possible to express the distribution function (*i.e.* the result of the time evolution of the distribution function provided by "FPI" for the *e-e* collisions) initialized with different temperature ratios, with the Laguerre distribution function by matching the moments of both distribution functions (section 2.3). Of course, this method is non-trivial and beyond a certain energy the Laguerre distribution function cannot express the distribution function any more. But, in section 2.4 we showed that the contribution of the high energy region in the density and energy equations is

negligible. But still, we can provide a good fit up to higher energy by adding more terms of generalized Laguerre polynomials and use more temperatures in the form of the Laguerre distribution function (2-1). Later in chapter 3 we provided the rates of change of the moment equations due to e-e collisions and also, we provided an algorithm to calculate the time evolution of the Laguerre distribution function summarized in Figure (4.1). Finally, we showed the results of the time evolution of the Laguerre distribution function for different initial temperature ratios and using different number of Laguerre terms and different forms of the Laguerre distribution function in chapter 4. The results show good agreement with the results obtained from "FPI".

Choosing the form of the Laguerre distribution function is not arbitrary and the structure of the actual distribution function needs to be considered. For example, for initial temperature ratio 4:1 $\left(\frac{T_c(t=0)}{T_h(t=0)} = \frac{1}{4}\right)$ a single temperature form of the Laguerre distribution function cannot represent the actual distribution function unless we use at least 16 terms of the generalized Laguerre polynomials (sub-section 2.5.3) whereas a two temperature form of the Laguerre distribution can represent the actual distribution function just by using 8 Laguerre terms (sub-section 2.5.4). Or, for initial temperature ratio 10:1 $\left(\frac{T_c(t=0)}{T_h(t=0)} = \frac{1}{10}\right)$ it is better to use the three temperature form of the Laguerre distribution function instead of the two temperature form (sub-sections 2.5.5 and 2.5.6). This is even more true for temperature ratios of 100:1 and 1000:1 (sub-sections 2.5.7 and 2.5.8).

The number of the Laguerre terms used for each population (cold, medium or hot) is also restricted by the structure of the actual distribution function. Previously, in section 2.3, we discussed the method of fitting a Laguerre distribution function to a reference distribution function by matching the even moments. Low moments are dominated by the cold component of the distribution function whereas the high moments are dominated by the hot component. Hence, we need to choose the number of Laguerre terms for the cold component according to the number of the moments dominated by colds.

$$M_k = \sum_{\eta=c,h} \int_0^\infty H_{\eta,k}(v)\,dv$$

Where,

$$H_{\eta,k}(v) = \frac{4}{\sqrt{\pi}} v^k T_\eta^{-\frac{3}{2}} a_{\eta 0}\, e^{-\frac{v^2}{T_\eta}}$$

The maximum contribution of the η component ($\eta = $ cold, hot) in the moment equation k occurs at the energy $vmax_{\eta,k}^2$:

$$\frac{d}{dv}\left(H_{\eta,k}(v)\right) = 0 \Rightarrow vmax_{\eta,k}^2 = \frac{kT_\eta}{2}$$

We define $R_{c,h,k}$ as the ratio of the Maximum contribution of the components.

$$R_{c,h,k} = \frac{Hmax_{c,k}(vmax_{c,k})}{Hmax_{h,k}(vmax_{h,k})} = \left(\frac{a_{c0}}{a_{h0}}\right)\left(\frac{T_c}{T_h}\right)^{\frac{k-3}{2}}$$

$R_{c,h,k}$ increases by reducing k, hence, the contribution of the cold component is dominant in low moments and the hots are dominant in high moments. Also, by decreasing the temperature ratio $\frac{T_c}{T_h}$, the domination of the hot component conceals the effect of the colds even at moments 6 and/or 8 (*i.e.* for temperature ratios $\frac{T_c}{T_h} \ll 0.01$).

Perspective

To make a code capable of emulating "FPI", the next steps will be:

Compute the non isotropic components of the distribution function in spherical harmonics using Legendre polynomials and generalized Laguerre polynomials for the velocity dependence. An initially anisotropic plasma, with the anisotropy being described by higher order Legendre polynomials ($l > 0$), will be allowed to relax towards an isotropic distribution by e-e and e-i (electron-ion) collisions.

Calculate the Vlasov part of the kinetic equation.(*i.e.* $\left(E \frac{\partial f}{\partial v_x} \right)$ and $\left(v_x \frac{\partial f}{\partial x} \right)$).

Generalize the computations for inhomogeneous plasma density and temperature.

One useful application of the present work could be to compute the rates of ionization [67] and excitation [68] in a plasma medium analytically by direct analytic integration of the Laguerre distribution function.

References

[1] T. Ohkawa, M. S. Chu, F. L. Hinton *et al.*, *Thermal and Electrical Properties of the Divertor Channel of Tokamak Plasmas*, Phys. Rev. Lett. **51**, 2101 (1983).

[2] J. D. Lindl and E. I. Moses, *Special Topic: Plans for the National Ignition Campaign (NIC) on the National Ignition Facility (NIF): On the threshold of initiating ignition experiments*, 050901 (2011).

[3] S. W. Haan, J. D. Lindl, D. A. Callahan *et al.*, *Point design targets, specifications, and requirements for the 2010 ignition campaign on the National Ignition Facility*, 051001 (2011).

[4] R. J. Goldston and P. H. Rutherford, *Introduction to Plasma Physics*, (1997).

[5] L. Boltzmann, *Lectures on gas theory. Translated by Stephen G. Brush*, ix, 490 p. (1964).

[6] M. N. Rosenbluth, W. M. MacDonald, D. L. Judd, *Fokker-Planck Equation for an Inverse-Square Force*, Phys. Rev. **107**, 1 (1957).

[7] A. G. Peeters and D. Strintzi, *The Fokker-Planck equation, and its application in plasma physics*, Annalen der Physik **17**, 142 (2008,).

[8] L. Spitzer and R. Härm, *Transport Phenomena in a Completely Ionized Gas*, Phys. Rev. **89**, 977 (1953).

[9] J. Dawson and C. Oberman, *High-Frequency Conductivity and the Emission and Absorption Coefficients of a Fully Ionized Plasma*, Physics of Fluids **5**, 517 (1962).

[10] J. Dawson and C. Oberman, *Effect of Ion Correlations on High-Frequency Plasma Conductivity*, Physics of Fluids **6**, 394 (1963).

[11] T. W. Johnston and J. M. Dawson, *Correct values for high-frequency power absorption by inverse bremsstrahlung in plasmas*, Physics of Fluids **16**, 722 (1973).

[12] A. B. Langdon, *Nonlinear Inverse Bremsstrahlung and Heated-Electron Distributions*, Phys. Rev. Lett. **44**, 575 (1980).

[13] J. P. Matte, M. Lamoureux, C. Moller *et al.*, *Non-Maxwellian electron distributions and continuum X-ray emission in inverse Bremsstrahlung heated plasmas*, Plasma Physics and Controlled Fusion **30**, 1665 (1988).

[14] K. Estabrook and W. L. Kruer, *Properties of Resonantly Heated Electron Distributions*, Phys. Rev. Lett. **40**, 1, 42 (1978).

[15] A. R. Bell, R. G. Evans, D. J. Nicholas, *Elecron Energy Transport in Steep Temperature Gradients in Laser-Produced Plasmas*, Phys. Rev. Lett. **46**, 243 (1981).

[16] J. P. Matte and J. Virmont, *Electron Heat Transport down Steep Temperature Gradients*, Phys. Rev. Lett. **49**, 1936 (1982).

[17] J. F. Luciani, P. Mora, J. Virmont, *Nonlocal Heat Transport Due to Steep Temperature Gradients*, Phys. Rev. Lett. **51**, 1664 (1983).

[18] P. Mora and J. F. Luciani, *Nonlocal electron transport in laser created plasmas*, Laser and Particle Beams **12**, 387 (1994).

[19] J. F. Luciani, P. Mora, R. Pellat, *Quasistatic heat front and delocalized heat flux*, Physics of Fluids **28**, 835 (1985).

[20] J. F. Luciani, P. Mora, A. Bendib, *Magnetic Field and Nonlocal Transport in Laser-Created Plasmas*, Phys. Rev. Lett. **55**, 2421 (1985).

[21] E. M. Epperlein, *Kinetic theory of laser filamentation in plasmas*, Phys. Rev. Lett. **65**, 2145 (1990).

[22] E. M. Epperlein and R. W. Short, *Nonlocal heat transport effects on the filamentation of light in plasmas*, Physics of Fluids B: Plasma Physics **4**, 2211 (1992).

[23] A. Tahraoui and A. Bendib, *Semicollisional heat flux in laser heated plasmas*, Physics of Plasmas **9**, 3089 (2002).

[24] V. Y. Bychenkov, W. Rozmus, V. T. Tikhonchuk *et al.*, *Nonlocal Electron Transport in a Plasma*, Phys. Rev. Lett. **75**, 4405 (1995).

[25] Z. Zheng, W. Rozmus, V. Y. Bychenkov *et al.*, *Nonlocal transport model in equilibrium two-component plasmas*, Physics of Plasmas **16**, 102301 (2009).

[26] J. R. Sanmartín, J. Ramírez, R. Fernández-Feria *et al.*, *Self-consistent, nonlocal electron heat flux at arbitrary ion charge number*, Physics of Fluids B: Plasma Physics **4**, 3579 (1992).

[27] J. Ramírez, J. R. Sanmartín, R. Fernández-Feria, *Nonlocal electron heat relaxation in a plasma shock at arbitrary ionization number*, Physics of Fluids B: Plasma Physics **5**, 1485 (1993).

[28] F. A. Bibi and JP. Matte, *Influence of the electron distribution function shape on nonlocal electron heat transport in laser-heated plasmas*, Phys. Rev. E **66**, 066414 (2002).

[29] M. K. Prasad and D. S. Kershaw, *Nonviability of some nonlocal electron heat transport modeling*, Physics of Fluids B: Plasma Physics **1**, 2430 (1989).

[30] M. K. Prasad and D. S. Kershaw, *Stable solutions of nonlocal electron heat transport equations*, Physics of Fluids B: Plasma Physics **3**, 3087 (1991).

[31] J. Delettrez, *Thermal electron transport in direct-drive laser fusion*, Can. J. Phys. **64**, 932–943 (1986).

[32] M. G. Haines, *Transport in laser-produced plasmas*, 139 (1988).

[33] P. A. Holstein, J. Delettrez, S. Skupsky *et al.*, *Modeling nonlocal heat flow in laser-produced plasmas*, Journal of Applied Physics **60**, 2296 (1986).

[34] F. Vidal, J. P. Matte, M. Casanova *et al.*, *Modeling and effects of nonlocal electron heat flow in planar shock waves*, Physics of Plasmas **2**, 1412 (1995).

[35] G. Gregori, S. H. Glenzer, J. Knight *et al.*, *Effect of Nonlocal Transport on Heat-Wave Propagation*, Phys. Rev. Lett. **92**, 205006 (2004).

[36] S. X. Hu, V. A. Smalyuk, V. N. Goncharov *et al.*, *Validation of Thermal-Transport Modeling with Direct-Drive, Planar-Foil Acceleration Experiments on OMEGA*, Phys. Rev. Lett. **101**, 055002 (2008).

[37] J. P. Matte, J. C. Kieffer, S. Ethier *et al.*, *Spectroscopic signature of non-Maxwellian and nonstationary effects in plasmas heated by intense, ultrashort laser pulses*, Phys. Rev. Lett. **72**, 1208 (1994).

[38] S. Chapman and T. G. Cowling, *The mathematical theory of non-uniform gases*, (1990).

[39] K. Abe, *Sonine Polynomial Solution of the Boltzmann Equation for Relaxation of Initially Nonequilibrium Distribution*, Physics of Fluids **14**, 492 (1971).

[40] K. Abe and Y. Ushimi, *Sonine polynomial solution of the Fokker-Planck equation*, Physics of Fluids **19**, 2047 (1976).

[41] I. K. Khabibrakhmanov and D. Summers, *Spectral representation of the isotropic Coulomb collisional operator*, Journal of Plasma Physics **58**, 475 (1997).

[42] JY. Ji and E. D. Held, *Analytical solution of the kinetic equation for a uniform plasma in a*

magnetic field, Phys. Rev. E **82**, 016401 (2010).

[43] JY. Ji and E. D. Held, *Full Coulomb collision operator in the moment expansion*, Physics of Plasmas **16**, 102108 (2009).

[44] JY. Ji, E. D. Held, C. R. Sovinec, *Moment approach to deriving parallel heat flow for general collisionality*, Physics of Plasmas **16**, 022312 (2009).

[45] JY. Ji and E. D. Held, *Exact linearized Coulomb collision operator in the moment expansion*, Physics of Plasmas **13**, 102103 (2006).

[46] E. D. Held, *Unified form for parallel ion viscous stress in magnetized plasmas*, Physics of Plasmas **10**, 4708 (2003).

[47] E. D. Held, J. D. Callen, C. C. Hegna, *Conductive electron heat flow along an inhomogeneous magnetic field*, Physics of Plasmas **10**, 3933 (2003).

[48] E. D. Held, J. D. Callen, C. C. Hegna *et al.*, *Conductive electron heat flow along magnetic field lines*, Physics of Plasmas **8**, 1171 (2001).

[49] D. D. Schnack, D. C. Barnes, D. P. Brennan *et al.*, *Computational modeling of fully ionized magnetized plasmas using the fluid approximation*, Physics of Plasmas **13**, 058103 (2006).

[50] E. D. Held, J. D. Callen, C. C. Hegna *et al.*, *Nonlocal closures for plasma fluid simulations*, Physics of Plasmas **11**, 2419 (2004).

[51] C. R. Sovinec, T. A. Gianakon, E. D. Held *et al.*, *NIMROD: A computational laboratory for studying nonlinear fusion magnetohydrodynamics*, Physics of Plasmas **10**, 1727 (2003).

[52] JY. Ji and E. D. Held, *Landau collision operators and general moment equations for an electron-ion plasma*, Physics of Plasmas **15**, 102101 (2008).

[53] M. Abramowitz and I. A. Stegun, *Handbook of Mathematical Functions: with Formulas, Graphs, and Mathematical Tables*, (1965).

[54] J. P. Matte, T. W. Johnston, J. Delettrez *et al.*, *Electron Heat Flow with Inverse Bremsstrahlung and Ion Motion*, Phys. Rev. Lett. **53**, 1461 (1984).

[55] A. Bendib, J. F. Luciani, J. P. Matte, *An improvement of the nonlocal heat flux formula*, Physics of Fluids **31**, 711 (1988).

[56] F. A. Bibi and J. Matte, *Nonlocal electron heat transport and electron-ion energy transfer in the presence of strong collisional heating*, Laser and Particle Beams **22**, 103 (2004).

[57] F. A. Bibi, J. Matte, J. Kieffer, *Fokker-Planck simulations of hot electron transport in solid density plasma*, Laser and Particle Beams **22**, 97 (2004).

[58] J. P. Matte, J. C. Kieffer, M. Chaker *et al.*, *Spectroscopic analysis of short-pulse laser-produced plasmas*, Laser and Particle Beams **12**, 455 (1994).

[59] M. Planck, *Über einen Satz der statistischen Dynamik and seine Erweiterung in der Quantentheorie*, Sitzungsberichte der Preussischen Akademie der Wissenschaften **24**, 324–341 (1917).

[60] A. Einstein, *Zur Theorie der Brownschen Bewegung*, Ann. Phys. (Leipzig) **19**, 371 (1906).

[61] A. D. Fokker, *Die mittlere Energie rotierender elektrischer Dipole im Strahlungsfeld. Annalen der Physik*, 810–820 (1914).

[62] L. D. Landau, *Kinetic equation for the Coulomb effect*, Phys. Z. Sowjetunion **10**, 154 (1936).

[63] F. A. Bibi, M. M. Shoucri, J. Matte, *Different Fokker-Planck approaches to simulate electron transport in plasmas*, Computer Physics Communications **164**, 60 (2004).

[64] D. Fowler, *The Binomial Coefficient Function*, The American Mathematical Monthly **103**, pp. 1 (1996).

[65] Wikipedia, *Binomial coefficient*, Available at: http://en.wikipedia.org/w/index.php?title=Binomial_coefficient&oldid=424293289 (Accessed 2011)

[66] Wikipedia, *Laguerre polynomials*, Available at: http://en.wikipedia.org/w/index.php?title=Laguerre_polynomials&oldid=423701213 (Accessed 2011)

[67] M. Gryzinski, *Classical Theory of Atomic Collisions. I. Theory of Inelastic Collisions*, Phys. Rev. **138**, A336 (1965).

[68] H. van Regemorter, *Rate of Collisional Excitation in Stellar Atmospheres.*, 906 (1962).

[69] J. D. Huba, *NRL Plasma Formulary*, (2006).

[1] T. Ohkawa, M. S. Chu, F. L. Hinton *et al.*, *Thermal and Electrical Properties of the Divertor Channel of Tokamak Plasmas*, Phys. Rev. Lett. **51**, 2101 (1983).

[2] J. D. Lindl and E. I. Moses, *Special Topic: Plans for the National Ignition Campaign (NIC) on the National Ignition Facility (NIF): On the threshold of initiating ignition experiments*, 050901 (2011).

[3] S. W. Haan, J. D. Lindl, D. A. Callahan *et al.*, *Point design targets, specifications, and requirements for the 2010 ignition campaign on the National Ignition Facility*, 051001 (2011).

[4] R. J. Goldston and P. H. Rutherford, *Introduction to Plasma Physics*, (1997).

[5] L. Boltzmann, *Lectures on gas theory. Translated by Stephen G. Brush*, ix, 490 p. (1964).

[6] M. N. Rosenbluth, W. M. MacDonald, D. L. Judd, *Fokker-Planck Equation for an Inverse-Square Force*, Phys. Rev. **107**, 1 (1957).

[7] A. G. Peeters and D. Strintzi, *The Fokker-Planck equation, and its application in plasma physics*, Annalen der Physik **17**, 142 (2008,).

[8] L. Spitzer and R. Härm, *Transport Phenomena in a Completely Ionized Gas*, Phys. Rev. **89**, 977 (1953).

[9] J. Dawson and C. Oberman, *High-Frequency Conductivity and the Emission and Absorption Coefficients of a Fully Ionized Plasma*, Physics of Fluids **5**, 517 (1962).

[10] J. Dawson and C. Oberman, *Effect of Ion Correlations on High-Frequency Plasma Conductivity*, Physics of Fluids **6**, 394 (1963).

[11] T. W. Johnston and J. M. Dawson, *Correct values for high-frequency power absorption by inverse bremsstrahlung in plasmas*, Physics of Fluids **16**, 722 (1973).

[12] A. B. Langdon, *Nonlinear Inverse Bremsstrahlung and Heated-Electron Distributions*, Phys. Rev. Lett. **44**, 575 (1980).

[13] J. P. Matte, M. Lamoureux, C. Moller *et al.*, *Non-Maxwellian electron distributions and continuum X-ray emission in inverse Bremsstrahlung heated plasmas*, Plasma Physics and Controlled Fusion **30**, 1665 (1988).

[14] K. Estabrook and W. L. Kruer, *Properties of Resonantly Heated Electron Distributions*, Phys. Rev. Lett. **40**, 1, 42 (1978).

[15] A. R. Bell, R. G. Evans, D. J. Nicholas, *Elecron Energy Transport in Steep Temperature Gradients in Laser-Produced Plasmas*, Phys. Rev. Lett. **46**, 243 (1981).

[16] J. P. Matte and J. Virmont, *Electron Heat Transport down Steep Temperature Gradients*, Phys. Rev. Lett. **49**, 1936 (1982).

[17] J. F. Luciani, P. Mora, J. Virmont, *Nonlocal Heat Transport Due to Steep Temperature Gradients*, Phys. Rev. Lett. **51**, 1664 (1983).

[18] P. Mora and J. F. Luciani, *Nonlocal electron transport in laser created plasmas*, Laser and Particle Beams **12**, 387 (1994).

[19] J. F. Luciani, P. Mora, R. Pellat, *Quasistatic heat front and delocalized heat flux*, Physics of Fluids **28**, 835 (1985).

[20] J. F. Luciani, P. Mora, A. Bendib, *Magnetic Field and Nonlocal Transport in Laser-Created Plasmas*, Phys. Rev. Lett. **55**, 2421 (1985).

[21] E. M. Epperlein, *Kinetic theory of laser filamentation in plasmas*, Phys. Rev. Lett. **65**, 2145 (1990).

[22] E. M. Epperlein and R. W. Short, *Nonlocal heat transport effects on the filamentation of light in plasmas*, Physics of Fluids B: Plasma Physics **4**, 2211 (1992).

[23] A. Tahraoui and A. Bendib, *Semicollisional heat flux in laser heated plasmas*, Physics of Plasmas **9**, 3089 (2002).

[24] V. Y. Bychenkov, W. Rozmus, V. T. Tikhonchuk *et al.*, *Nonlocal Electron Transport in a Plasma*, Phys. Rev. Lett. **75**, 4405 (1995).

[25] Z. Zheng, W. Rozmus, V. Y. Bychenkov *et al.*, *Nonlocal transport model in equilibrium two-component plasmas*, Physics of Plasmas **16**, 102301 (2009).

[26] J. R. Sanmartín, J. Ramírez, R. Fernández-Feria *et al.*, *Self-consistent, nonlocal electron heat flux at arbitrary ion charge number*, Physics of Fluids B: Plasma Physics **4**, 3579 (1992).

[27] J. Ramírez, J. R. Sanmartín, R. Fernández-Feria, *Nonlocal electron heat relaxation in a plasma shock at arbitrary ionization number*, Physics of Fluids B: Plasma Physics **5**, 1485 (1993).

[28] F. A. Bibi and JP. Matte, *Influence of the electron distribution function shape on nonlocal electron heat transport in laser-heated plasmas*, Phys. Rev. E **66**, 066414 (2002).

[29] M. K. Prasad and D. S. Kershaw, *Nonviability of some nonlocal electron heat transport modeling*, Physics of Fluids B: Plasma Physics **1**, 2430 (1989).

[30] M. K. Prasad and D. S. Kershaw, *Stable solutions of nonlocal electron heat transport equations*, Physics of Fluids B: Plasma Physics **3**, 3087 (1991).

[31] J. Delettrez, *Thermal electron transport in direct-drive laser fusion*, Can. J. Phys. **64**, 932–943 (1986).

[32] M. G. Haines, *Transport in laser-produced plasmas*, 139 (1988).

[33] P. A. Holstein, J. Delettrez, S. Skupsky *et al.*, *Modeling nonlocal heat flow in laser-produced plasmas*, Journal of Applied Physics **60**, 2296 (1986).

[34] F. Vidal, J. P. Matte, M. Casanova *et al.*, *Modeling and effects of nonlocal electron heat flow in planar shock waves*, Physics of Plasmas **2**, 1412 (1995).

[35] G. Gregori, S. H. Glenzer, J. Knight *et al.*, *Effect of Nonlocal Transport on Heat-Wave Propagation*, Phys. Rev. Lett. **92**, 205006 (2004).

[36] S. X. Hu, V. A. Smalyuk, V. N. Goncharov *et al.*, *Validation of Thermal-Transport Modeling with Direct-Drive, Planar-Foil Acceleration Experiments on OMEGA*, Phys. Rev. Lett. **101**, 055002 (2008).

[37] J. P. Matte, J. C. Kieffer, S. Ethier *et al.*, *Spectroscopic signature of non-Maxwellian and nonstationary effects in plasmas heated by intense, ultrashort laser pulses*, Phys. Rev. Lett. **72**, 1208 (1994).

[38] S. Chapman and T. G. Cowling, *The mathematical theory of non-uniform gases*, (1990).

[39] K. Abe, *Sonine Polynomial Solution of the Boltzmann Equation for Relaxation of Initially Nonequilibrium Distribution*, Physics of Fluids **14**, 492 (1971).

[40] K. Abe and Y. Ushimi, *Sonine polynomial solution of the Fokker-Planck equation*, Physics of Fluids **19**, 2047 (1976).

[41] I. K. Khabibrakhmanov and D. Summers, *Spectral representation of the isotropic Coulomb collisional operator*, Journal of Plasma Physics **58**, 475 (1997).

[42] JY. Ji and E. D. Held, *Analytical solution of the kinetic equation for a uniform plasma in a magnetic field*, Phys. Rev. E **82**, 016401 (2010).

[43] JY. Ji and E. D. Held, *Full Coulomb collision operator in the moment expansion*, Physics of

Plasmas **16**, 102108 (2009).

[44] JY. Ji, E. D. Held, C. R. Sovinec, *Moment approach to deriving parallel heat flow for general collisionality*, Physics of Plasmas **16**, 022312 (2009).

[45] JY. Ji and E. D. Held, *Exact linearized Coulomb collision operator in the moment expansion*, Physics of Plasmas **13**, 102103 (2006).

[46] E. D. Held, *Unified form for parallel ion viscous stress in magnetized plasmas*, Physics of Plasmas **10**, 4708 (2003).

[47] E. D. Held, J. D. Callen, C. C. Hegna, *Conductive electron heat flow along an inhomogeneous magnetic field*, Physics of Plasmas **10**, 3933 (2003).

[48] E. D. Held, J. D. Callen, C. C. Hegna *et al.*, *Conductive electron heat flow along magnetic field lines*, Physics of Plasmas **8**, 1171 (2001).

[49] D. D. Schnack, D. C. Barnes, D. P. Brennan *et al.*, *Computational modeling of fully ionized magnetized plasmas using the fluid approximation*, Physics of Plasmas **13**, 058103 (2006).

[50] E. D. Held, J. D. Callen, C. C. Hegna *et al.*, *Nonlocal closures for plasma fluid simulations*, Physics of Plasmas **11**, 2419 (2004).

[51] C. R. Sovinec, T. A. Gianakon, E. D. Held *et al.*, *NIMROD: A computational laboratory for studying nonlinear fusion magnetohydrodynamics*, Physics of Plasmas **10**, 1727 (2003).

[52] JY. Ji and E. D. Held, *Landau collision operators and general moment equations for an electron-ion plasma*, Physics of Plasmas **15**, 102101 (2008).

[53] Stegun and M. Abramowitz, *Handbook of Mathematical Functions: with Formulas, Graphs, and Mathematical Tables*, (1965).

[54] J. P. Matte, T. W. Johnston, J. Delettrez *et al.*, *Electron Heat Flow with Inverse Bremsstrahlung and Ion Motion*, Phys. Rev. Lett. **53**, 1461 (1984).

[55] A. Bendib, J. F. Luciani, J. P. Matte, *An improvement of the nonlocal heat flux formula*, Physics of Fluids **31**, 711 (1988).

[56] F. A. Bibi and J. Matte, *Nonlocal electron heat transport and electron-ion energy transfer in the presence of strong collisional heating*, Laser and Particle Beams **22**, 103 (2004).

[57] F. A. Bibi, J. Matte, J. Kieffer, *Fokker-Planck simulations of hot electron transport in solid density plasma*, Laser and Particle Beams **22**, 97 (2004).

[58] J. P. Matte, J. C. Kieffer, M. Chaker *et al.*, *Spectroscopic analysis of short-pulse laser-produced plasmas*, Laser and Particle Beams **12**, 455 (1994).

[59] M. Planck, *Über einen Satz der statistischen Dynamik and seine Erweiterung in der Quantentheorie*, Sitzungsberichte der Preussischen Akademie der Wissenschaften **24**, 324–341 (1917).

[60] A. Einstein, *Zur Theorie der Brownschen Bewegung*, Ann. Phys. (Leipzig) **19**, 371 (1906).

[61] A. D. Fokker, *Die mittlere Energie rotierender elektrischer Dipole im Strahlungsfeld. Annalen der Physik*, 810–820 (1914).

[62] L. D. Landau, *Kinetic equation for the Coulomb effect*, Phys. Z. Sowjetunion **10**, 154 (1936).

[63] F. A. Bibi, M. M. Shoucri, J. Matte, *Different Fokker-Planck approaches to simulate electron transport in plasmas*, Computer Physics Communications **164**, 60 (2004).

[64] D. Fowler, *The Binomial Coefficient Function*, The American Mathematical Monthly **103**, pp. 1 (1996).

[65] Wikipedia, *Binomial coefficient*, Available at: http://en.wikipedia.org/w/index.php?title=Binomial_coefficient&oldid=424293289 (Accessed 2011)

[66] Wikipedia, *Laguerre polynomials*, Available at: http://en.wikipedia.org/w/index.php?title=Laguerre_polynomials&oldid=423701213 (Accessed 2011)

[67] M. Gryzinski, *Classical Theory of Atomic Collisions. I. Theory of Inelastic Collisions*, Phys. Rev. **138**, A336 (1965).

[68] H. van Regemorter, *Rate of Collisional Excitation in Stellar Atmospheres.*, 906 (1962).

[69] J. D. Huba, *NRL Plasma Formulary*, (2006).

Appendix A – Reduction of the moment equations to temperature equations

In this appendix, we explain how we eliminate the $a_{\eta i}(t)$'s in the normalised equations (2-16), to obtain a set of s coupled nonlinear equations for the s temperatures. We first rewrite (2-16) by substituting $(k' = \frac{k}{2})$:

$$\sum_{\eta=1}^{s} T_\eta(t)^{(k'-1)} g_{\eta k'0}(t) = MN_{2k'}, \qquad k' = 0,1,\dots,(N_M - 1),$$

$$C_{k'i} = \binom{-k'+i}{i},$$

Note that, as k' and i are integers, $C_{k'i} = 0$ if $i \geq k'$.

We have defined

$$g_{\eta k'n}(t) = \sum_{i=n}^{N_\eta} C_{k'(i-n)}\, a_{\eta i}(t) \qquad\qquad\qquad\qquad \text{(A-1)}$$

which is identical to (2-16) when $n=0$.

Here, (s) is the number of temperatures, and the index n is introduced to count the number of eliminations we do in the system of equations.

Note:

The Binomial coefficients satisfy a recursive relation (by using the definition of the Binomial coefficient (1-16) to (1-18)):

$$C_{ki} - C_{(k+1)i} = \binom{-k+i}{i} - \binom{-k+i-1}{i}$$

$$= \frac{(i-k)(i-k-1)\dots(1-k)}{i!} - \frac{(i-k-1)\dots(1-k)(-k)}{i!}$$

$$= \frac{(i-k-1)\dots(1-k)[(i-k)-(-k)]}{i!} = \frac{(i-k-1)\dots(1-k)}{(i-1)!} = C_{k(i-1)}$$

where,

$$C_{k(i-1)} = 0, \; if \; i \leq 0 \qquad\qquad\qquad\qquad\qquad \text{(A-2)}$$

And consequently,

$$g_{\eta k_1 n}(t) - g_{\eta(k_1+1)n}(t) = \sum_{i=n+1}^{N_\eta} C_{k_1(i-n-1)}\, a_{\eta i}(t) = g_{\eta k_1(n+1)}(t)$$

Where,

$$g_{\eta k_1(N_\eta+1)}(t) = 0 \qquad\qquad\qquad\qquad\qquad\qquad \text{(A-3)}$$

We use (A-2) and (A-3) to simplify our equations.

For any two neighbor equations *i.e.* MN_{2l} and MN_{2l+2} we can write:

$$(-T_1(t))MN_{2l} + MN_{2l+2} = -T_1(t)^l g_{1l1}(t) + \sum_{\eta=2}^{s}\left((-T_1(t))T_\eta(t)^{(l-1)}\,g_{\eta l0}(t) + \right.$$

$$\left. T_\eta(t)^l\,g_{\eta(l+1)0}(t)\right) \tag{A-4}$$

By doing this, we have eliminated $a_{10}(t)$ in (A-4).

Similarly, for MN_{2l+2} and MN_{2l+4} we get:

$$(-T_1(t))MN_{2l+2} + MN_{2l+4} = -T_1(t)^{(l+1)} g_{1(l+1)1}(t) + \sum_{\eta=2}^{s}\left((-T_1(t))T_\eta(t)^l\,g_{\eta(l+1)0}(t) + \right.$$

$$\left. T_\eta(t)^{(l+1)}\,g_{\eta(l+2)0}(t)\right) \tag{A-5}$$

By multiplying (A-4) by $(-T_1)$ and adding it to (A-5) we get:

$$(-T_1(t))^2 MN_{2l} + 2(-T_1(t))MN_{2l+2} + MN_{2l+4} =$$

$$T_1(t)^{(l+1)} g_{1l2}(t) + \sum_{\eta=2}^{s}\left((-T_1(t))^2 T_\eta(t)^{(l-1)}\,g_{\eta l0}(t) + 2(-T_1(t))T_\eta(t)^l\,g_{\eta(l+1)0}(t) + \right.$$

$$\left. T_\eta(t)^{(l+1)}\,g_{\eta(l+2)0}(t)\right) \tag{A-6}$$

Repeating this process for $(N_1 + 1)$ times we get:

$$\sum_{i_1=0}^{N_1+1}\binom{N_1+1}{i_1}(-T_1(t))^{N_1+1-i_1} MN_{2(l+i_1)} =$$

$$(-1)^{N_1+1}T_1(t)^{(l+N_1)}\underbrace{g_{1l(N_1+1)}(t)}_{=0} +$$

$$\sum_{\eta=2}^{s}\sum_{i_1=0}^{N_1+1}\binom{N_1+1}{i_1}(-T_1(t))^{N_1+1-i_1} T_\eta(t)^{(l-1+i_1)} g_{\eta(l+i_1)0}(t) \tag{A-7}$$

Obviously, all of the $a_{1i}(t)$'s are eliminated in (A-7) by using $(N_1 + 2)$ normalized moment equations *i.e.* $(MN_{2l}, MN_{2(l+1)}, \dots, MN_{2(l+N_1+1)})$. The same process by using $(MN_{2(l+1)}, MN_{2(l+2)}, \dots, MN_{2(l+N_1+2)})$ leads us to (A-8):

$$\sum_{i_1=0}^{N_1+1}\binom{N_1+1}{i_1}(-T_1(t))^{N_1+1-i_1} MN_{2(l+i_1+1)} =$$

$$\sum_{\eta=2}^{s}\sum_{i_1=0}^{N_1+1}\binom{N_1+1}{i_1}(-T_1(t))^{N_1+1-i_1} T_\eta(t)^{(l+i_1)} g_{\eta(l+i_1+1)0}(t) \tag{A-8}$$

From now on, we will try to eliminate the $a_{2i}(t)$'s from the equations. We first multiply (A-7) by $(-T_2(t))$ and add it to (A-8) we get:

$$\sum_{i_1=0}^{N_1+1}\binom{N_1+1}{i_1}(-T_1(t))^{N_1+1-i_1}\left((-T_2(t))MN_{2(l+i_1)} + MN_{2(l+i_1+1)}\right) =$$

$$\sum_{i_1=0}^{N_1+1}\binom{N_1+1}{i_1}(-T_1(t))^{N_1+1-i_1}\left(-T_2(t)^l g_{2(l+i_1+1)1}(t)\right) +$$

$$\sum_{i_1=0}^{N_1+1}\binom{N_1+1}{i_1}(-T_1(t))^{N_1+1-i_1}\left(\sum_{\eta=3}^{s}\left((-T_2(t))T_\eta(t)^{(l+i_1-1)}\,g_{\eta(l+i_1)0}(t) + \right.\right.$$

$$\left.\left. T_\eta(t)^{(l+i_1)}\,g_{\eta(l+i_1+1)0}(t)\right)\right) \tag{A-9}$$

Continuing this process for $(N_2 + 1)$ times, all of the $a_{2i}(t)$'s will be eliminated. We get:

$$\sum_{i_1=0}^{N_1+1} \sum_{i_2=0}^{N_2+1} \binom{N_1+1}{i_1} \left(-T_1(t)\right)^{N_1+1-i_1} \times \binom{N_2+1}{i_2} \left(-T_2(t)\right)^{N_2+1-i_2} MN_{2(l+i_1+i_2)} =$$

$$\sum_{i_1=0}^{N_1+1} \binom{N_1+1}{i_1} \left(-T_1(t)\right)^{N_1+1-i_1} \left((-1)^{N_2+1} T_2(t)^{l+N_2} \underbrace{g_{2(l+i_1)(N_2+1)}(t)}_{=0} \right) +$$

$$\sum_{i_1=0}^{N_1+1} \sum_{i_2=0}^{N_2+1} \binom{N_1+1}{i_1} \left(-T_1(t)\right)^{N_1+1-i_1} \times$$

$$\binom{N_2+1}{i_2} \left(-T_2(t)\right)^{N_2+1-i_2} \sum_{\eta=3}^{s} T_\eta(t)^{(l+i_1+i_2-1)} g_{\eta(l+i_1+i_2)0}(t) \tag{A-10}$$

Continuing with the process, eventually, we can get:

$$\sum_{i_1=0}^{N_1+1} \sum_{i_2=0}^{N_2+1} \cdots \sum_{i_s=0}^{N_s+1} \binom{N_1+1}{i_1} \left(-T_1(t)\right)^{N_1+1-i_1} \times \binom{N_2+1}{i_2} \left(-T_2(t)\right)^{N_2+1-i_2} \times \cdots \times$$

$$\binom{N_s+1}{i_s} \left(-T_s(t)\right)^{N_s+1-i_s} \times MN_{2(l+i_1+i_2+\cdots+i_s)} = 0 \tag{A-11}$$

By varying $(l = 0,1, \dots, s-1)$, we can get (s) equations adequate to calculate (s) temperatures.

Appendix B – Coefficients $C_{\eta p}(v,t)$ and $D_{\eta p}(v,t)$ of the collision operator for the basis functions

B.1. Calculating $C_{\eta p}(v,t)$ i.e. the friction coefficient in (3-8):

In (3-8) first by substituting $\left(F_{\eta p}(u,t)\right)$ from (3-6), we get:

$$C_{\eta p}(v,t) = \frac{16\sqrt{\pi}\,\alpha}{v^2} T_\eta(t)^{-\frac{3}{2}} A_{\eta p}(v,t) \tag{B-1}$$

Here,

$$A_{\eta p}(v,t) = \int_0^v u^2 \exp\left(-\frac{u^2}{T_\eta(t)}\right) L_p^{\left(\frac{1}{2}\right)}\left(\frac{u^2}{T_\eta(t)}\right) du \tag{B-2}$$

Changing the variable $\left(\frac{u^2}{T_\eta(t)} \to x\right)$ (B-2) becomes:

$$A_{\eta p}(v,t) = \left(\frac{1}{2}\right) T_\eta(t)^{\frac{3}{2}} \int_0^{\frac{v^2}{T_\eta(t)}} x^{\frac{1}{2}} \exp(-x) L_p^{\left(\frac{1}{2}\right)}(x)\, dx \tag{B-3}$$

For $(p=0)$ (B-3) becomes:

$$A_{\eta 0}(v,t) = \left(\frac{1}{2}\right) T_\eta(t)^{\frac{3}{2}} \int_0^{\frac{v^2}{T_\eta(t)}} x^{\frac{1}{2}} \exp(-x) L_0^{\left(\frac{1}{2}\right)}(x)\, dx = \left(\frac{1}{2}\right) T_\eta(t)^{\frac{3}{2}} \int_0^{\frac{v^2}{T_\eta(t)}} x^{\frac{1}{2}} \exp(-x)\, dx =$$

$$\left(\frac{1}{2}\right) T_\eta(t)^{\frac{3}{2}} \left|-e^{-x}\sqrt{x} + \frac{\sqrt{\pi}}{2} \mathrm{Erf}(\sqrt{x})\right|_0^{\frac{v^2}{T_\eta(t)}} = \left(\frac{1}{2}\right) T_\eta(t)^{\frac{3}{2}} \left(\frac{\sqrt{\pi}}{2} \mathrm{Erf}\left(\sqrt{\frac{v^2}{T_\eta(t)}}\right) - e^{-\frac{v^2}{T_\eta(t)}}\sqrt{\frac{v^2}{T_\eta(t)}}\right),\quad p=0$$

$$\tag{B-4}$$

And for $(p \geq 1)$ we can use (B-5) given by using the Rodrigues formula (in ref. [53] equation 22.11.6) for the generalized Laguerre polynomials to simplify (B-3).

$$L_p^{(\alpha)}(x) = \frac{x^{-\alpha}e^x}{p!}\frac{d^p}{dx^p}\left(e^{-x}x^{p+\alpha}\right) \tag{B-5}$$

(B-3) then becomes:

$$A_{\eta p}(v,t) = \left(\frac{1}{2}\right) T_\eta(t)^{\frac{3}{2}} \int_0^{\frac{v^2}{T_\eta(t)}} x^{\frac{1}{2}} e^{-x} \left(\frac{x^{-\frac{1}{2}} e^x}{p!} \frac{d^p}{dx^p}\left(e^{-x} x^{p+\frac{1}{2}}\right)\right) dx, \quad p \geq 1 =$$

$$\left(\frac{1}{2}\right) T_\eta(t)^{\frac{3}{2}} \left(\frac{1}{p!}\right) \int_0^{\frac{v^2}{T_\eta(t)}} \frac{d^p}{dx^p}\left(e^{-x} x^{p+\frac{1}{2}}\right) dx, \quad p \geq 1 =$$

$$\left(\frac{1}{2}\right) T_\eta(t)^{\frac{3}{2}} \left(\frac{1}{p!}\right) \left|\underbrace{\frac{d^{p-1}}{dx^{p-1}}\left(e^{-x} x^{p+\frac{1}{2}}\right)}_{I}\right|_0^{\frac{v^2}{T_\eta(t)}}, \quad p \geq 1 \tag{B-6}$$

We can write (B-5) for $\left(L_{p-1}^{\left(\frac{3}{2}\right)}(x)\right)$ as below:

$$L_{p-1}^{\frac{3}{2}}(x) = \frac{x^{-\frac{3}{2}} e^x}{(p-1)!} \frac{d^{p-1}}{dx^{p-1}}\left(e^{-x} x^{p+\frac{1}{2}}\right) \tag{B-7}$$

We use (B-7) for part I in (B-6):

$$A_{\eta p}(v,t) = \left(\frac{1}{2}\right) T_\eta(t)^{\frac{3}{2}} \left(\frac{1}{p!}\right) \left|(p-1)! \, x^{\frac{3}{2}} e^{-x} L_{p-1}^{\left(\frac{3}{2}\right)}(x)\right|_0^{\frac{v^2}{T_\eta(t)}}, \quad p \geq 1 \Rightarrow$$

$$A_{\eta p}(v,t) = \left(\frac{1}{2p}\right) v^3 e^{-\frac{v^2}{T_\eta(t)}} L_{p-1}^{\left(\frac{3}{2}\right)}\left(\frac{v^2}{T_\eta(t)}\right), \quad p \geq 1 \tag{B-8}$$

Considering (B-1), (B-4) and (B-8) we can write:

$$C_{\eta p}(v,t) = \begin{cases} 8\sqrt{\pi}\,\alpha \left(\frac{\sqrt{\pi}}{2v^2}\,\mathrm{Erf}\left(\sqrt{\frac{v^2}{T_\eta(t)}}\right) - T_\eta(t)^{-\frac{1}{2}}\frac{e^{-\frac{v^2}{T_\eta(t)}}}{v}\right), & p = 0 \\[4mm] \left(\frac{8\sqrt{\pi}\,\alpha}{p}\right) T_\eta(t)^{-\frac{3}{2}} v \, e^{-\frac{v^2}{T_\eta(t)}} L_{p-1}^{\left(\frac{3}{2}\right)}\left(\frac{v^2}{T_\eta(t)}\right), & p \geq 1 \end{cases} \tag{B-9}$$

B.2. Calculating $D_{\eta p}(v,t)$ i.e. the parallel diffusion coefficient in (3-8):

In (3-8) we have:

$$D_{\eta p}(v,t) = \left(\underbrace{\frac{4\pi\alpha}{3} \int_v^\infty u \, F_{\eta p}(u,t)\,du}_{I_D} + \underbrace{\left(\frac{4\pi\alpha}{3v^3}\right) \int_0^v u^4 F_{\eta p}(u,t)\,du}_{II_D}\right) \tag{B-10}$$

Part I_D in (B-10) is:

$$I_D = \frac{4\pi\alpha}{3} \int_v^\infty u \, F_{\eta p}(u,t)\,du \tag{B-11}$$

Now by substituting $F_{\eta p}(u,t)$ from (3-6):

$$I_D = \frac{16\sqrt{\pi}\alpha}{3} T_\eta(t)^{-\frac{3}{2}} B_{\eta p}(v,t) \tag{B-12}$$

Where,

$$B_{\eta p}(v, t) = \int_{v}^{\infty} u \, \exp\left(-\frac{u^2}{T_\eta(t)}\right) L_p^{\left(\frac{1}{2}\right)}\left(\frac{u^2}{T_\eta(t)}\right) du \qquad (B\text{-}13)$$

By changing the variable $\left(x \to \frac{u^2}{T_\eta(t)}\right)$ (B-13) becomes:

$$B_{\eta p}(v, t) = \left(\frac{1}{2}\right) T_\eta(t) \int_{\frac{v^2}{T_\eta(t)}}^{\infty} e^{-x} L_p^{\left(\frac{1}{2}\right)}(x) \, dx \qquad (B\text{-}14)$$

Here, we derive a formula in order to simplify (B-14).

We calculate the derivative of the expression below:

$$\frac{d}{dx}\left(e^{-x} L_p^{(\alpha)}(x)\right) = -e^{-x} L_p^{(\alpha)}(x) + e^{-x} \frac{d}{dx}\left(L_p^{(\alpha)}(x)\right) \qquad (B\text{-}15)$$

Differentiating the generating function of generalized Laguerre polynomials, (eq. 22.9.15 of ref. [53]) leads to:

$$\frac{d}{dx} L_p^{(\alpha)}(x) = -L_{p-1}^{(\alpha+1)}(x) \qquad (B\text{-}16)$$

Now, we use (B-16) (for $k = 1$ and $\alpha = \frac{1}{2}$) in (B-15):

$$\frac{d}{dx}\left(e^{-x} L_p^{(\alpha)}(x)\right) = -e^{-x} L_p^{(\alpha)}(x) - e^{-x} L_{p-1}^{(\alpha+1)}(x) = -e^{-x}\left(L_p^{(\alpha)}(x) + L_{p-1}^{(\alpha+1)}(x)\right) \qquad (B\text{-}17)$$

There is another useful equation (in ref. [53] equation 22.7.30):

$$L_p^{(\alpha)}(x) + L_{p-1}^{(\alpha+1)}(x) = L_p^{(\alpha+1)}(x) \qquad (B\text{-}18)$$

Using (B-18), we can write (B-17) as:

$$\frac{d}{dx}\left(e^{-x} L_p^{(\alpha)}(x)\right) = -e^{-x} L_p^{(\alpha+1)}(x) \qquad (B\text{-}19)$$

And moreover, by integrating both sides of (B-19):

$$\int_{x_1}^{x_2} e^{-x} L_p^{(\alpha+1)}(x) = -\left|e^{-x} L_p^{(\alpha)}(x)\right|_{x_1}^{x_2} = e^{-x_1} L_p^{(\alpha)}(x_1) - e^{-x_2} L_p^{(\alpha)}(x_2) \qquad (B\text{-}20)$$

Using (B-20), we can write (B-14) as:

$$B_{\eta p}(v, t) = \left(\frac{1}{2}\right) T_\eta(t) \int_{\frac{v^2}{T_\eta(t)}}^{\infty} e^{-x} L_p^{\left(\frac{1}{2}\right)}(x) \, dx = -\left(\frac{1}{2}\right) T_\eta(t) \left|e^{-x} L_p^{\left(-\frac{1}{2}\right)}(x)\right|_{\frac{v^2}{T_\eta(t)}}^{\infty} =$$

$$\left(\frac{1}{2}\right) T_\eta(t) \, e^{-\frac{v^2}{T_\eta(t)}} L_p^{\left(-\frac{1}{2}\right)}\left(\frac{v^2}{T_\eta(t)}\right) \qquad (B\text{-}21)$$

As a result, (B-12) becomes:

$$I_D = \frac{16\sqrt{\pi}\alpha}{3} T_\eta(t)^{-\frac{3}{2}} B_{\eta p}(v, t) = \frac{8\sqrt{\pi}\alpha}{3} T_\eta(t)^{-\frac{1}{2}} e^{-\frac{v^2}{T_\eta(t)}} L_p^{\left(-\frac{1}{2}\right)}\left(\frac{v^2}{T_\eta(t)}\right) \qquad (B\text{-}22)$$

Now, we proceed with part II_D in (B-10):

119

$$II_D = \left(\frac{4\pi\alpha}{3v^3}\right) \int_0^v u^4 F_{\eta p}(u,t)\, du = \left(\frac{16\sqrt{\pi}\alpha}{3v^3}\right) T_\eta(t)^{-\frac{3}{2}} G_{\eta p}(v,t) \tag{B-23}$$

Where,

$$G_{\eta p}(v,t) = \int_0^v u^4 \exp\left(-\frac{u^2}{T_\eta(t)}\right) L_p^{\left(\frac{1}{2}\right)}\left(\frac{u^2}{T_\eta(t)}\right) du \tag{B-24}$$

By changing variable $\left(x \to \frac{u^2}{T_\eta(t)}\right)$ (B-24) becomes:

$$G_{\eta p}(v,t) = \left(\frac{1}{2}\right) T_\eta(t)^{\frac{5}{2}} \int_0^{\frac{v^2}{T_\eta(t)}} x^{\frac{3}{2}} e^{-x} L_p^{\left(\frac{1}{2}\right)}(x)\, dx \tag{B-25}$$

For $(p = 0)$, using the definition of the Error function and integrating by parts, we get:

$$G_{\eta 0}(v,t) = \left(\frac{1}{2}\right) T_\eta(t)^{\frac{5}{2}} \int_0^{\frac{v^2}{T_\eta(t)}} x^{\frac{3}{2}} e^{-x} L_0^{\left(\frac{1}{2}\right)}(x)\, dx = \left(\frac{1}{2}\right) T_\eta(t)^{\frac{5}{2}} \int_0^{\frac{v^2}{T_\eta(t)}} x^{\frac{3}{2}} e^{-x}\, dx$$

$$= \left(\frac{1}{2}\right) T_\eta(t)^{\frac{5}{2}} \left| e^{-x}\left(-\frac{3\sqrt{x}}{2} - x^{\frac{3}{2}}\right) + \frac{3\sqrt{\pi}}{4} Erf(\sqrt{x}) \right|_0^{\frac{v^2}{T_\eta(t)}}, \qquad p = 0 \Rightarrow$$

$$G_{\eta 0}(v,t) =$$

$$\left(\frac{1}{2}\right) T_\eta(t)^{\frac{5}{2}} \left(-\left(\frac{3}{2} v T_\eta(t)^{-\frac{1}{2}} + v^3 T_\eta(t)^{-\frac{3}{2}}\right) e^{-\frac{v^2}{T_\eta(t)}} + \right.$$

$$\left. \frac{3\sqrt{\pi}}{4} Erf\left(\sqrt{\frac{v^2}{T_\eta(t)}}\right) \right), \qquad\qquad p = 0 \tag{B-26}$$

And for $(p = 1)$, (B-25) becomes:

$$G_{\eta 1}(v,t) = \left(\frac{1}{2}\right) T_\eta(t)^{\frac{5}{2}} \int_0^{\frac{v^2}{T_\eta(t)}} x^{\frac{3}{2}} e^{-x} L_1^{\left(\frac{1}{2}\right)}(x)\, dx$$

$$= \left(\frac{1}{2}\right) T_\eta(t)^{\frac{5}{2}} \int_0^{\frac{v^2}{T_\eta(t)}} \left(\frac{3}{2} x^{\frac{3}{2}} - x^{\frac{5}{2}}\right) e^{-x}\, dx, \qquad\qquad p = 1 \Rightarrow$$

$$G_{\eta 1}(v,t) =$$

$$\left(\frac{1}{4}\right) T_\eta(t)^{\frac{5}{2}} \left(\left(3 v T_\eta(t)^{-\frac{1}{2}} + 2 v^3 T_\eta(t)^{-\frac{3}{2}} + 2 v^5 T_\eta(t)^{-\frac{5}{2}}\right) e^{-\frac{v^2}{T_\eta(t)}} - \right.$$

$$\left. \frac{3}{2}\sqrt{\pi} Erf\left(\sqrt{\frac{v^2}{T_\eta(t)}}\right) \right), \qquad\qquad p = 1 \tag{B-27}$$

For $(p \geq 2)$ we can use (B-5) and write (B-25) as:

$$G_{\eta p}(v,t) = \left(\tfrac{1}{2}\right) T_\eta(t)^{\frac{5}{2}} \int_0^{\frac{v^2}{T_\eta(t)}} x^{\frac{3}{2}} e^{-x} \left(\frac{x^{-\frac{1}{2}} e^x}{p!} \frac{d^p}{dx^p} \left(e^{-x} x^{p+\frac{1}{2}} \right) \right) dx =$$

$$\left(\tfrac{1}{2}\right) T_\eta(t)^{\frac{5}{2}} \left(\tfrac{1}{p!}\right) \int_0^{\frac{v^2}{T_\eta(t)}} x \underbrace{\left(\frac{d^p}{dx^p} \left(e^{-x} x^{p+\frac{1}{2}} \right) \right) dx}_{dU} , \qquad p \geq 2 \qquad\qquad \text{(B-28)}$$

Integrating by parts, leads (B-28) to become:

$$dU = \left(\frac{d^p}{dx^p} \left(e^{-x} x^{p+\frac{1}{2}} \right) \right) dx \Rightarrow$$

$$U = \frac{d^{p-1}}{dx^{p-1}} \left(e^{-x} x^{p+\frac{1}{2}} \right)$$

$$G_{\eta p}(v,t) = \left(\tfrac{1}{2}\right) T_\eta(t)^{\frac{5}{2}} \left(\tfrac{1}{p!}\right) \left(\left. |x \cdot U| \right|_0^{\frac{v^2}{T_\eta(t)}} - \int_0^{\frac{v^2}{T_\eta(t)}} U \, dx \right) =$$

$$\left(\tfrac{1}{2}\right) T_\eta(t)^{\frac{5}{2}} \left(\tfrac{1}{p!}\right) \left(\left. \left|x \frac{d^{p-1}}{dx^{p-1}} \left(e^{-x} x^{p+\frac{1}{2}} \right) \right|_0^{\frac{v^2}{T_\eta(t)}} \right. - \int_0^{\frac{v^2}{T_\eta(t)}} \frac{d^{p-1}}{dx^{p-1}} \left(e^{-x} x^{p+\frac{1}{2}} \right) dx \right) =$$

$$\left(\tfrac{1}{2}\right) T_\eta(t)^{\frac{5}{2}} \left(\tfrac{1}{p!}\right) \left(\left. \left|x \frac{d^{p-1}}{dx^{p-1}} \left(e^{-x} x^{p+\frac{1}{2}} \right) \right|_0^{\frac{v^2}{T_\eta(t)}} \right. - \left. \left|\frac{d^{p-2}}{dx^{p-2}} \left(e^{-x} x^{p+\frac{1}{2}} \right) \right|_0^{\frac{v^2}{T_\eta(t)}} \right), \qquad p \geq 2$$

$$\text{(B-29)}$$

Using (B-5):

$$\frac{d^{p-1}}{dx^{p-1}} \left(e^{-x} x^{p+\frac{1}{2}} \right) = (p-1)! \; x^{\frac{3}{2}} L_{p-1}^{\left(\frac{3}{2}\right)}(x) \, e^{-x}$$

$$\frac{d^{p-2}}{dx^{p-2}} \left(e^{-x} x^{p+\frac{1}{2}} \right) = (p-2)! \; x^{\frac{5}{2}} L_{p-2}^{\left(\frac{5}{2}\right)}(x) \, e^{-x}$$

$$G_{\eta p}(v,t)$$

$$= \left(\tfrac{1}{2}\right) T_\eta(t)^{\frac{5}{2}} \left(\tfrac{1}{p!}\right) \left(\left. \left|(p-1)! \; x^{\frac{5}{2}} L_{p-1}^{\left(\frac{3}{2}\right)}(x) \, e^{-x} \right|_0^{\frac{v^2}{T_\eta(t)}} \right. - \left. \left|(p-2)! \; x^{\frac{5}{2}} L_{p-2}^{\left(\frac{5}{2}\right)}(x) \, e^{-x} \right|_0^{\frac{v^2}{T_\eta(t)}} \right),$$

$$p \geq 2$$

$$G_{\eta p}(v,t) = \left(\tfrac{1}{2}\right) \left(\tfrac{1}{p(p-1)}\right) \left((p-1)v^5 L_{p-1}^{\left(\frac{3}{2}\right)}\left(\tfrac{v^2}{T_\eta(t)}\right) e^{-\frac{v^2}{T_\eta(t)}} - v^5 L_{p-2}^{\left(\frac{5}{2}\right)}\left(\tfrac{v^2}{T_\eta(t)}\right) e^{-\frac{v^2}{T_\eta(t)}} \right), \quad p \geq 2$$

$$\text{(B-30)}$$

And using (B-18):

$$G_{\eta p}(v,t) = \left(\frac{1}{2}\right)\left(\frac{1}{p(p-1)}\right)\left(p\,v^5\,L_{p-1}^{\left(\frac{3}{2}\right)}\left(\frac{v^2}{T_\eta(t)}\right)e^{-\frac{v^2}{T_\eta(t)}} - v^5\,L_{p-1}^{\left(\frac{5}{2}\right)}\left(\frac{v^2}{T_\eta(t)}\right)e^{-\frac{v^2}{T_\eta(t)}}\right),\ p \geq 2 \quad \text{(B-31)}$$

Considering (B-23), (B-26), (B-27) and (B-31) we can write:

$$II_D = \left(\frac{8\sqrt{\pi}\alpha}{3v^3}\right)T_\eta(t)\left(-\left(\frac{3}{2}vT_\eta(t)^{-\frac{1}{2}} + v^3 T_\eta(t)^{-\frac{3}{2}}\right)e^{-\frac{v^2}{T_\eta(t)}} + \frac{3\sqrt{\pi}}{4}Erf\left(\sqrt{\frac{v^2}{T_\eta(t)}}\right)\right), \qquad p = 0$$

$$II_D$$

$$= \left(\frac{4\sqrt{\pi}\alpha}{3v^3}\right)T_\eta(t)\left(\left(3\,v\,T_\eta(t)^{-\frac{1}{2}} + 2\,v^3 T_\eta(t)^{-\frac{3}{2}} + 2\,v^5 T_\eta(t)^{-\frac{5}{2}}\right)e^{-\frac{v^2}{T_\eta(t)}}\right.$$

$$\left. -\frac{3}{2}\sqrt{\pi}\,Erf\left(\sqrt{\frac{v^2}{T_\eta(t)}}\right)\right), \qquad p = 1$$

$$II_D = \left(\frac{8\sqrt{\pi}\alpha}{3}\right)v^2 T_\eta(t)^{-\frac{3}{2}}\left(\frac{1}{2}\right)\left(\frac{1}{p(p-1)}\right)\left(p\,L_{p-1}^{\left(\frac{3}{2}\right)}\left(\frac{v^2}{T_\eta(t)}\right)e^{-\frac{v^2}{T_\eta(t)}} - L_{p-1}^{\left(\frac{5}{2}\right)}\left(\frac{v^2}{T_\eta(t)}\right)e^{-\frac{v^2}{T_\eta(t)}}\right),\ p \geq 2$$

$$\text{(B-32)}$$

Adding (B-22) and (B-32), in (B-10), we can simplify it to obtain (B-33) for the case $(p = 0)$, (B-34) for the case $(p = 1)$ and (B-35) for the cases $(p \geq 2)$:

$$D_{\eta 0}(v,t) = 4\sqrt{\pi}\alpha\,T_\eta(t)^{-\frac{1}{2}}\left(-\frac{T_\eta(t)}{v^2}e^{-\frac{v^2}{T_\eta(t)}} + \frac{\sqrt{\pi}}{2}\left(\frac{T_\eta(t)}{v^2}\right)^{\frac{3}{2}}Erf\left(\sqrt{\frac{v^2}{T_\eta(t)}}\right)\right),\ p = 0 \quad \text{(B-33)}$$

$$D_{\eta 1}(v,t) = 4\sqrt{\pi}\alpha\,T_\eta(t)^{-\frac{1}{2}}\left(\left(\frac{T_\eta(t)}{v^2}+1\right)e^{-\frac{v^2}{T_\eta(t)}} - \frac{\sqrt{\pi}}{2}\left(\frac{T_\eta(t)}{v^2}\right)^{\frac{3}{2}}Erf\left(\sqrt{\frac{v^2}{T_\eta(t)}}\right)\right),\ p = 1 \quad \text{(B-34)}$$

$$D_{\eta p}(v,t) = \frac{8\sqrt{\pi}\alpha}{3}T_\eta(t)^{-\frac{1}{2}}\left(e^{-\frac{v^2}{T_\eta(t)}}L_p^{\left(-\frac{1}{2}\right)}\left(\frac{v^2}{T_\eta(t)}\right) + \frac{v^2}{T_\eta(t)}\left(\frac{1}{p(p-1)}\right)\left(p\,L_{p-1}^{\left(\frac{3}{2}\right)}\left(\frac{v^2}{T_\eta(t)}\right)e^{-\frac{v^2}{T_\eta(t)}}\right.\right.-$$

$$\left.\left.L_{p-1}^{\left(\frac{3}{2}\right)}\left(\frac{v^2}{T_\eta(t)}\right)e^{-\frac{v^2}{T_\eta(t)}}\right)\right),\ p \geq 2 \qquad\qquad \text{(B-35)}$$

Appendix C -Collision operator for the basis functions

C.1. Collision operator for the case $(p = 0)$.

We substitute $C_{\eta p}(v,t)$ and $D_{\eta p}(v,t)$ from (3-9) and (3-10) in (3-8). And also, we write the

Laguerre distribution function $F_{\zeta q}(v,t)$ and its derivative with respect to (v) in the equation.

$$F_{\zeta q}(v,t) = \frac{4}{\sqrt{\pi}} T_\zeta(t)^{-\frac{3}{2}} e^{-\frac{v^2}{T_\zeta(t)}} L_q^{\left(\frac{1}{2}\right)}\left(\frac{v^2}{T_\zeta(t)}\right) \tag{C-1}$$

$$\frac{\partial F_{\zeta q}(v,t)}{\partial v} = -\frac{8}{\sqrt{\pi}} v\, T_\zeta(t)^{-\frac{5}{2}} e^{-\frac{v^2}{T_\zeta(t)}} L_q^{\left(\frac{3}{2}\right)}\left(\frac{v^2}{T_\zeta(t)}\right) \tag{C-2}$$

$$Coll\{F_{\zeta q}(v,t), F_{\eta 0}(v,t)\} = \frac{1}{v^2}\frac{\partial}{\partial v}\left[v^2\left(D_{\eta 0}(v,t)\frac{\partial F_{\zeta q}(v,t)}{\partial v} + C_{\eta 0}(v,t)F_{\zeta q}(v,t)\right)\right] =$$

$$\left(32\,\alpha\,T_\zeta(t)^{-\frac{3}{2}}\right)\frac{1}{v^2}\frac{\partial}{\partial v}\left[e^{-\frac{v^2}{T_\zeta(t)}}\left(T_\eta(t)^{-\frac{1}{2}}v\,e^{-\frac{v^2}{T_\eta(t)}} - \frac{\sqrt{\pi}}{2}\,\text{Erf}\left(\sqrt{\frac{v^2}{T_\eta(t)}}\right)\right)L_{q-1}^{\left(\frac{3}{2}\right)}\left(\frac{v^2}{T_\zeta(t)}\right)\right] \tag{C-3}$$

(C-3) is a simple derivative and could be easily calculated by considering the derivative of the

generalized Laguerre polynomials mentioned in (B-16). After simplifying the result:

$$Coll\{F_{\zeta q}(v,t), F_{\eta 0}(v,t)\} =$$

$$-\left(\frac{64 e^{-\frac{v^2}{T_\zeta(t)}}\alpha}{T_\zeta(t)^{\frac{7}{2}}\sqrt{T_\eta(t)}}\right)\left(-\sqrt{\pi}\,Erf\left(\frac{v}{\sqrt{T_\eta(t)}}\right)\sqrt{T_\eta(t)}\left(\frac{1}{2v}\right)\left(-L_q^{\left(\frac{3}{2}\right)}\left(\frac{v^2}{T_\zeta}\right)T_\zeta(t) + L_q^{\left(\frac{5}{2}\right)}\left(\frac{v^2}{T_\zeta}\right)T_\eta(t)\right) + \right.$$

$$\left. e^{-\frac{v^2}{T_\eta(t)}}T_\zeta(t)\left(-\frac{L_q^{\left(\frac{1}{2}\right)}\left(\frac{v^2}{T_\zeta}\right)T_\zeta(t)}{T_\eta(t)} + \frac{L_q^{\left(\frac{5}{2}\right)}\left(\frac{v^2}{T_\zeta}\right)T_\eta(t)}{T_\zeta(t)}\right)\right),\quad p = 0 \tag{C-4}$$

C.2. Collision operator for the case $(p = 1)$.

We substitute $C_{\eta p}(v,t)$ and $D_{\eta p}(v,t)$ from (3-9) and (3-11) in (3-8). And also, we write the

Laguerre distribution function $F_{\zeta q}(v,t)$ and its derivative with respect to (v) in the equation.

$$Coll\{F_{\zeta q}(v,t), F_{\eta 1}(v,t)\} = \frac{1}{v^2}\frac{\partial}{\partial v}\left[v^2\left(D_{\eta 1}(v,t)\frac{\partial F_{\zeta q}(v,t)}{\partial v} + C_{\eta 1}(v,t)F_{\zeta q}(v,t)\right)\right] =$$

$$\left(32\,\alpha\,T_\eta(t)^{-\frac{3}{2}}T_\zeta(t)^{-\frac{3}{2}}\right)\frac{1}{v^2}\frac{\partial}{\partial v}\left[\left(-\left(\frac{T_\eta(t)}{T_\zeta(t)}\right)\left((T_\eta(t)+v^2)e^{-\frac{v^2}{T_\eta(t)}} - \right.\right.\right.$$

$$\left.\left.\frac{\sqrt{\pi}}{2}\left(\frac{T_\eta(t)^{\frac{3}{2}}}{v}\right)Erf\left(\sqrt{\frac{v^2}{T_\eta(t)}}\right)\right)\left(v\,e^{-\frac{v^2}{T_\zeta(t)}}L_q^{\left(\frac{3}{2}\right)}\left(\frac{v^2}{T_\zeta(t)}\right)\right) + v^3\,e^{-\frac{v^2}{T_\eta(t)}}e^{-\frac{v^2}{T_\zeta(t)}}L_q^{\left(\frac{1}{2}\right)}\left(\frac{v^2}{T_\zeta(t)}\right)\right)\right] \quad \text{(C-5)}$$

By calculating the derivative with respect to (v) in (C-5) and after some simplifications we get:

$$Coll\{F_{\zeta q}(v,t), F_{\eta 1}(v,t)\} = -32\,e^{-\frac{v^2\left(T_\zeta(t)+T_\eta(t)\right)}{T_\zeta(t)\,T_\eta(t)}}\,\alpha\,T_\zeta(t)^{-\frac{3}{2}}T_\eta(t)^{-\frac{3}{2}}\left(L_q^{\left(\frac{1}{2}\right)}\left(\frac{v^2}{T_\zeta(t)}\right)\left(-3+\frac{2v^2}{T_\eta(t)}\right)+\right.$$

$$L_q^{\left(\frac{3}{2}\right)}\left(\frac{v^2}{T_\zeta(t)}\right)\left(\frac{T_\eta(t)}{T_\zeta(t)}\right) +$$

$$\left. L_q^{\frac{5}{2}}\left(\frac{v^2}{T_\zeta(t)}\right)\left(\frac{T_\eta(t)}{T_\zeta(t)^2}\right)\left(\frac{e^{\frac{v^2}{T_\eta(t)}}\sqrt{\pi}}{v}T_\eta(t)^{\frac{3}{2}}Erf\left[\frac{v}{\sqrt{T_\eta(t)}}\right]-2\left(v^2+T_\eta(t)\right)\right)\right), \quad p=1 \quad \text{(C-6)}$$

C.3. Collision operator for the cases $(p \geq 2)$.

We substitute $C_{\eta p}(v,t)$ and $D_{\eta p}(v,t)$ from (3-9) and (3-12) in (3-8). And also, we write the Laguerre distribution function $F_{\zeta q}(v,t)$ and its derivative with respect to (v) in the equation.

$$Coll\{F_{\zeta q}(v,t), F_{\eta p}(v,t)\} = \frac{1}{v^2}\frac{\partial}{\partial v}\left[v^2\left(D_{\eta p}(v,t)\frac{\partial F_{\zeta q}(v,t)}{\partial v} + C_{\eta p}(v,t)F_{\zeta q}(v,t)\right)\right] =$$

$$\left(32\,\alpha\,T_\eta(t)^{-\frac{3}{2}}T_\zeta(t)^{-\frac{3}{2}}\right)\frac{1}{v^2}\frac{\partial}{\partial v}e^{-v^2\left(\frac{1}{T_\eta(t)}+\frac{1}{T_\zeta(t)}\right)}v^3\left(-\frac{2}{3}\left(\frac{T_\eta(t)}{T_\zeta(t)}\right)\left(L_p^{\left(-\frac{1}{2}\right)}\left(\frac{v^2}{T_\eta(t)}\right)+\right.\right.$$

$$\left.\left.\frac{v^2}{T_\eta(t)}\left(\frac{1}{p(p-1)}\right)\left(p\,L_{p-1}^{\left(\frac{3}{2}\right)}\left(\frac{v^2}{T_\eta(t)}\right) - L_{p-1}^{\left(\frac{5}{2}\right)}\left(\frac{v^2}{T_\eta(t)}\right)\right)\right)L_q^{\left(\frac{3}{2}\right)}\left(\frac{v^2}{T_\zeta(t)}\right) + \left(\frac{1}{p}\right)L_{p-1}^{\left(\frac{3}{2}\right)}\left(\frac{v^2}{T_\eta(t)}\right)L_q^{\left(\frac{1}{2}\right)}\left(\frac{v^2}{T_\zeta(t)}\right)\right)$$

$$\text{(C-7)}$$

By calculating the derivative with respect to (v) in (C-7) and after some simplifications we get:

$$Coll\{F_{\zeta q}(v,t), F_{\eta p}(v,t)\} =$$

$$\frac{32\,\alpha}{p(p-1)T_\zeta(t)^{\frac{3}{2}}T_\eta(t)^{\frac{3}{2}}}\, e^{-\frac{v^2\left(T_\zeta(t)+T_\eta(t)\right)}{T_\zeta(t)T_\eta(t)}}\left(2p(p-1)\,L_p^{\left(\frac{1}{2}\right)}\left(\frac{v^2}{T_\eta(t)}\right)L_q^{\left(\frac{1}{2}\right)}\left(\frac{v^2}{T_\zeta(t)}\right)+\right.$$

$$2p\left(\frac{v^2}{T_\zeta(t)}\right)\left(\frac{T_\eta(t)}{T_\zeta(t)}\right)L_{p-1}^{\left(\frac{1}{2}\right)}\left(\frac{v^2}{T_\eta(t)}\right)L_q^{\left(\frac{5}{2}\right)}\left(\frac{v^2}{T_\zeta(t)}\right)-2\left(\frac{v^2}{T_\zeta(t)}\right)\left(\frac{T_\eta(t)}{T_\zeta(t)}\right)L_{p-1}^{\left(\frac{3}{2}\right)}\left(\frac{v^2}{T_\eta(t)}\right)L_q^{\left(\frac{5}{2}\right)}\left(\frac{v^2}{T_\zeta(t)}\right)+$$

$$\left.(1-p)\left(\frac{T_\eta(t)}{T_\zeta(t)}\right)L_{p-1}^{\left(\frac{1}{2}\right)}\left(\frac{v^2}{T_\eta(t)}\right)L_q^{\left(\frac{3}{2}\right)}\left(\frac{v^2}{T_\zeta(t)}\right)\right),\ p\ge 2 \qquad\text{(C-8)}$$